UCLouvain
Faculté des sciences
Louvain Institute of Biomolecular Science and Technology

Regulatory functions of a plant TSPO-related protein during abiotic stress

Thèse présentée par **Paweł Jurkiewicz** en vue de l'obtention du grade de Docteur en Sciences

Promoteur:	Henri Batoko
Membres du jury:	Bernard Knoops (Président)
	René Rezsohazy (Secrétaire)
	Charles Hachez
	Jean-Jacques Lacapère
	Pierre Morsomme
	Celine Vanhee

Septembre 2018

Rodzinie i Przyjaciołom

Acknowledgements

This PhD thesis was a great adventure full of little victories and defeats. Step by step under heavy workload it was progressing towards the goals. It taught me to accept failures and prioritize things. However, looking from a distance, it has just one face: that was the time of my professional and personal growth.

Particular thanks go to my supervisor Prof. Henri Batoko. Accepted as an Erasmus student in 2012, I met you saying "my door is always open". Indeed, after six years I've got to know you as an outstanding investigator, always full of motivation and brilliant ideas. Always professional and helpful. The rock. Thank you for all those moments we spent on tough scientific discussions and those we were in stitches by joking. Good luck for your future projects!

Doing science without collaboration is like going from Belgium to Poland by foot and blindfolded. Does not work. I acknowledge all our collaborators for materials, ideas and benchwork done to elevate the final value of our research.

In addition, I would like to thank all the members of my jury for their time, critical reading of this manuscript and helpful comments. It was my true pleasure to be surrounded by such fantastic friendly people.

Big "thank you" goes also to all my lab colleagues, the current and the former ones, working hard on TSPO-related topics. Thank you for all your sacrifice, scientific support, ideas and good humour. I will miss you.

The FYMO unit was my second home during these five years. I am grateful I could have worked in this environment. I thank every single member of my big FYMO family: PIs, students, technicians and members of administrative staff. Everyone contributed, even a wee bit, to make this dream come true.

Dziękuję również moim kochanym Rodzicom oraz Rodzicom Agi, bez pomocy których ta wspaniała przygoda mogłaby okazać się niemożliwa do zrealizowania. Dziękuję za nieustające wsparcie i motywację.

"Malowanie, gipsogładzie, solidnie." Greg, teraz na pewno wyślę Ci tę tezę!!! (Edzia, Tobie również, a Mały będzie miał co drzeć i malować.)

Myślę, że cała ta historia nie wydarzyłaby się, gdyby nie pomoc Prof. Stanisława Ułaszewskiego. To dzięki Pana szerszemu poglądowi na naukę mogłem wyjechać do Belgii i tam rozpocząć tę wielką życiową podróż. Dziękuję!

Na sam koniec dziękuję mojej własnej, niedawno stworzonej, wspaniałej Rodzinie. To właśnie dzięki Wam przeżywam tutaj najpiękniejsze chwile mojego życia.

Oby tak dalej!

Paweł
Louvain-la-Neuve, wrzesień 2018

Table of contents

Abbreviations

3D	three-dimensional
AAO	abscisic aldehyde oxidase
AAPT	amino-alcohol phosphotransferase
ABA	abscisic acid
ABA-GE	abscisic acid glucosyl ester
ABC	ATP-binding cassette
ABF	ABA responsive element binding factor
ABI	ABA-Insensitive
acyl-ACP	acyl-chain attached to an acyl-carrier-protein
AIM/LIR	Atg8-interacting motifs/LC3-interacting regions
AIT	ABA importing transporter
AREB	ABA responsive element binding protein
ARM	armadillo repeat domain
AtDTX50	*Arabidopsis thaliana* detoxification efflux carrier 50
ATG	autophagy-related
AtHB7	*Arabidopsis thaliana* homeobox 7
AtTSPO	*Arabidopsis thaliana* Translocator protein
AtVPS34	*Arabidopsis thaliana* vacuolar protein sorting 34
B3-MAPKKK	B3-group Raf-like mitogen-activated protein kinase kinase kinase
BATS	Barkor/ATG14 autophagosome targeting sequence
BG	beta-glucosidase
BiFC	bimolecular fluorescence complementation
BiP	lumenal binding proteins
BSA	bovine serum albumin
bZIP	basic leucine zipper
C	Celsius (unit)
CaMV 35S	cauliflower mosaic virus 35S promoter
Ci	Curie (unit)
CL	cardiolipin
CLS	CL synthase
CNS	central nervous system

CoA	coenzyme A
CRAC	cholesterol recognition/amino acid consensus
CRLs	cullin-RING ligases
CSP	chemical shift perturbations
DAG	diacylglycerol
DBI	diazepam-binding inhibitor
DDM	n-Dodecyl β-D-maltoside
DMPC	1,2-Dimyristoyl-sn-glycero-3-phosphocholine
DMPG	1,2-Dimyristoyl-sn-glycero-3-phosphorylglycerol
DMSO	dimethyl sulfoxide
DNA	deoxyribonucleic acid
DRE	drought-responsive element
DTT	dithiotreitol
ECL	enhanced chemiluminescence
EDTA	ethylene diamine tetra-acetic acid
ENTH	epsin N-terminal homology
ER	endoplasmic reticulum
ERAD	endoplasmic reticulum-associated protein degradation
ERG6	sterol 24-C-methyltransferase
FA	fatty acid
Fab1	forms aploid and binucleate cells 1
FAO	fatty acid oxidation
FAX1	fatty acid export 1
Flvcr	feline leukemia virus subgroup C receptor
FRET	Förster resonance energy transfer
FYVE	Fab1/YOTB/Vac1/EEA1
G3P	glycerol-3-phosphate
GFP	green fluorescent protein
GPAT	G3P acyltransferase
GST	glutathione S-transferase
HAB	homolog of ABA-insensitive
HCCA	alpha-cyano-4-hydroxycinnamic acid
HECT	homologous to the E6-AP carboxyl terminus

HEPES	4-(2-hydroxyethyl)-1-piperazine ethanesulfonic acid
HIP	hybrid intrinsic protein
HMG-CoA	hydroxymethylglutaryl-CoA
HPTLC	high performance thin layer chromatography
HRP	horseradish peroxidase
HsPIPK1α	*Homo sapiens* PI4P 5-kinase
HSQC	heteronuclear single quantum coherence
IBP	isoquinoline-binding protein
IP_3	inositol 1,4,5-trisphosphate
IP_4	inositol 1,3,4,5-tetrakisphosphate
IP_5	inositol 1,3,4,5,6-pentakisphosphate
IP_6	inositol 1,2,3,4,5,6-hexakisphosphate
IPTG	isopropyl-β-D-thiogalactoside
K	Kelvin (unit)
KanR	kanamycin resistance
KAT	K^+-influx channel
kDa	kilodalton (unit)
Kir	inward-rectifier potassium channel
KO	knockout
KOD	potassium deuteroxide
LACS9	long chain acyl-CoA synthetase 9
LD	lipid droplets
LDAP	lipid droplet-associated proteins
LED	light-emitting diode
Lin	linker domain
LPA	lysophosphatidic acid
LPAT	LPA acyltransferase
LS	Linsmaier and Skoog
MALDI-TOF	matrix-assisted laser desorption/ionization-time-of-flight
MATE	multidrug and toxic compound extrusion
MBR	mitochondrial benzodiazepine receptor
MES	2-(N-morpholino)ethanesulfonic acid
MHz	megahertz (unit)

MIP	major intrinsic protein
MORN	membrane occupation and recognition nexus
MPTP	mitochondrial permeability transition pore
MS	Murashige and Skoog
MST	microscale thermophoresis
MTM	myotubularin-type phosphatase
mTSPO	mouse Translocator protein 1
NCED	9-cis-epoxy carotenoid dioxygenase
ndi	nutrient deprivation-induced
Ni-NTA	nickel- nitrilotriacetic acid
NIP	nodulin26-like intrinsic protein
NMR	nuclear magnetic resonance
NRT	nitrate transporter
NT	N-terminal domain
OE	overexpressor
OMM	outer mitochondrial membrane
ORP	oxysterol-binding proteins
OST1	open stomata 1
PA	phosphatidic acid
PAP	PA phosphatase
PBR	peripheral-type benzodiazepine receptor
PC	phosphatidylcholine
PCR	polymerase chain reaction
PDR	pleiotropic drug resistance
PE	phosphatidylethanolamine
PEG	polyethylene glycol
PG	phosphatidylglycerol
PGP	PG phosphate
PGPP	PGP phosphatase
PGPS	PGP synthase
PH	pleckstrin homology
PI	phosphatidylinositol
PIK	PI kinase

PIP	PI phosphate
PIP	plasma membrane intrinsic protein
PIP2	PI bis-phosphate
PIP2;7	plasma membrane intrinsic protein isoform 2;7
PIP3	PI tris-phosphate
PIPK	PIP kinase
PIS	PI synthase
PIs	phosphoinositides
PK11195	isoquinolinecarboximide
PL	phospholipids
PLC	phospholipase C
PP2C	protein phosphatase 2C
PPIX	protoporphyrin IX
PRE	plastid responsive element
PS	phosphatidylserine
PSD	PS decarboxylase
PSS	PS synthase
PTEN	phosphatase and tensin homolog deleted on chromosome ten
PUB	plant U-box
PVDF	polyvinylidene difluoride
PX	phox homology
PYL	pyrabactin resistance-like
PYR	pyrabactin resistance
RCAR	regulatory component of ABA receptors
RING	really interesting new gene
RIP	regulated intramembrane proteolysis
RLS1	ring finger of seed longevity
RNA	ribonucleic acid
ROS	reactive oxygen species
RPN10	26S proteasome non-ATPase regulatory subunit
RT-qPCR	reverse transcription quantitative PCR
S1P, S2P	subtilisin-like site-specific proteases 1 and 2

SD	standard deviation
SDR	short-chain alcohol dehydrogenase/reductase
SDS	sodium dodecyl sulfate
SDS-PAGE	SDS-polyacrylamide gel electrophoresis
SE	standard error
SIP	small basic intrinsic protein
SKOR	stelar K^+ outward rectifying
SNF1	sucrose non-fermenting 1
SnRK2	SNF-related protein kinase
ss-DNA	single stranded DNA
SSP	secondary structure propensity
STAR	steroidogenesis acute regulatory protein
SYP	syntaxin of plants
TAG	triacylglycerol
TBS	tris-buffered saline
TE	thioesterase
TEV	tobacco etch virus
TIP	tonoplast intrinsic protein
TM	transmembrane domain
TNF-α	tumor necrosis factor alpha
Tris	2-Amino-2-(hydroxymethyl)propane-1,3-diol
TRPV1	transient receptor potential vanilloid 1
TSP	trimethylsilyl-[2,2,3,3-d_4]-propionate
TSPO	Translocator protein
UBI10	ubiquitin 10
UND	U-box N-terminal domain
UPR	unfolded protein response
UPS	ubiquitin-proteasome system
USER	uracil-specific excision reagent
UV	ultraviolet
v/v	volume/volume
VDAC1	voltage-dependent anion channel 1
w/v	weight/volume
WT	wild type

XIP	uncategorized intrinsic protein
YD	yeast extract, dextrose
YFP	yellow fluorescent protein
ZEP	zeaxanthin epoxidase

Abstract

Translocator proteins (TSPO) are evolutionarily conserved polytopic membrane proteins. Structurally, they share a core transmembrane domain made of five α-helices. However, the length and structure of their termini appear to be kingdom-specific. After more than forty years of extensive studies, the biological role of TSPO is still highly discussed. It seems that, from bacteria to humans, these nonessential proteins are upregulated during cellular stresses to sense and regulate redox homeostasis through tetrapyrrole metabolism. The molecular mechanism of this ancient regulatory role persists nowadays with variations from species to species. In addition, recent evidences in animal cells suggest that TSPO may modulate lipid metabolism.

The *Arabidopsis thaliana* TSPO (AtTSPO) is an abiotic stress-induced membrane protein with a plant-specific polybasic N-terminal extension. In particular, AtTSPO is highly induced by osmotic stress. The presence of AtTSPO in the cell is tightly regulated and the degradation of AtTSPO requires heme binding and an active autophagy pathway. AtTSPO physically interacts with the plasma membrane aquaporin PIP2;7 *in vivo* and targets the aquaporin for autophagic degradation during osmotic stress.

In this work, we present evidence supporting a role for plant TSPO in the cell energy homeostasis in a tissue-specific manner. We showed that AtTSPO can enhance fatty acids and lipid droplets (LD) accumulation in mature seeds but limiting LD levels in seedlings. Moreover, we show that AtTSPO binds the signaling lipid $PI(4,5)P_2$ through its N-terminal polybasic extension. The N-terminus extension of AtTSPO can also mistarget a $PI(4,5)P_2$ biosensor from the plasma membrane to the Golgi membranes where AtTSPO is localized in the plant cell. Deletion of the N-terminus, or defined point mutations within, prevented AtTSPO-PIP2;7 interaction *in vivo*.

These findings support a functional divergence of plant TSPO from their bacterial and animal counterparts, through the evolutionary acquisition of a lipid-interacting N-terminal extension.

PART I: INTRODUCTION

Translocator proteins (TSPO) are found in almost all species ranging from prokaryotes to humans. TSPO possess five alpha-helical transmembrane segments that form a structurally conserved TspO/MBR domain. The best-characterized mammalian TSPO was described more than forty years ago (Braestrup and Squires, 1977; Braestrup et al., 1977), and a bacterial ortholog, TspO, has also been extensively studied (Zeng and Kaplan, 2001; Guo et al., 2015; Batoko et al., 2015). However, the biological functions of TSPO are still not clear. It seems that these ancient proteins have evolved a common role in stress sensing and response with some mechanistic variations from species to species.

TSPO from higher plants share a peculiar N-terminal extension, absent in their animal and bacterial counterparts. It is not yet known whether this N-terminal extension of plant TSPO has any functional attribute. However, some of the shared characteristics of these extensions are striking: i) they are rich in basic amino acid residues that contribute to an overall positive charge of the peptide, ii) they are of variable length of >30 residues with a remarkable conservation of some key charged residues close to the first transmembrane segment. The host laboratory showed recently that the Arabidopsis TSPO (AtTSPO) is induced by osmotic stress and physically interacts with a highly-expressed plasma membrane aquaporin, PIP2;7. Under osmotic stress, AtTSPO appears to titrate newly translated PIP2;7 molecules *en route* to the plasma membrane. The interaction complex is subsequently targeted to vacuolar degradation via the autophagic pathway, therefore limiting PIP2;7-dependent water transport activity at the plasma membrane of affected cells.

The network of plant responses to osmotic stress involves lipids metabolism and in particular signaling phosphoinositides (PIs). These minor signaling lipids can be recognized and bound by specific proteins harboring defined lipid binding domains. However, linear or spatial polybasic stretch of amino acids formed by some regulatory proteins can also generate functional electrostatic interactions with PIs.

This project aims at deciphering the role of the N-terminal extension of AtTSPO and its potential involvement in lipids signaling and regulation of AtTSPO-PIP2;7 interaction.

The literature review will introduce TSPO proteins as well as aquaporins, followed by a review of current knowledge on lipids and their signaling roles in the cell.

Chapter 1: TSPO

Translocator proteins (TSPO) represent a diverse family of ubiquitous membrane proteins with biological roles linked to detrimental physiological conditions and homeostasis. Structurally, they have evolved a conserved structure made of five core transmembrane spans, while the length of their termini appears to be kingdom-specific. The first characterized member was the mammalian 18 kDa Translocator protein which has an extended C-terminus containing a cholesterol binding motif. In contrast, higher plants TSPO lack the C-terminal extension but instead they possess a lengthened N-terminus with an intriguing polybasic motifs property. In this chapter, we will give an overview on the functions fulfilled by TSPO proteins across biological kingdoms. We will introduce emerging data debunking a long-lasting consensus on TSPO role in animal cells followed by state-of-the-art in TSPO from Arabidopsis. We will end by characterizing a novel regulatory function of TSPO in plant cell under osmotic stress by targeting a highly expressed aquaporin PIP2;7 for degradation.

1.1. Historical overview

In the late seventies, an interest arose in animal research to identify binding sites for diazepam, a drug belonging to the family of benzodiazepines. Existence of such binding sites/receptor was evidenced for the first time in murine peripheral tissues in addition to brain tissues (Braestrup and Squires, 1977). This observation was also confirmed in human tissues (Braestrup et al., 1977). Further investigation showed that this putative receptor was present in most peripheral tissues like kidneys, and precisely enriched in kidneys' mitochondria (Mohler and Okada, 1977; Squires and Braestrup, 1977).
The two different binding sites were speculated to correspond to two different proteins as their binding properties varied biochemically. For example, chlorodiazepam was not able to displace diazepam from central nervous system (CNS) receptor binding site but it successfully displaced diazepam from peripheral tissues receptor binding site (Squires and Braestrup, 1977). The proteins responsible of generating benzodiazepine

binding in peripheral tissues were called peripheral-type benzodiazepine receptor (PBR) to distinguish them from the central ones (Gavish et al., 1999; Lacapere and Papadopoulos, 2003). However, further research showed that PBR were also present in CNS tissues (Patel and Marangos, 1982; Anholt et al., 1984). As from its identification, the putative peripheral receptor attracted much interest and its name evolved as novel functions were ascribed to this protein, including mitochondrial benzodiazepine receptor (MBR), mitochondrial diazepam-binding inhibitor (DBI) receptor complex, PK11195-binding site (PK11195-isoquinoline carboximide; a high-affinity synthetic diagnostic ligand) and isoquinoline-binding protein (IBP). Although these names defined certain biochemical properties of the protein, none of them reflected its true nature and biological role. Hence, the protein was renamed in 2006 Translocator protein (TSPO) reflecting a consensual view of researchers in the field (Papadopoulos et al., 2006), although the possible substrate(s), if any, translocated across biological membrane are still under fierce debate.

1.2. Evolutionarily conserved domain and functions of TSPO proteins from different kingdoms of life

Translocator proteins (TSPO) are conserved, ubiquitous membrane proteins identified initially as benzodiazepine-binding proteins in mammalian cells. Recent genetic and biochemical studies have challenged the accepted model that TSPO are essential and required for steroidogenesis in animals. Instead, evidence from different kingdoms of life suggests that TSPO are encoded by nonessential genes that are temporally upregulated in cells encountering conditions of oxidative stress, including inflammation and tissue injury. In this section, we discuss how TSPO may be involved in complex homeostasis signaling mechanisms. We suggest that a shared and ancient physiological role of TSPO may be to modulate oxidative stress, irrespective of the cell type or subcellular localization of the protein, in part through a subtle regulation of tetrapyrrole metabolism.

1.2.1. The conflicting and elusive physiological role for TSPO in animal cells (*adapted from a co-authored publication: Batoko et al., 2015*)

TSPO are structurally well-conserved five α-helical transmembrane proteins found in most species from bacteria to humans. The so-called TspO/MBR domain corresponding to the five α-helical transmembrane segments is conserved (>25% identity between TSPO from different species), but the termini of TSPO are evolutionary divergent. For example, plant TSPO possess a positively charged N-terminal extension that is absent in bacterial and animal TSPO (Figure 1.1). Animal mitochondrial TSPO (hereafter referred to as TSPO1) was first identified as a diazepam-binding protein found in peripheral tissues; hence the previous denomination as peripheral-type benzodiazepine receptor (Braestrup et al., 1977). Further research showed that TSPO are not genuine receptor proteins and are ubiquitously expressed in many tissues and cell types including the central nervous system (CNS) in mammals. The most studied animal isoform, TSPO1, is primarily found in the mitochondrial outer membrane. A less characterized TSPO1 paralog, TSPO2, has been described in some mammals and in avian species (Fan et al., 2009; Nakazawa et al., 2009), but its expression appears to be restricted to developing red blood cells and the protein is localized in the membrane of the endoplasmic reticulum.

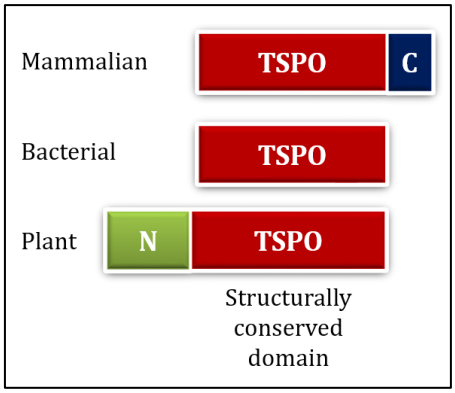

Figure 1.1. Schematic view of mammalian, bacterial and plant TSPO. Although the primary structure of TSPO proteins is fairly conserved, all members of TSPO protein

family possess in common a structurally conserved core membrane spanning domain made of five α-helices (in red). An extended C-terminus is specific of animal TSPO, while higher plant TSPO have a specific N-terminal extension.

Animal TSPO1 has been implicated in many cellular processes including cell proliferation and differentiation, apoptosis, immunomodulation, tetrapyrrole biosynthesis, oxidative stress, steroid biosynthesis, and mitochondrial physiology (Anholt et al., 1986; Mukhin et al., 1989; Krueger and Papadopoulos, 1990; Rupprecht et al., 2010). The most studied physiological role of TSPO1, including its possible involvement in diseases and malfunctions of the CNS, relates to its modulation of steroid hormones production. In particular, TSPO1 is thought to be required and essential for the translocation of cholesterol from the outer mitochondrial membrane (OMM) to the inner mitochondrial membrane, a limiting step for steroidogenesis (Mukhin et al., 1989; Krueger and Papadopoulos, 1990; Rupprecht et al., 2010). Accordingly, TSPO1 is enriched in steroidogenic tissues such as the adrenal cortex and testicular Leydig cells. Acute steroidogenic responses are mediated by the delivery of cholesterol to the OMM by steroidogenesis acute regulatory protein (STAR) (Lin et al., 1995; Miller, 2013), most likely at the mitochondria-associated endoplasmic reticulum membrane (Prasad et al., 2015). It is not yet clear whether TSPO1 and STAR cooperate in this action. On the one hand, STAR mutations cause congenital lipoid adrenal hyperplasia, with no steroidogenesis, suggesting that the soluble STAR protein is essential for steroidogenesis (Caron et al., 1997; Bhangoo et al., 2006). On the other hand, STAR is not expressed in some steroidogenic tissues such as the human placenta (Bhangoo et al., 2006). Also, TSPO1 is not expressed in some cell lines such as Jurkat cells, which are capable of producing steroid hormones (Carayon et al., 1996; Gonzalez-Polo et al., 2005; Tu et al., 2014). Anecdotal data suggest that TSPO1 is encoded by an essential gene (Papadopoulos et al., 1997) and the literature largely describes TSPO1 as indispensable for steroidogenesis in animal tissues and cultured cells (Papadopoulos et al., 1997, 2006; Rupprecht et al., 2010). Therefore, recent findings demonstrating that knockdown or knockout of TSPO1 in different cell types had no effect on viability and, importantly, that tspo1$^{-/-}$ mice and flies (*Drosophila melanogaster*) were

viable and showed unaltered steroidogenesis (Banati et al., 2014; Taylor et al., 2014; Morohaku et al., 2014; Lin et al., 2014; Tu et al., 2014) came as an intriguing surprise. Other findings appear to show a complex response of mouse to targeted tissue-specific deletion of TSPO1 (Fan et al., 2015). Additionally, recent evidence, contrary to previous suggestions, shows that TSPO1 is not involved in the regulation of the mitochondrial permeability transition pore (MPTP) (Sileikyte et al., 2014), suggesting that its role in mitochondrial physiology is far from clear. A recent review extensively discussed the data supporting a role of TSPO1 in steroidogenesis and mitochondrial physiology (Selvaraj and Stocco, 2015) and other views exist on this complex subject (Fan et al., 2015). Therefore, here we highlight some of the conflicting observations in animal cells regarding the physiological role of TSPO and provide alternative explanations in light of recent findings, including breakthrough structural analyses. We critically analyze data regarding the role of TSPO in animal and non-animal cells and conclude that a conserved function of TSPO, with some cell-dependent mechanistic variations, is to regulate the cellular responses to signal transduction pathway activation through modulation of oxidative stress.

1.2.1.1. TSPO1 binds cholesterol but is not a cholesterol transporter

TSPO1 can bind cholesterol *in vitro* and *in vivo* through a cholesterol recognition/amino acid consensus (CRAC) sequence [-L/V-$(X)_{1-5}$-Y-$(X)_{1-5}$-R/K; single amino acid code, with X representing any amino acid] in its transmembrane (TM) 5 domain (Li and Papadopoulos, 1998). Consistent with the apparent role of TSPO1 in steroidogenesis, it has been deduced from molecular simulation and low resolution structural studies of mitochondrial and bacterial TSPO that they form a channel-like structure as a monomer or oligomer, respectively, that may accommodate the transport of cholesterol or other lipophilic molecules (Papadopoulos et al., 2006; Korkhov et al., 2010; Rupprecht et al., 2010; Girard et al., 2012; Teboul et al., 2012; Li et al., 2013; Jaremko et al., 2014) (Figure 1.2).

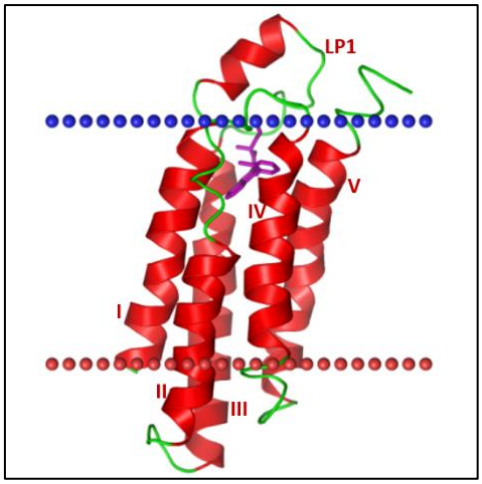

Figure 1.2. 3D NMR structure of recombinant mouse TSPO1 monomer. Protein was stabilized by PK11195 binding (magenta ribbon located in the ligand-binding pocket) obtained in dodecylphosphocholine micelles (Jaremko et al., 2014). The five membrane α-helices are numbered with Roman numerals. The broken lines indicate approximately the limits of the membrane region, with red representing the cytosolic face. Adapted from Batoko et al., 2015.

A human polymorphic TSPO1 mutation resulting in an A147T substitution, one helical turn preceding the cholesterol binding motif, reduces cholesterol binding *in vitro* and is associated *in vivo* with increased psychiatric disorders. These clinical observations were interpreted as the consequence of reduced neurosteroid formation (Costa et al., 2009; Rupprecht et al., 2010). However, the TSPO1 A147T substitution and corresponding substitution in bacterial TSPO not only reduced cholesterol binding, but also altered PK11195 and Ro5-4864 binding (Li et al., 2015; Guo et al., 2015). The A147T equivalent in *Rhodobacter sphaeroides* TSPO (RsTSPO), A139T, appears to structurally modify the positioning of L142 and F144, which are important for cholesterol binding, within the conserved CRAC motif in TM5 (Li et al., 2015). In addition, the side chain of the conserved alanine (A147 or equivalent) protrudes into the PK11195 and Ro5-4864 binding pocket such that its mutation is expected to interfere with those ligands' binding (Guo et al., 2015). If TSPO1 is somehow involved in cholesterol transport from the OMM, and this transport step requires cholesterol binding by the CRAC motif, it is difficult to understand how PK11195 could enhance

steroidogenesis through TSPO1 as consistently reported (Krueger and Papadopoulos, 1990; Papadopoulos et al., 1997; 1997, 2006; Rupprecht et al., 2010). Structural evidence suggests that PK11195 binding by TSPO1 should interfere with cholesterol binding at the CRAC motif. In contrast to STAR, there is no direct biochemical evidence, such as by *in vitro* reconstitution, that any TSPO protein can transport cholesterol. Moreover, the CRAC motif is not conserved in plant TSPO and the A147T substitution is constitutively present in the animal TSPO2 paralog, suggesting that cholesterol binding and/or transport is not the primary evolutionarily conserved biological role of TSPO. The hypothesized TSPO1-mediated transport of cholesterol is constrained by the compact crystal structure, as shown in Figure 1.3 for bacterial TSPO dimers, rendering an internal pore-like transport mechanism through the monomer or transport through the tight dimer interface less conceivable (Li et al., 2015). The functional dimer's tight hydrophobic interface represents about 15% of the monomers and the central core appears to be occupied by TM3, at least in RsTSPO (Li et al., 2015), which harbors a well-conserved G/A-XXX-G/A motif favoring transmembrane α-helix dimerization (Moore et al., 2008).

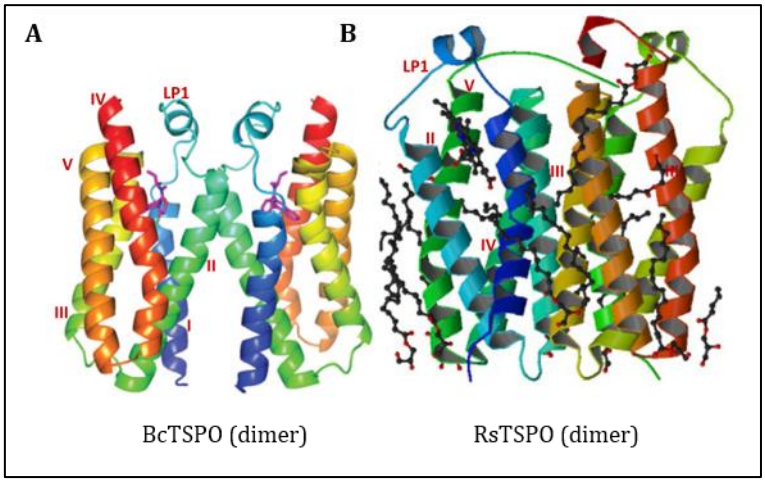

Figure 1.3. A comparison of the 3D structure of bacterial TSPO proteins. (A) Ribbon drawing of a crystal structure of the *Bacillus cereus* TSPO (BcTSPO) functional dimer complexed with PK11195 in the lipidic cubic phase (Guo et al., 2015). The five membrane a-helices of one monomer are numbered with Roman numerals. **(B)** Ribbon drawing of a crystal structure of the *Rhodobacter sphaeroides* TSPO (RsTSPO) apo-dimer in the lipidic

cubic phase (Li et al., 2015). Some lipid molecules are shown as ball-and-stick drawings. The five membrane α-helices of one monomer are numbered with Roman numerals. Adapted from Batoko et al., 2015.

The biological meaning of cholesterol binding and the mechanism by which animal TSPO1 might transport cholesterol remain to be determined. Transient overexpression of TSPO1 in macrophages enhances cholesterol efflux by inducing cholesterol transporters and reducing macrophage lipid content (Taylor et al., 2014). A cell-specific knockout of TSPO1 in mouse resulted in increased lipid droplets (Fan et al., 2015). The non-mitochondrial TSPO2 was shown to be involved in cholesterol redistribution (Fan et al., 2009). It may be that TSPO expression somehow regulates lipid metabolism and the presence of TSPO in a biological membrane could increase the sterol content within that given membrane through protein–sterol interaction. Early *in vitro* studies using isolated animal mitochondria showed that PK11195 stimulated steroid synthesis at the mitochondrial level by acting on cholesterol already available in the OMM, since addition of excess cholesterol in the media did not enhance steroid synthesis (Krueger and Papadopoulos, 1990). It may be that increased cholesterol levels in the OMM due to TSPO1 expression indirectly enhance cholesterol translocation rate to the mitochondrial inner membrane and hence steroidogenesis.

1.2.1.2. TSPO bind but do not transport porphyrins across biological membranes

Besides cholesterol, another class of endogenous TSPO ligands are porphyrins, specifically heme and its direct precursor protoporphyrin IX (PPIX) (Verma et al., 1987). These are cyclic tetrapyrroles synthesized through a conserved eight-step enzymatic pathway in the prokaryote-derived organelles (mitochondria or plastids) of eukaryotic cells. TSPO from distantly related species bind heme and PPIX *in vitro* and *in vivo* (Verma et al., 1987; Ozaki et al., 2010; Vanhee et al., 2011; Guo et al., 2015). Recombinant RsTSPO was copurified with an unidentified cyclic porphyrin (Li et al., 2015). Although the published literature repeatedly

mentions that TSPO, and in particular TSPO1, is a porphyrin transporter, no published experimental evidence supports this claim.

Unbound heme can be extremely toxic to the cell. Although we know little about heme trafficking, the transport of heme across biological membranes appears to be energy-dependent (Korolnek and Hamza, 2014). Heme produced in the mitochondria has to reach hemoproteins distributed in other membrane-bound compartments of the cell and the cytosol. In mammals, heme export from the mitochondria is mediated by the antiporter Flvcr1b, a mitochondrial splice variant of the plasma membrane heme exporter feline leukemia virus subgroup C receptor 1 (Flvcr1) (Chiabrando et al., 2012). Overexpression of Flvcr1b promoted heme synthesis and *in vitro* erythroid differentiation, whereas silencing of Flvcr1b in cultured HeLa cells resulted in mitochondrial heme accumulation (Chiabrando et al., 2012). TSPO knockdown in zebrafish resulted in depletion of red blood cells and downregulation of globin biosynthesis (Rampon et al., 2009). It was suggested that this phenotype could be due to PPIX accumulation, as this accumulation is known to induce maturation arrest of reticulocytes and erythropoiesis ability (Yamamoto et al., 2014). The PPIX-related cytoprotective effects of TSPO may relate to binding and sequestration of PPIX rather than its transport *per se* across biological membranes. Unbound PPIX is highly toxic; in the presence of light, it reacts with molecular oxygen to generate singlet oxygen, a reactive oxygen species (ROS). Free PPIX can also inhibit soluble guanylate cyclase activity and heme oxygenase, which degrades free heme to prevent it from reaching toxic concentrations (Korolnek and Hamza, 2014). TSPO was shown to prevent PPIX accumulation in a glioblastoma cell line. Exposure of TSPO-knockdown glioblastoma cells to light led to cell death, suggesting that TSPO downregulation enhanced PPIX accumulation and ROS formation (Zeno et al., 2012). Overexpression of a plant TSPO can protect against photodynamic-related cell death, which is induced by boosting the levels of photoreactive porphyrins (Vanhee et al., 2011). How TSPO could protect the cell from porphyria-related physiological disorders is not yet clear. It was shown that purified *Chlorobium tepidum* TSPO can photooxidize PPIX *in vitro* (Ginter et al., 2013). *Bacillus cereus* TSPO (BcTSPO) and *Xenopus*

tropicalis TSPO1 can also photooxidize PPIX *in vitro* (Guo et al., 2015). These enzymatic activities were light-dependent and irreversible, and in presence of saturating PK11195 concentration the PPIX decay was substantially but not completely inhibited (Guo et al., 2015), suggesting that, at least *in vitro*, both PPIX and PK11195 may be competing for the same binding groove within TSPO. In BcTSPO, PPIX degradation required W51 and W138, the latter of which is evolutionarily well conserved among TSPO. W138F substitution greatly reduced but did not abolish the catalytic degradation of PPIX, while W51F but also the A142T (equivalent to the human polymorphic A147T mutation) substitution triggered complete inhibition of PPIX photodegradation (Guo et al., 2015). Interestingly, the carbonyl group of PK11195 forms a hydrogen bond with the indole-NH groups of W51 and W138 of BcTSPO, within the ligand-binding pocket (Guo et al., 2015). It may be that the free or excited state of PPIX is reversibly stabilized by binding to TSPO. An additional layer of cellular protection may be provided by the enzymatic photodegradation of PPIX by some TSPO, and this specific enzymatic activity requires defined residues such as A142, W51, and/or W138 (BcTSPO numbering, or equivalent in other TSPO). Instead of acting as a transporter as suggested previously, it may be that TSPO bind heme and PPIX as a regulatory cellular protection mechanism against oxidative stress otherwise generated by the free form of these porphyrins.

1.2.2. ROS signaling attenuation by TSPO in bacteria, plant and microglial cells

The first evidence of TSPO acting as a regulator of tetrapyrrole metabolism came from the facultative photoheterotrophic bacterium *R. sphaeroides*. These bacterial cells meet their energetic needs for growth through aerobic respiration. Under low oxygen levels or anaerobic conditions, *R. sphaeroides* generates intracellular membrane compartments containing bacteriochlorophylls, carotenoids, and light-harvesting complexes. Under anaerobic conditions they also produce the nonessential RsTSPO, and RsTSPO is downregulated in aerobically growing cells (Zeng and Kaplan, 2001). The outer membrane-localized

RsTSPO regulates a repressor/antirepressor (PpsR/AppA) system that in turn represses photosynthesis genes under light and aerobic conditions. Interestingly, the antirepressor AppA is a hemoprotein. It was suggested that RsTSPO may be involved in the efflux of coproporphyrin III, an intermediate in PPIX, heme, and chlorophyll biosynthesis, and that the transcriptional effects of RsTSPO could be explained by the accumulation of an AppA coactivator (Zeng and Kaplan, 2001). However, an RsTSPO-knockout strain can still secrete coproporphyrin III, suggesting that this efflux activity is not RsTSPO-dependent. Heme and/or PPIX sequestration, and possibly PPIX photodegradation by RsTSPO *in vivo*, could indirectly regulate the activity of the PpsR/AppA system and therefore indirectly regulate the expression of the target genes. Thus, RsTSPO may regulate oxygen and light responses in *R. sphaeroides* by modulating tetrapyrrole metabolism (Figure 1.4). Rat TSPO1 can functionally complement the absence of RsTSPO, suggesting functional conservation between the bacterial and animal TSPO. A signaling regulatory role was also assigned to *Sinorhizobium meliloti* TSPO (SmTSPO). *S. meliloti* is a plant symbiotic bacterium that is sensitive to nutrient deprivation.

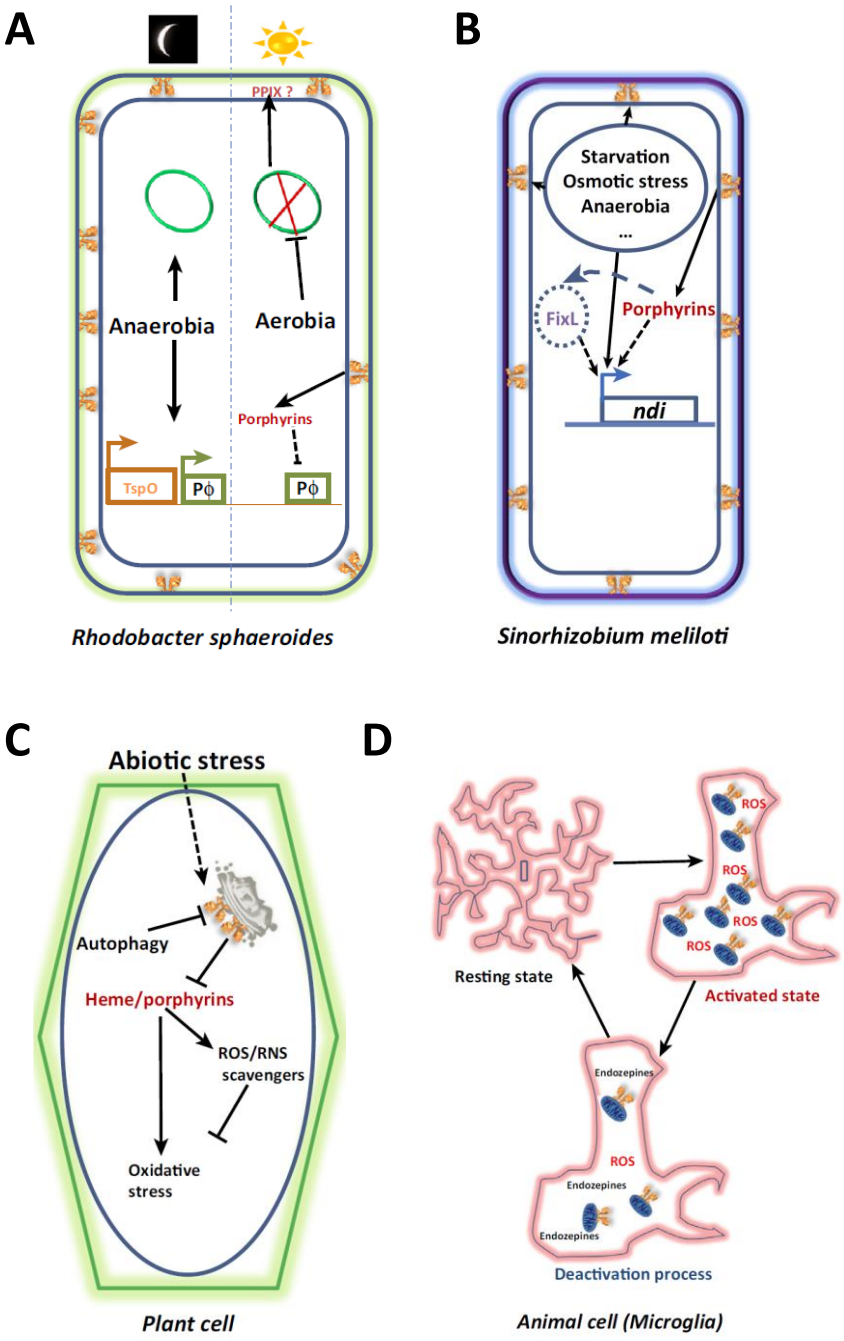

Figure 1.4. Regulation of oxidative stress signaling by Translocator proteins (TSPO) in different cell types. Arrows indicate positive regulatory steps and bars negative regulation, while the interrupted lines suggest hypothetical regulatory steps. **(A)** In the facultative photoheterotrophic bacterium *Rhodobacter sphaeroides*, TSPO (TspO)

expression is upregulated by low levels of oxygen and/or in the dark (left side) simultaneously with the induction of the photosynthetic genes (Pφ) and the biogenesis of the light-harvesting membrane compartment (green circle). TSPO (illustrated as the gold structures anchored to the outer cellular membrane) regulate the expression of the photosynthetic genes through an antirepressor/repressor system (not shown). Under aerobic conditions (right side), the metabolism of the cell shifts to respiration and the photosynthetic apparatuses are degraded, probably liberating unbound porphyrins, which are potential ligands of TSPO. TSPO regulate the levels of free porphyrins in the cell and indirectly inhibit the expression of the Pφ. **(B)** In *Sinorhizobium meliloti*, starvation and stressful conditions induce TSPO, which regulates the expression of the nutrient deprivation-induced (ndi) genes through modulation of the levels of free porphyrins. Under low-oxygen conditions, TSPO is epistatic to the oxygen-sensing two- component kinase FixL in the regulation of the ndi genes. **(C)** In higher plants, TSPO is induced by abiotic stresses and can be found mainly in the membrane of the Golgi apparatus in the cell. The level of TSPO in the cell is tightly regulated and downregulation of TSPO through the autophagy pathway requires heme binding; thus, TSPO was proposed to act as an unbound cytosolic heme scavenger (Vanhee et al., 2011). Consistent with this hypothesis, overexpressed TSPO is toxic to the cell and induced oxidative stress by interfering with the activity of hemoproteins involved in reactive oxygen/nitrogen species (ROS/RNS) scavenging. **(D)** Activated microglia accumulate ROS and upregulate the expression of mitochondrial TSPO. TSPO mediates negative regulation of microglial activation via the binding of secreted endozepines by astrocytes, contributing therefore to re-establishing the 'resting' state of the microglia and inflammation. Adapted from Batoko et al., 2015.

The nutrient deprivation-induced (*ndi*) loci A and B are induced by carbon and nitrogen deprivation and also by osmotic stress, oxygen limitation, and entry to the stationary growth phase (Davey and De Bruijn, 2000). Deletion of the gene encoding SmTSPO prevented *ndi* expression and the absence of SmTSPO could be complemented by RsTSPO expressed from a copy *in trans* (Davey and De Bruijn, 2000). It was suggested that SmTSPO interaction with heme or a biosynthetic precursor indirectly modulates *ndi* expression (Figure 1.4). SmTSPO is epistatic to FixL, an oxygen-sensing two-component kinase, in regulating *ndi* expression under low oxygen tension (Davey and De Bruijn, 2000).
Characterized plant TSPO so far were shown to be involved, at least in part, in redox homeostasis by modulating tetrapyrrole metabolism. In the moss *Physcomitrella patens*, one of the TSPO (PpTSPO1) was shown to control PPIX levels. PpTSPO1 is targeted to the mitochondria and induced by oxidative stress and its absence can trigger PPIX accumulation (Frank et al., 2007). In contrast to the moss *P. patens* with five TSPO genes, TSPO are mostly encoded by a single gene in higher plants. The *Arabidopsis thaliana* TSPO (AtTSPO) is transiently induced by abiotic stress and, when constitutively expressed, can alleviate induced porphyria in the

plant cell (Vanhee et al., 2011). AtTSPO is targeted to the early secretory pathway and was shown to bind PPIX *in vitro* and heme *in vitro* and *in vivo*. Heme binding required a histidine (H91) at the beginning of TM2 (Vanhee et al., 2011), within the TSPO's ligand-binding pocket. Expression of AtTSPO appears to be highly regulated. Overexpression of AtTSPO can be toxic, partly because the active downregulation of AtTSPO through a selective autophagic pathway also results in the scavenging of cytosolic free heme. It was shown that downregulation of AtTSPO was concomitant with decreased levels of free heme in plant cells subjected to osmotic stress (Vanhee et al., 2011). Heme oxygenases in the plant cell are plastidic enzymes. Reported findings suggest that AtTSPO is possibly involved in the transient clearance of excess cytosolic unbound heme and probably iron recycling during stress (Vanhee et al., 2011). Thus, AtTSPO might modulate redox homeostasis of the plant cells through heme/PPIX binding and scavenging during stress. However, as illustrated in Figure 1.4, continuous heme scavenging by constitutively expressed AtTSPO may be detrimental to the cell by interfering with the activity of hemoproteins, including those involved in ROS scavenging.

Microglia are immune cells (macrophages) and major sensors of homeostasis disruption within the CNS. Under normal physiological conditions, microglial cells are morphologically ramified (also known as 'resting' state). In the case of an insult or injury to the nervous system, the ramified microglial cells are transformed in a multistep process into an amoeboid motile form (also known as 'activated' state) (Figure 1.4). This activation process is triggered by as-yet-unknown signaling molecules (exogenous and/or endogenous). Activated microglial cells release cytokines that induce inflammation, such as tumor necrosis factor alpha (TNF-α) and interleukin 1β, as well as ROS and nitric oxide. Activated microglial cells are implicated in the protection of the nervous system and the etiology of neurodegenerative diseases (Wang et al., 2014). TSPO1 is upregulated during the microglial activation process (Bae et al., 2014; Wang et al., 2014), suggesting that TSPO1 is involved in inflammation management by these cells. For instance, it was shown in retinal inflammation and injury that TSPO1 upregulation in microglial cells paralleled the increase of endozepines in astrocytes and Müller cells.

The uptake of secreted endozepines by activated microglia regulates TSPO-dependent signaling in these cells and the reversible activation process (Bae et al., 2014). Endozepines, PK11195, and Ro5-4864 inhibit ROS production in activated microglia, suggesting a TSPO-dependent negative regulatory effect after the inflammatory response. TSPO-mediated signaling regulated features of microglial activation such as ROS production, TNF-α expression and secretion, and microglial proliferation (Bae et al., 2014; Wang et al., 2014). Consistently, immune response gene expression was affected in tspo1$^{-/-}$ tissues (Tu et al., 2014). The latest structural breakthroughs and findings in non-animal species are coming together to shed new light into the biological role of these enigmatic membrane proteins. Clarifying the physiological role of TSPO would require a thorough molecular understanding of the action of endogenous ligands on these proteins, including the likely evolutionary specificities. It seems that, from bacteria to humans, these ancient but nonessential proteins are upregulated during cellular stress to sense and regulate redox homeostasis through tetrapyrrole metabolism, with mechanistic variations from species to species (Figure 1.5). This may be the conserved and common physiological role of TSPO, in addition to species-specialized functions acquired through their evolution.

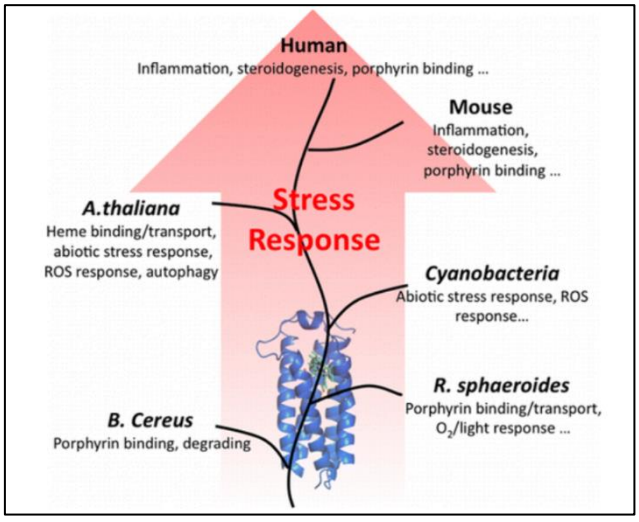

Figure 1.5. Induction of TSPO under various stress conditions appears to be a common theme for all the members of the TSPO family. Adapted from Li et al., 2016.

1.3. Higher plants TSPO and their peculiar N-terminal extension

Since their discovery in 1970s, TSPO proteins are extensively studied mostly in mammals to uncover their physiological role. Members of this family of proteins were uncharacterized in plants until recently (Corsi et al., 2004; Lindemann et al., 2004; Guillaumot et al., 2009; Vanhee et al., 2011). The best characterized plant TSPO is from *Arabidopsis thaliana* (AtTSPO). Higher plants TSPO are encoded mostly by a single gene, in contrast to the situation in Bryophyta. The genome of a representative moss, *Physcomitrella patens*, encodes five putative TSPO but only PpTSPO1 has been characterized to some extend (Frank et al., 2007).

In Arabidopsis, AtTSPO is encoded by a single intronless gene, At2g47770, whose expression is regulated by basic leucine zipper type (bZIP) transcription factors AREB1 (ABA–responsive element binding protein), AREB2 and ABF3 (ABA–responsive element binding protein) (Figure 1.6). The latter are involved in ABA-responsive element-dependent ABA signaling (Yoshida et al., 2010).

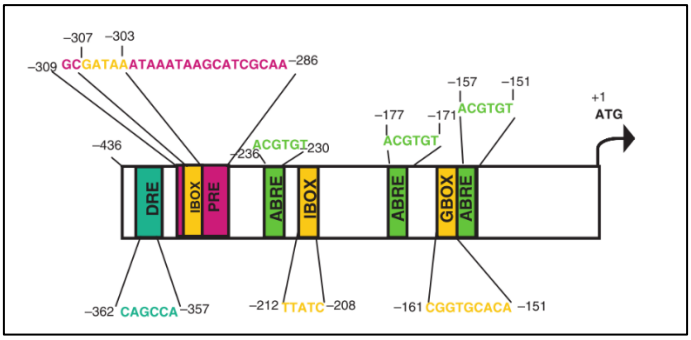

Figure 1.6. Schematic representation of a promoter region of AtTSPO. ATG (+1) represents the beginning of the At2g47770 (AtTSPO) exon. The shown exon-preceding motifs are drought-responsive element (DRE); abscisic acid-responsive element (ABRE), light-responsive elements IBOX and GBOX, and the plastid responsive element (PRE). Adapted from Guillaumot et al., 2009.

Under normal conditions, AtTSPO is constitutively expressed only in dehydrated tissues like pollen grains or seeds and to some extend in senescing leaves. However, the expression of AtTSPO in vegetative tissues is only triggered by abiotic stresses, such as ion deficiency, salt

and osmotic stress or exogenous abscisic acid treatment (Kreps et al., 2002; Seki et al., 2002; Zimmermann et al., 2004; Winter et al., 2007; Guillaumot et al., 2009; Hermans et al., 2010) (Figure 1.7). In contrast to

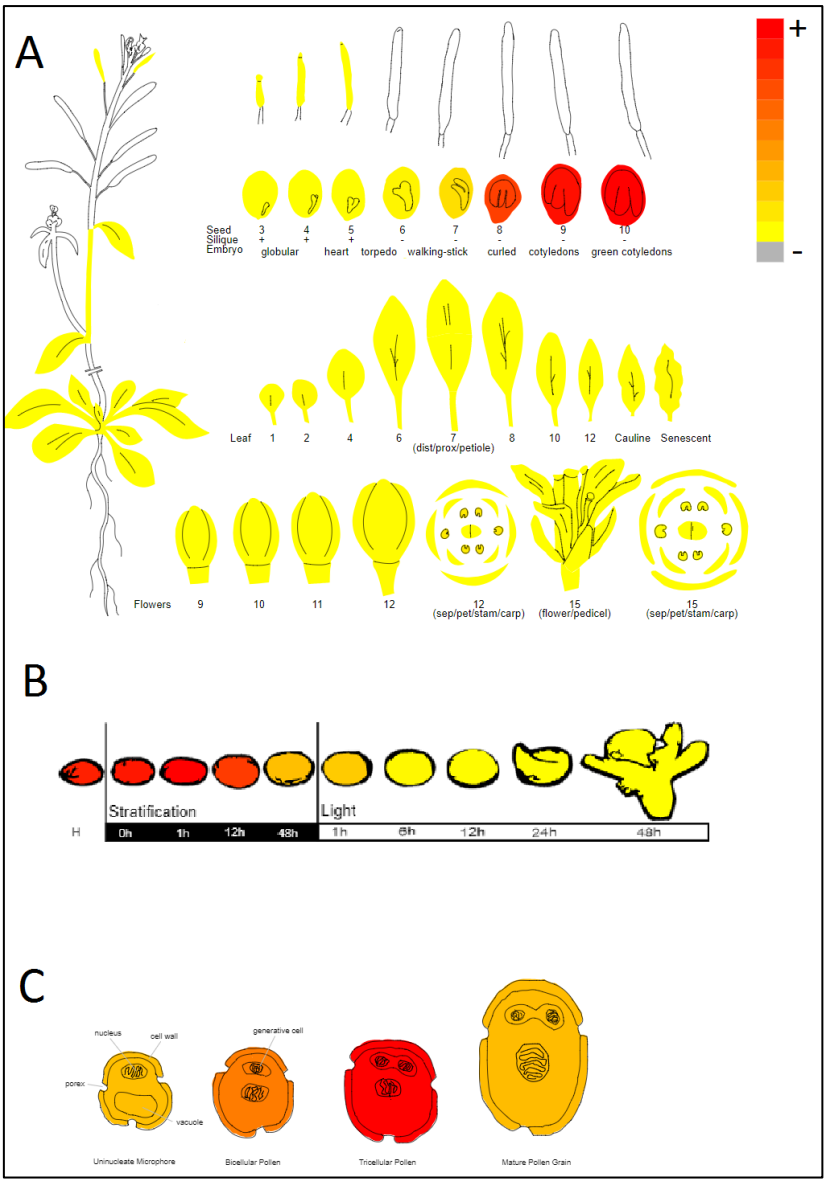

Figure 1.7. Expression profile of AtTSPO. The data were obtained from the BAR website (http://bar.utoronto.ca/eplant). Yellow indicates a poor expression of the genes while red indicates a high expression level of the gene. **(A)** No AtTSPO expression is observed in vegetative tissues under normal conditions but it is highly expressed in mature seeds. **(B)** AtTSPO expression decreases upon seed germination. **(C)** AtTSPO is expressed during pollen maturation.

mammalian TSPO1 protein, AtTSPO is an endoplasmic reticulum and Golgi-localized protein and Arabidopsis knockout and knockdown mutants are viable under normal growing conditions (Guillaumot et al., 2009).

AtTSPO is also post-translationally regulated. Induced or overexpressed AtTSPO is actively degraded through a selective autophagy pathway. Selective targeting of AtTSPO to the autophagy pathway requires heme and the ubiquitin-like autophagy-related 8 (ATG8) binding (Vanhee et al., 2011; Veljanovski and Batoko, 2014). Hemin affinity chromatography, pulldown assay, and *in vivo* labeling with the fluorescent heme analog palladium mesoprotoporphyrin IX showed that AtTSPO binds heme *in vitro* and *in vivo*. This binding requires the histidine residue at position 91 (H91) but not that at position 115 (H115), both residues being relatively well conserved in plant TSPO (Vanhee et al., 2011). ABA-dependent AtTSPO induction was accompanied by an increase in unbound heme levels in plant cells, and downregulation of AtTSPO coincided with the return to steady state levels of unbound heme, suggesting that a physiological consequence of active AtTSPO downregulation may be heme scavenging. Furthermore, overexpression of AtTSPO attenuated aminolevulinic acid-induced porphyria in the plant cells, supporting a role for AtTSPO in cytosolic porphyrin scavenging during abiotic stress (Vanhee et al., 2011).

More recent work from the host laboratory uncovered a regulatory interaction between AtTSPO and the plasma membrane aquaporin PIP2;7 (Hachez et al., 2014). Pull-down assays and fluorescence imaging approaches revealed that AtTSPO physically interacts with PIP2;7 at the endoplasmic reticulum and Golgi membranes *in planta*. Intriguingly, constitutive expression of fluorescently-tagged PIP2;7 in AtTSPO over-expressing transgenic lines resulted in patchy distribution of the fluorescence, reminiscent of the pattern of constitutively expressed YFP-AtTSPO in Arabidopsis (Figure 1.8). Mutational stabilization of AtTSPO such as expression of the mutant form containing a H91A substitution or pharmacological inhibition of the autophagy pathway affected concomitantly the detected levels of PIP2;7, suggesting that the complex containing both proteins is degraded through the autophagy.

Co-expression of AtTSPO and PIP2;7 resulted in decreased levels of PIP2;7 in the plasma membrane and abolished the membrane water permeability mediated by transgenic PIP2;7 (Hachez et al., 2014).

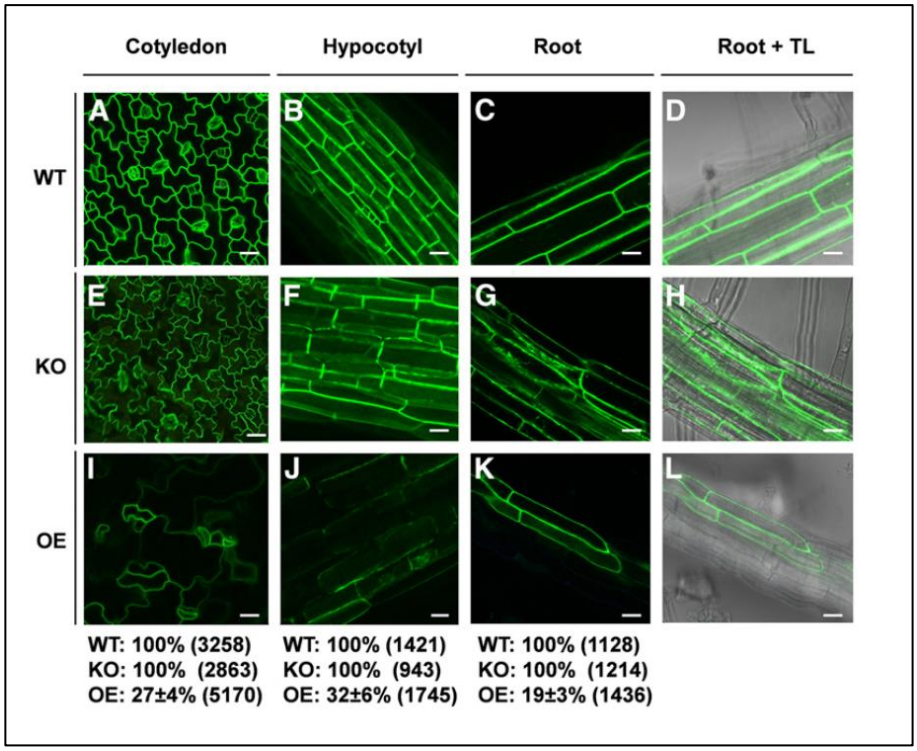

Figure 1.8. Overexpression of AtTSPO differentially regulates the expression of constitutively expressed YFP-PIP2;7. Representative confocal images of transgenic Arabidopsis seedlings overexpressing YFP-PIP2;7. Images of cotyledons ([A], [E] and [I]), hypocotyls ([B], [F] and [J]), and roots ([C], [G] and [K]) merged with transmitted light images ([D], [H] and [L]) from the wild-type background (WT), a knockout line for TSPO (KO), or a transgenic line overexpressing TSPO (OE). The percentage of cells (in parenthesis the total number of cells analyzed) showing detectable YFP-PIP2;7 fluorescence from random samples and acquired images using identical settings are given ± the SE of the mean for each organ. Bars = 20 μm. Adapted from Hachez et al., 2014.

TSPO proteins from all kingdoms of life possess a structurally conserved core TspO/MBR domain, but in addition they have evolved kingdom-specific structure of their termini. In animals, an extended C-terminal part contains a cholesterol binding domain (Li and Papadopoulos, 1998). Higher plants TSPO contain an N-terminus extension rich in charged amino acid residues. The primary sequence of this extension is poorly

conserved among plant proteins, but is characterized, as in AtTSPO, by a high frequency of charged residues (23/50 residues in AtTSPO, with a net charge of +3; Figure 1.9) (Guillaumot et al., 2009).

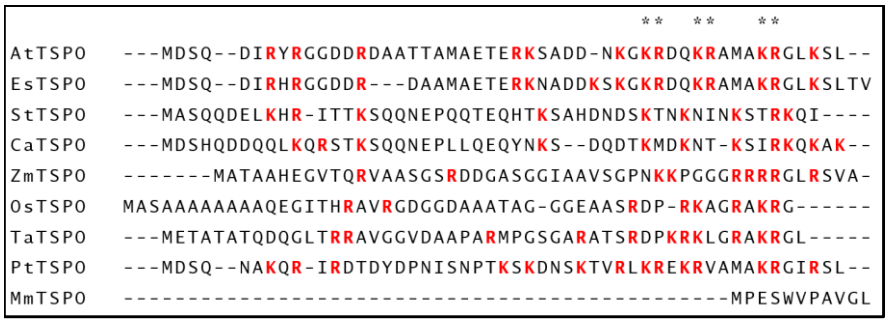

Figure 1.9. The higher plants-specific N-terminal extension of TSPO proteins is positively charged. ClustalW alignment of 50 N-terminal amino acids of higher plants (monocots and dicots) TSPO. At, *Arabidopsis thaliana*; Es, *Eutrema salsugineum*; St, *Solanum tuberosum*; Ca, *Capsicum annuum*; Zm, *Zea mays*; Os, *Oryza sativa*; Ta; *Triticum aestivum*; Pt; *Populus trichocarpa*. Positively charged amino acids were highlighted in red (neutral pH) and the conserved lysine/arginine residues close to the first transmembrane domain were indicated by asterisks. Mouse TSPO (Mm; *Mus musculus*) was added to illustrate no conservation of the elongated N-terminus nor the positively charged residues.

Chapter 2: Aquaporins and regulation of their activity

Aquaporins are protein channels that facilitate diffusion of water and other small solutes through biological membranes. Their importance in maintaining the plant water balance during various developmental stages is reflected by their large number encoded by plant genomes. However, water is not the only substrate of these channels since some of the plant aquaporins have been shown to transport ammonia, urea and glycerol, gases (carbon dioxide), as well as hydrogen peroxide and metalloids (reviewed in Chaumont and Tyerman, 2014). Therefore, aquaporins play also important roles in metabolism and signaling. In this chapter, we will briefly describe classification and structure of aquaporins followed by an overview on aquaporin regulation pathways including a regulatory mechanism involving Arabidopsis TSPO protein.

2.1. The discovery of aquaporins

Water is the most abundant substance in all living organism and is crucial to maintain life. For decades, the mechanism of water passage through phospholipid bilayers was thought to be ruled by simple diffusion. This mechanism requires a relatively high energy of activation (more than 10 kcal/mol). Hence, it stayed in opposition to observations of rapid bulk movement of water in some cell types (activation energy less than 5 kcal/mol), reminiscent of water diffusing freely without any barriers (Eggena, 1983). In addition, application of diuretic and antidiuretic compounds or blocking agents such as mercury salts provoked transient variations in membrane water permeability suggesting an existence of "hydrophilic pores" within the membranes (Stein and Danielli, 1956). However, the precise nature and role of these predicted water channels remained elusive for almost forty years.

Water channels were first characterized and named aquaporins in the early nineties, first in mammals (Preston et al., 1992) and then in plants (Maurel et al., 1993). They are membrane-anchored proteins with a molecular mass ranging from 21 to 34 kDa that form channels facilitating selective transport of water and other small solutes across biological phospholipid bilayers (Chaumont et al., 2005). Aquaporins are

found in almost every living organism, ranging from bacteria to metazoans and are a part of the Major Intrinsic Protein (MIP) superfamily. Arabidopsis and maize genomes contain more than 30 genes encoding aquaporins (Chaumont et al., 2001; Johanson et al., 2001) that cluster in different subfamilies according to their similarities in amino acid sequence. The phylogeny analysis of maize and Arabidopsis aquaporins allowed their classification into four subfamilies: Plasma Membrane Intrinsic Proteins (PIPs); Tonoplast Intrinsic Proteins (TIPs); Nodulin26-like Intrinsic Proteins (NIPs) and Small basic Intrinsic Proteins (SIPs) (Figure 2.1).

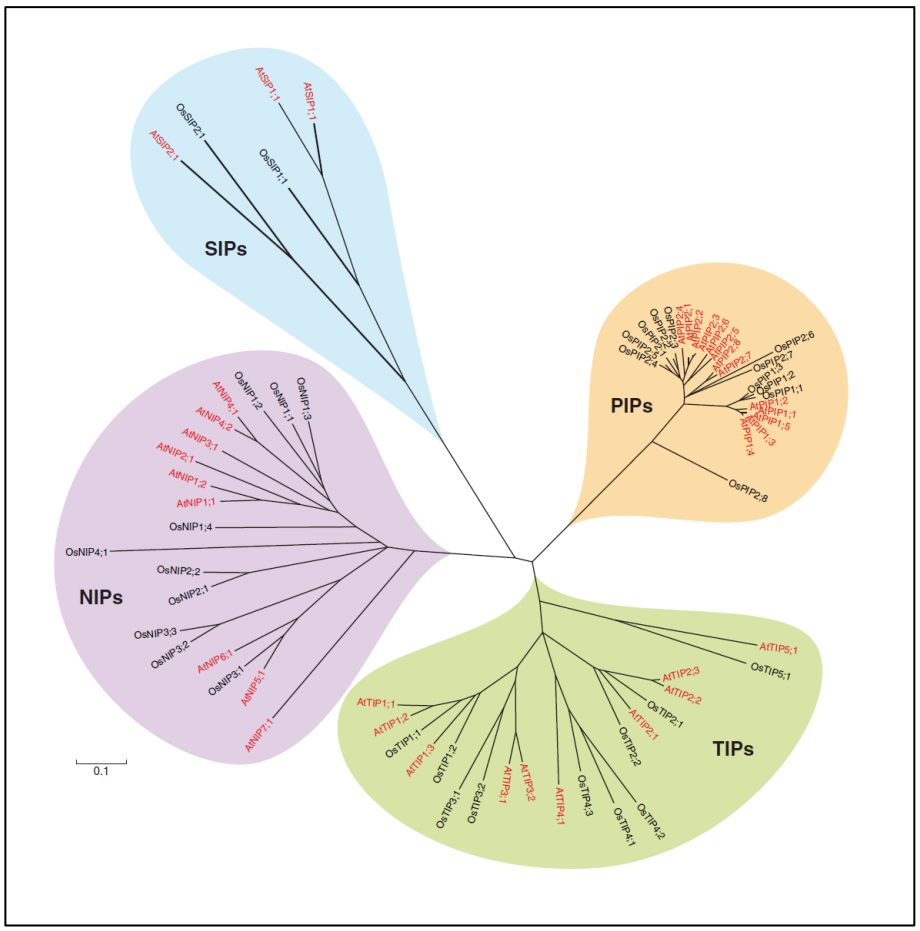

Figure 2.1. Phylogenetic tree of the Arabidopsis (red) and rice (black) aquaporin families. The diversity of aquaporins in plants reflects a high dynamics of their genomes. While some families were lost in certain plant clades (for instance XIPs in

monocotyledons), genomic rearrangements have caused the expansion of the plant water channel family. These events have occurred during different stages of plant evolution. The division of PIPs into two subfamilies and TIPs into five subfamilies probably occurred early since members of these subfamilies are present in all higher plants. Adapted from Maurel et al., 2015.

Additional aquaporins were also characterized and subsequently categorized into the following subfamilies: GlpF-like Intrinsic Proteins (GIPs), Hybrid Intrinsic Proteins (HIPs) and Uncategorized Intrinsic Proteins (XIPs) (Danielson and Johanson, 2008).

2.2. Molecular structure of aquaporins

The first structurally characterized aquaporin at the atomic scale was AQP1 from mammals (Murata et al., 2000; Sui et al., 2001). Few years later, the first structure of a plant aquaporin, SoPIP2;1 from spinach, was published (Törnroth-Horsefield et al., 2006) (Figure 2.2). Topologically, aquaporins are comprised of six transmembrane domains with their C- and N-terminal ends facing the cytoplasm. The size of each monomer is 60 and 40 Angström (Å) in length and width, respectively (Sui et al., 2001).

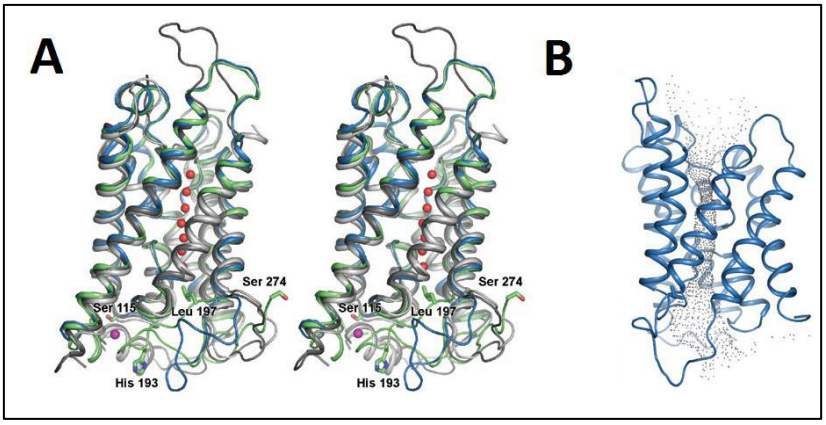

Figure 2.2. The first three-dimensional structure of a plant aquaporin. (A) Models of spinach SoPIP2;1 aquaporin in its open (blue) and closed (green) conformations overlaid on the model of mammalian AQP0 (light grey) and AQP1 (grey). **(B)** Structure of SoPIP2;1 which is conserved in all aquaporins. Adapted from Törnroth-Horsefield et al., 2006.

Aquaporins interact and assemble as tetramers where one monomer interacts physically with two neighboring monomers (Figure 2.3). Tetramers do not structure a common channel but each monomer within the complex forms a single transmembrane water pore (Murata et al., 2000; Bienert et al., 2012).

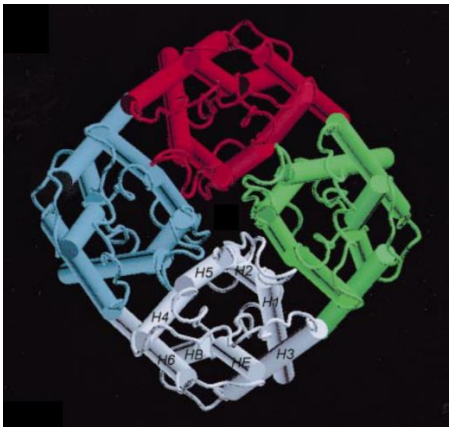

Figure 2.3. Cylinder model of assembled AQP1 tetramer. End-on view from the extracellular surface. Adapted from Murata et al., 2000.

2.3. Plasma membrane Intrinsic Proteins (PIPs)

As mentioned earlier, aquaporins are phylogenetically categorized into several families, yet we will only focus on PIP family, since the aquaporin of our interest is the Arabidopsis PIP2;7 (see below).

PIP comprises the largest subfamily of aquaporins with a molecular weight of around 30 kDa. Plant PIP aquaporins are divided into two groups, PIP1 and PIP2. In general, PIP1s and PIP2s are expressed simultaneously in the same plant cells, although some isoforms are organ- or tissue-specific or they are expressed during different developmental stages or under different environmental conditions (Hachez et al., 2006, 2008). PIP2s, in contrast to PIP1s exhibit high water transport activity.

When expressed alone, PIP2s in plants are targeted to the plasma membrane while PIP1s are retained in the ER. However, PIP aquaporins naturally assemble as homo- and heterotetramers (Fotiadis et al., 2001; Fetter et al., 2004; Zelazny et al., 2007; Berny et al., 2016). The interaction

between two isoforms results in the localization of the complex to the plasma membrane. The water transport mediated by the tetramers is increased as compared to PIP2s expressed alone, as explained by the synergistic effect (Fetter et al., 2004; Temmei et al., 2005; Zelazny et al., 2007; Vandeleur et al., 2009; Bellati et al., 2010; Chevalier et al., 2014; Yaneff et al., 2015; Berny et al., 2016).

2.4. Regulation of aquaporins activity

Recent studies showed that aquaporins as not only water homeostasis regulators but also important actors in metabolic, nutrient and signaling roles (reviewed in Chaumont and Tyerman, 2014). Such broad range of functions imposes that these membrane channels must be precisely regulated by the plant cell at multiple levels. In this section, we briefly describe the characterized aquaporin regulatory pathways including the recently uncovered novel regulatory mechanism involving the Arabidopsis multistress-induced membrane protein TSPO.

2.4.1. Aquaporin expression

Aquaporin genes are expressed under varying physiological conditions in a tissue- and organ-specific manner. Studies on expression have provided evidence for involvement of PIPs in controlling the radial transcellular water transport and cell osmoregulation (Luu and Maurel, 2005; Hachez et al., 2006; Prado and Maurel, 2013). In general, *PIP* expression is predominant in roots but some isoforms are partially or even exclusively expressed in leaves (Sakurai et al., 2005; Prado et al., 2013). Interestingly, higher levels of PIP mRNA and/or proteins were measured during the day as compared to night. This suggests a regulation by circadian rhythm and a correlation with the diurnal control of transpiration (Moshelion et al., 2002; Lopez et al., 2003; Cochard et al., 2006; Vandeleur et al., 2009; Hachez et al., 2012).

2.4.2. Post-translational regulation of aquaporins

The time to respond to environmental stimuli at the cellular/tissue/organ level requires varying mechanisms of aquaporin regulation. Responses to long-term cues generally could include the

regulation of aquaporin expression and anatomical plant modifications while the need for rapid responses to short-term adversities within minutes are rather mediated by post-translational modifications (Horie et al., 2012; Vandeleur et al., 2014). Many post-translational modifications of aquaporins were shown to regulate channel activity as well as abundance in the destination membrane (Chaumont and Tyerman, 2014; Maurel et al., 2015). These modifications encompass phosphorylation, methylation, protonation, ubiquitination, formation of disulfide bridge and heteromerization, and regulate aquaporin trafficking and gating (Chaumont and Tyerman, 2014; Kapilan et al., 2018).

2.4.2.1. Aquaporin gating

The gating of aquaporins involves closure and opening of the channels, a mechanism that is known to be regulated by phosphorylation, protonation and binding of divalent cations (Aroca et al., 2005; Verdoucq et al., 2008).

An aquaporin gating mechanism has been put forward using dynamic modeling based on the solved structure of spinach aquaporin in its open and closed form (Hedfalk et al., 2006; Törnroth-Horsefield et al., 2006). The closed form is stabilized by the interaction network involving divalent cation binding site (most likely Ca^{2+} *in vivo*) (Törnroth-Horsefield et al., 2006; Nyblom et al., 2009). Phosphorylation of three potential sites (serine residues at positions 115, 188 and 274) probably leads to the channel opening while the protonation of histidine 193 renders the closed conformation even tighter (Törnroth-Horsefield et al., 2006; Nyblom et al., 2009; Frick et al., 2013).

2.4.2.2. Aquaporin trafficking

Research devoted to regulation of plant aquaporin activity by trafficking involved mostly members of PIP family (Luu and Maurel, 2005; Hachez et al., 2013). Recently, it was demonstrated that the transmembrane domain 3 (TM3) of PIP1;2 or PIP2;5 from *Zea mays* discriminates between ER and plasma membrane localization, respectively, and that a highly conserved LxxxA motif in the TM3 of PIP2;5 regulates its export from the ER (Chevalier et al., 2014).

PIP trafficking is also regulated by syntaxins (Hachez et al., 2014). PIP aquaporins are inserted into the plasma membrane through a physical interaction with a syntaxin of plants 121 (SYP121). Moreover, plant cells expressing PIP2;7 with a non-functional SYP121 showed reduced water permeability at the plasma membrane (Hachez et al., 2014).

2.4.2.3. AtTSPO-mediated negative regulation of PIP2;7

It was demonstrated in the host laboratory that when coexpressed, AtTSPO can downregulate the level of PIP2;7 in the plasma membrane (Hachez et al., 2014). AtTSPO was shown to physically interact with PIP2;7 within membranes of the early secretory pathway, resulting in targeting of the heterocomplex AtTSPO-PIP2;7 to the vacuole for degradation through the autophagy pathway (Figure 2.4). This interesting observation suggest that during osmotic stress for example, the transient expression of AtTSPO reduces the abundance of PIP2;7 at the plasma membrane to temporally protect the plant cell from water deficit. However, the molecular mechanisms of this interaction conducive of physiological consequences are not yet clear.

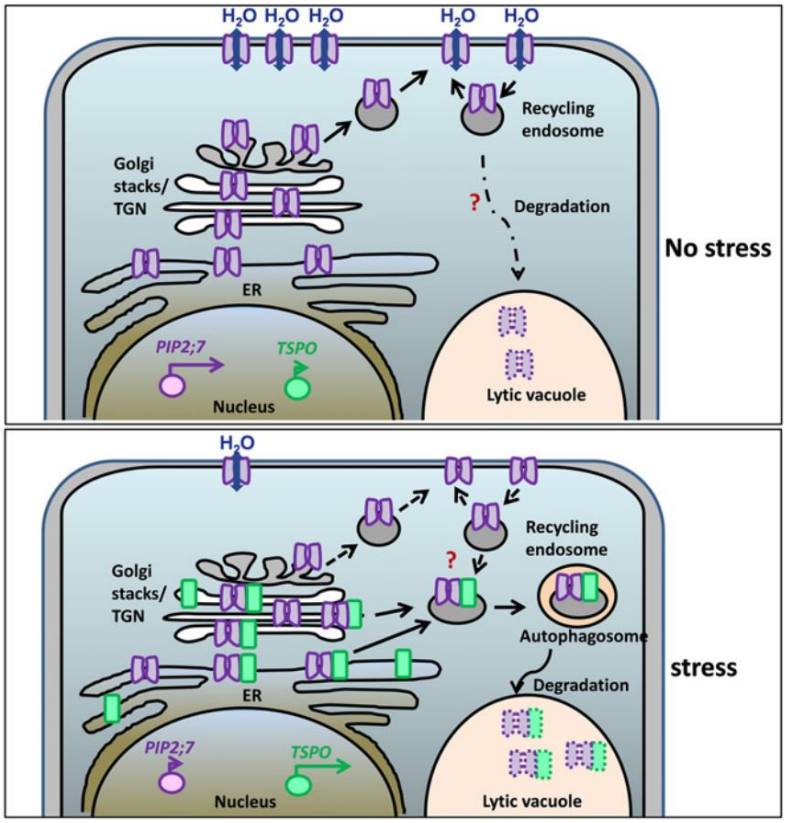

Figure 2.4. Model of abiotic stress-induced AtTSPO-mediated downregulation of PIP2;7. Under normal conditions (upper panel) AtTSPO level is undetectable and PIP2;7 is targeted to the plasma membrane to mediate the water transport. The long-term regulation of PIP2;7 could involve recycling through endosomes and degradation in vacuole. However, when water-related stress sets in (bottom panel), increased ABA levels upregulate expression of AtTSPO that is targeted to the ER/Golgi. Aquaporin abundance at the plasma membrane has to be decreased to prevent cell and plant from water loss. For simultaneous and efficient cleansing of PIP2;7 from the plasma- and internal membranes, the endosomal pathway could be accompanied by the AtTSPO-mediated titration of PIP2;7 molecules *en route* to the plasma membrane and subsequent degradation of the complex through the autophagic pathway. Adapted from Hachez et al., 2014.

Different mechanism exist to regulate the activity and number of aquaporins at the plasma membrane (as described in this chapter). However, a transient titration of aquaporin molecules *en route* to the peripheries of the cell by AtTSPO and subsequent degradation through the autophagy pathway is novel in plant and could contribute to a rapid, albeit transient, reduction of water movement through the plasma membrane.

Chapter 3: Plant phospholipids

Lipids are a ubiquitous and highly diverse group of compounds that plays three major roles in the living cells. First, as anhydrous lipid droplets composed of triacylglycerols (TAG) and sterol esters, they serve as efficient energy storage because of their relatively reduced state. Second, polar lipids consisting of a hydrophobic and a hydrophilic region form the matrix of biological membranes. The tendency of hydrophobic moieties to self-associate and the propensity of the hydrophilic parts to interact with each other and with water molecules is the physical principle of the spontaneous formation of membranes (van Meer et al., 2008). Finally, lipids act as first or second messengers in cellular processes of signal recognition and transduction. In this chapter, we will present a short literature review on phospholipids. We will focus on phosphoinositides, a group of minor signaling molecules, and the mechanisms of protein-phosphoinositide interactions and their relevance in plant development.

3.1. Phospholipids: structure and classification

Phospholipids (Figure 3.1) are ubiquitous in nature and comprise the most abundant group of lipids in cellular membranes. They are composed of two major regions: a hydrophilic region, commonly called a "head group" and a hydrophobic tail made of fatty acids, both regions being attached to a glycerol backbone (Nakamura, 2017).

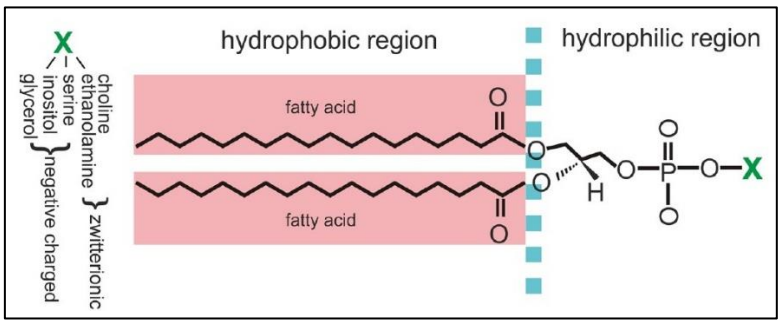

Figure 3.1. Schematic representation of a glycerophospholipid. Within the hydrophilic region the polar head may be zwitterionic (in case the phosphate group is linked to choline or ethanolamine group) or negatively charged (when phosphate is linked to serine, inositol or glycerol). Adapted from Zhao and Lappalainen, 2012.

The broad class of phospholipids may be further subdivided into several lower classes (Table 3.1). The primary classification based on the composition of the hydrophilic region and the secondary classification based on the hydrophobic chain composition: assembly of two acyl tails of variable length (mainly 16- or 18-carbon) and number and position of double bonds. For instance, PA (18:1(9Z)/18:1(9Z)) is an 18-carbon acyl chain phosphatidic acid with 1 double bound at position 9 in both acyl chains.

Table 3.1. Main classes of phospholipids and their abbreviations. Highlighted by grey rectangle is the class whose presence in plants has not been reported to date (Simon et al., 2014). Adapted from Fahy et al., 2011.

Class	Abbreviation
Phosphatidylcholines	PC
Phosphatidylethanolamines	PE
Phosphatidylserines	PS
Phosphatidylglycerols	PG
Phosphatidic acids	PA
Phosphatidylinositols	PI
Phosphatidylinositol phosphates	PIP
Phosphatidylinositol bis-phosphates	PIP2
Phosphatidylinositol tris-phosphates	PIP3
Cardiolipins	CL
Phosphatidylglycerol phosphates	PGP
Glyceropyrophosphates	PPA
CDP-glycerols	CDP-DG
Glycosylglycerophospholipids	[glycan]-GP
Glycerophosphoinositolglycans	[glycan]-PI
Glycerophosphonocholines	PnC
Glycerophosphonoethanolamines	PnE

3.2. Phosphoinositides: landmarks of cellular membranes and purely signaling phospholipids

The complex interplay of cellular processes at and within the membranes is partially regulated by signaling phospholipids. They are found only in low amounts in membranes and are generated transiently in a dynamic manner. One excellent example for such regulatory lipids are phosphoinositides. The term phosphoinositides (PIs) describes seven types of phosphorylated phosphatidylinositol. They are minor constituents of cell membranes (less than 1% of total phospholipids) (Vermeer et al., 2009; Munnik and Nielsen, 2011). Structurally, PIs are composed of a glycerol backbone esterified in positions sn-1 and sn-2 by two fatty acid chains and linked by a phosphate group in position sn-3 to an inositol ring (Payrastre et al., 2001).

The biosynthesis of PIs in plants is similar to the situation in other eukaryotes. All PIs are derived from phosphatidylinositol (Figure 3.2) by phosphorylation of different positions of the inositol head group (Munnik and Nielsen, 2011). In plants, only five out of seven known PIs have been found (Heilmann and Heilmann, 2015). They include three monophosphorylated (PI3P, PI4P and PI5P) and two bisphosphorylated isomers ($PI(3,5)P_2$ and $PI(4,5)P_2$). The presence of $PI(3,4)P_2$ and $PI(3,4,5)P_3$ in plants was not yet experimentally documented .

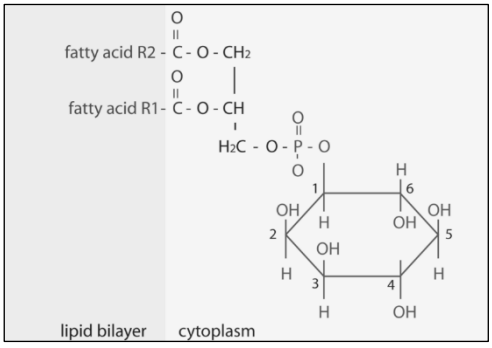

Figure 3.2. The chemical structure of phosphatidylinositol. Adapted from De Craene et al., 2017.

The phosphorylation of phosphatidylinositol (PI) to PI monophosphates, such as PI3P or PI4P is catalyzed by PI kinases (Figure 3.3). The genome

of Arabidopsis encodes only one PI 3-kinase (AtVPS34) (Munnik and Testerink, 2009). AtVPS34 is an active PI 3-kinase (Welters et al., 1994) albeit up to date no in-depth study has been reported on its substrate specificity. AtVPS34 shares the highest sequence similarity with mammalian type III PI 3-kinases phosphorylating the 3-position of the PI inositol ring, but not that of PI-monophosphates or PI-bisphosphates (Heilmann, 2016b). PI3P plays housekeeping functions in plants since the knock-out of the AtVPS34 gene results in gametophytic lethality (Lee et al., 2008). PI3K activity is inhibited by wortmannin or related drugs (Vermeer et al., 2006). Wortmannin treatment led to the understanding of PI3P contribution in numerous plant events including autophagy, endosomal trafficking, defense-related ROS production, endocytosis, and ABA-dependent guard cell signaling (Vermeer et al., 2006; Ischebeck et al., 2010).

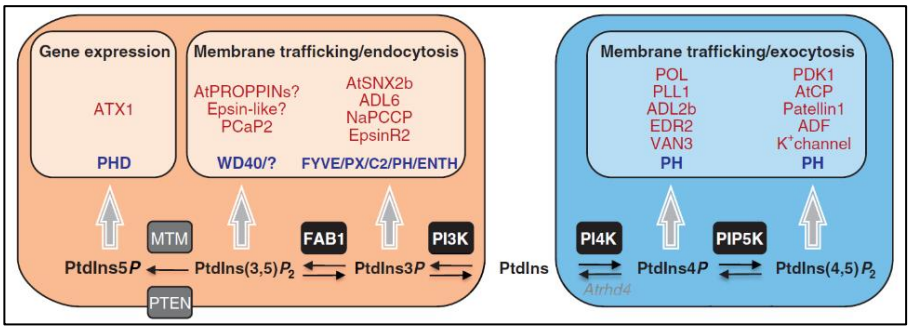

Figure 3.3. Biosynthesis of PIs and their role in cell signaling. PIs are generated from the structural lipid, phosphatidylinositol (PtdIns). Five isomers can be formed through phosphorylation and dephosphorylation of the inositol headgroup, at the D-3, D-4, or D-5 position, via specific kinases (black boxes) and phosphatases (grey boxes). Each lipid exhibits unique identities in structure and function for signaling. Described protein targets for individual lipids are indicated in red. Specific lipid-binding domains are indicated in blue. Adapted from Munnik and Nielsen, 2011.

Cytosolic effectors bind PI3P by either PX (Phox Homology) or FYVE (Fab1/YOTB/Vac1/EEA1) domains, and proteins containing these domains have been also characterized in Arabidopsis (Jensen et al., 2001; van Leeuwen et al., 2004; Wywial and Singh, 2010). Fluorescently tagged-FYVE domains used as PI3P biosensors localize mainly to the late endosomes and multivesicular bodies (Vermeer et al., 2006; Simon et al.,

2014). A sorting nexin involved in endosome to vacuole trafficking, AtSNX2b, was demonstrated to bind PI3P via its conserved PX domain (Phan et al., 2008). Other effector proteins regulating vesicular trafficking and binding PI3P by distinct lipid-binding domains include NaPCCP (C2 domain), ADL6 (PH domain) and EpsnR2 (ENTH domain (epsin N-terminal homology)) (Lee et al., 2002; Lee et al., 2007; Lee et al., 2008) (Figure 3.3).

PI3P is also fundamental for autophagy. Autophagy is a pathway for degradation of cellular macromolecules and recycling of unwanted or damaged cell components during stress conditions or specific developmental stages. The fundamental aspect of autophagy is the formation of double-membrane structures called autophagosomes surrounding the material destined for vacuolar degradation (Liu and Bassham, 2012). Genetic and biochemical studies in yeast resulted in the partial characterization of the components of the autophagy machinery, and one of these fundamental constituents has been identified as type III PI 3-kinase complex (Suzuki et al., 2013). The catalytic subunit of this complex, VPS34, is essential for the canonical autophagy (Funderburk et al., 2010). During initiation of the autophagosome formation in animals and yeast, ATG14 targets the PI 3-kinase complex to ER/mitochondria contact sites for localized synthesis of PI3P (Hamasaki et al., 2013). However, ATG14 is absent in plants, thus a corresponding component should exist to regulate the localization of the PI 3-kinase complex (Batoko et al., 2017). ATG1 activates the components of the PI 3-kinase complex through phosphorylation and the active VPS34 generates PI3P at the phagophore (Jao et al., 2013; Russell et al., 2013; Egan et al., 2015; Park et al., 2016). Enrichment in this specific lipid triggers the recruitment of PI3P-binding autophagy components, for instance ATG2 and ATG18 (Batoko et al., 2017).

PI4P is the major plant phosphoinositide (~80% of total PIs) (Munnik and Vermeer, 2010). It is synthesized through phosphorylation of PI at the 4-position of inositol, a reaction catalyzed by a family of PI 4-kinases (PI4K). In contrast to PI3K, there exist four active isoforms of PI 4-kinases in Arabidopsis (PI4Kα1, PI4Kα2, PI4Kβ1 and PI4Kβ2), which also resemble mammalian homologs. An additional γ-subfamily of eight genes

encode type II PI4-kinases but most likely they represent a group of inactive PI 4-kinases (Galvão et al., 2008). PI4P in plants plays a central role in polarized membrane trafficking during tip-growth (Preuss et al., 2006; Vermeer et al., 2009). This polarized pattern of cell expansion is characteristic for pollen tubes and root hairs growth and involves delivery of secretory vesicles to an apical plasma membrane domain. Subcellular localization of PI4P using a cognate biosensor showed that the PI4P localized to an apical plasma membrane domain but also is dynamically present in trans-Golgi network and recycling endosomes (Thole et al., 2008; Vermeer et al., 2009; Simon et al., 2014). PI4P also regulates polarity during cell differentiation in other developmental processes. During cell division, PI4P localizes at the cell plate (Vermeer et al., 2009) and the double knock-out plants for kinases pi4kb1/pi4kb2 are division-defective (Kang et al., 2011).

Although PI5P has been detected in plants (Meijer et al., 2001), the biosynthesis pathway of this minor phosphoinositide remains unclear. It is likely that PI5P is generated by dephosphorylation of a PI-bisphosphate precursor (Figure 3.3). In Arabidopsis, there are likely 2 types of PI-3 phosphatases: PTEN (phosphatase and tensin homolog deleted on chromosome ten; 3 genes) and MTM (myotubularin-type phosphatase; 2 genes). Both types exhibit phosphatase activity towards $PI(3,5)P_2$ (Ding et al., 2009). AtPTEN1 is exclusively expressed in pollen grains and has a key role for pollen tube development. *AtPTEN1* knock-out plants are lethal and RNAi suppression causes cell death after mitosis (Gupta, 2002).

PI3P and PI4P are substrates for PI3P 5-kinases and PI4P 5-kinases, respectively, yielding $PI(3,5)P_2$ and $PI(4,5)P_2$. Four isoforms of PI3P 5-kinases are encoded in Arabidopsis that are homologous to the Fab1 (Forms Aploid and Binucleate cells) kinase from the yeast *S. cerevisiae* (Mueller-Roeber and Pical, 2002). To date, only one Fab1 enzyme has been shown to catalyze the transformation of PI3P to $PI(3,5)P_2$ *in vitro* (Bak et al., 2013). In addition, there exist a strong, albeit indirect evidence that Fab1 enzymes also generate $PI(3,5)P_2$ *in vivo* (Hirano et al., 2015).

The most abundant group of phosphoinositide kinases in Arabidopsis is PI4P 5-kinases. They are represented by eleven isoforms (PIP5K1–11),

categorized in two subfamilies (Mueller-Roeber and Pical, 2002). Isoforms PIP5K10 and PIP5K11 belong to the subfamily A and are structurally similar to animal PI4P 5-kinases. Subfamily B gathers all the remaining nine isoform (PIP5K1-PIP5K9). They contain additional N-terminal domains (NT), a membrane occupation and recognition nexus repeat domain (MORN) and a variable linker domain (Lin) (Heilmann, 2016b). Enzymes of both subfamilies catalyze the *in vitro* conversion of PI4P to $PI(4,5)P_2$, but also to a lesser degree, PI3P to $PI(3,5)P_2$ (Stenzel et al., 2008; Ischebeck et al., 2008, 2011).

$PI(4,5)P_2$ is localized mainly to the plasma membrane (Simon et al., 2014), where it fulfills a broad range of functions such as anchoring signaling and membrane trafficking proteins (Figure 3.4). $PI(4,5)P_2$ can also be cleaved by phospholipase C (PLC) into the soluble inositol 1,4,5-trisphosphate (IP_3) and the membrane-bound diacylglycerol (DAG) (McLaughlin and Murray, 2005; Suh et al., 2006). IP_3 induces the release of calcium from intracellular stores in animal cells (Berridge, 1993). However, no similar IP_3 receptor mediating calcium release has been described in land plants sequenced so far (Krinke et al., 2007). It is likely that IP_3 acts as a precursor for inositol polyphosphates, such as inositol 1,3,4,5-tetrakisphosphate (IP_4), inositol 1,3,4,5,6-pentakisphosphate (IP_5) and inositol 1,2,3,4,5,6-hexakisphosphate (IP_6) that could play a phytohormone receptor function (Heilmann and Heilmann, 2013). On the other hand, DAG in plants is rapidly phosphorylated to phosphatidic acid (PA) that has a signaling function (Figure 3.4). Increased levels of PA were observed during osmotic and drought stresses, phytohormone treatment, wounding and pathogen attack (Wang et al., 2000; Testerink and Munnik, 2005; Bargmann et al., 2009).

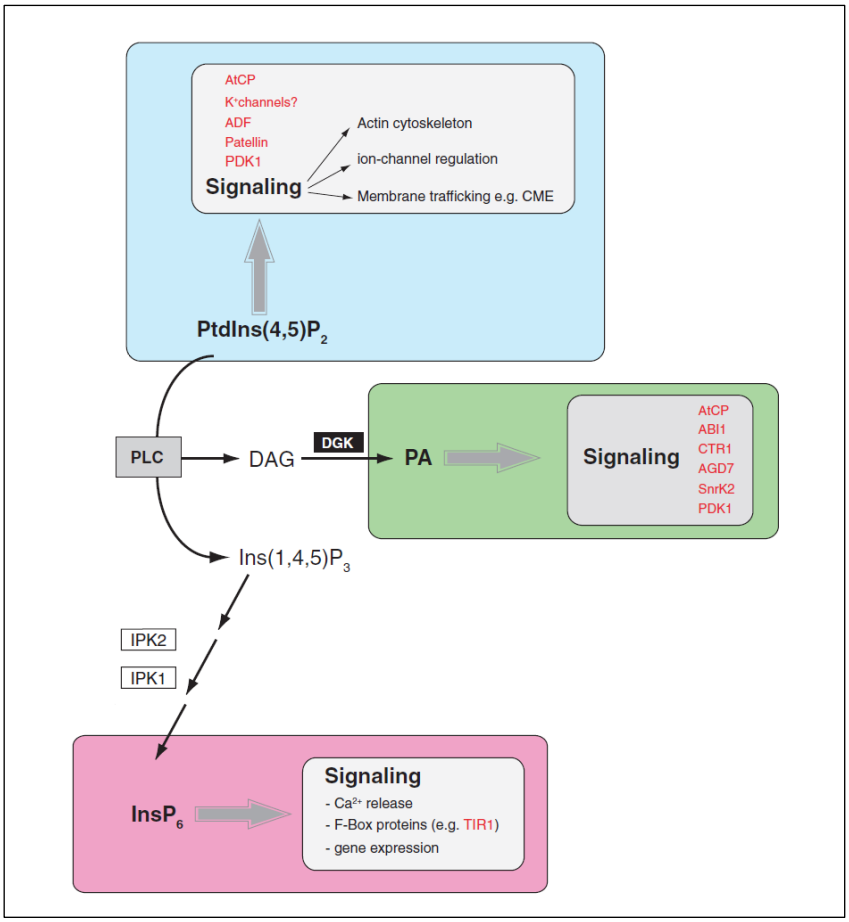

Figure 3.4. The PI(4,5)P$_2$-dependent signaling pathway. Hydrolysis of PI(4,5)P$_2$ by phospholipase C (PLC) generates IP$_3$, which can be stepwise phosphorylated into IP$_6$ by the two inositolpolyphosphate multikinases, IPK2 and IPK1. Diacylglycerol (DAG) is rapidly converted into phosphatidic acid (PA) which acts as a signaling molecule. For more details, see text. Adapted from Munnik and Vermeer, 2010.

PI(4,5)P$_2$ also regulates plasma membrane channels (Table 3.2). In animals, the best characterized channels are the inward-rectifier potassium channels (Kir) and they are activated by PI(4,5)P$_2$ (Hilgemann et al., 2001). Also, several voltage-gated potassium channels are PI(4,5)P$_2$-sensitive. In contrast, PI(4,5)P$_2$ inhibits the TRPV1 (Transient Receptor Potential Vanilloid 1) capsaicin receptor channel of the pain and heat pathway (Chuang et al., 2001). Many more channels in animal cells seem to be phosphoinositide-dependent. In plants, the phosphoinositide-dependent channel regulation is only characterized to some extend.

$PI(4,5)P_2$ enhanced the activity of the Arabidopsis SKOR channel (Stelar K^+ Outward Rectifying) and the K^+-influx channel KAT1, and the tomato K^+-influx channel LKT1 expressed in *Xenopus* oocytes (Liu et al., 2005). Also, accumulation of $PI(4,5)P_2$ in guard cells inhibited anion-release channels promoting cell swelling and stomatal opening (Lee et al., 2007). In contrast, a cleavage product of $PI(4,5)P_2$ diffuses into the cytosol where it releases calcium from an intracellular storages by activating a ligand-gated Ca^{2+} channel. It is still unknown by what molecular mechanism phosphoinositides influence Ca^{2+} channel, but a likely candidate is not IP_3 but IP_6 (Figure 3.4).

Table 3.2. Regulation of ion channels by $PI(4,5)P_2$ in animals. The word "activation" refers broadly to any kind of enhancement of channel activity. Adapted from Suh and Hille, 2005.

Channel	Effects
Inward-rectifier K^+channels	
Kir1 (ROMK)	Activation
Kir2	Activation
Kir3 (GIRK)	Activation
Kir6 (K_{ATP})	Activation
Voltage-gated K^+channels	
Kv	Removal of inactivation
KCNQ	Activation
HERG	Activation, slowing inactivation
Two-P domain K^+channels	
TASK1	Activation
TASK3	Activation
TREK1	Activation, more sensitive to mechanogating, pH_i
TRAAK	Activation dependent on mechanical stimulation
Voltage-gated Ca^{2+}channels	
$Ca_v2.1$ (P/Q-type)	Slow rundown, shift of voltage dependence
$Ca_v2.2$ (N-type)	Stabilization and activation
Sensory transduction channels	
TRPV1	Inhibition, less sensitive to H^+, capsaicin, heat
TRPM5	Slow desensitization, more bitter, sweet tastes
TRPM7	Direct activation
TRPM8	Activation, more sensitive to cold
Transduction channels in hair cell (TRPA1)	Current activation, rapid adaptation
CNG (cGMP-gated)	Inhibition, enhancement of transducin–phosphodiesterase coupling
Na^+channel	
ENaC	Direct binding to βENaC and activation
Cl^-channel	
CFTR	Activation (– phosphorylation) Inhibition (+ phosphorylation)
Ca^{2+}-release channels	
$Ins(1,4,5)P_3$ receptor	Inhibition
Ryanodine receptor	Activation

Elevated levels of $PI(4,5)P_2$ in plants were reported in response to salt-induced hyperosmotic stress (Zonia and Munnik, 2004). In particular,

genetic and biochemical studies showed that plant response to white light illumination involves an increase of $PI(4,5)P_2$ in the plasma membrane of guard cells inducing stomatal opening, hence enhancing evapotranspiration. The increased $PI(4,5)P_2$ in the plasma membrane of stomatal guard cells was responsible of anion channels inhibition (Lee et al., 2007).

Interestingly, $PI(4,5)P_2$ is also a key regulator of autophagy, as demonstrated in mammalian cells (Tan et al., 2016). Autophagosome has the kinase that generates $PI(4,5)P_2$ and the autophagy regulator ATG14 interacts with both the enzyme and its product during autophagosome initiation. $PI(4,5)P_2$ binding to ATG14 regulates ATG14 interaction with VPS34 and Beclin 1/ATG6, a protein complex catalysing the production of PI3P at the autophagosome initiation site, as described earlier in this thesis (Tan et al., 2016).

3.2.1. Protein-phosphoinositide interactions in plant development

In recent years, PIs have emerged as key regulators of plant development, since many severe plant phenotypes were reported when PI metabolism was altered. They encompass lethality, reduced stomatal closure, impaired thermotolerance, vascular, pollen, root and general growth defects, and many others (reviewed in Heilmann, 2016a). However, because a detailed information on the molecular PIs targets in plants is still limited, the interpretation of reported phenotypes remains a challenge.

PIs act as signal transmitters through diverse mechanisms. As intact lipids, they bind to target proteins or influence the properties of the membrane into which they are inserted. In degraded form, they act as precursors for the downstream formation of soluble inositol polyphosphates (IPPs) (Figure 3.5). Intact PIs localize mainly to the cytosolic leaflet of cellular membranes (Balla, 2013) and they do not display uniform distribution within membranes but they are enriched in membrane domains (Kusano et al., 2008; Ischebeck et al., 2008, 2011; Vermeer et al., 2009). To impact membrane properties, plants synthesize different species of PIs under particular conditions (for instance under

salinity stress). They may vary on the level of saturation of their fatty acids (König et al., 2007), a factor that influences the lateral mobility of PIs within the plane of the membrane and regulates their association with particular membrane domains (Mukherjee et al., 1999; Cho et al., 2006). For the functional interaction with target proteins, PIs act mainly through their head groups, which are unique in their phosphorylation pattern and are recognized by PIs-binding protein domains such as FYVE finger (Fab1/YOTB/Vac1/EEA1), phox homology (PX) or pleckstrin homology (PH) (Munnik and Nielsen, 2011).

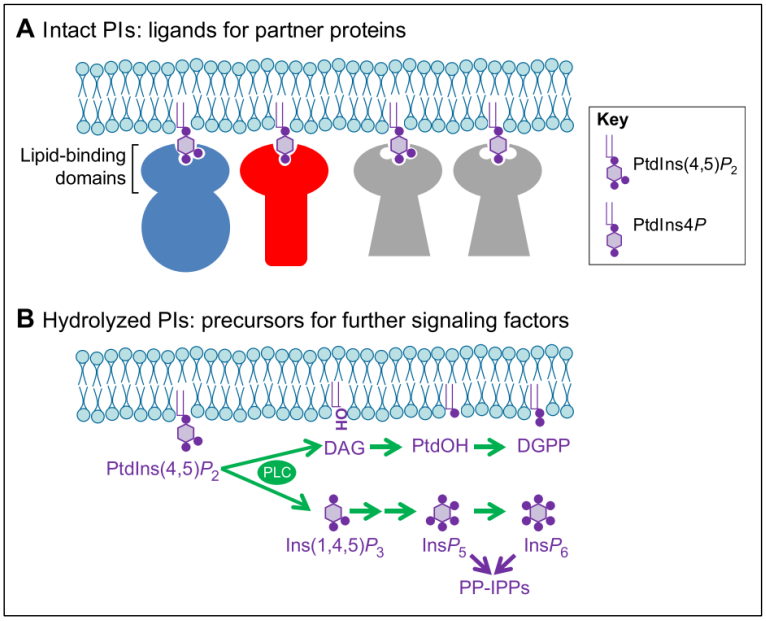

Figure 3.5. Modes of PIs action. (A) The binding of a phosphoinositide to a protein serves as a recruitment signal or have effects on the localization or function of the target protein. Some PIs recognition domains are highly specific for particular PIs. For instance, some pleckstrin homology (PH) domain-containing proteins (dark blue) have a strong preference for PI(4,5)P_2, whereas others (red) bind preferentially to PI4P. However, majority of PH domains do not exhibit such preferences, and proteins harboring these domains (gray) can bind to any given PIs. The specificity of PI function is thus likely manifested by additional factors. **(B)** The hydrolysis of PI(4,5)P_2 by phospholipase C (PLC) yields diacylglycerol (DAG) and inositol polyphosphates (IPPs). In plants, DAG is rapidly phosphorylated to phosphatidic acid (PtdOH) and possibly further to diacylglycerol pyrophosphate (DGPP). An Ins(1,4,5)P_3-sensitive calcium channel is absent in plants and Ins(1,4,5)P_3 instead appears to act as a precursor for IPPs, including InsP_5, InsP_6 or pyrophosphorylated IPPs (PP-IPPs). Adapted from Heilmann, 2016a.

Not every PIs-binding domain is highly specific towards a particular PI species (Figure 3.5). Moreover, some PIs-binding domains, such as PH domains, are poorly conserved in their primary sequence but are rather characterized by their three-dimensional fold. It is therefore difficult to identify such domains by sequence analysis as they may be shaped only transiently upon interaction with other protein partners (van Rossum et al., 2005).

3.2.1.1. The electrostatic/hydrogen bond switch model helps to explain a protein-anionic lipids interaction

One general property of the anionic phospholipids-binding domains is the presence of basic amino acids (Jensen et al., 2001; Whitley et al., 2003; Testerink and Munnik, 2005). Studies on phosphoinositide-binding domains demonstrated that specific PI binding implicates electrostatic interactions between the negatively-charged phosphate residues in the PIs and basic amino acids (lysine, arginine) in the proteins (Whitley et al., 2003).

Interestingly, it has been reported only for phosphatidic acid so far, that a simple electrostatic interaction is supported by a hydrogen bond formed by the head group upon deprotonation (Kooijman et al., 2007). When the side chain of lysine or arginine in a binding peptide detects the head group of PA, it comes into proximity (around 3.5 Å) and creates a hydrogen bond increasing the negative charge of PA due to the further deprotonation of its head group. Elevated negative charge strengthens the electrostatic attraction, locks the lysine or arginine on the head group of PA and results in a docking of the peptide on a PA molecule (Kooijman et al., 2007). It is likely that similar mechanism may underlie specific binding of effector proteins to PIs.

PART II: OBJECTIVES

The biological role of TSPO proteins in animal cells remains murky and even controversial after four decades of extensive studies. One key question is whether these membrane proteins share any ancient function, and in parallel have evolved cell-type specific functions. This argument stems from the continuous list of cellular activities and pathways shown to be affected one way or another by this enigmatic protein. A novel proposed function of TSPO in animal cells could be their involvement in lipid metabolism and regulation.

Recently, the host laboratory has uncovered a regulatory interaction between AtTSPO and a highly-expressed plasma membrane aquaporin, PIP2;7. However, the molecular determinants underlying this interaction remain unknown. In addition, a careful analysis of TSPO structures also provides some evolutionary distinctive hints, distinguishing for instance plant TSPO from their bacterial and mammalian relatives. In this project, **we will check whether (and how) the Arabidopsis TSPO may be involved in lipid metabolism.**

The presence of a plant-specific N-terminal extension rich in basic residues in AtTSPO is intriguing. **We will investigate its possible involvement in the molecular mechanism of protein-protein and protein-lipid interactions** in connection with the regulation of PIP2;7 levels in the plasma membrane during osmotic stress.

PART III: RESULTS AND DISCUSSION

The data presented herein have been published or discussed in the following manuscripts:

1. **Jurkiewicz P., Melser S., Maucourt M., Ayeb H., Veljanovski V., Maneta-Peyret L., Hooks M., Rolin D., Moreau P. and Batoko H.** (2018). The multistress-induced Translocator protein (TSPO) differentially modulates storage lipids metabolism in seeds and seedlings. The Plant Journal, doi: 10.1111/tpj.14028.
2. **Jurkiewicz P., Senicourt L., Lequin O., Lacapère JJ. and Batoko H**. Functional divergence within TSPO family: the role of a plant-specific conserved N-terminal extension. (Manuscript under consideration for Nature Communications).
3. **Jurkiewicz P. and Batoko H.** (2018). Protein degradation mechanisms modulate abscisic acid signaling and responses during abiotic stress. Plant Science 267:48-54.
4. **Batoko H., Jurkiewicz P. and Veljanovski V.** (2015). Translocator proteins, porphyrins and abiotic stress: new light? Trends in Plant Science 20:261-263.
5. **Batoko H., Veljanovski V. and Jurkiewicz P.** (2015). Enigmatic Translocator protein (TSPO) and cellular stress regulation. Trends in Biochemical Sciences 40:497-503.

Adapted versions of articles no. 1 and 2 are presented in Chapter 4 and 5, respectively. Articles no. 3, 4 and 5 are delivered to each member of the jury as hardcopies. They can also be found using the following DOI:

article 3	https://doi.org/10.1016/j.plantsci.2017.10.017
article 4	https://doi.org/10.1016/j.tplants.2015.03.009
article 5	https://doi.org/10.1016/j.tibs.2015.07.001

Chapter 4: The multistress-induced Translocator protein (TSPO) differentially modulates storage lipids metabolism in seeds and seedlings

The Plant Journal, doi: 10.1111/tpj.14028

Pawel Jurkiewicz[1], Su Melser[2§], Mickaël Maucourt[3], Haitham Ayeb[1], Vasko Veljanovski[1$], Lilly Maneta-Peyret[2], Mark Hooks[3], Dominique Rolin[3], Patrick Moreau[2,4*] and Henri Batoko[1*]

[1] Louvain Institute of Biomolecular Science and Technology (LIBST), UCLouvain, Croix du Sud 4-5, L7.07.14, 1348 Louvain-la-Neuve, Belgium

[2] CNRS-University of Bordeaux, UMR 5200 Membrane Biogenesis Laboratory, INRA Bordeaux Aquitaine, 33140 Villenave d'Ornon, France.

[3] Plateforme Métabolome Bordeaux, MetaboHUB, Bordeaux Functional Genomic Center, IBVM, CS 20032 F-33140 Villenave d'Ornon, France

[4] Bordeaux Imaging Center, UMS 3420 CNRS, US4 INSERM, University of Bordeaux, 33000 Bordeaux, France.

4.1. Abstract

Translocator proteins (TSPO) are conserved membrane proteins extensively studied in mammals but their function is still unclear. Angiosperm TSPO are transiently induced by abiotic stresses in vegetative tissues. We showed previously that constitutive expression of the Arabidopsis TSPO (AtTSPO) could be detrimental to the cell. Degradation of AtTSPO requires an active autophagy pathway. We show here that genetic modifications of TSPO expression in plant and yeast cells reduces the levels of cytoplasmic lipid droplets (LD). Transgenic Arabidopsis seedlings overexpressing AtTSPO contain less LD as compared to wild type. LD levels were increased in Arabidopsis AtTSPO knockout seedlings. Deletion of the *Schizosaccharomyces pombe* TSPO resulted in an increase of LD level in the cell. As compared to the wild type, the mutant strain was more sensitive to cerulenin, an inhibitor of fatty acids and sterol biosynthesis. We found that in contrast to seedlings, overexpression of AtTSPO (OE) resulted in up to 50% increase in seeds fatty acids as compared to wild type (WT). A time course experiment revealed that after 4 days of seeds imbibition, the levels of triacylglycerol (TAG) was still higher in the OE seeds as compared to WT or knockout (KO) seeds. However, the *de novo* synthesis of phospholipids and TAG after 24 hours of imbibition was substantially reduced in OE seeds as compared to WT or KO seeds. Our findings support a plant TSPO role in energy homeostasis in a tissue-specific manner, enhancing fatty acids and LD accumulation in mature seeds and limiting LD levels in seedlings.

4.2. Introduction

The phytohormone abscisic acid (ABA) is active during abiotic stress and induces the expression of a subset of plant genes during vegetative growth. Plants transcriptional responses to ABA come in two waves: an early transient response peaking at about 3 h and a late sustained response from 10 h onwards (reviewed in Finkelstein, 2013). Transcription factors, protein kinases and phosphatases and other regulatory proteins of unknown function are found in the group of so-called “early” affected genes (Fujita et al., 2006; Yamaguchi-Shinozaki and Shinozaki, 2006). Late embryonic abundant (LEA) proteins, chaperonins,

enzymes, ion and water-channel proteins, and reactive oxygen species (ROS) scavengers constitute the "late" affected genes, and are presumed to contribute to plant adaptation to the stress (Fujita et al., 2006; Yamaguchi-Shinozaki and Shinozaki, 2006).

The Arabidopsis Translocator protein-related (AtTSPO) is induced by various abiotic stress in the plant cell albeit transiently (Kreps et al., 2002; Seki et al., 2002; Zimmermann et al., 2004; Winter et al., 2007; Guillaumot et al., 2009; Hermans et al., 2010; Vanhee et al., 2011). ABA-induced AtTSPO expression peaks at about 3 h and is one of the most strongly induced "early" genes. However, the biological role of the encoded protein during stress is not yet fully understood. AtTSPO is a 5-α helical membrane protein encoded by a single locus (At2g47770) in Arabidopsis, and belongs to the so-called tryptophan-rich sensory protein/peripheral-type benzodiazepine receptor (TspO/MBR) group of proteins (Papadopoulos et al., 2006). Translocator proteins (TSPO) are well conserved from Archaea to Metazoans (Gavish et al., 1999; Lacapere and Papadopoulos, 2003; Papadopoulos et al., 2006; Batoko et al., 2015). The level of AtTSPO is tightly regulated in the plant cell. AtTSPO in only transiently expressed in Arabidopsis cell during stress, and induced or constitutively expressed AtTSPO is actively downregulated through the selective autophagy pathway (Vanhee et al., 2011; Hachez et al., 2014; Veljanovski and Batoko, 2014). AtTSPO targeting to this cellular homeostatic pathway requires heme binding, and a point mutation reducing heme binding *in vitro* stabilizes the protein *in vivo* (Vanhee et al., 2011; Hachez et al., 2014). It has been proposed that, among other roles, AtTSPO could act as a scavenger of toxic free porphyrins (including heme) during stress in the plant cell (Vanhee et al., 2011; Hachez et al., 2014). In addition, autophagic degradation of AtTSPO could modify the plant cell lipids metabolism through the *de novo* generation of the double-membrane autophagosomes. Indeed, recent studies have suggested direct links between active autophagy and lipid metabolism (Koga et al., 2010; Lapierre et al., 2011; Li et al., 2015; Gomez et al., 2017).

Since their identification in the late 70's (Braestrup et al., 1977), TSPO have been the subject of intensive research, almost exclusively in animal cells, to pinpoint their function. Considerable evidence indicates that it

plays regulatory roles in steroidogenesis and apoptosis and is involved in various human diseases, including metastatic cancer, inflammation-associated diseases of the central nervous system and anxiety disorders (Li et al., 2016). One of the main functions attributed to mammalian TSPO is their possible involvement in steroid metabolism and mitochondrial physiology (reviewed in Rupprecht et al., 2010) although recent evidence has cautioned these acceptations (Morohaku et al., 2014; Sileikyte et al., 2014; Tu et al., 2014; Batoko et al., 2015; Li et al., 2016; Guilarte et al., 2016). However, there is a growing appreciation for the potential roles TSPO play in environmental stress and human disease.

It is thought that a conserved function of TSPO irrespective of their subcellular localization could be their involvement in stress and redox homeostasis, and through evolution, these ubiquitous membrane proteins may have acquired additional species- and possibly cell type-specific functions (Stoebner et al., 2001; Gatliff et al., 2014; Batoko et al., 2015; Fan et al., 2015; Li et al., 2016; Guilarte et al., 2016). It was shown recently that mammalian TSPO1 mediates adipose tissue homeostasis since mitochondrial TSPO1 expression was substantially reduced in white and brown adipose tissues in mouse models of obesity (Thompson et al., 2013). Conditional steroidogenic cell-targeted deletion of TSPO resulted in the accumulation of lipid droplets (Fan et al., 2015), while overexpression of TSPO in macrophages triggered a depletion of cholesterol and a reduction of neutral lipid mass (Taylor et al., 2014). How TSPO could be involved in lipid metabolism is not yet clear. In addition, a whole organism screening for gluconeogenesis activators in zebrafish uncovered TSPO physiological ligands, suggesting the possible involvement of TSPO in energy homeostasis (Gut et al., 2013).

Lipid droplets are found in almost all nucleated cells and represent a reservoir of neutral lipids that can be broken down when energy or fatty acids are required in the cell (Hashemi and Goodman, 2015). Two types of lipid droplets are found in the plant cell: i) cytoplasmic droplets containing mainly triacylglycerol (TAG) and sterol esters surrounded by a single membrane derived from the cytoplasmic leaflet of the ER, and ii) plastoglobules derived from the thylakoid membrane in plastids and containing antioxidant molecules protecting the photosynthetic

apparatus from oxidative stress. Another excess carbon energy storage macromolecule found in the chloroplast of plant cells is starch. Recent evidence suggest that TAG are not only reserve energy in the plant cell but are also involved in stress responses. They usually serve to transiently sequester free fatty acids that can be harmful to the cell (Fan et al., 2013; Yang et al., 2015; Yang and Benning, 2018). In this work, we show that expression of AtTSPO differentially affects TAG accumulation in seeds and in seedlings. In light of these findings, we discuss the possible regulatory role of AtTSPO in the energy homeostasis of the plant cell during water-related stress.

4.3. Results

4.3.1. Constitutive expression of AtTSPO modifies TAG metabolism during seedling establishment

Plant TSPO are upregulated during abiotic stress and during senescence. LD are known to increase during similar physiological or developmental conditions. TAG in LD could serve transiently to sequester harmful free fatty acids generated by membrane remodeling during stress (reviewed in Xu and Shanklin, 2016; Yang and Benning, 2018). We therefore compared TAG and polar lipids levels in WT, AtTSPO knockout (KO), and overexpressing (OE) transgenic seedlings. Four day-old seedlings grown on synthetic medium and under strictly monitored and reproducible environmental conditions were compared. As shown in Figure 4.1A, the average relative level of TAG in the OE seedlings (pool of two independent homozygote lines OE8 and OE9) was reduced to ~10% of WT levels, after normalization. In contrast, the TAG level of the KO seedlings (pool of two independent homozygote TDNA insertion lines KO1 and KO2 seedlings, see also supplemental Figure 4.S1) was ~130% of that observed in the WT seedlings ($p<0.001$). In addition, the TAG over phospholipids (TAG/PL) ratio increased in the KO seedlings with respect to their WT counterpart ($p<0.05$), and drastically decreased in the OE seedlings ($p<0.01$) (Figure 4.1B). These results suggest that at this growth stage, overexpression of AtTSPO has a relatively negative effect on TAG accumulation and conversely, the lack of AtTSPO increases TAG accumulation. Expressed AtTSPO during this growth stage could

therefore be involved in reduced biosynthesis of TAG and LD, or their enhanced consumption.

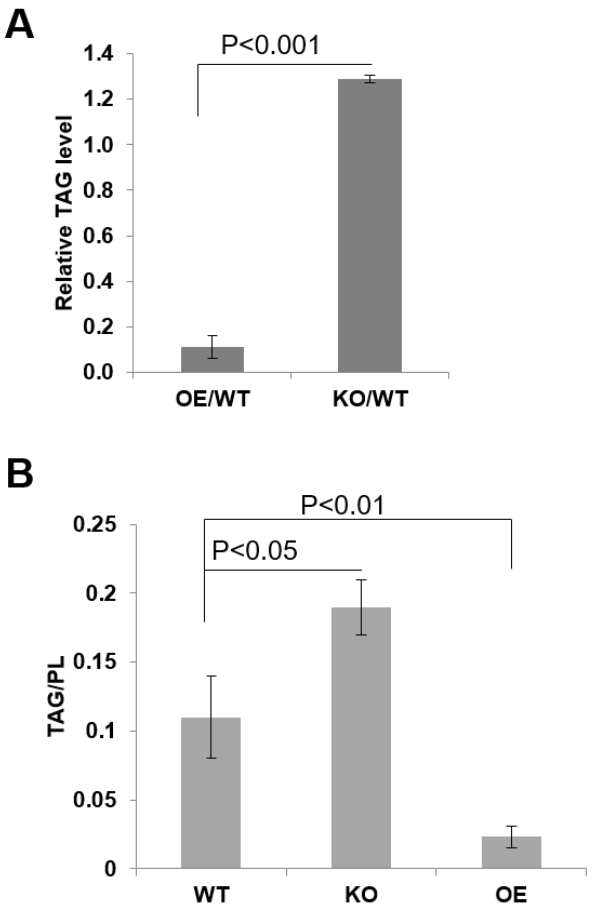

Figure 4.1. The Arabidopsis AtTSPO regulates the level of triacylglycerol in seedlings. (A) Triacylglycerol was quantified in 4-day-old seedling extracts and expressed as a fraction of the WT value for transgenic plants overexpressing AtTSPO (OE8) or knocked-out for AtTSPO (KO1). **(B)** Polar lipids from the same samples as in **(A)** were quantified and the ratio of TAG/PL was calculated for the WT, KO and OE seedlings. The error bars in **(A)** and **(B)** represent the standard deviation from three independent experiments.

4.3.2. AtTSPO can modulate the level of cytoplasmic lipid droplets in Arabidopsis

Next, we examined the relative amount of cytoplasmic lipid droplets in the sampled 4-day-old seedlings as a possible source of the observed TAG

content variations. Cytoplasmic lipid droplets are single layer membrane compartment in the cell and contain lipid reserves essentially made of TAG and sterol esters (Chapman and Ohlrogge, 2012). Cytoplasmic lipid droplets can be stained *in vivo* with different dyes. We compared the commonly used Nile red (James et al., 2010; McLachlan et al., 2016) to LD540 (Spandl et al., 2009), and the recently described blue-fluorescent LD dyes for live-cell imaging in plant (Kuntam et al. 2015). We found that LD540 perfectly co-localized with the well-characterized LD marker ERG6-RFP in yeast with little or no staining of non-LD structures (supplemental Figure 4.S2). Arabidopsis seedlings were incubated in 1 ng/ml of LD540 (a generous gift from Dr. Thiele, Max Planck Institute of molecular cell biology and genetics, Dresden, Germany) for 30 min and the stained lipids droplets were imaged by confocal microscopy. The optical sections were taken across the mesophyll cell layer of the cotyledon, and representative images are shown in Figure 4.2A. We confirmed by western blotting the expression of AtTSPO in all the genotypes tested, using the large subunit of RUBISCO as loading control (Figure 4.2B). As shown in Figure 4.2A (upper panels), very little LD540 fluorescence could be seen in the AtTSPO overexpressing OE8 cotyledon as compared to the WT and the KO1 sample. The latter showed larger LD and more overall LD540 fluorescence as compared to WT (see also supplemental Figure 4.S3). It may be that during osmotic stress conducive of AtTSPO expression, the plant cell remodels its polar membrane lipids by modifying the mobilization and synthesis of TAG. These observations suggest that AtTSPO could be part of a regulatory mechanism controlling the homeostasis between membrane lipids and reserve lipids during water limitation in the cell, for example in desiccated seeds or during periods of osmotic stress. LD are also required for clearance of toxic proteins and are involved in autophagosome biogenesis and fusion (Koga et al., 2010; Li et al., 2014; Moldavski et al., 2015; Shpilka et al., 2015). We reasoned that the observed reduced levels of LD in presence of AtTSPO could be linked to the regulatory degradation of the protein through the autophagy pathway. If so, the relatively stable mutant AtTSPO^{H91A} (Vanhee et al., 2011; Hachez et al., 2014) should have less effect as compared to the WT protein on LD content. Indeed, the level

of LD in Arabidopsis transgenic plant overexpressing AtTSPO^{H91A} was comparable to that of the WT plant (Figure 4.2A, compare LD540 panels WT, OE8 and H91A-1). Similar results were obtained from independent transgenic lines (see also supplemental Figure 4.S3). These results suggest that, at least in the plant cell, the regulatory degradation of TSPO could enhance LD breakdown or decrease LD biogenesis.

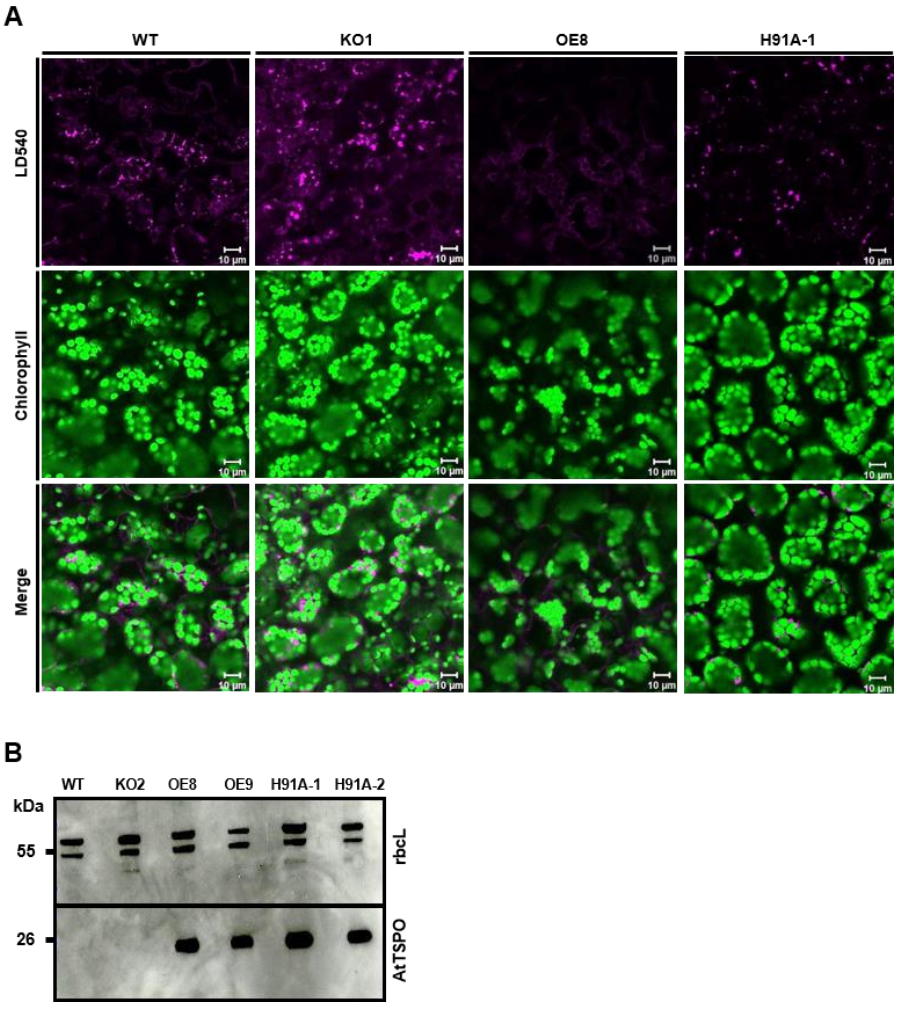

Figure 4.2. AtTSPO but not the point mutant AtTSPO^{H91A} reduces the level of lipid droplets in 4-day old Arabidopsis cotyledons. Representative confocal images of cotyledon from WT, KO and AtTSPO overexpressing transgenic plants stained with the lipid droplet-specific dye LD540. **(A)** Lipid droplets (magenta) and chlorophyll autofluorescence (green) are shown from a single optical section passing through the mesophyll cell layer. **(B)** Western blotting of AtTSPO expression (lower panel) from

protein extract of WT, KO2, two independent homozygous transgenic lines overexpressing wild type AtTSPO (OE8 and OE9) or the point mutant variant AtTSPO^{H91A} (H91A-1 and H91A-2); the large subunit of RUBISCO (rbcL) was used as loading control (upper panel). Scale bar: 10 µm.

4.3.3. Inactivation of the *S. pombe* TSPO gene increases the number of lipid droplets in the mutant cell

Next, we wanted to investigate whether TSPO involvement in the regulation of TAG through cytoplasmic lipid droplets is not a peculiarity of the plant TSPO, but possibly a shared functional role by distantly related TSPO. We took advantage of the fact that the fission yeast genome encodes (SPBC725.10) and expresses a TSPO protein (here after called SpTSPO). Interestingly, SPBC725.10 is upregulated during nitrogen starvation and its deletion (strain ΔSPBC725.10) enhances sensitivity to the autophagy-inducible drug rapamycin (Doi et al., 2015), and its overexpression increases viability at the stationary growth phase (Ohtsuka et al., 2013). We first confirmed by PCR that the SPBC725.10 locus was indeed disrupted in strain ΔSPBC725.10 (Figure 4.3A). Genotyping the strains showed that the disruption cassette could be amplified only from genomic DNA retrieved from ΔSPBC725.10 (lane tspo KO) but not from the WT strain (lane WT), using a combination of gene-specific and disruption cassette-specific primers. The WT and mutant *S. pombe* strains were grown in liquid culture up to the stationary phase and stained for lipid droplets with LD540. Representative confocal images are presented in Figure 4.3B. LD540-stained LD were quantified after confocal imaging of at least 45 randomly selected cells from each strain. The ΔSPBC725.10 null mutant cells contained about 25% more LD than the WT cells (Figure 4.3C, $p<0.05$). A detailed quantification of neutral lipids normalized to proteins content (Figure 4.4A) or the ratio of the neutral lipid species (Figure 4.4B) showed that the mutant cells accumulate more diacylglycerol, triacylglycerol and esters ($p<0.05$), while the level of free fatty acids and sterols was similar to that of the WT cells. These results suggest that in *S. pombe*, the expression of the endogenous SpTSPO may be limiting the number of LD, and deletion of the corresponding gene increases the biosynthesis and/or limits the consumption of LD. This observation is reminiscent of what was recently

described in steroidogenic mammalian cells in which the mitochondrial TSPO1 was genetically knocked-out (Fan et al., 2015). To test the hypothesis that TSPO could enhance LD breakdown, we grew WT and mutant *S. pombe* cells in rich medium up to the stationary phase. The cells were then harvested and plated (by streaking or as a serial dilution drop test) on solid medium supplemented with cerulenin, an inhibitor of β-keto-acyl ACP synthase and HMG-CoA synthase (Figure 4.5). In presence of this drug inhibiting both fatty acids and sterols biosynthesis, cell growth is dependent upon the consumption of LD reserves. As shown in Figure 4.5, the ΔSPBC725.10 null mutant (KO) cells failed to grow and were more sensitive to cerulenin than the WT cells, suggesting that SpTSPO expression and activity may be required for efficient breakdown of the LD reserves. We therefore concluded that TSPO involvement in reserve lipids metabolism in eukaryotic cells could be an evolutionary conserved metabolic role of these membranes proteins.

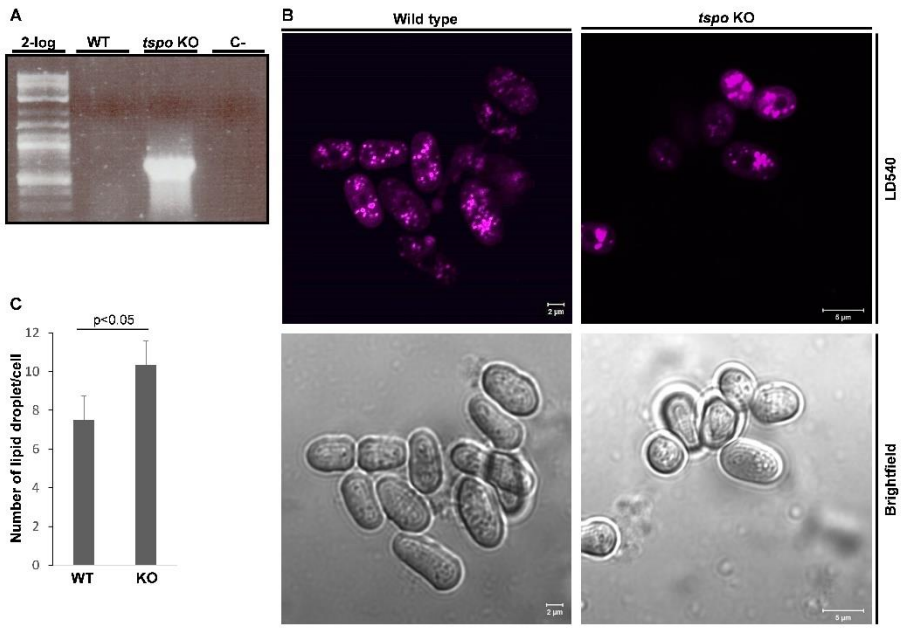

Figure 4.3. Inactivation of the *S. pombe* endogenous TSPO gene increases the number of lipid droplets per cell. (A) Genotyping of the mutant strain (tspo KO) showing PCR amplification of the insertion cassette using as control the wild type genomic DNA and a DNA-free sample (C-). **(B)** WT and mutant cells were grown overnight at 30°C and stained with LD540. Micrographs show representative confocal images of lipid

droplets (magenta, upper panels) and corresponding transmitted light image (lower panels) images. **(C)** Inactivation of SpTSPO (KO, n=45) increases the number of LD as compared to WT cells (n=45). The bar on each histogram represents standard deviation.

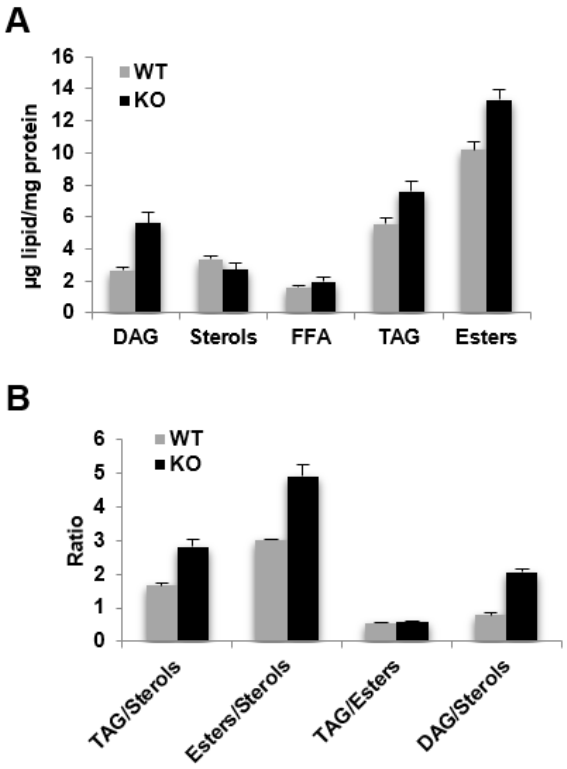

Figure 4.4. Inactivation of SpTSPO enhances neutral lipids accumulation. (A) Neutral lipids (diacylglycerol, DAG; triacylglycerol, TAG; sterols, esters) and free fatty acids (FFA) were quantified and normalized against total proteins (WT = 6.6 mg, KO = 1.9 mg) from *S. pombe* cells grown overnight in YD medium at 30°C. **(B)** Ratio of neutral lipids in WT and mutant (KO) cells.

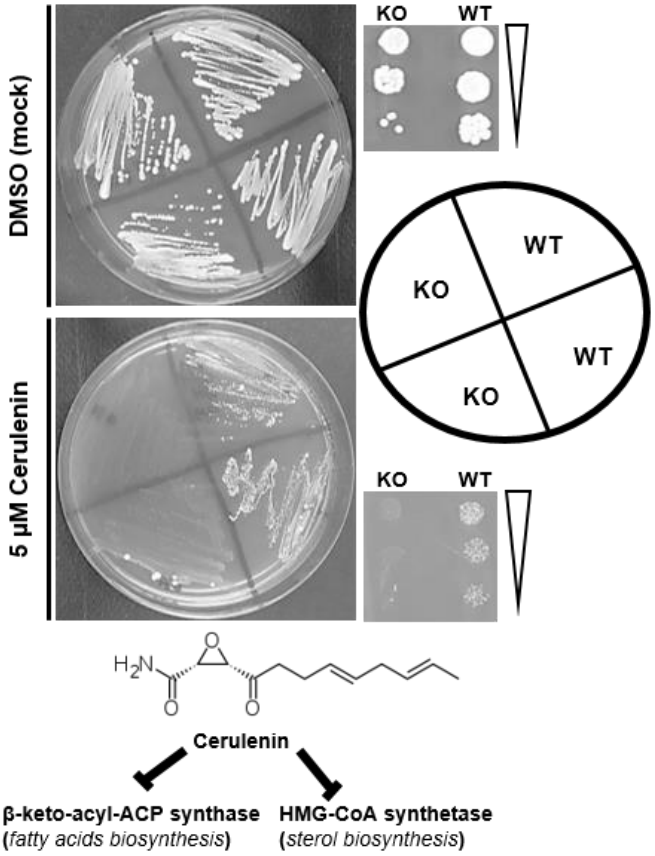

Figure 4.5. Inactivation of SpTSPO increases the sensitivity to cerulenin, the fatty acids and sterol biosynthesis inhibitor. WT and mutant *S. pombe* were grown in liquid YD medium up to stationary phase, then the cells were streaked (left plates) or plated as a dilution series (drop test) on the same media containing DMSO (<0.1%, mock) or 5 µM cerulenin. The plates were imaged after incubation for 5 days at 30°C; the structure of cerulenin and its target enzymes in lipid biosynthesis are shown at the bottom.

4.3.4. Constitutive expression of AtTSPO modifies seed lipids metabolism during germination

We showed previously that AtTSPO is mainly expressed in mature seeds and is only transiently induced during abiotic stress in vegetative tissues (Guillaumot et al., 2009; Vanhee et al., 2011; Hachez et al., 2014). We wondered whether expressed AtTSPO in seeds could affect reserve mobilization during seed imbibition. We first compared the ratio of TAG over phospholipids of WT, KO and AtTSPO OE seeds after one day imbibition (Figure 4.6A). We consistently observed that this ratio was

statistically the same for WT and KO seeds, while it was about 40% higher for OE seeds, suggesting either a relatively reduced consumption of TAG during imbibition of OE seeds or illustrating a possible higher amount of TAG in the starting/germinating seeds. We then conducted a time course experiment, monitoring the levels of TAG from day-2 up to day-10, comparing WT and KO germinating seeds to seeds from independent transgenic lines overexpressing either AtTSPO (OE1 and OE2) or its point mutant variant AtTSPO^{H91A} (H91A-1 and H91A-2) (Figure 4.6B). Interestingly, the levels of TAG in AtTSPO overexpressing seeds was at least 2-fold higher as compared to WT and KO seeds levels at day-2 and day-4, in agreement with the data obtained after one day imbibition. TAG levels diminished with time in all the samples but the slope of TAG decrease in overexpressing lines was similar or even higher at the early time points than those of WT or KO lines. Therefore, our results seem to be more in favor of a higher amount of TAG in the starting/germinating seeds than a reduced consumption of TAG during imbibition of OE seeds. Moreover, the ratio of TAG over phosphatidylcholine plus phosphatidylethanolamine followed the same trend (Figure 4.6C), suggesting that the effect of overexpressed AtTSPO on TAG metabolism is limited in time and developmentally.

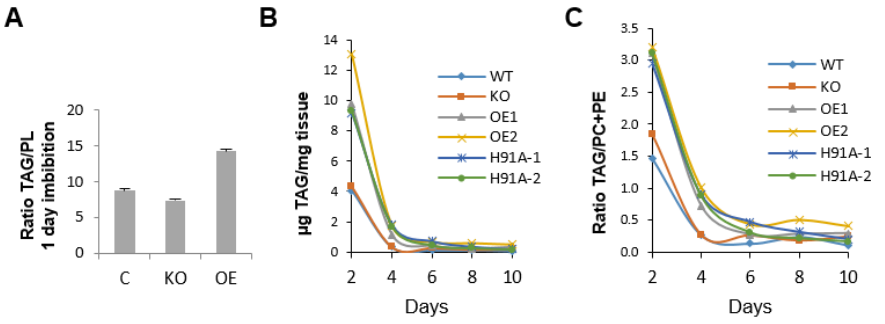

Figure 4.6. Higher TAG levels are found in Arabidopsis lines overexpressing AtTSPO after one-day imbibition up to 4 days of germination. (A) Ratio of TAG to phospholipids (PL) in WT, KO, OE and point mutant variant AtTSPO^{H91A} lines imbibed for 24h (100 seeds). **(B)** TAG amounts in seedlings from WT, KO, OE and point mutant variant AtTSPO^{H91A} lines (50-100 seedlings per line) in a kinetic of germination up to 10 days. **(C)** Ratio of TAG to phospholipids (PL) in WT, KO, OE and point mutant variant AtTSPO^{H91A} lines in a kinetic of germination up to 10 days.

We showed previously that the level of AtTSPO is tightly regulated in the plant cell. For instance, ABA-dependent upregulation of AtTSPO expression is only transient, and overexpression of AtTSPO under the control of a strong constitutive promoter (p35S) or a mild endogenous constitutive promoter resulted in few cells accumulating the protein (Guillaumot et al., 2009; Hachez et al., 2014). We examined the levels of AtTSPO during Arabidopsis seeds imbibition in a time course experiment (Figure 4.7A) and consistently found that AtTSPO levels decreases steadily, becoming almost undetectable by western blotting after 24h of seed imbibition in water, corroborating previous observations (Hachez et al., 2014).

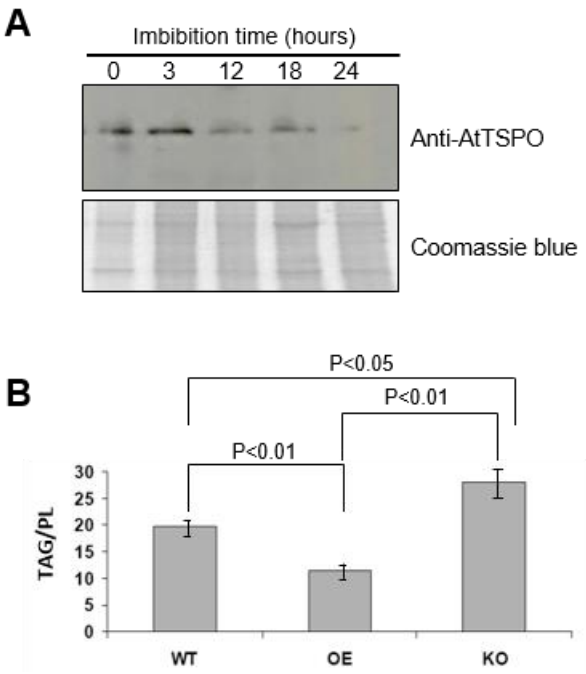

Figure 4.7. The Arabidopsis TSPO protein (AtTSPO) modulates lipids content and metabolism in seeds. (A) Downregulation of AtTSPO during seed imbibition. Arabidopsis WT seeds were incubated in water at room temperature for imbibition and sampled at the mentioned time point; total protein extracts (30 µg) were analyzed by western blotting using the anti-AtTSPO antibody at a dilution of 1:5000; a Coomassie blue-stained replica of the gel is shown in the bottom panel as a loading control. **(B)** Incorporation of radioactive acetate into triacylglycerol (TAG) and polar lipids (PL) was measured after 24h imbibition of the WT, OE, and KO seeds; each histogram represents the ratio of TAG/PL for the specified seed type and the error bar represents standard deviation (n=3).

We could not find any striking difference in terms of the germination rate between the WT Arabidopsis seeds and transgenic lines overexpressing AtTSPO (OE, pool of homozygous lines) or seeds derived from independent KO lines (lines SALK_066561C (KO1) and SALK_135023C (KO2)). To understand the potential role of overexpressed AtTSPO on TAG levels during germination and seedling establishment, we analyzed the incorporation of radioactive acetate into TAG and polar lipids. As shown in Figure 4.7B, constitutive expression of AtTSPO (OE histogram) resulted in reduced synthesis of TAG compared to polar lipids. Consistently, a higher level of TAG over polar lipids was found in the imbibing KO seeds. Therefore, we can consider that when TAG levels are high (in OE starting/germinating seeds), *de novo* TAG synthesis is lower during imbibition (downregulation); and when TAG levels are low in KO starting/germinating seeds, *de novo* TAG synthesis is higher (upregulation). These results suggest that during seed germination and seedling establishment, AtTSPO is actively degraded, and constitutive expression of this stress-induced protein modulates somehow TAG (and polar lipids) synthesis during these growth stages.

4.3.5. Constitutive expression of AtTSPO substantially increases the level of fatty acids in dry seeds

To follow up on the observed enhanced TAG in germinating seeds from transgenic plant overexpressing AtTSPO, we checked whether the observed differences are already present in the harvested seeds. We first compared the weight of the seeds and found that apart from the KO seeds that were about 20% lighter, the transgenic and WT seeds had statistically equivalent weight (Figure 4.8A). However, seeds from AtTSPO overexpressing plant had up to 50% more fatty acids as compared to WT seeds. Accordingly, KO seeds had about 25% less fatty acids as compared to the WT seeds (Figure 4.8B). Most fatty acids species were increased in transgenic lines overexpressing AtTSPO, with a remarkable enhancement for C18:1, C18:2, C18:3 and C20:1 (Figure 4.8C). This unexpected effect of overexpression of AtTSPO in the seeds contrasts with recent findings in mammalian cells where loss of TSPO

enhanced lipids accumulation in adipose tissues (Thompson et al., 2013; Fan et al., 2015).

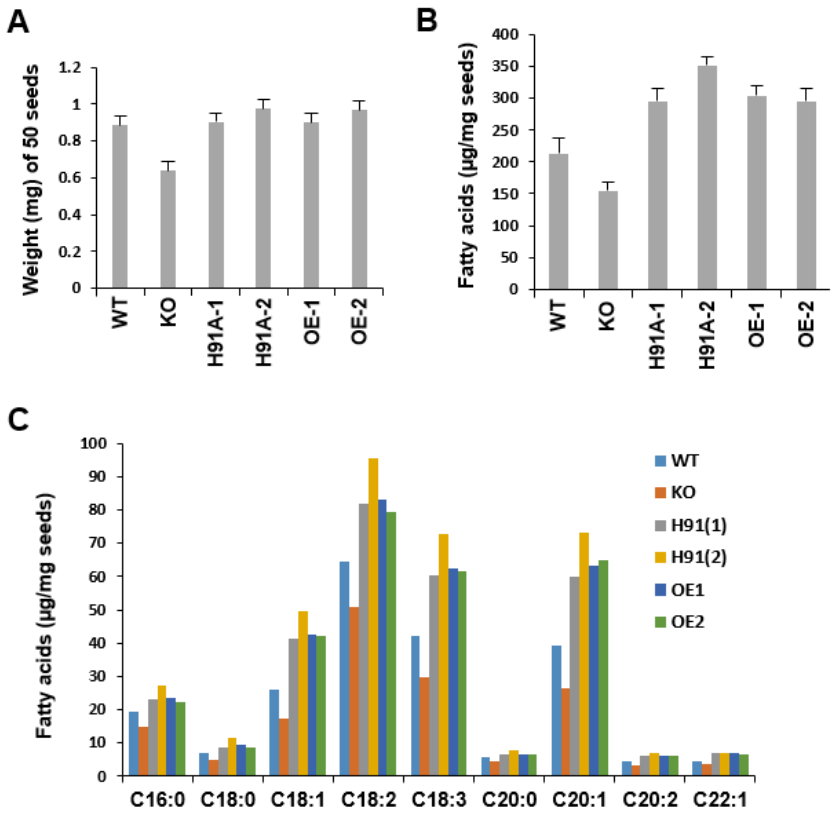

Figure 4.8. Higher TAG levels are found in dry seeds of Arabidopsis lines overexpressing AtTSPO. (A) Weight of dry seeds from WT, KO, OE and point mutant variant AtTSPO^{H91A} lines. **(B)** TAG amounts determined by measuring the fatty acid amounts of dry seeds from WT, KO, OE and point mutant variant AtTSPO^{H91A} lines. **(C)** Detail of fatty acids measured in dry seeds from WT, KO, OE and point mutant variant AtTSPO^{H91A} lines.

4.3.6. Constitutive expression of AtTSPO reduces starch levels but not soluble sugars in the plant cell

Conventionally, starch is synthesized by autotrophic plant cells during the day and hydrolyzed during the night to provide the energy fueling growth. The derived sugar metabolism also provides intermediates and building blocks for fatty acids biosynthesis (Chapman and Ohlrogge, 2012; Santelia et al., 2015). The conversion of sucrose into fatty acids in

particular can regulate the levels of TAG accumulation in seeds (Chapman and Ohlrogge, 2012). However, primary starch can be degraded in the light in response to abiotic and biotic stress to meet the changes in energy and carbon demand that are required to counteract these stress (Santelia et al., 2015). To investigate whether other energy reserves or other metabolites apart from lipids could be affected by the constitutive expression of AtTSPO in Arabidopsis, we first compared the starch content of WT, KO (KO1) and OE (OE8) siliques and ran a comparative metabolites profiling of 4 day-old seedlings from the same genotypes. Mature siliques were analyzed for their starch content expressed as glucose equivalent (Figure 4.9A).

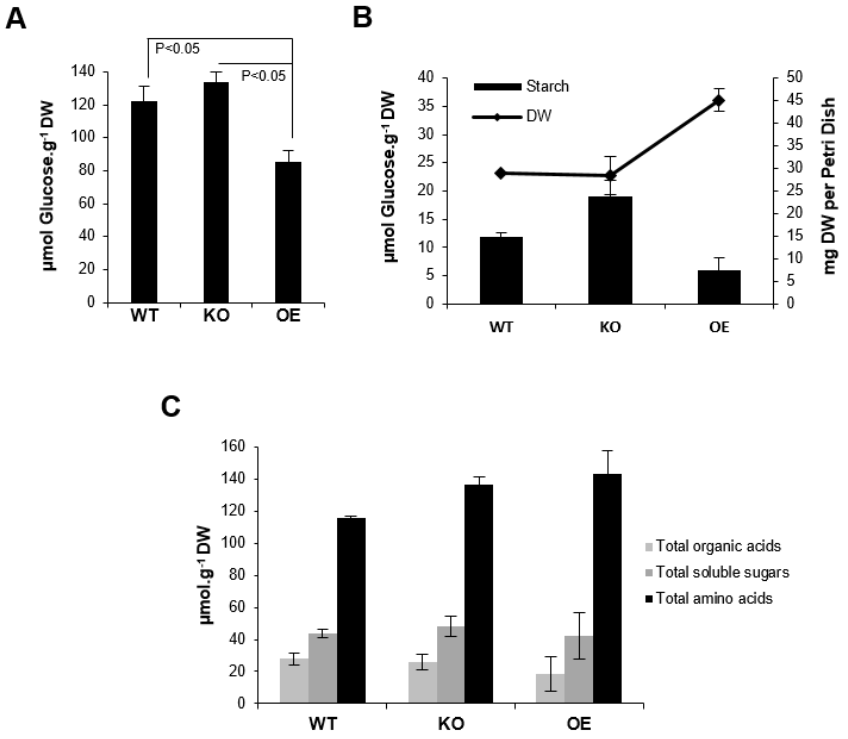

Figure 4.9. Overexpression of AtTSPO impacts starch and biomass accumulation in mature silique and Arabidopsis seedlings. (A) Mature siliques were sampled from WT, KO (KO1), and OE (pool of OE8 and OE9) plants and the starch content was quantified as equivalent glucose and normalized to the dry weight. **(B)** The starch content of Arabidopsis seedlings (4-day-old) was measured and normalized to the dry weight of seedlings. The bar represents the standard deviation of the mean from 3 independent experiments. **(C)** A portion of the samples as in **(D)** was used for metabolomics analysis. The bar represents the standard deviation of the mean for each category of metabolites.

We found no statistical difference between the WT and KO siliques in terms of starch content (~120 µmol glucose/g dry weight). In comparison, the starch content of the OE siliques was substantially reduced (~80 µmol glucose/g dry weight). These results suggest that constitutive expression of AtTSPO is detrimental to the accumulation of carbon reserves in siliques. To extend these findings, we compared starch and biomass accumulation in 4-day-old seedlings derived from WT, KO and OE seedlings. Equal number (around 150) of seedlings were grown on ½ strength MS medium (3 independent experiments with 3 replicate plates per line) under controlled conditions. As shown in Figure 4.9B, the OE seedlings accumulated more biomass than the WT and KO seedlings. In contrast, the starch content was the lowest in the OE seedlings (less than 50% of the WT level). As anticipated, the highest starch content was observed in KO seedlings (~150% of the level in the WT seedlings, $p<0.05$). These results suggest that AtTSPO regulates carbon and lipid reserve levels in the plant cell. After a quantitative metabolite profiling by ^{1}H-NMR, we compared soluble sugars (glucose, fructose and sucrose), organic acids (acetate, fumarate, citrate, formate, and malate) and amino acids (alanine, asparagine, aspartate, gamma-aminobutyric acid, glutamine, glutamate, isoleucine, lysine, phenylalanine, serine, tryptophan, valine, and pyroglutamate) in the same samples. As shown in Figure 4.9C, no significant differences could be seen for the independent substances or categories of metabolites between the seedlings from the three genotypes, suggesting that these metabolic intermediates are not affected by the presence or absence of AtTSPO. It may be that constitutive expression of AtTSPO reduces the levels of starch, an energy reserve between photosynthetic activity and cellular carbon metabolism, in addition to the neutral lipids reserve.

4.4. Discussion

We showed previously that the level of AtTSPO is tightly regulated in the plant cell (Guillaumot et al., 2009; Vanhee et al., 2011; Hachez et al., 2014). The plant cell downregulates stress-induced or constitutively expressed AtTSPO via a selective autophagy pathway (Vanhee et al., 2011; Hachez et al., 2014). The potential detrimental physiological effects

to the plant cell of a continuous presence of AtTSPO are not yet clear. Unexpectedly, we found that overexpression of AtTSPO resulted in a substantial increase in fatty acids levels in dry seeds. We also present evidence that constitutive expression of AtTSPO reduced lipids and carbon reserves in germinating seed or seedling. In contrast, inactivation of AtTSPO enhanced LD levels in the same tissues. We extended these observations to yeast cells by showing that inactivation of the fission yeast *S. pombe* TSPO homolog resulted in an increased number of LD and enhanced sensitivity to cerulenin. These data suggest that TSPO proteins may play a role in regulation of lipids and carbon homeostasis in the cell. In plant vegetative tissues in particular, TSPO expression could be involved in TAG homeostasis, while in seed tissues, overexpression of TSPO induces upregulation of TAG biosynthesis pathway.

The effect of AtTSPO in vegetative tissues is reminiscent of what was recently described in mammalian cells. Mitochondrial TSPO1 was shown to be downregulated (transcript and protein) in both white and brown adipose tissues of mouse models pertaining to obesity as compared to control animals (Thompson et al., 2013). Conditional knockout of TSPO1 in mouse steroidogenic cells resulted in the accumulation of LD (Fan et al., 2015). It is not yet clear how mechanistically TSPO could regulate the biosynthesis or consumption/degradation of LD. We showed in the plant cell that the relatively stable mutant variant of AtTSPO, AtTSPO^{H91A}, had limited effect on LD content of the cell, suggesting a potential link between AtTSPO regulatory degradation and LD levels. Increased sensitivity to cerulenin in absence of SpTSPO may suggest that the mutant cells are more affected by the inhibition of intermediate and long-chain lipid synthesis. It is worth mentioning that knockout mice for TSPO1 was reported gaining prominently more gonadal and subcutaneous fat than the control mice, and increase in adipocyte hypertrophy and LD. These modifications were accompanied by decreased lipolysis and downregulation of hormone-sensitive and adipose triglyceride lipase (Tu et al., 2016).

In response to abiotic stress, potentially toxic free fatty acids released from membrane remodeling are channeled to LD to protect the integrity of the cellular membrane system (Yang and Benning, 2018). Hence,

during abiotic stress or senescence, there is an increase of LD in mesophyll cells. Given that AtTSPO is only transiently expressed during abiotic stress, it is not surprising that constitutive expression of the protein induces downregulation of LD. The LD fatty acids may be used by the cell to generate autophagosomes required to get rid of the "toxic" AtTSPO accumulating in the cell. We showed previously that constitutive expression of AtTSPO could be detrimental to the plant cell (Guillaumot et al., 2009; Vanhee et al., 2011).

On the other hand, LD could also attenuate AtTSPO role in redox regulation. Recent findings are expanding the biological roles of LD in eukaryotic cells apart from the energy reserve function commonly ascribed to these particular membrane compartments. It was shown for instance that LD can act as antioxidant organelles (Bailey et al., 2015), and other studies suggest that oxidative stress enhances the biosynthesis of LD (Liu et al., 2015). It was shown in *Drosophila* glia cells that during hypoxia-triggered production of ROS, LD can sequester polyunsaturated fatty acids away from the plasma membrane, shielding these lipids from harmful peroxidation (Bailey et al., 2015).

The additional reduction in starch because of overexpressed AtTSPO suggests that this stress-induced protein could be part of a regulatory hub for cellular energy homeostasis. The effect of AtTSPO on energy reserve could be indirect. High throughput experiments suggest that overexpression of SpTSPO increases viability of the cell at stationary phase and deletion of SpTSPO decreases cell population growth on glucose (Ohtsuka et al., 2013). A whole organism screening for gluconeogenesis in zebrafish for drugs activating fasting metabolism uncovered the isoquinoline carboxamide PK11195 and the benzodiazepine-related compound Ro5-4864 (clonazepam) (Gut et al., 2013), both of which are known as high affinity TSPO ligands (Papadopoulos et al., 2006).

The plant fatty acid synthesis for TAG and membranes differs fundamentally from other eukaryotes, because in the plant cell this takes place exclusively in plastids as opposed to the cytosol, and the synthases involved are structured as dissociable complexes with distinctive acyl carrier protein (Chapman and Ohlrogge, 2012). Interestingly, we found

that overexpression of AtTSPO resulted in a substantial increase in TAG and fatty acids in dry seeds. It may be that AtTSPO affects differently lipids metabolism in seeds as compared to vegetative tissues. Our results support the view that TSPO regulates TAG accumulation in dry seeds, and that TSPO regulates TAG consumption during seedling establishment/plant development. Understandably, consumption of the lipid reserves during seed imbibition was correlated to AtTSPO degradation. AtTSPO may also be involved in the regulation of the number, size, and morphodynamics of the LD in a tissue-dependent manner, complementing the role of well characterized proteins such as LDAP (lipid droplet-associated proteins) and SEIPIN (Horn et al., 2013; Cai et al., 2015).

4.5. Experimental procedures

4.5.1. Generation, growth and treatments of the transgenic plant lines

Genetic constructions, transformation, selection and selfing of transgenic Arabidopsis lines and validation of the AtTSPO knockout line KO1 (TDNA insertional line salk_066561C) were described elsewhere (Guillaumot et al., 2009; Vanhee et al., 2011; Hachez et al., 2014). Arabidopsis seeds were surface-sterilized before they were sown on half strength MS (Murashige and Skoog, 1962) solid sterile medium containing 0.7% agar and buffered at pH 5.8 in the presence of 0.5% (w/v) MES. Total proteins extraction from seedlings was as described (Vanhee et al., 2011). We followed standard protocols for SDS-PAGE and western blotting. The anti-large subunit of RUBISCO antibodies were from Agrisera and used at the recommended dilution. The anti-AtTSPO antibody has been described elsewhere (Guillaumot et al., 2009) and was used at 1/5000.

4.5.2. Yeast strains and growth conditions

The fission yeast SPBC725.10 gene encoding SpTSPO was disrupted using the KanR cassette. For PCR-mediated genotyping, we used the KanR specific primer 5’-CAAGGAGGGTATTCTGGGCC-3’ in combination with the primer 5’-CTCCTTCCCTTCTGTGACG-3', annealing 212 bp upstream of the ATG start codon of SPBC725.10. The WT and the mutant strains

were a kind gift from Dr. D. Hermand (Université de Namur, Belgium). The yeast were grown in liquid or 2% agar-solidified complete YD medium at 30°C.

4.5.3. Lipid droplets staining and imaging

In preliminary experiments, we used 4-day-old Arabidopsis seedlings and compared Nile red (Sigma), LD540 (Spandl et al., 2009) and the blue-fluorescent lipid dyes Ac-201 and Ac-202 (Kuntam et al., 2015) for their efficiency and specificity in LD staining. In our experimental conditions, we found that LD540 was the best dye for LD staining *in vivo*. About 15 Arabidopsis seedlings were vacuum infiltrated (-1 bar) for 30 min in 1 ng/ml LD540 followed by 3 washes (1 ml each) with sterile water. *S. pombe* cells were grown in liquid YD medium up to the stationary phase, then incubated in 1 ng/ml LD540 (added to the culture medium) for 15 min, followed by 3 washes with sterile distilled water. The sample were immediately imaged (excitation 488 nm, Zeiss LSM 710). Identical settings were used for the confocal imaging of the samples to be compared and the collected images processed using IMARIS (Bitplane, Switzerland) and assembled using Microsoft PowerPoint. LD were counted from Z-stacks (0.5 µm optical sections, with a total stack of up to 7 µm) of 45 cells per sample.

4.5.4. Lipid analysis

Seeds were imbibed (or not) at 22°C under continuous light in the presence or absence of radiolabelled acetate (2µCi/ assay). After 24h of imbibition (or not), the seeds were heated to 70°C in isopropanol for 15 min to inactivate lipases, and ground using an ultra-Turax. Lipids were extracted three times by chloroform:methanol (1:1, v/v) at room temperature, and then washed three times with 0.9% NaCl. The solvent was evaporated under N_2 and lipids were dissolved in an appropriate volume of chloroform:methanol (1:1, v/v). Polar lipids were separated by HPTLC (60F254 plates, Merck, Darmstadt, Germany), using the solvent system methyl acetate:n-propanol:chloroform:methanol:0.25% aqueous KCl (25:25:25:10:9, v/v) according to (Heape et al., 1985), and neutral lipids were separated by HPTLC using a solvent system hexane:ethylether:acetic acid (90:15:2, v/v) (Laloi et al., 2007). Lipids

were identified by co-migration with known standards and quantified by densitometric analysis (Macala et al., 1983) using a TLC scanner 3 (CAMAG, Muttenz, Switzerland) after primuline staining (van Echten-Deckert, 2000). For more precise quantification, individual lipids were scrapped off the HPTLC plates and their fatty acids were determined and quantified by gas chromatography after conversion to the corresponding methyl esters by hot methanolic H_2SO_4 according to Browse et al., 1986. Fatty acid quantification was performed by incorporating a C17 internal standard.

When required, radiolabelled acetate was added and radiolabelled lipids were separated by HPTLC and analyzed using a Storm PhosphorImager (GE Healthcare) and the ImageQuant software (Applied Biosystems).

For yeast lipid analysis, *S. pombe* cells were grown in YD medium overnight (OD_{600} of 0.37x20 for WT cells and 0.11x20 for mutant cells) and then pelleted by centrifugation at 5000 g for 10 min. The pelleted cells were washed, resuspended in sterile water and disrupted with glass beads using TissueLyser II (Qiagen) for 3 x 30s. Proteins were quantified using BCA (total proteins 6.6 mg for WT and 1.9 mg for mutant) followed by lipids extraction by chloroform:methanol (2:1, v/v) at room temperature. The extracted lipids were washed 3 times with 0.9% NaCl, lyophilized and then resuspended in 200 µl chloroform:methanol (1:1, v/v). Neutral lipids were separated on HPTLC plate, eluted with hexane:diethyl ether: acetic acid (90:15:2, v/v) for quantification as above.

4.5.5. Extraction and ^{1}H-NMR analysis of polar compounds

Polar metabolites were extracted from 30 mg of lyophilized powder with an ethanol-water series at 80°C (Moing et al., 2004). The supernatants were combined, dried under vacuum and lyophilized. Each lyophilized extract was solubilized in 500 µL of 200 mM deuterated potassium phosphate buffer solution pH 6.0, containing 3mM ethylene diamine tetra-acetic acid disodium salt (EDTA), titrated with KOD solution to pH 6 when necessary, and lyophilized again. The lyophilized titrated extracts were stored in darkness under vacuum at room temperature, before ^{1}H-NMR analysis which was completed within one week.

For ^{1}H-NMR analysis, 500 µL of D_2O with sodium trimethylsilyl-[2,2,3,3-d_4]-propionate (TSP, 0.01% mg/mL final concentration for chemical shift calibration) were added to each lyophilized titrated extract. The mixture was centrifuged at 17700*g* for 5 min at room temperature. The supernatant was then transferred into a 5 mm NMR tube for acquisition. Quantitative ^{1}H-NMR spectra were recorded at 500.162 MHz and 300 K on an Avance III spectrometer (BrukerBiospin, Wissembourg, France) using a 5mm ATMA broadband inverse probe, a 90° pulse angle and an electronic reference for quantification (Digital ERETIC, Bruker TopSpin 3.0). The assignments of metabolites in the NMR spectra were made by comparing the proton chemical shifts with literature or database values (Fan, 1996; Ulrich et al., 2008; Ferry-Dumazet et al., 2011; Wishart et al., 2013), and by comparison with spectra of authentic compounds and by spiking the samples. For absolute quantification, two calibration curves (glucose and fructose: 1.25 mM to 50 mM) were prepared and analyzed under the same conditions. The glucose calibration was used for the quantification of all compounds, as a function of the number of protons of selected resonances, except fructose that was quantified using its own calibration curve. The metabolite concentrations were calculated using AMIX (version 3.9.14, Bruker) and Excel (Microsoft, Redmond, WA, USA) software.

4.6. Author's contribution

P.M. and H.B. conceived and designed the experiments, all authors contributed experimental data, D.R., P.M. and H.B. analyzed and discussed the data, P.M. and H.B. wrote the paper and H.B. supervised the research.

4.7. Accession numbers

Sequence data from this article can be found in The Arabidopsis Information Resource (TAIR: http://www.arabidopsis.org/) under the following accession number AtTSPO (AT2G47770), and in the Scientific Resource for fission yeast (PomBase: http://www.pombase.org) under the following accession number SPBC725.10.

4.8. Acknowledgements

We thank Dr. D. Hermand (Université de Namur, Belgium) for generously providing the *S. pombe* strains, D. Masquelier for her technical assistance, F. Doignon for the help in growing *S. pombe* strains for the neutral lipid analyses, and the imaging platform IMABIOL (ISV/UCL). Lipid analyses were performed at the CGFB Bordeaux Metabolome Facility- MetaboHUB (ANR-11-INBS-0010). This work was partly funded by the Wallonia-Brussels Federation Joint Research Action (ARC grant #11/16-036 to H.B.), and the Belgian Funds for Scientific Research (FNRS) (CR grant #19516174 and PDR grant # 6794930 to H.B.). V.V was a FNRS postdoctoral researcher and H.B. is a Senior Research Associate of the FRS-FNRS. This work was also partly funded by the CNRS and the University of Bordeaux (L.M-P. and P.M.). S.M. was supported through an ANR grant (BLAN07-1_182875) to P.M.

4.9. Supplemental figures

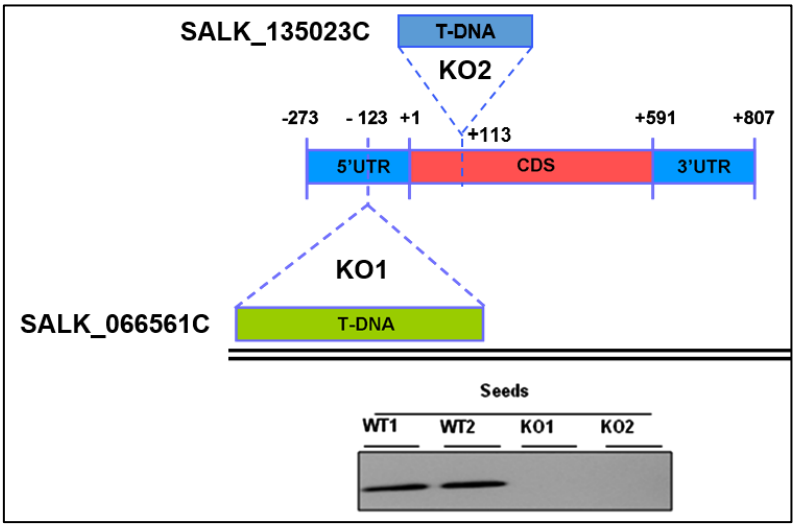

Figure 4.S1. Characterization of AtTSPO TDNA insertional mutant lines used in this study.

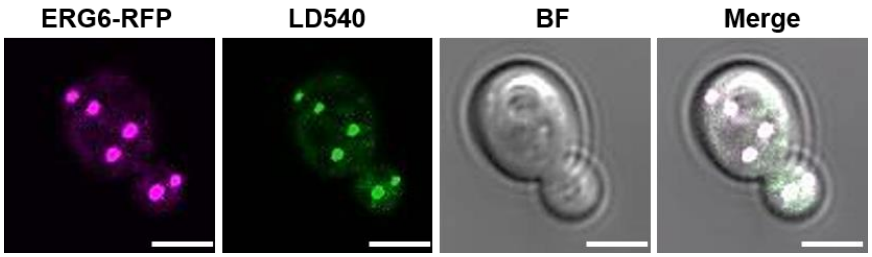

Figure 4.S2. LD540 is a lipid droplet-specific fluorescent dye.

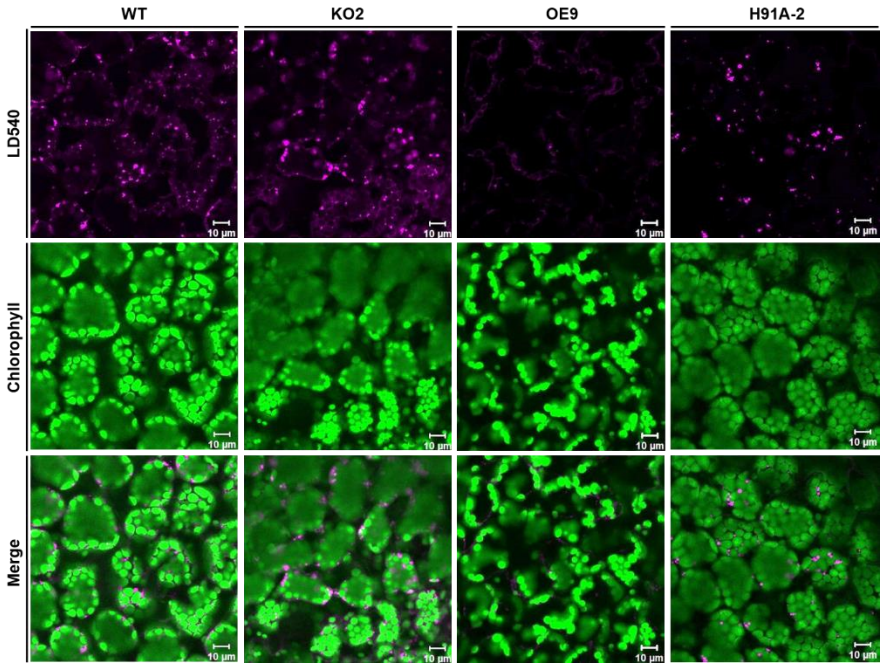

Figure 4.S3. Independent transgenic Arabidopsis lines showed the same lipid droplet phenotype as in figure 4.2.

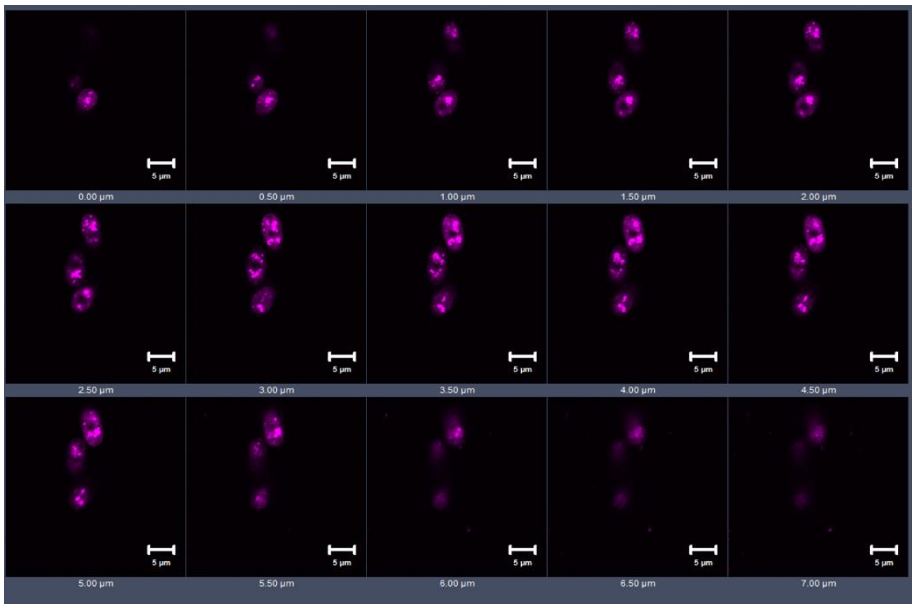

Figure 4.S4: Representative Z-stack confocal images used for lipid droplets quantification in yeast. Scale bar = 5 µm.

4.10. Model for AtTSPO-dependent modulation of storage lipids levels

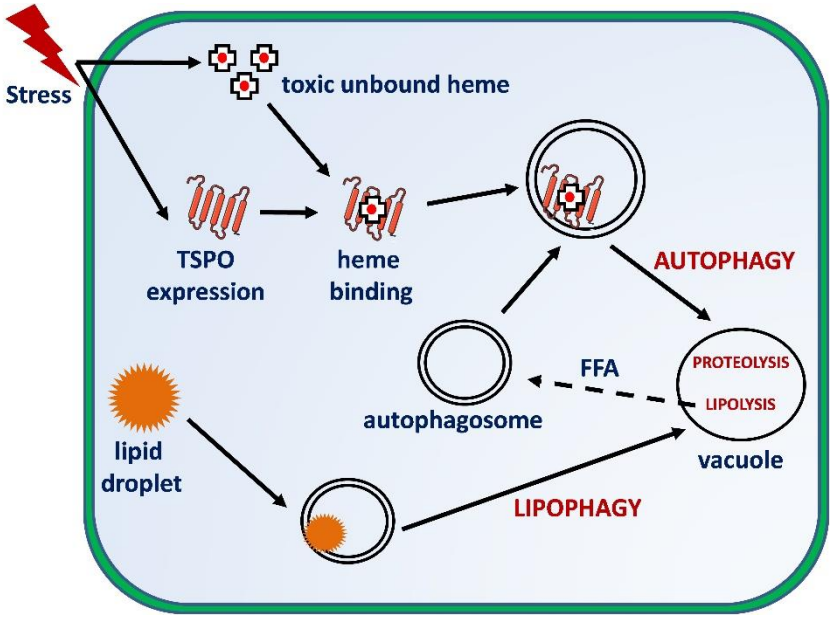

Figure 4.10. Proposed model of AtTSPO-dependent lipid droplets breakdown. Abiotic stress conditions upregulate the levels of unbound cytosolic toxic porphyrins. In parallel, AtTSPO expression is induced and the protein binds free heme. Heme binding and an active autophagy pathway are the prerequisites of AtTSPO degradation and heme scavenging. Lipid droplets comprise a huge pool of lipids which upon lipophagy and subsequent lipolysis in the vacuole come back as free fatty acids that contribute to the autophagosome formation. Enhanced degradation of AtTSPO boosts the breakdown of lipid droplets, which was not the case for AtTSPO^{H91A}, a stable form of AtTSPO. We speculate (not shown in the scheme) that the presence of AtTSPO during reserve accumulation in the seed can enhance LD levels as revealed by the contrast between KO and OE seeds in term of LD levels. Dashed arrow indicates a multistep process.

The cellular level of AtTSPO is tightly regulated in the plant cell, and the protein is readily degraded through a selective autophagy pathway. The potential detrimental physiological effects of a continuous presence of AtTSPO in the plant cell are not yet fully understood. We demonstrated that overexpression of AtTSPO resulted in an increase in fatty acids levels in dry seeds and that constitutive expression of AtTSPO reduced lipids and carbon reserves in germinating seed or seedling. In contrast, inactivation of AtTSPO enhanced LD levels in the same tissues. These observations seem not to be peculiar to plant TSPO since we were able to reproduce the data using yeast cells. Indeed, inactivation of the *S. pombe* TSPO homolog resulted in an increased number of LD and enhanced sensitivity to cerulenin.

The effect of AtTSPO in vegetative tissues seems similar to what was recently described in animal cells. The level of mitochondrial TSPO1 was shown to be downregulated in adipose tissues of mouse models of obesity as compared to control animals. In addition, knockout of TSPO1 in mouse steroidogenic cells resulted in the accumulation of LD. We suggest that TSPO proteins may play an evolutionarily conserved regulatory role in lipids homeostasis.

Lipids are perceived as not only a reservoir of cellular energy or building blocks for biological membranes, but also as potential messengers in cellular processes of signal recognition and transduction. One group of purely signaling lipids are phosphoinositides. These molecules comprise less than 1% of total cellular pool of lipids but they greatly control many processes in the plant cell, some of them being relevant to stress perception and response. Sequence analysis of plant TSPO indicates that these proteins have evolved an N-terminal domain composed of 30-50 amino acid residues. Intriguingly, approximately half of these residues are charged and the overall charge of the N-terminal extension is positive. We were curious, whether AtTSPO could bind any of the plant phospholipids. It is known in the literature that such positively charged protein domains can generate specific or pleiotropic binding to signaling anionic lipids. We addressed the function of the N-terminus of AtTSPO in light of protein-protein interaction underlying the response to osmotic stress.

Chapter 5: Functional divergence within TSPO family: the role of a plant-specific conserved N-terminal extension as a PI(4,5)P_2 effector domain

Manuscript under consideration for Nature Communications

Pawel Jurkiewicz[1], Lucile Senicourt[2], Olivier Lequin[2], Jean-Jacques Lacapere[2] and Henri Batoko[1*]

[1] Louvain Institute of Biomolecular Science and Technology (LIBST), UCLouvain, Croix du Sud 4-5, L7.07.14, 1348 Louvain-la-Neuve, Belgium.

[2] Sorbonne Université, École Normale Supérieure, PSL University, CNRS, Laboratoire des Biomolécules, 4 place Jussieu, 75005 Paris, France.

5.1. Abstract

The function of conserved Translocator proteins (TSPO) is still highly debated after more than four decades of investigation. These membrane proteins may have evolved to fulfil certain cell type-specific functions or mechanisms to respond to various types of cellular stress. However, no experimental data are available to mechanistically explain functional divergence among these enigmatic proteins. *Arabidopsis thaliana* Translocator-related protein (AtTSPO) is a stress-induced membrane protein with a plant-specific polybasic N-terminal extension. We showed previously that the plasma membrane aquaporin PIP2;7 interacts with AtTSPO *in vivo* and undergoes AtTSPO-dependent autophagic degradation during osmotic stress. We show herein that purified AtTSPO, the plant-specific N-terminal extension alone, or a chimeric mouse TSPO variant containing the plant-specific N-terminus, can bind PI(4,5)P_2 *in vitro* and modify the level of PIP2;7 molecules at the plasma membrane *in vivo*. Expression of AtTSPO but not mouse TSPO delocalized a PI(4,5)P_2 biosensor from the plasma membrane to the Golgi membranes, where AtTSPO is localized in the plant cell. Deletion of the plant-specific N-terminal extension or defined point mutations affecting PI(4,5)P_2 binding prevented AtTSPO-PIP2;7 interaction *in vivo*. These findings support a functional divergence of plant TSPO from their bacterial and animal counterparts via the evolutionary acquisition of a lipid-interacting N-terminal extension and define AtTSPO as PI(4,5)P_2 effectors in plants.

5.2. Introduction

Translocator proteins (TSPO) are polytopic membrane proteins that are found in organisms ranging from prokaryotes to humans (Kreps et al., 2002; Seki et al., 2002; Zimmermann et al., 2004; Papadopoulos et al., 2006; Guillaumot et al., 2009; Fan et al., 2012; Li et al., 2015; Guo et al., 2015). The primary structure of TSPO is evolutionarily conserved and consists of five α-helical transmembrane segments that form the TspO/MBR domain (Jaremko et al., 2014; Li et al., 2015; Guo et al., 2015). Although TSPO have been extensively studied since their discovery in the 1970s (Braestrup and Squires, 1977), varying findings across species and

experimental models have resulted in an unclear picture of the exact molecular functions of TSPO.

The best-studied TSPO is the animal isoform TSPO1, an 18 kDa protein localized to the outer mitochondrial membrane. TSPO1 is involved in various cellular processes including cell proliferation and differentiation, apoptosis, immunomodulation, tetrapyrrole biosynthesis, oxidative stress and mitochondrial physiology (Anholt et al., 1986; Mukhin et al., 1989; Krueger and Papadopoulos, 1990; Rupprecht et al., 2010). The best-characterized biological role of TSPO1 is in steroidogenesis, in which it has been shown to be indispensable, based on its involvement in binding and transport of cholesterol from the cytosol to the inner mitochondrial membrane (Mukhin et al., 1989; Krueger and Papadopoulos, 1992; Li and Papadopoulos, 1998). The recognition of cholesterol by TSPO1 requires presence of the so-called cholesterol recognition amino acid consensus (CRAC), encompassing the end of the fifth transmembrane segment (Li and Papadopoulos, 1998; Jamin et al., 2005). Although bacterial TSPO have also been shown to bind cholesterol *in vitro*, the CRAC domain is not conserved among plant TSPO (Li and Papadopoulos, 1998). Despite reports suggesting that TSPO1 is encoded by an essential gene, recent findings (Morohaku et al., 2014; Sileikyte et al., 2014; Stocco, 2014) revealed that a lack of TSPO1 had no effect on cultured cells or animal viability and did not alter steroidogenesis, contradicting the widely-held view of an essential physiological role for TSPO1 in animal cells. Nevertheless, recent studies have suggested the involvement of TSPO1 in lipid metabolism in animal cells (Thompson et al., 2013; Taylor et al., 2014; Fan et al., 2015; Tu et al., 2016). High expression of TSPO1 has been consistently found in steroid-producing cells and conditional deletion of TSPO1 in steroidogenic cells results in the accumulation of lipid droplets (Fan et al., 2015). The involvement of TSPO1 in mitochondrial physiology is also under debate (Morin et al., 2016; Zhao et al., 2016; Gatliff et al., 2017). Additionally, TSPO1 knockout in a Leydig cell line resulted in increased mitochondrial fatty acid oxidation (FAO) and upregulation of FAO-associated genes (Tu et al., 2016).

TSPO have also been described in plants (Corsi et al., 2004; Lindemann et al., 2004; Guillaumot et al., 2009; Vanhee et al., 2011). The termini of TSPO are evolutionary divergent, supporting functional divergence across species: an extended C-terminus is unique to animal TSPO, while higher plant TSPO have a plant-specific N-terminal extension of variable length (>30 residues). These plant-specific N-terminal extensions are structurally divergent but share the common property of being rich in charged residues and, in particular, in basic residues with an overall net positive charge. Functional studies of plant TSPO and structure-function analysis of bacterial and mammalian TSPO (Jaremko et al., 2014; Li et al., 2015; Guo et al., 2015) suggest that these proteins act in sensing and responding to stress . TSPO involvement in stress homeostasis could be a conserved ancestral function of these proteins with some species-dependent mechanistic variation (Batoko et al., 2015; Li et al., 2016). The *Arabidopsis thaliana* TSPO (AtTSPO) is transiently induced by abiotic stress such as osmotic stress or by the stress phytohormone abscisic acid (ABA) (Kreps et al., 2002; Seki et al., 2002; Guillaumot et al., 2009; Vanhee et al., 2011). AtTSPO is encoded by a single intronless gene and is highly regulated both at the transcriptional and post-translational levels. AtTSPO transcripts peak rapidly (3-6 hours) after ABA treatment, and the induced protein is actively degraded by a selective autophagy pathway and becomes undetectable approximately 72 hours after ABA-dependent induction (Vanhee et al., 2011; Finkelstein, 2013). AtTSPO localizes mainly in the Golgi membranes but can also be found in the ER membranes of the plant cell (Guillaumot et al., 2009). The time-limited presence of AtTSPO in the plant cell may contribute to the osmotic stress response. Indeed, we showed previously that AtTSPO physically interacts with the highly expressed plasma membrane aquaporin PIP2;7 in the Golgi membranes (Hachez et al., 2014). Under osmotic stress, AtTSPO interacts with PIP2;7 molecules *en route* to the plasma membrane. The resulting protein complex is subsequently targeted to the vacuole via the autophagic pathway. Therefore, under osmotic stress conditions, AtTSPO-dependent regulation of PIP2;7 reduces water transport activity at the plasma membrane of the plant cell.

The signaling network underlying plant responses to water-related stresses involves lipids and, in particular, phosphoinositides (Munnik and Nielsen, 2011; Heilmann and Heilmann, 2015; Heilmann, 2016). Chemically, phosphoinositides (PIs) are phosphorylated phosphatidylinositols and account for less than 1% of the total cellular pool of membrane phospholipids (Munnik and Nielsen, 2011). Five of the seven naturally occurring PIs have been identified in plants (Munnik and Nielsen, 2011): three monophosphorylated (PI3P, PI4P and PI5P) and two bisphosphorylated isomers (PI(3,5)P_2 and PI(4,5)P_2). Although considered minor cellular phospholipids, PIs are important signaling molecules that regulate membrane trafficking, endo/exocytosis, autophagy and ion channels, among other things (Kihara et al., 2001; Liu et al., 2005; Zoncu et al., 2007; Tan et al., 2016). Elevated levels of both PI(3,5)P_2 and PI(4,5)P_2 were reported in response to salt-induced hyperosmotic stress (Zonia and Munnik, 2004). In particular, genetic and biochemical studies have shown that plant responses to white light illumination involve an increase in PI(4,5)P_2 in the plasma membrane of guard cells, which induces stomatal opening, and hence, enhances evapotranspiration. An increased PI(4,5)P_2 level in the plasma membrane of stomatal guard cells was responsible for anion channel inhibition (Lee et al., 2007). Interestingly, PI(4,5)P_2 is also a key regulator of autophagy, as demonstrated in mammalian cells. Autophagosomes have a kinase that generates PI(4,5)P_2, and the autophagy regulator ATG14 interacts with both the kinase and its product during autophagosome initiation. PI(4,5)P_2 binding to ATG14 regulates ATG14 interaction with VPS34 and Beclin 1/ATG6, a protein complex catalysing the production of PI3P at the autophagosome initiation site (Tan et al., 2016). The regulatory role of PIs affects the localization and function of proteins with specific PI-binding domains such as FYVE (Fab1/YOTB/Vac1/EEA1) finger, phox homology (PX) and pleckstrin homology (PH) domains (Munnik and Nielsen, 2011). In plants, several proteins have been demonstrated to interact with PIs via such domains (Agorio et al., 2017). In addition to these specific interacting domains, linear or spatial polybasic stretches within some regulatory proteins can

generate pleiotropic or specific functional electrostatic interactions with PIs (Zheng et al., 2002).

In this work, we present evidence demonstrating that the evolutionarily conserved plant-specific polybasic N-terminus of AtTSPO binds PI(4,5)P_2, and that this binding regulates both the interaction with PIP2;7 *in vivo* and the subsequent degradation of the protein complex through selective autophagy. Interestingly, addition of the plant-specific polybasic N-terminus to mouse TSPO1 conferred binding properties to PI(4,5)P_2 and regulated PIP2;7 in plant cells.

5.3. Results

5.3.1. The N-terminal extension of AtTSPO is necessary for protection from plant tissue dehydration

AtTSPO expression is higher during osmotic stress. However, this expression is only transient in plant tissues. We showed previously that expressed AtTSPO could physically interact with defined aquaporin molecules intracellularly, *en route* to the plasma membrane, resulting in a reduction in water transport across the plasma membrane during osmotic stress (Hachez et al., 2014). Consistent with these findings, we also showed that the constitutive expression in plant cells of AtTSPO or of the more stable point mutant variant AtTSPO (H91A) resulted in transgenic plants exhibiting reduced water loss compared to wild-type plants when subjected to dehydration. This physiological role and the underlying molecular mechanism appear to be unique to plant TSPO. We wondered whether this phenomenon is associated with the plant-specific N-terminal extension.

To investigate this possibility, we generated transgenic plants overexpressing a truncated version of AtTSPO that lacks the first 41 amino acids (p35S::Venus-AtTSPO$^{\Delta N}$), and compared the water loss exhibited by these plants to that of wild-type (WT) plants, AtTSPO knockout (KO) plants, and available transgenic plants expressing either AtTSPO constitutively (p35S::AtTSPO) or the stable point mutant variant (p35S::AtTSPO^{H91A}) (Figure 5.1). Plants grown on agar plates (nearly 100% humidity) were transferred to a filter paper and then allowed to

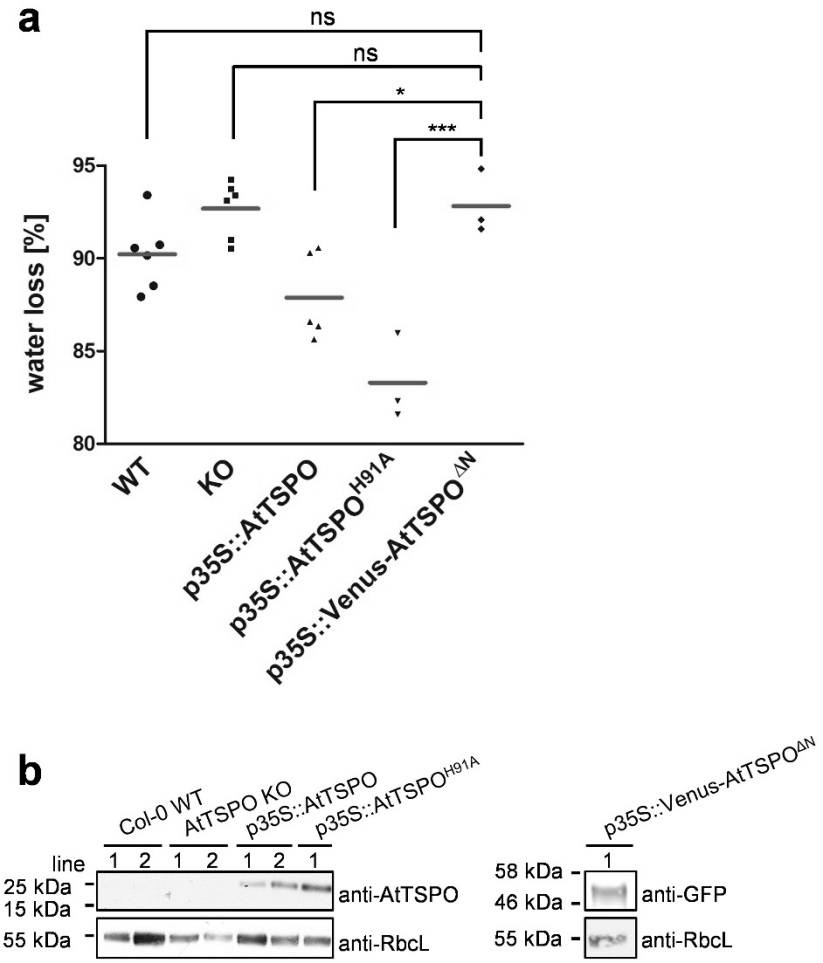
a
ns
ns
*
***
water loss [%]
95
90
85
80
WT
KO
p35S::AtTSPO
p35S::AtTSPO H91A
p35S::Venus-AtTSPO ΔN
b
Col-0 WT
AtTSPO KO
p35S::AtTSPO
p35S::AtTSPO H91A
p35S::Venus-AtTSPO ΔN
line
1 2 1 2 1 2 1
1
25 kDa
15 kDa
55 kDa
anti-AtTSPO
anti-RbcL
58 kDa
46 kDa
55 kDa
anti-GFP
anti-RbcL

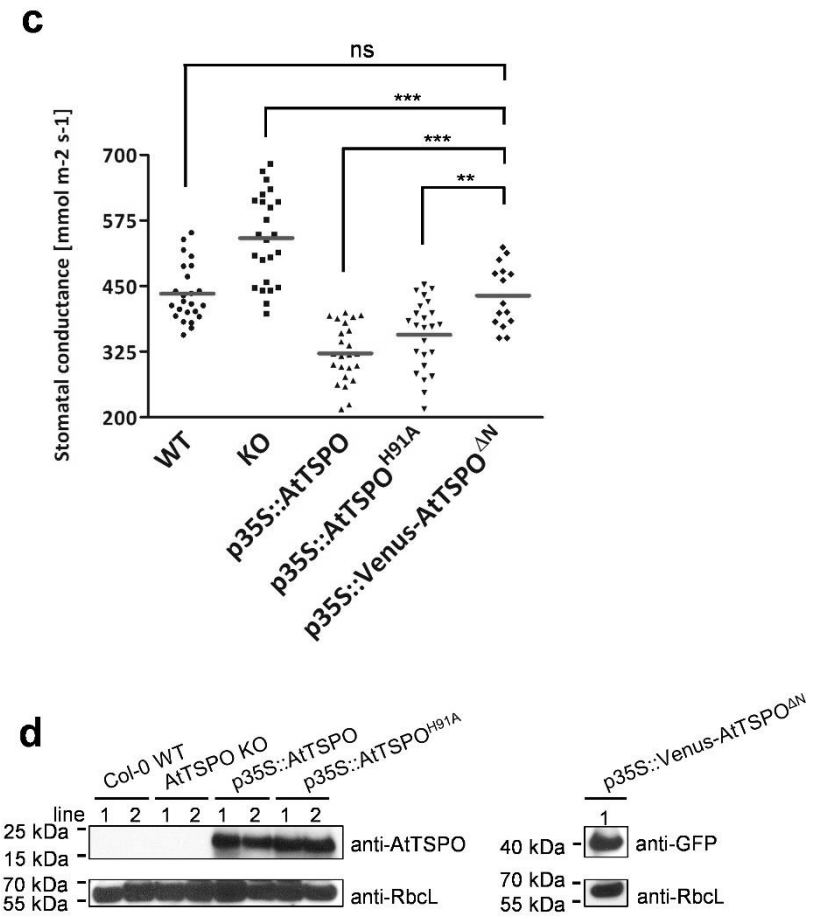

Figure 5.1. Arabidopsis plants expressing the N-terminus truncated AtTSPO are more affected by water loss as compared to plants overexpressing the full-length AtTSPO. (a) Percentage of water loss after 120 min from 7 day-old seedlings grown *in vitro* and subjected to dehydration on weighing paper at room temperature. WT, wild-type; KO, TDNA insertional knockout line for AtTSPO; p35S::AtTSPO, AtTSPO overexpressing line; p35S::AtTSPO^{H91A}, transgenic line overexpressing a stable form of AtTSPO, harboring the point substitution H91A; p35S::Venus-AtTSPO$^{\Delta N}$, line overexpressing a Venus-tagged N-terminus truncated variant of AtTSPO. Two independent lines of WT, KO and AtTSPO overexpressing plants were used and one line of plants overexpressing AtTSPO^{H91A} and Venus-AtTSPO$^{\Delta N}$. Lines were tested in triplicates (30-50 seedlings as a replicate). Shown are individual measurements and the grey horizontal line defines the mean for each data set. For statistical significance evaluation one-way ANOVA followed by Tukey's test was performed. *, $p<0.05$; ***, $p<0.001$; ns, not significant. **(b)** Western blot performed on total protein extracts from seedlings assayed in water loss experiment. **(c)** Stomatal conductance recorded from intact leaves of soil-grown mature plants under phytotron conditions. Genotypes are as in **a**. Two

independent lines of WT, KO, AtTSPO and AtTSPO^{H91A} overexpressing plants were used and one line of plants overexpressing Venus-AtTSPO$^{\Delta N}$. For each line, we tested 4 plants (2-3 rosette leaves per plant). Shown are individual measurements and the grey horizontal line defines the mean for each data set. Statistical analysis conducted as in **a**; additionally **, $p<0.01$. **(d)** Western blot performed on total protein extracts from leaves assayed in stomatal conductance experiment.

dehydrate at room temperature, after which their relative water loss was measured after up to 2 hours of incubation (Figure 5.1a). Under conditions of dehydration, we found that, as expected, KO seedlings had the highest water loss, while p35S::AtTSPO and p35S::AtTSPO^{H91A} plants had the lowest. Notably, we found no significant difference in water loss between WT plants and p35S::Venus-AtTSPO$^{\Delta N}$ plants, suggesting that deletion of the plant-specific N-terminus abolished the impact of the constitutive expression of AtTSPO on the regulation of water loss by the transgenic plants. Consistent with prior findings, tagging the protein at the N-terminus had no effect on this property of AtTSPO (Hachez et al., 2014) (see also below). We also verified transgene expression in all the lines used (Figure 5.1b and 5.1d).

Since water loss is associated with evapotranspiration through stomatal opening (which is regulated by the ABA signaling pathway), we next examined the stomatal conductance of mature plants of the same lines grown on soil. Stomatal conductance measurements on rosette leaves after they had bolted (Figure 5.1c) revealed a correlation with the level of water loss observed in the seedlings grown *in vitro* (Figure 5.1a), indicating that the N-terminal extension is required for regulation of water loss mediated by constitutively expressed AtTSPO. Thus, constitutive expression of AtTSPO had a physiological impact on stomatal opening.

5.3.2. The N-terminal extension of AtTSPO is required for the interaction with PIP2;7 *in planta*

Since AtTSPO-mediated reduction in water loss appears to require the N-terminal extension of AtTSPO, and since we have previously shown that AtTSPO interacts with PIP2;7 *in vitro* (Hachez et al., 2014), we decided to examine whether the N-terminal extension was required for this interaction *in vivo*. To this end, we conducted a bimolecular fluorescence complementation (BiFC) experiment using constructs depicted in Figure

5.2a. While interaction of full-length AtTSPO-containing construct with a complementing PIP2;7-containing construct was easily detectable, no detectable BiFC signal was observed with the truncated AtTSPO construct lacking the first 41 residues at the N-terminus (Figure 5.2b). As shown previously (Hachez et al., 2014), the interaction of AtTSPO and PIP2;7 is visible in the ER and Golgi membranes (Figure 5.2b), and the truncated AtTSPO localized to the Golgi membranes (Supplemental Figure 5.S1). Expression of all the tested constructs was verified by western blot (Figure 5.2c), and quantification of the BiFC signal (Figure 5.2d) suggested that the Venus fluorescence detectable with the truncated construct was reduced to that of background levels (see also Figure 5.S2 for smaller deletions and Figure 5.S3 for the signal quantification methodology). We conclude that truncation of the N-terminus abolished the AtTSPO-PIP2;7 interaction *in vivo*.

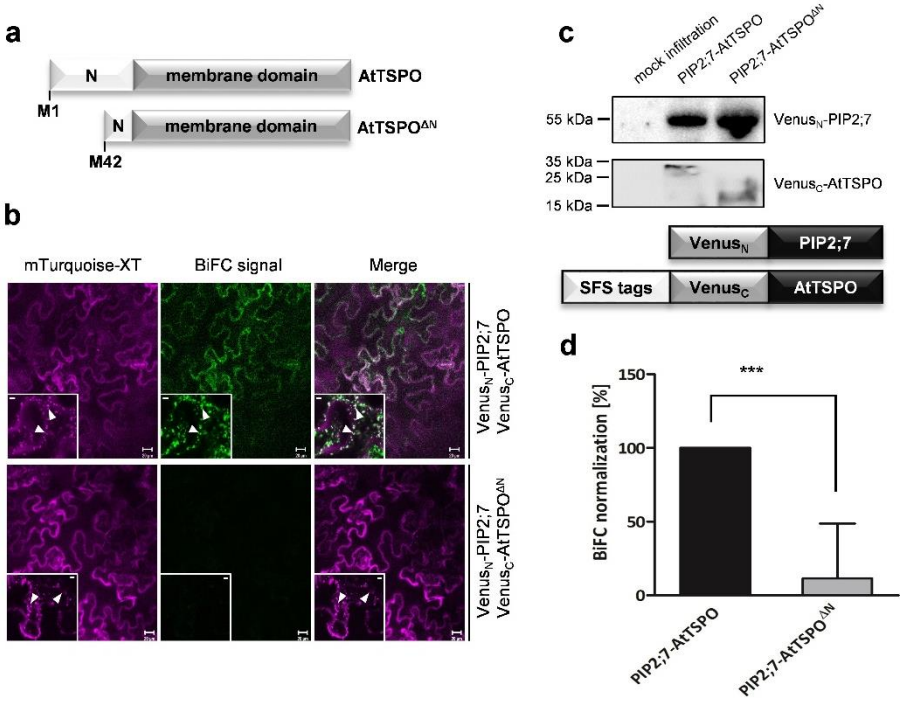

Figure 5.2. The plant specific N-terminus extension of AtTSPO is required for AtTSPO interaction with the Arabidopsis PIP2;7 *in vivo*. (a) Schematic representation of AtTSPO genetic constructs prepared for BiFC. As a positive control we used both full-length PIP2;7 and AtTSPO. N-terminus truncated variant starts with the methionine at the

position 42. **(b)** Representative confocal images of tobacco epidermal cells transiently coexpressing $Venus_N$-PIP2;7 and $Venus_C$-AtTSPO or $Venus_N$-PIP2;7 and $Venus_C$-AtTSPO$^{\Delta N}$. Xylosyltransferase-mTurquoise fluorescent chimera (in magenta) was imaged as a cell transfection control (Golgi marker) and for signal quantification purposes. Low magnification images qualitatively demonstrate the occurrence or lack of BiFC (in green) and the insets with high magnification images show Golgi stacks (arrowheads). Bars = 20 µm and 5 µm for low and high magnification, respectively. Experiment was repeated three times. **(c)** Western blot from total extracts of infiltrated leaves areas imaged in BiFC approach. PIP2;7 expression was detected by anti-GFP. AtTSPO full-length and truncated form were detected by anti-FLAG (the StrepII-FLAG-SrepII tags fusion, coined SFS in this figure, was originally cloned upstream $Venus_C$). Non-infiltrated leaf area was used as a negative control. **(d)** Quantification of the signal shows a drastic reduction of BiFC and hence interaction between PIP2;7 and truncated AtTSPO mutant (grey histogram) as compared to full-length AtTSPO (black histogram). For statistical significance evaluation, an independent samples t-test was performed using Graphpad Prism. ***, $p<0.001$.

5.3.3. Modification of PIP2;7 abundance at the plasma membrane by AtTSPO requires the plant-specific N-terminal extension

Since overexpression of AtTSPO was previously seen to drastically reduce the abundance of PIP2;7 at the plasma membrane (Hachez et al., 2014), we decided to test if the N-terminal extension of AtTSPO is required for this observed depletion. We extracted plasma membrane-enriched fractions (Supplementary Figure 5.S4) from Arabidopsis suspension cell lines stably expressing GFP-tagged full-length AtTSPO and AtTSPO$^{\Delta N}$, and assessed the relative abundance of PIP2;7 in these preparations by immunoblotting. We used the plant plasma membrane H+-ATPase (PMA) to normalize the data. Consistent with our prior findings, the plasma membrane fraction from positive control cells expressing full-length AtTSPO exhibited significantly lower amounts of PIP2;7 than did untransformed cells (Figure 5.3b). However, no reduction in PIP2;7 levels was seen in AtTSPO$^{\Delta N}$-expressing cells in comparison to wild-type cells, suggesting that the core membrane-bound TspO/MBR domain of TSPO is not required for PIP2;7 depletion.

Since the N-terminal extension of TSPO is unique to plants, we decided to test the species specificity of this requirement by adding the plant-specific N-terminal extension to mouse TSPO1 homologue by generating a chimeric AtTSPO^{Nter}-mTSPO construct. As with the AtTSPO constructs, the chimeric construct also localized within Golgi membranes in the plant cell (data not shown). In contrast to the unaltered mouse TSPO1 construct that did not elicit reduction in levels of PIP2;7, expression of

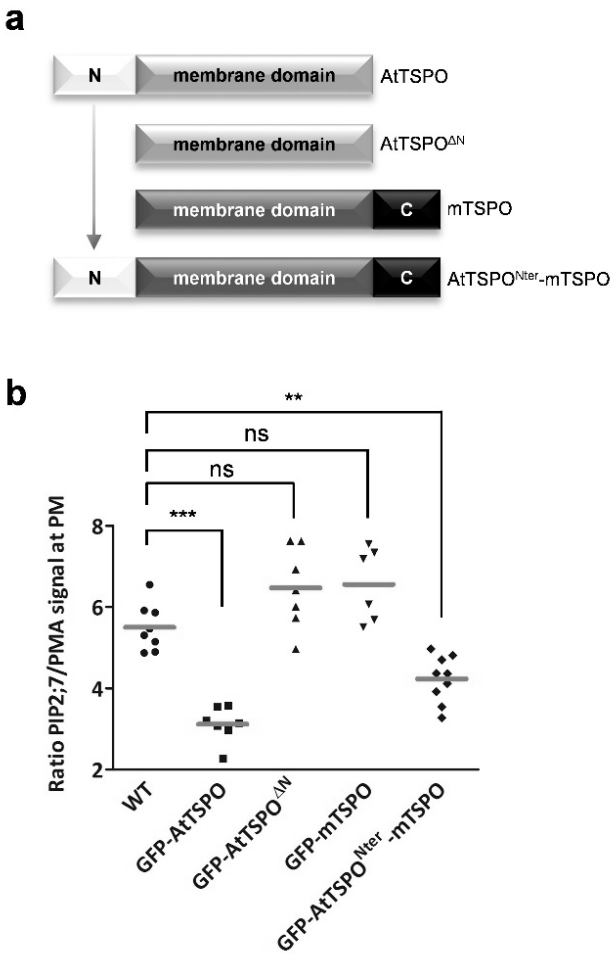

Figure 5.3. Modification of the aquaporin PIP2;7 abundance at the plasma membrane requires the plant-specific N-terminus extension. (a) Schematic representation of genetic constructs expressed stably in Arabidopsis suspension cells. To assess the function of AtTSPO N-terminus, we used the mouse homolog (mTSPO) as a negative control and as a carrier protein for the plant N-terminus. Each construct was N-terminally tagged with GFP. **(b)** Plasma membrane fractions were extracted from Arabidopsis suspension cells and relative amount of PIP2;7 aquaporin was assessed by western blotting. Plasma membrane proton ATPase (PMA) was used as reference protein for the signal quantification. Shown are individual measurements (PIP2;7 signal normalized against PMA signal from 6-9 replicates coming from two independent plasma membrane preparations) and the grey horizontal line defines the mean. Statistical significance analysis was performed with one-way ANOVA followed by Tukey's test. **, $p<0.01$; ***, $p<0.001$; ns, not significant.

the chimeric construct led to decreased levels of PIP2;7 in the plasma membrane. However, the efficiency of reduction (~30%) was lower that

seen with full-length AtTSPO (~60%) (Figure 5.3b), indicating some functional specificity of the N-terminal extension to plants. We conclude that the TSPO-dependent PIP2;7 depletion from the plasma membrane requires the plant-specific polybasic N-terminal extension.

5.3.4. AtTSPO binds defined signaling lipids via its positively charged N-terminus

The N-terminal extension of higher plants TSPO is rich in arginine and lysine residues, although the overall amino acids conservation is relatively low as exemplified in Figure 5.4a. It is well documented in the literature that such positively charged regions could generate electrostatic interactions with negatively charged molecules, for instance with anionic lipids (Zheng et al., 2002). As shown in Figure 5.4b, we performed lipids overlay using purified full-length AtTSPO and commercially available spotted membrane and anionic lipids (PIP strip).

a

b

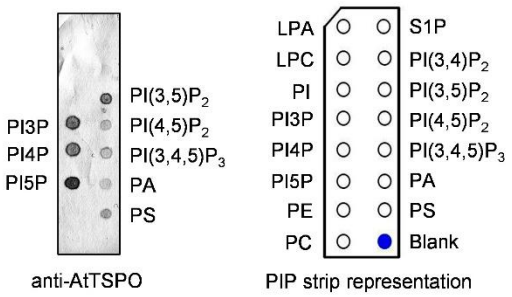

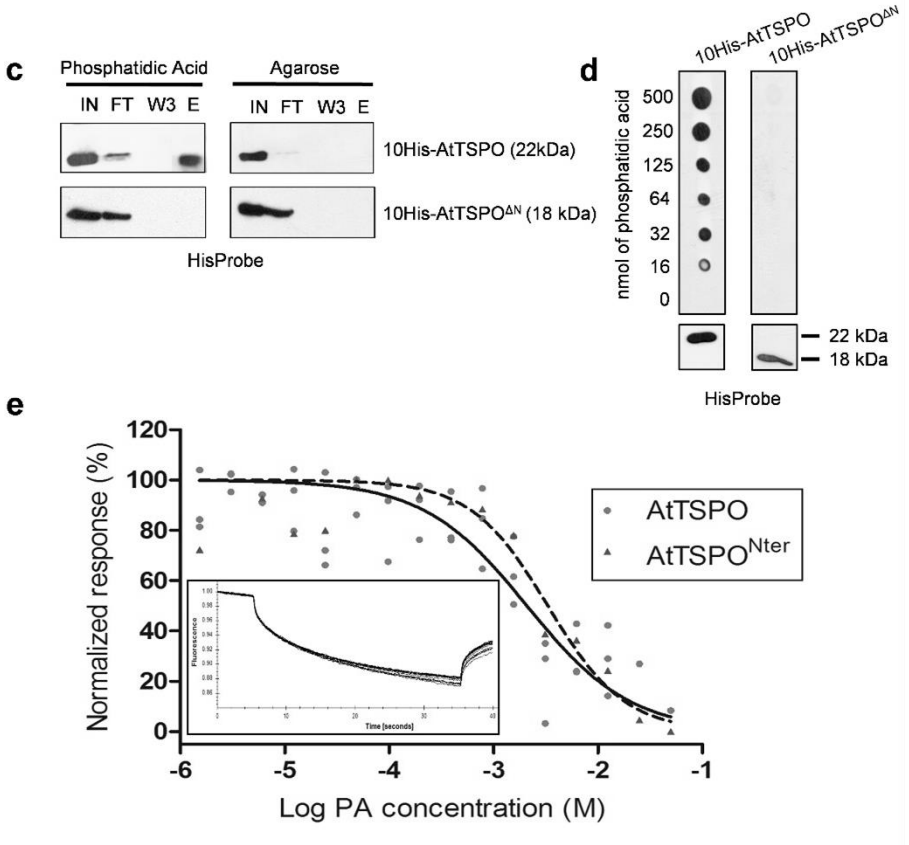

Figure 5.4. Purified AtTSPO binds defined anionic lipids *in vitro* and the binding requires the N-terminal peptide. (a) The higher plants-specific N-terminal extension of TSPO proteins is positively charged. ClustalW alignment of 50 N-terminal amino acids of higher plants (monocots and dicots) TSPO. At, *Arabidopsis thaliana*; Es, *Eutrema salsugineum*; St, *Solanum tuberosum*; Ca, *Capsicum annuum*; Zm, *Zea mays*; Os, *Oryza sativa*; Ta; *Triticum aestivum*; Pt; *Populus trichocarpa*. Positively charged amino acids were highlighted in red (neutral pH) and the conserved lysine/arginine residues close to the first transmembrane domain were shown in grey rectangles. Mouse TSPO (Mm; *Mus musculus*) was added to illustrate no conservation of the elongated N-terminus nor the positively charged residues. **(b)** Initial screening of AtTSPO ligands yielded several candidates from the group of anionic lipids. AtTSPO purified from the yeast was incubated with spotted lipids in PIP Strip overlay assay (right panel; PA, phosphatidic acid; LPA, lyso-PA; PC, phosphatidylcholine; LPC, lyso-PC; PI, phosphoinositol; PE, phosphatidylethanolamine; S1P, sphingosine phosphate; PS, phosphatidylserine) followed by the detection with anti-AtTSPO antibodies (left panel). **(c)** The plant specific N-terminal extension is involved in AtTSPO-anionic lipids interaction *in vitro.* Lipid-dependent pull-down of AtTSPO. Purified AtTSPO or AtTSPO$^{\Delta N}$ (IN) were incubated with PA or agarose resin (negative control). The flowthrough (FT) was collected and after washes (last wash W3) fractions were eluted (E) and probed using HisProbe. **(d)** Ten histidine-tagged AtTSPO or N-terminus truncated AtTSPO expressed and solubilized from yeast microsomes were incubated with spotted gradient of phosphatidic acid

concentrations followed by the detection with HisProbe. The bottom panel shows a control detection of both proteins. **(e)** Thermophoresis analyses of AtTSPO full-length and the N-terminal peptide titrated against phosphatidic acid concentrations. Protein samples were labeled by the red fluorescent dye NT-647-NHS (Nanotemper Technologies, Germany). Non-linear fit of changes in thermophoresis signal of labeled full-length protein (continuous line) yielded a K_d of 2.1 ± 0.4 mM while the fit for the N-terminal peptide (dotted line) yieleded a K_d of 3.3 ± 0.9 mM. The rectangular insert is a representative record of the fluorescence over time (5 seconds cold, 30 seconds hot, 5 seconds cold). Shown are all the recorded data points (AtTSPO in dots, AtTSPO$^{\Delta N}$ in triangles).

The purified AtTSPO appeared to bind all the spotted phosphoinositides but one, PI(3,4)P_2, and also phosphatidic acid (PA) and phosphatidylserine (PS) (Figure 5.4b). To confirm the possible interaction with anionic lipids and the putative involvement of the positively charged N-terminus extension of AtTSPO in these interactions, we used PA as a representative anionic lipid for further analyses *in vitro*. We used pull-down assay and immobilized PA (Figure 5.4c) and a membrane spotted gradient of PA (Figure 5.4d) to show that indeed purified AtTSPO binds PA *in vitro*. The interaction requires the 41 first amino acids of the protein, since the truncated variant of AtTSPO, AtTSPO$^{\Delta N}$, devoid of its plant-specific N-terminus extension, could not bind PA anymore (Figure 5.4d). Next, we expressed and purified the N-terminus peptide (first 49 residues) of AtTSPO almost to homogeneity (Supplemental Figure 5.S5) and compared its PA binding capacity to that of full-length AtTSPO using microscale thermophoresis (MST; Figure 5.4e). This approach bases on the detection of a temperature-induced change in fluorescence of a target molecule in function of the concentration of a non-fluorescent ligand. The observed change in fluorescence is due to directed movement of particles in a microscopic temperature gradient and can be affected by binding events. Any change of the chemical microenvironment of the fluorescent probe, as well as changes in the hydration shell of biomolecules result in a relative change of the fluorescence detected when a temperature gradient is applied and can be used to determine binding affinities. As shown in Figure 5.4e, the N-terminus peptide alone could bind PA, albeit with a slightly lower affinity as compared to the full-length AtTSPO (K_d of 2.1 mM for the purified AtTSPO and 3.3 mM for the peptide). These results suggest that

the plant specific N-terminal extension of AtTSPO is responsible for the binding to defined anionic lipids *in vitro* probably through electrostatic/hydrogen bond interactions (Kooijman et al., 2007).

Among the phosphoinositides that AtTSPO bound to (Figure 5.4b), we were particularly interested in PI(4,5)P_2, as its roles in ABA signaling, plant osmotic stress responses (Zonia and Munnik, 2004); and autophagosome initiation (Tan et al., 2016) suggest mechanistic links to the autophagic regulation of stress-induced AtTSPO-PIP2;7 interaction (Hachez et al., 2014). Using thermophoresis measurements, we checked whether the N-terminal peptide of AtTSPO is required for AtTSPO-phosphoinositide interactions (Figure 5.5a). Titration of histidine-tagged full-length AtTSPO and truncated AtTSPO$^{\Delta N}$ against a range of PI(4,5)P_2 concentrations revealed a decrease in fluorescence for full-length AtTSPO, indicating that it bound PI(4,5)P_2 (Figure 5.5a). In contrast, no binding was observed with AtTSPO$^{\Delta N}$ (Figure 5.5a). Additionally, no binding was observed between full-length AtTSPO and phosphatidylcholine (PC), indicating specificity of interaction with PI(4,5)P_2.

Next, we checked whether the purified N-terminus of AtTSPO (AtTSPO^{Nter}) alone is sufficient for the interaction with PI(4,5)P_2 (Figure 5.5b). Using a lipid overlay technique, we observed that both the full-length AtTSPO (consistent with previous observations) and its derived N-terminal peptide could bind to PI3P, PI4P and PI(4,5)P_2. In contrast, and interestingly, mouse TSPO did not bind PI(4,5)P_2, suggesting that the binding determinant for PI(4,5)P_2 is not within the membrane domain of TSPO that is conserved between species. The chimeric mouse TSPO protein (AtTSPO^{Nter}-mTSPO) whose N-terminus is extended with the plant-specific N-terminal extension could bind PI(4,5)P_2, albeit with relatively reduced affinity compared to that of full-length AtTSPO or its N-terminal peptide alone (Figure 5.5c). We used PI3P as the positive control lipid for testing the binding activity of all the purified protein variants. Together, these data demonstrate that the plant-specific N-terminus of AtTSPO is a *bona fide* determinant for binding to PI(4,5)P_2 and other phosphoinositides.

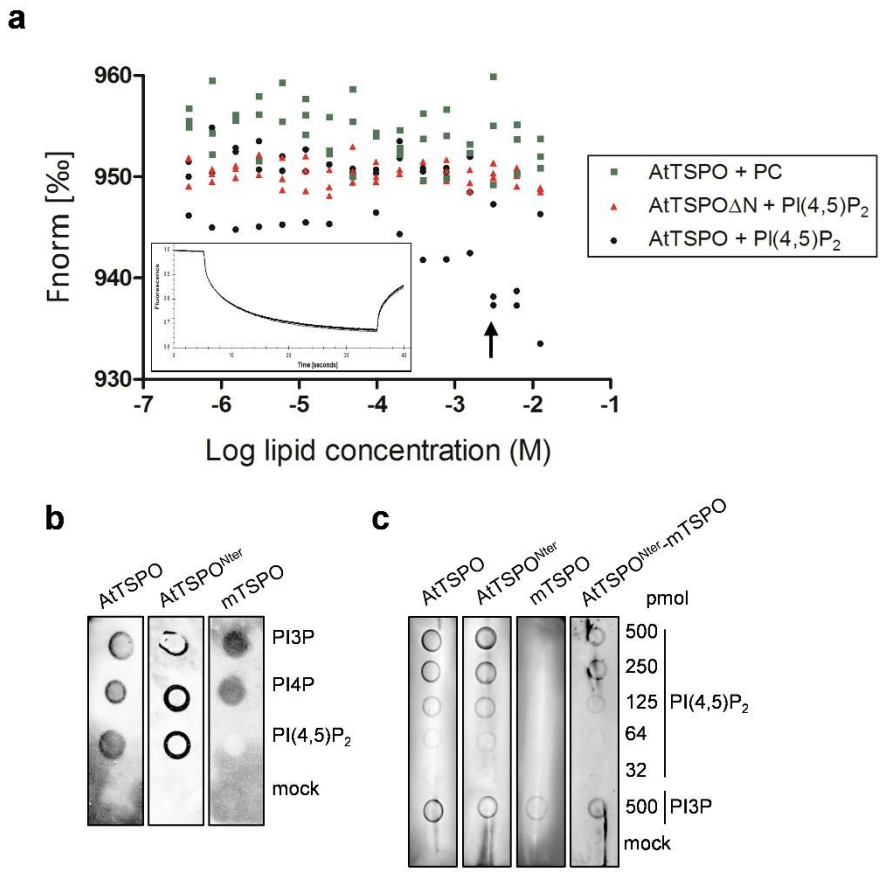

Figure 5.5. The AtTSPO N-terminal peptide is a PI(4,5)P_2 lipid binding moiety. **(a)** The N-terminus truncated AtTSPO cannot bind PI(4,5)P_2 *in vitro*. Thermophoresis analyses of TSPO full-length and N-terminal deletion titrated against PI(4,5)P_2 concentrations. Protein samples were labeled through their polyhistidine tags by the RED-tris-NTA dye (Nanotemper Technologies, Germany). The thermophoretical movement of labeled TSPO increases (normalized fluorescence decreases) upon binding of PI(4,5)P_2. Phosphatidylcholine was used as a negative control lipid. Both data sets: AtTSPO + PI(4,5)P_2 and AtTSPO$^{\Delta N}$ + PI(4,5)P_2 were compared using two-way ANOVA followed by the Bonferroni multiple comparison post-hoc test. The threshold of lipid concentration that gives rise to statistical significance of the data ($p<0.01$) is 1.56 mM (indicated by the arrow). Non-linear regression-based modeled K_d of AtTSPO-PI(4,5)P_2 interaction is 2.3 ± 0.7 mM. The rectangular insert is a representative record of the fluorescence over time (5 seconds cold, 30 seconds hot, 5 seconds cold). Shown are all the recorded values. **(b)** Purified mouse TSPO homolog lacking the plant-specific N-terminus does not bind PI(4,5)P_2 *in vitro* in contrast to plant full-length protein and isolated N-terminal peptide. Five hundred pmol of given phosphoinositide was spotted on nitrocellulose membrane, incubated with purified proteins followed by detection with anti-AtTSPO (for isolated N-terminus) or HisProbe (for AtTSPO and mTSPO). Two percent DDM (n-dodecyl-β-D-maltoside) was used as a mock control. **(c)** Adding the plant AtTSPO N-terminus to the mouse TSPO resulted in a chimeric protein capable of binding PI(4,5)P_2 *in vitro.* Purified proteins were incubated with a gradient of PI(4,5)P_2 concentrations and

detected using anti-AtTSPO antibodies (for N-terminal peptide and N-terminus attached to mTSPO) and HisProbe (for AtTSPO and mTSPO). PI3P was spotted as a positive control for mTSPO binding. Two percent DDM was used as a mock control. Experiments in **b** and **c** were performed at least two times.

5.3.5. AtTSPO-mediated localization shift of a PI(4,5)P_2 biosensor from the plasma membrane to the Golgi membrane requires the N-terminal extension

The subcellular distribution of plant phosphoinositides is membrane specific (Hammond et al., 2012; Holthuis and Menon, 2014; Simon et al., 2014). Under normal growth conditions, PI(4,5)P_2 is mainly localized at the plasma membrane in Arabidopsis (Simon et al., 2014), while AtTSPO is found in the endoplasmic reticulum and in the Golgi apparatus (Guillaumot et al., 2009) (Supplemental Figure 5.S1). In order to understand which subcellular compartment is involved in the interaction between AtTSPO and PI(4,5)P_2, we used a plant-validated genetically encoded PI(4,5)P_2-specific biosensor (Simon et al., 2014). We first generated stable transgenic lines of Arabidopsis suspension cells that expressed a double mCherry-tagged PI(4,5)P_2-binding domain from phospholipase C, and under the control of a mild constitutive promoter, to limit possible interference with the cell physiology. Using ABA treatment to mimic osmotic stress conducive to AtTSPO expression (Guillaumot et al., 2009), we observed a partial redistribution of the PI(4,5)P_2 biosensor from the plasma membrane to the cytosol, suggesting a possible depletion of the lipid pool from the membrane or a concomitant catabolism and reduced biosynthesis of PI(4,5)P_2 after ABA treatment (Supplemental Figure 5.S8).

To investigate whether the expression of AtTSPO could modify the distribution of PI(4,5)P_2 in the plant cell, we retransformed the PI(4,5)P_2 biosensor-expressing cells with GFP-tagged AtTSPO or AtTSPO$^{\Delta N}$ under the control of a constitutive CaMV p35S promoter. Confocal imaging revealed that in the absence of AtTSPO, the biosensor localized to the periphery of expressing cells, which is consistent with a previous report showing that this construct mainly localized to the plasma membrane (Simon et al., 2014) (Figure 5.6a, upper panels, control cells). Notably, in cells coexpressing GFP-AtTSPO (Figure 5.6a, middle panels), little or no

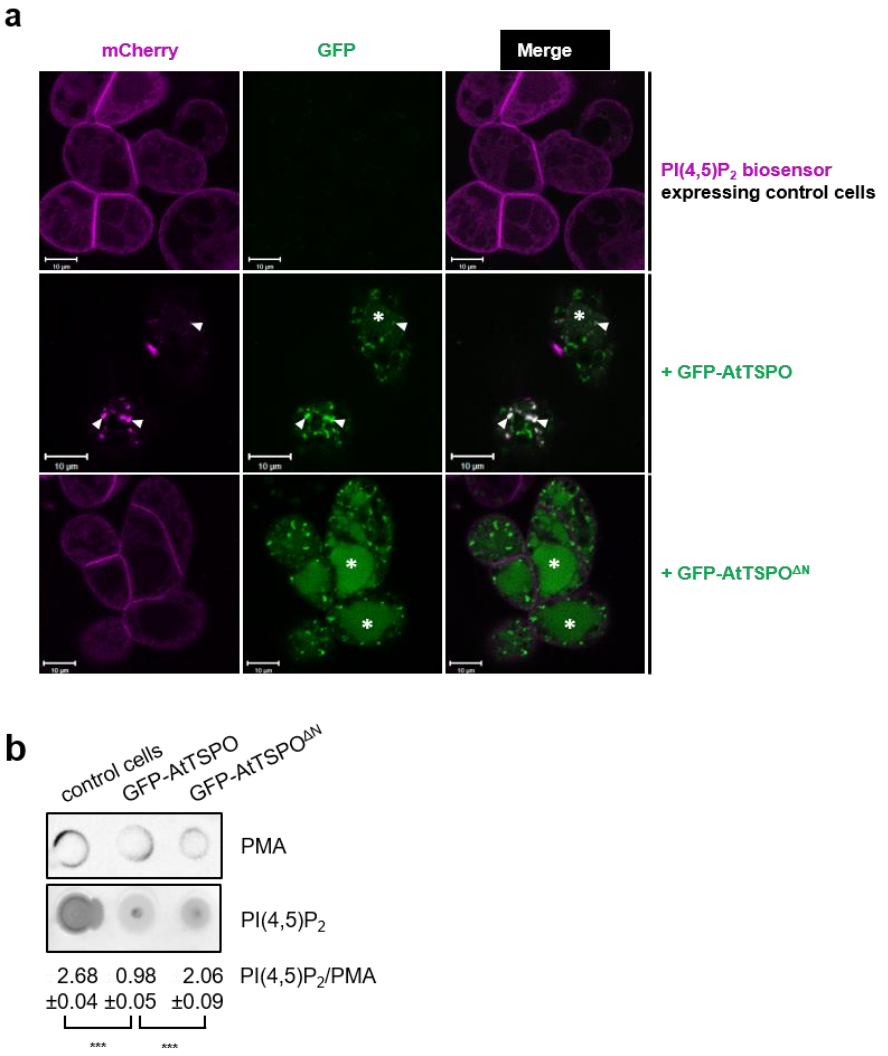

Figure 5.6. In presence of the full-length AtTSPO but not AtTSPO$^{\Delta N}$, the PI(4,5)P_2 biosensor was depleted from the plasma membrane and partially colocalized with AtTSPO in the Golgi membranes. (a) Representative confocal images of Arabidopsis suspension cells stably coexpressing the PI(4,5)P_2 biosensor (mCherry-tagged double pleckstrin homology domain from phospholipase C; in magenta) and the full-length AtTSPO or AtTSPO$^{\Delta N}$ (GFP-tagged; in green). The arrowheads indicate mCherry and GFP signals colocalizing at Golgi membranes. * indicate GFP fluorescence in the vacuole. Bars = 10 µm. See Supplemental Figure 5.S10 for colocalization profile. **(b)** Solubilized plasma membrane-enriched fractions from cells as imaged in (**a)** were spotted on nitrocellulose membrane and relative level of PI(4,5)P_2 was detected using monoclonal anti-PI(4,5)P_2 antibodies (Enzo Life Sciences, USA). For signal quantification (ImageJ 1.51 software) we used plasma membrane proton ATPase (PMA) as a control. Statistical significance analysis was performed with one-way ANOVA followed by Tukey's test. ***, $p<0.001$. Data is the mean and SD of three technical replicates. Experiment was performed two times.

PI(4,5)P_2 biosensor fluorescence could be detected at the cell periphery, but instead, strong fluorescence could be seen within the cell in mobile punctate structures. The biosensor colocalized with the GFP-AtTSPO on the punctate structures, which we identified to be Golgi stacks, as GFP-AtTSPO is mainly localized in the Golgi membranes (Guillaumot et al., 2009). In contrast, coexpressing the truncated form of AtTSPO (GFP-AtTSPO$^{\Delta N}$) (Figure 5.6a, bottom panels) had no distinct effect on the distribution of the biosensor fluorescence. GFP fluorescence from the full-length AtTSPO or the truncated form could also be detected in cell vacuoles (asterisks), suggesting that truncation of the plant-specific N-terminus of AtTSPO did not preclude its targeting to and degradation in the vacuole.

To check whether, as suspected (Supplemental Figure 5.S8), expression of AtTSPO results in a reduction in the levels of PI(4,5)P_2 at the plasma membrane, we prepared plasma membrane-enriched fractions from the tested cell lines and probed these fractions in a dot blot experiment for their PI(4,5)P_2 content using a specific antibody against this lipid (Yakir-Tamang and Gerst, 2009) (Figure 5.6b). We used an anti-H+-ATPase (PMA) to normalize the quantified signal. The expression of AtTSPO resulted in a reduction of approximately two-thirds in the levels of PI(4,5)P_2 in the plasma membrane-enriched fraction. In comparison, levels of PI(4,5)P_2 were reduced by 23% when the N-terminus truncated AtTSPO was expressed (Figure 5.6b). These results suggest that the plant-specific N-terminus is required for efficient AtTSPO-induced depletion of PI(4,5)P_2 from the plasma membrane and its co-localization with AtTSPO in Golgi membranes.

Since the biosynthesis of PI(4,5)P_2 is catalyzed by PI4P 5-kinase at the plasma membrane via the phosphorylation of PI4P (Munnik and Vermeer, 2010), we hypothesized that AtTSPO-induced accumulation of PI(4,5)P_2 in the Golgi membranes is associated with the enrichment of a PI4P 5-kinase and the relatively low levels of PI4P present within the Golgi compartment (Simon et al., 2014). We transiently expressed an mCherry-tagged human PI4P 5-kinase (mCherry-HsPIPK1α) and compared its localization in wild-type tobacco with that in tobacco plants stably expressing YFP-AtTSPO. No difference in subcellular localization of

the kinase was observed, suggesting that AtTSPO-dependent enrichment of PI(4,5)P_2 in the Golgi membranes may not be a consequence of the mistargeting of a PI4P 5-kinase to this compartment (Supplementary Figure 5.S9). It is possible that AtTSPO acts as a PI(4,5)P_2 effector whose expression in the Golgi membranes initiates the enrichment of PI(4,5)P_2 within that membrane compartment.

5.3.6. Lysine/arginine couples in the N-terminal extension of AtTSPO are required for both PI(4,5)P_2 binding and interactions with aquaporin PIP2;7 *in vivo*

In order to identify the key amino acid residues in the N-terminus of AtTSPO that are involved in the interaction with PI(4,5)P_2, we performed liquid NMR analysis of the 50-amino acid purified N-terminus labelled with ^{15}N and ^{13}C (Supplementary Figure 5.S5). The good spectral quality of the purified peptide (Figure 5.7a) allowed for effective recording of the 2D and triple resonance 3D spectra needed to gain full ^{1}H, ^{15}N, and ^{13}C assignments. Chemical shift analysis revealed that the peptide was poorly structured and did not adopt a stable globular fold. Interestingly, calculation of the secondary structure propensity (SSP) score (Marsh et al., 2006) revealed that two regions (R15-R27 and D31-K45) had a significant tendency to form α-helices (Figure 5.7b). The N-terminal peptide showed no interaction with calcium or zwitterionic lipids (DMPC bicelles). In contrast, the peptide interacted with negatively charged bicelles (DMPG), as revealed by changes in HSQC spectra (Figure 5.7a), leading to an increased stabilization of the C-terminal R36-R45 helical segment (Figure 5.7b). The titration of the peptide with micelles of PI(4,5)P_2 induced larger changes in ^{1}H-^{15}N HSQC spectra than those observed with DMPG bicelles (Figure 5.7a and 5.7c) suggesting stronger interactions with PI(4,5)P_2. The ^{1}H-^{15}N cross-peaks of residues belonging to the 34-49 segment completely disappeared (Figure 5.7c), which indicates a tight association of the C-terminal region of the peptide with

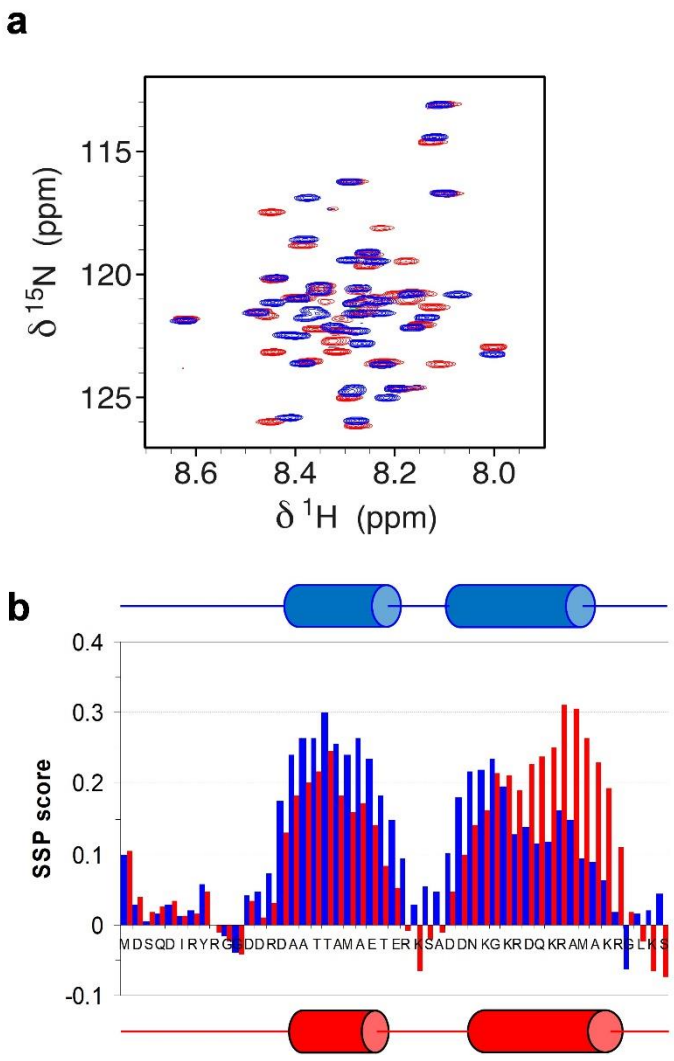
a
115
120
125
δ 15N (ppm)
8.6
8.4
8.2
8.0
δ 1H (ppm)
b
0.4
0.3
0.2
0.1
0
-0.1
SSP score

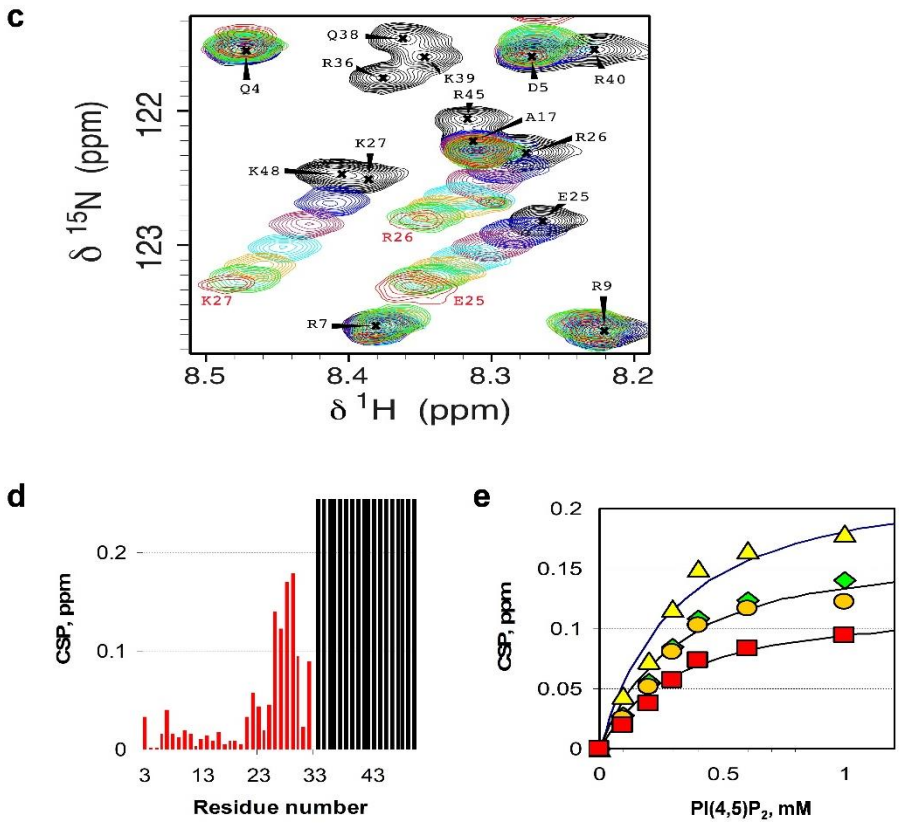

Figure 5.7. The recombinant AtTSPO N-terminal peptide interacts with anionic DMPG and PI(4,5)P_2 lipids. **(a)** 2D ^{1}H-^{15}N HSQC spectrum (500 MHz, 30° C) of 100 mM AtTSPO^{Nter} in the absence (blue) and in the presence (red) of 25 mM DMPG / 50 mM DHPC bicelles. **(b)** Secondary Structure Propensity (SSP) score in the absence (blue) and in the presence (red) of DMPG/DHPC bicelles. **(c)** Selected region in 2D ^{1}H-^{15}N HSQC showing different behaviours of residues upon titration of AtTSPO^{Nter} with increasing amounts of PI(4,5)P_2 (0 mM, black; 0.1 mM, blue; 0.2 mM, maroon; 0.3 mM, cyan; 0.4 mM, orange; 0.6 mM, green; 1 mM, red). Residues R36, Q38, K39, R40, K48 disappear at the first addition of PI(4,5)P_2 while residues E25, R26, K27 show progressive chemical shift perturbations. **(d)** ^{1}H,^{15}N Chemical Shift Perturbations (CSP) after addition of 1 mM PI(4,5)P_2. Residues 34-49 that disappear at the first point of the titration are indicated by grey shading. CSPs were calculated as |Dd(^{1}H)| + |Dd(^{15}N)|/10. **(e)** CSP of E26 (green squares), R27 (orange circles), K28 (yellow triangles), A30 (red squares) as a function of PI(4,5)P_2 concentration added.

PI(4,5)P_2. Other residues along segment 20-32 exhibited a progressive chemical shift variation upon titration, corresponding to a fast-exchange regime (Figure 5.7c and 5.7d). Monitoring these chemical shift perturbations upon titration (Figure 5.7d) allowed the estimation of a K_d

in the range of 0.15 mM for the interaction between these residues and PI(4,5)P_2.

Our analyses of the N-terminal extension of AtTSPO revealed several key amino acids that could interact with PI(4,5)P_2, with the C-terminal region of the peptide being most affected upon interaction. Interestingly, this segment contains three positively charged coupled lysine/arginine residues that could potentially contribute to the interaction at positions K35-R36, K39-R40, and K44-R45 (Figure 5.7c). To test our hypothesis that interaction with PI(4,5)P_2 is required for AtTSPO to interact with PIP2;7, we generated point substitutions of these residue couples and tested the binding strengths of the mutants to PIP2;7 by BiFC. Double substitution mutants AtTSPO$^{K35A/R36A}$ and AtTSPO$^{K39A/R40A}$ and a quadruple mutant AtTSPO$^{K39A/R40A/K44A/R45A}$ (Figure 5.8) were generated. A Golgi-localized xylosyltransferase tagged with the monomeric variant of a cyan fluorescent protein (mTurquoise) was used as a transfection control (Gookin and Assmann, 2014) and for both colocalization and normalization of the BiFC signal (Supplemental Figure 5.S3). As expected, coexpression of wild-type AtTSPO and PIP2;7 generated a mainly Golgi-localized BiFC signal (Figure 5.8a, upper panels, arrowheads). Notably, all the tested mutant combinations generated substantially lower BiFC signals (Figure 5.8a), less than 20% of the level generated by the wild-type protein (Figure 5.8b). These results suggest that mutations in residues putatively involved in PI(4,5)P_2 binding to the N-terminus of AtTSPO also reduced the efficiency of its interaction with aquaporin PIP2;7 *in vivo*.

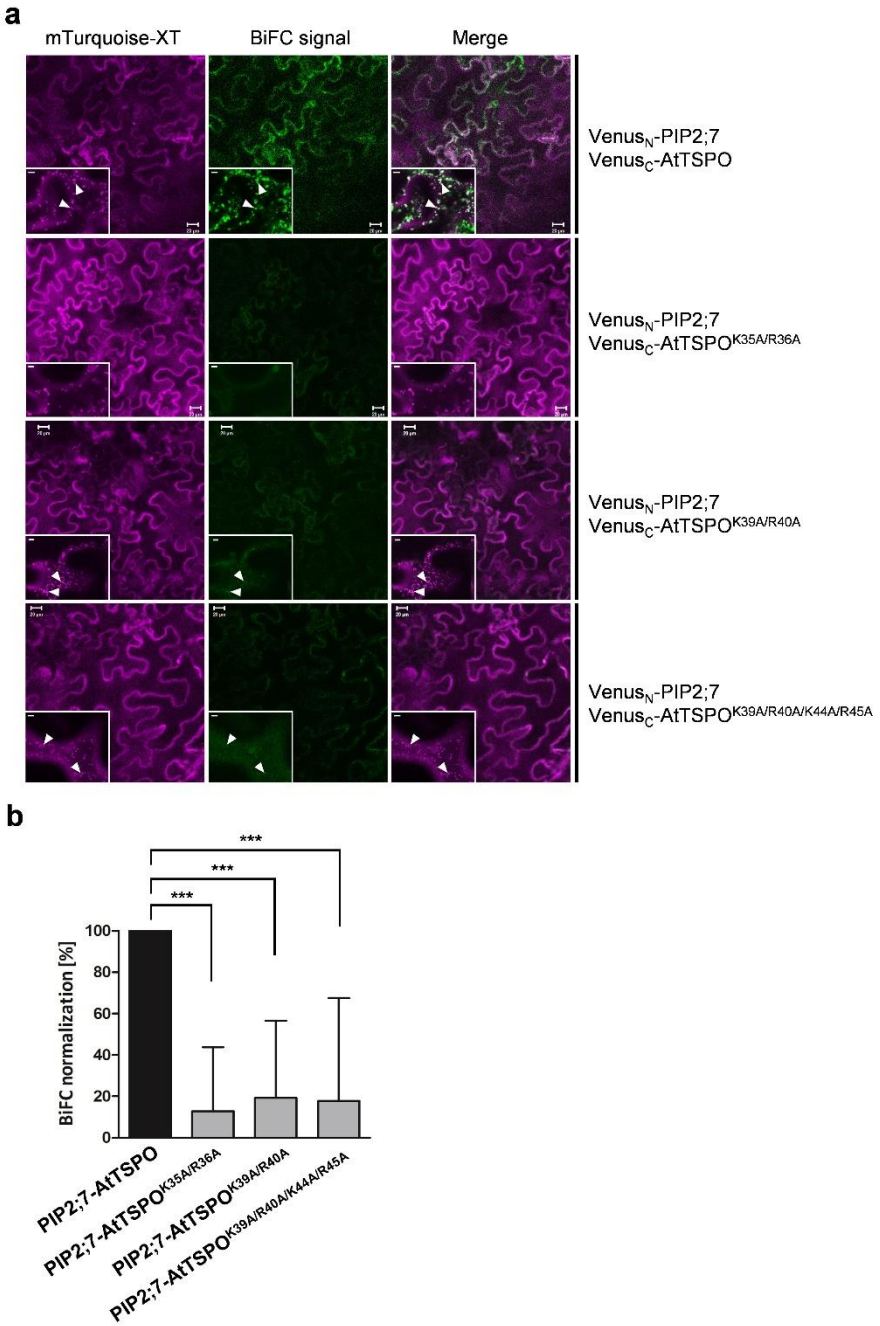

Figure 5.8. Defined positively charged lysine-arginine couples in the N-terminal region of AtTSPO are involved in its interaction *in vivo* with PIP2;7. **(a)** Representative confocal images of tobacco epidermal cells transiently coexpressing

Venus$_N$-PIP2;7 and Venus$_C$-AtTSPO or Venus$_N$-PIP2;7 and Venus$_C$-AtTSPO point mutants. Xylosyltransferase-mTurquoise fluorescent chimera (in magenta) was imaged as a cell transfection control (Golgi marker) and for signal quantification purpose. A combination of full-length PIP2;7 and AtTSPO were used as a positive control for the BiFC signal. Low magnification images qualitatively demonstrate the occurrence and distribution of BiFC (in green) in the transfected area and the insets with high magnification images show Golgi stacks (arrowheads). In case of PIP2;7-AtTSPO$^{K35A/R36A}$, no colocalization of the BiFC signal with the Golgi marker was detected. Bars = 20 µm and 5 µm for low and high magnification, respectively. Experiment was repeated three times **(b)** Quantitative data of the signal shows a drastic reduction of BIFC between PIP2;7 and AtTSPO mutants as compared to full-length AtTSPO. Statistical analysis based on one-way ANOVA followed by Tukey's test. ***, $p<0.001$. See supplemental data for quantification procedure.

5.3.7. PI(4,5)P_2 mediates AtTSPO-PIP2;7 interaction *in vitro*

To confirm that PI(4,5)P_2 is required for AtTSPO-PIP2;7 interaction, we used thermophoresis to monitor the contribution of PI(4,5)P_2 to the interaction *in vitro*. We used a transgenic line expressing Venus-PIP2;7 (Hachez et al., 2014) to solubilize the protein from the microsomal fraction and titrated the protein against AtTSPO concentrations in the presence and absence of PI(4,5)P_2 *in trans*. The thermophoretic dynamics of Venus-PIP2;7 were monitored via the fluorescence of the Venus tag. As shown in Figure 5.9, we did not observe an interaction between AtTSPO and Venus-PIP2;7 in the absence of PI(4,5)P_2 or in the presence of 50 µM phosphatidylcholine (Figure 5.9b, red and green points, respectively). In contrast, in the presence of 50 µM PI(4,5)P_2, Venus-PIP2;7 fluorescence increased (Figure 5.9b, black triangles), generating a 2 plateau-pattern against AtTSPO concentrations and clearly indicating the occurrence of a protein-protein interaction. Indeed, we could perform a non-linear fit of changes in Venus fluorescence only in presence of PI(4,5)P_2 (Figure 5.9c). These results demonstrate that AtTSPO-PIP2;7 interactions are modulated by PI(4,5)P_2.

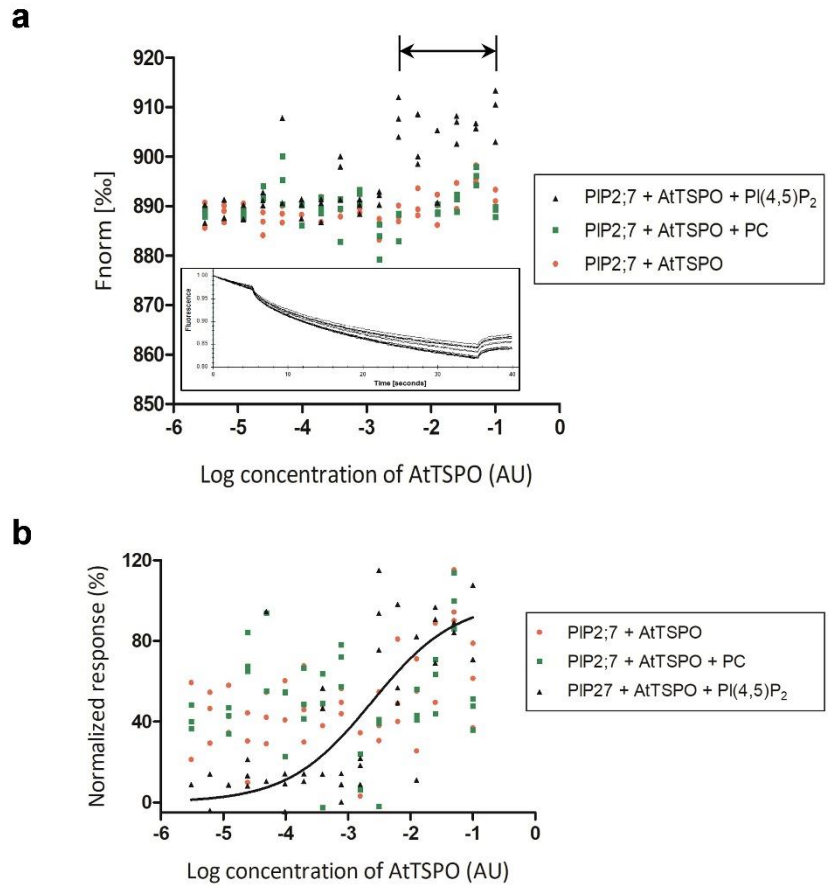

c

	PIP2;7 + AtTSPO	PIP2;7 + AtTSPO + PC	PIP2;7 + AtTSPO + PI(4,5)P_2
Hill slope value	0.1591	0.01414	0.6465
Statistical difference of Hill slope value over PIP2;7 + AtTSPO + PI(4,5)P_2	p=0.0011	p<0.0001	---

Figure 5.9. The AtTSPO-PIP2;7 *in vitro* interaction can only be detected in presence of PI(4,5)P_2. (a) Thermophoresis analyses of YFP-PIP2;7 titrated against AtTSPO concentrations. PIP2;7 movement was followed through the YFP fluorescence. Depending on experiment, 50 µM PI(4,5)P_2, phosphatidylcholine (PC, negative control) or no lipid was added. The thermophoretical motion of Venus-PIP2;7 decreases (normalized fluorescence increases) upon binding of AtTSPO in presence of 50 µM PI(4,5)P_2 but not PC nor in absence of lipids. Horizontal arrow indicates the bound-state plateau region. The rectangular insert is a representative recorded fluorescence timetrace. Shown are all recorded data points. **(b)** Data were normalized and fitted using non-linear regression

model yielding a typical sigmoidal binding curve only in presence of PI(4,5)P_2. **(c)** Hill slope values from **b** were compared statistically. Low p values indicate no steepness similarity between fitted curves.

5.4. Discussion

Owing to their conserved N-terminal extension, plant TSPO are structurally different from bacterial and animal TSPO. This study aimed at understanding the physiological role, if any, of the N-terminal extension found in plant TSPO, and its specific evolutionary significance. We discovered a previously unknown complex mechanism involving AtTSPO, the signaling lipid PI(4,5)P_2 and the highly expressed plasma membrane aquaporin PIP2;7, underlying the plant cellular response to dehydration.

TSPO involvement to stress response appears to be a common feature of these conserved proteins (Li et al., 2016). So far, a molecular mechanism explaining such a response and the cellular components involved has not been described in any cell type. We showed that when expressed, the plant AtTSPO reduces the level of a highly expressed aquaporin, PIP2;7, at the cell surface (Hachez et al., 2014) (Figure 5.3), as a mean of reducing water lost by the cell. This modulation of aquaporin levels at the cell surface requires the plan-specific N-terminal extension of AtTSPO. Interestingly, the mouse mitochondrial TSPO1 homolog (mTSPO) expressed in the plant cell did not affect the level of PIP2;7 at the cell surface. However, a chimeric version of the same protein ($AtTSPO^{Nter}$-mTSPO), containing the plant-specific N-terminus of AtTSPO, was able to lower the level of PIP2;7 at the plasma membrane (Figure 5.3). It may be that this conserved N-terminal extension of plant TSPO absent in animal and bacterial TSPO has through evolution, provided plant TSPO with a specific function related to cellular response and adaptation to osmotic stress.

Unexpectedly, we found that the N-terminal extension of AtTSPO binds the signaling lipid PI(4,5)P_2 *in vitro* and *in vivo*, and this binding is a prerequisite for AtTSPO intracellular physical and functional interaction with the aquaporin PIP2;7 (Figures 5.5, 5.6 and 5.7). Cells expressing AtTSPO showed accumulation of a PI(4,5)P_2 biosensor on the Golgi membrane instead of the plasma membrane as seen in control cells

or cells expressing a truncated version of AtTSPO devoid of its N-terminal extension. These results suggest that in presence of AtTSPO, the Golgi membrane become enriched in free PI(4,5)P_2 possibly at the expense of the plasma membrane. We did not find any significant difference between cells expressing AtTSPO and control cell for their overall PI(4,5)P_2 levels (Supplementary Figure 5.S11), but a net depletion of this lipid in the plasma membrane fractions of the cells expressing AtTSPO as compared to control cells or cells expressing the truncated variant of AtTSPO (Figure 5.6). Circumstantial observation suggested a positive correlation between PI(4,5)P_2 relative abundance in the plasma membrane, increased active aquaporins and increased osmotic water permeability of the plant cell plasma membrane (Ma et al., 2014). Consistent with these observations, expression of AtTSPO reduced the levels of PI(4,5)P_2 and PIP2;7 at the plasma membrane and hence reduced water loss by the corresponding transgenic plants as compared to wild type plants. It is not yet known whether PI(4,5)P_2 directly or indirectly modulates the structure-function of plasma membrane aquaporins although others channels are known to bind and are regulated by PI(4,5)P_2 (Chuang et al., 2001; Hilgemann et al., 2001; Liu et al., 2005; Lee et al., 2007). Free PI(4,5)P_2 are normally found in the plasma membrane as exemplified by the subcellular localization of the cognate biosensor and biochemical analyses (van Leeuwen et al., 2007; Simon et al., 2014; Heilmann and Heilmann, 2015). It has been debated whether intracellular PI(4,5)P_2 signaling exists in intracellular compartments of eukaryotic cells although increasing evidence supports specific and essential functions for intracellular PI(4,5)P_2 (Tan et al., 2015). PI(4,5)P_2 is poorly detected on intracellular compartments likely because of the lack of free PI(4,5)P_2 as it is bound to effectors that associate with its biosynthetic kinases (PI4P5Ks). This work provides evidence that the expression of AtTSPO triggers the accumulation of detectable levels of potentially free PI(4,5)P_2 on the Golgi membrane. It is not clear how this new intracellular PI(4,5)P_2 signaling platform is generated. PI(4,5)P_2 is an important regulatory lipid of the plasma membrane and little is known how cells regulate their plasma membrane levels of PI(4,5)P_2 more so in the plant cell. It was shown recently that the lipid transfer activity of defined ER-resident

oxysterol-binding proteins (ORP) is regulated by the plasma membrane levels of PI(4,5)P_2. In particular, the recruitment of ORP8 to ER-PM contact sites in mammalian cells is called only when PI(4,5)P_2 levels in the plasma membrane are high, to transfer its precursor (PI4P) back to the ER membrane and therefore slow their conversion to PI(4,5)P_2 (Sohn et al., 2018). In fact, after synthesis, plasma membrane PI4P can be either converted to PI(4,5)P_2 or be delivered to the ER by ORP5/8 proteins to be dephosphorylated by ER-resident phosphatases (Sohn et al., 2018). Generated PI(4,5)P_2 in intracellular membrane compartments including the ER, the Golgi and endosomes, regulates endocytosis, exocytosis, cytoskeleton dynamics and autophagy. At these intracellular compartment, PI(4,5)P_2 binds to effector proteins (Tan et al., 2015). Generation of PI(4,5)P_2 requires the recruitment of phosphatidylinositol phosphate kinases and in particular PI4P5Ks to the target membrane typically by the same effectors binding PI(4,5)P_2. In plants, up to 11 PI4P 5-kinase isoforms are encoded by the Arabidopsis genome (Munnik and Testerink, 2009) and studies of Arabidopsis PI4P 5-kinase isoforms are scarce. It seems that the isoform activities are cell-type specific, and that their overexpression results in unfavourable phenotypes (Ischebeck et al., 2008). In contrast, heterologous expression of a distantly related PI4P 5-kinase from *Homo sapiens* (HsPIPK1α) in Arabidopsis yielded a functional kinase and did not trigger meaningful phenotypical changes (Anderson et al., 1999; Ma et al., 2014). We found that coexpression of a functional PI4P5K and AtTSPO did not modify the subcellular localization of the kinase (Supplemental Figure 5.S9). Recently it was shown that in addition to PI3P, PI5P, PI(4,5)P_2 is involved in the initiation, trafficking of membrane precursors and fusion of the autophagosome with the lytic compartment. Nucleation of the autophagosome initiation membrane requires the Vacuolar Protein Sorting (VPS) 34 complex, which generates PI3P. The VPS34 complex is recruited to the autophagosome initiation sites by ATG14/Barkor, which binds PI3P through its Barkor/ATG14 autophagosome targeting sequence (BATS) domain. The ATG14 carboxyl-terminal BATS domain also binds PI4P5K and PI(4,5)P_2 (Tan et al., 2016). Although an ATG14-related protein has not yet been characterized in plants, putative candidate genes are present

in deciphered plant genomes. Generation of PI(4,5)P_2 signaling on the autophagosome initiation membrane could facilitate the targeting of AtTSPO-containing complex to this site. We found that binding of PI(4,5)P_2 is not indispensable to the autophagy-dependent degradation of AtTSPO since the N-terminus truncated form of the protein could still be translocated to the vacuole (Figure 5.6). However, binding of PI(4,5)P_2 is necessary for AtTSPO to interact with the aquaporin PIP2;7. This could happen as the autophagosome is initiated at the vicinity of AtTSPO-containing organelles, the cytosolic N-terminus of AtTSPO may come into close contact with the autophagosome initiation membrane enriched in PI(4,5)P_2 and PI3P (Figure 5.8c). How the AtTSPO-containing complex is extracted and translocated to the autophagosomal membrane is still unknown.

Structural analysis suggest that lipid binding by the N-terminal extension of AtTSPO may induce conformation changes in the protein. We showed that ^{1}H-^{15}N cross-peaks of residues belonging to the 34-49 segment, close to the first transmembrane span of the AtTSPO, completely disappeared after interaction of the peptide with PI(4,5)P_2. It may be that the conformational change induced by PI(4,5)P_2 binding is required to expose residues allowing the interaction with PIP2;7 within the lipid bilayer. The 34-49 segment contains key arginine/lysine residues involved in PI(4,5)P_2 binding *in vitro*, and their mutation resulted in dramatic reduction of AtTSPO capability to interact with PIP2;7 *in vivo*.

In conclusion, this work provides evidence that as a response to osmotic stress, the induced Arabidopsis TSPO, localized mainly in the Golgi membrane of the plant cell, triggers a depletion of PI(4,5)P_2 from the plasma membrane and its subsequent enrichment in the Golgi membrane containing AtTSPO. Moreover, we showed that AtTSPO binds PI(4,5)P_2 through its polybasic plant-specific N-terminus as a requirement for its interaction with the plasma membrane aquaporin PIP2;7. This molecular mechanism provides a basis for the functional divergence among TSPO proteins, by demonstrating that the plant lineage-conserved N-terminal extension rich in polybasic residues determines the involvement of TSPO in the osmotic stress response.

5.5. Methods

5.5.1. Plant materials and growth conditions

We used *Arabidopsis thaliana* (ecotype Columbia-0) wild type and transgenic plants expressing full-length AtTSPO, point mutant AtTSPO^{H91A} or Venus-tagged AtTSPO$^{\Delta N}$ (first 41 amino acids removed), each construct under the control of the p35S promoter (Guillaumot et al., 2009; Vanhee et al., 2011). An Arabidopsis homozygous TDNA insertional line (KO) in *TSPO* was described by Guillaumot et al., 2009. Seeds sterilization and growth conditions were as described previously (Guillaumot et al., 2009).

The wild type Arabidopsis suspension cell culture (ecotype Landsberg *erecta*) (May and Leaver, 1993) was agitated in the dark on a rotary shaker and diluted 10-fold weekly in the freshly sterilized LS medium (Duchefa Biochemie cat. no. L0230; 4.43 g L^{-1}, adjusted to pH 5.7 with KOH, 3% sucrose, 50 µg L^{-1} of kinetin, 500 µg L^{-1} of 1-naphthalene acetic acid; Duchefa Biochemie).

5.5.2. Water loss and stomatal conductance assays

To assess the dehydration tolerance, the wild-type, TSPO knockout and AtTSPO, AtTSPO^{H91A} and Venus-AtTSPO$^{\Delta N}$ overexpressing plants were grown on half-strength MS medium in a growth chamber (16h/8h light/dark conditions, 22–25°C, 90 µmol photons sec^{-1} m^{-2}). Seven days after germination, seedlings were transferred on a weighing paper and weighted on a microbalance at time 0 and after 120 minutes. Water loss was expressed as percentage of the original weight of seedlings.

For stomatal conductance assay, mature but not yet flowering Arabidopsis plants were grown under controlled phytotron conditions (16h/8h light/dark photoperiod, 20°C, 65% humidity, 120 µmol photons sec^{-1} m^{-2}) and integral rosette leaves were subjected *in situ* to the abaxial stomatal conductance measurements according to manufacturer's protocol (automatic mode, SC-1 LEAF POROMETER, Decagon Devices, USA).

5.5.3. Plant suspension cells transformation and plasma membrane preparation

Transgenic Arabidopsis suspension cell lines were raised by co-cultivation with *Agrobacterium* (van Leene et al., 2007) (timentin, Goldbio #T-104-2, was used to replace vancomycin). We used pCambia3300 USER vector cloning system (Nour-Eldin et al., 2006) to generate mGFP5-TSPO fusions driven by the p35S promoter. The GFP-tagged AtTSPO, AtTSPO$^{\Delta N}$, mTSPO (mouse homolog) and AtTSPO^{Nter}-mTSPO (N-terminus of AtTSPO added to the mouse protein) chimeras were created by PCRs using the primers listed in the Supplemental Table 5.S1. In case of the GFP-AtTSPO$^{\Delta N}$, a 7 amino acid-long linker (GAGAGAG) was introduced in between to flexibilize the chimeric protein.

The vector encoding the PI(4,5)P_2 phosphoinositide sensor (Simon et al., 2014) was a generous gift from Dr. Yvon Jaillais (Ecole Normale Superieure Lyon) and Dr. Teun Munnik (University of Amsterdam).

Plasma membrane-enriched fraction of Arabidopsis wild-type and transgenic suspension cells was prepared by two-phase partitioning (Santoni, 2007).

5.5.4. BiFC experiments and cell imaging

In BiFC assays, we took advantage of the pDOE12 vector (Gookin and Assmann, 2014) (received from Dr. Sarah Assmann, Pennsylvania State University, USA) encoding the split Venus at the N-terminus of the protein of interest (Venus split into N- and C parts consisting of 210 amino acids and 29 amino acids, respectively). Full-length AtTSPO and AtPIP2;7 cDNAs were PCR-amplified from templates described previously (Hachez et al., 2014). N-terminus truncated variants of AtTSPO were PCR-generated. All the lysine/arginine point mutants of AtTSPO were created by overlapping PCR-mediated site-directed mutagenesis. Primers used in this assay are listed in the Supplementary Table 5.S1. Transient expression in tobacco (*Nicotiana tabacum*) was performed through *Agrobacterium* (GV3101::pMP90)-mediated transfection as described before (Batoko et al., 2000). Confocal imaging using a Zeiss LSM710 confocal microscope equipped with a spectral detector was performed as described (Guillaumot et al., 2009; Vanhee et al., 2011; Hachez et al.,

2014). The mTurquoise was exited with 445 nm laser and its fluorescence used to detect transfected cell and for Golgi colocalization of the BiFC signal. The reconstituted mVenus fluorescence after BiFC was excited with a 514 nm argon multiline laser. To quantify the BiFC signal, we imaged five independent randomly chosen (but not overlapping) areas of the infiltrated or non-infiltrated leaf. Pixel intensities from mTurquoise and mVenus channels were acquired along two diagonals of each image (around 700 intensity measurements per diagonal) using ZEN2012 software (Zeiss). An average signal intensity was calculated from 10 diagonals. An average signal intensity from non-infiltrated leaves was for background subtraction. Ratio between an average BiFC/mTurquoise signal intensity was calculated and normalized against the positive control (combination AtPIP2;7-AtTSPO full-length).

The human phosphatidylinositol 4-phosphate 5-kinase type-1 alpha fused to mCherry (mCherry-HsPIPK1α), shown to be functional in the plant cell (Ma et al., 2014), was expressed in tobacco leaf through *Agrobacterium*-mediated transiently expression. The construct was expressed both in wild type plant and in a stable transgenic line overexpressing YFP-AtTSPO. Confocal imaging of the resulting mCherry signal in leaf epidermal cells was achieved using a 561 nm excitation laser.

5.5.5. TSPO purification for *in vitro* biochemical assays

Yeast transformation was performed by the LiAc/ss-DNA/PEG method as described before (Gietz and Schiest, 2007). The 10 histidine-tagged AtTSPO and AtTSPO$^{\Delta N}$ proteins were expressed and purified from *S. cerevisiae* following the optimized protocol (Vanhee et al., 2010).

The 6His-mTSPO (pET-15b vector) and 10His-tagged AtTSPO N-terminus fused to mTSPO (GST-fusion in pGEX-4T-2 vector) were expressed and purified from *E. coli* BL21 (DE3). Protein expression was induced with 1 mM isopropyl-β-D-thiogalactoside (IPTG) at 28°C for 4 hours. Bacteria were collected and the pellet resuspended in buffer A [50mM Tris, pH 8.0, 300mM NaCl, 10% glycerol, 20mM imidazole, proteases inhibitors cocktail (Sigma)] supplemented with 1 mg/ml lysozyme and 1000 U benzonase (Sigma) and incubated for 15 minutes at room temperature

with gentle shaking. Cells were lysed by sonication (3 min, amplitude 60, 10-second pulses, Ultrasonic processor, Vibra-Cell, USA). Bacterial membranes containing overexpressed TSPO were obtained by two steps of centrifugation at 4°C. Lysed cells were spun down for 30 min at 15,000 g followed by the supernatant centrifugation for 1 hour at 250,000 g. Sedimented membranes were resuspended in buffer A and solubilized by adding n-Dodecyl-β-D-maltoside (DDM) to the final concentration 2% for 1 hour at room temperature on a rotary wheel. Solubilized membranes solution was then centrifuged at 150,000 g for 30 min at 4°C and the supernatant was mixed with Ni-NTA matrix (Qiagen) pre-equilibrated with solubilization buffer lacking imidazole. The binding was performed at room temperature for 3 hours. After this time, the flow through was collected and the beads washed 4 times in buffer A (0.2% DDM) with increasing imidazole concentrations (20, 20, 40 and 60mM). Bound proteins were eluted with 300 mM imidazole in buffer A and dialyzed on the PD-10 desalting columns (GE Healthcare) against imidazole-free buffer A. At this step, mTSPO was concentrated and frozen in aliquots.

After dialysis, AtTSPO^{Nter}-mTSPO fusion protein was subjected to a second purification step by an overnight digestion at room temperature with His-tagged-TEV protease (0.1µg/ml; produced and shared by Marc Boutry's laboratory, UCLouvain, Louvain-la-Neuve, Belgium). Then, the mixture was applied on the nickel-affinity column and processed as previously. Washing fractions containing the protein of interest were pooled, dialyzed, concentrated and frozen for downstream biochemical applications.

Appropriated DNA primers designed for expression and purification of TSPO were listed in the Supplemental Table 5.S1.

5.5.6. Expression and purification of N-terminus of AtTSPO for structural studies

AtTSPO^{Nter} construct (residues 1-49) was expressed from pGEX-4T-2 vector in *E. coli* BL21 (DE3) bacteria as a GST fused 10xHis-tagged protein containing a TEV (Tobacco Etch Virus) protease cleavage site. To get labeled protein, bacteria were cultured in M9 minimal medium

supplemented with [^{15}N]-NH_4Cl and [^{13}C]-Glucose at 1 and 4 g per liter, respectively. The protein expression in cells cultured in the presence of 0.1 mg/ml ampicillin was induced with 1 mM isopropyl-β-D-thiogalactoside (IPTG) at 37°C for 4 hours. Bacteria were collected, proteases inhibitors cocktail (Roche) was added before lysis (by sonication) in 50 mM Hepes-NaOH, 500 mM NaCl at pH 7.8, and centrifugation at 14,000 g during 20 min. The protein in the supernatant was purified with Ni-NTA resin (Qiagen) and eluted with 250 mM imidazole. The purified proteins were dialyzed against 50 mM Hepes-NaOH at pH 7.8, overnight at room temperature and then digested by His-tagged-TEV protease (0.1µg/ml) overnight (16-20h) at room temperature. The cleaved AtTSPO^{Nter} was purified from GST fusion protein and protease with Ni-NTA resin since His-tagged GST and TEV proteins were retained on the column. The purified protein was dialyzed against 10 mM sodium phosphate, 1 mM NaN_3 at pH 7.8 to perform structural studies. SDS-PAGE analysis was performed at the different steps to follow the purification.

Purified AtTSPO^{Nter} was characterized by (i) dot-blot and by (ii) mass spectroscopy. Spots of AtTSPO^{Nter} on PVDF membrane for dot-blot were first incubated with serum polyclonal rabbit antibody (Guillaumot et al., 2009), second with anti-rabbit coupled to alkaline phosphatase that was revealed with specific substrate (BCIP/NBT Sigma-Fast).

Aliquots of purified AtTSPO^{Nter} were mixed with HCCA matrix and mass determined using 5-17 kDa standard set protein (Proteomics Sigma) with MALDI-TOF (DE-Pro, ABSciex).

Concentration of purified AtTSPO^{Nter} was determined by UV spectroscopy using calculated extinction coefficient (280 nm) of 0.256 for 1 mg/ml.

Appropriated DNA primers designed for expression and purification of AtTSPO^{Nter} were listed in the Supplemental Table 5.S1.

5.5.7. CD spectroscopy

Measurements were carried out on a JASCO (France) spectropolarimeter with 1 mm cuvette at room temperature.

5.5.8. Bicelles and PI(4,5)P_2 micelle

Bicelles were prepared as previously described(Caillon et al., 2013). Briefly, solutions of 25 mM of 1,2-dimyristoyl-*sn*-glycero-3-phosphocholine or 1,2-dimyristoyl-*sn*-glycero-3-phospho-(1'-*rac*-glycerol) (DMPG or DMPC, Avanti-polar lipids) and 50 mM of 1,2-dihexanoyl-*sn*-glycero-3-phosphocholine (DHPC, Avanti-polar lipids) in 10 mM sodium phosphate at pH 6.1-6.2 were mixed (vortex 1 min) and submitted to 3 freeze-thaw cycles. 1,2-dioleoyl-*sn*-glycero-3-phospho-(1'-myo-inositol-4',5'-bisphosphate) PI(4,5)P_2 micelles were formed by adding 10 mM sodium phosphate at pH 6.1-6.2 to powder and the solution was sonicated to perform good mixing (stock solution was 5 mM).

5.5.9. Diffusion Light Scattering

Measurements were carried out with a protein solution DynaPro-99 apparatus (Yatt Technology). Size (radius) of the (DMPC/DMPG) bicelles and PI(4,5)P_2 micelles were determined to be 4.1±0.2 and 65±20 nm, respectively.

5.5.10. NMR spectroscopy

NMR samples were prepared in 5 mm NMR tubes and contained ~100 µM ^{15}N, ^{13}C- labeled AtTSPO^{Nter} in 10 mM sodium phosphate at pH 6.2, H_2O/D_2O (90:10 v/v). 0.1 mM sodium 2,2-dimethyl-2-silapentane-d_6-5-sulfonate (DSS, Sigma) was used as an internal chemical shift reference. Protease inhibitor cocktail (Roche) and EDTA (1 mM) were added in to prevent any degradation. Experiments were recorded on a Bruker 500 MHz Avance III spectrometer equipped with a TCI cryoprobe. Resonances were assigned using 2D ^{1}H-^{15}N HSQC and 3D ^{1}H-^{15}N-^{13}C HNCACB, CBCA(CO)NH, HNCA, HNCO and HN(CA)CO spectra acquired at 20°C. NMR experiments were processed with Bruker TopSpin 3.2 or NMRPipe (Delaglio et al., 1995) and analyzed with NMRFAM-SPARKY program (Lee et al., 2015). Secondary structure analysis was based on SSP score (Marsh et al., 2006) calculated from $^{13}C^{\alpha}$, $^{13}C^{\beta}$, ^{13}CO, ^{1}HN and ^{15}N chemical shifts.

2D ^{1}H-^{15}N-HSQC spectra of AtTSPO^{Nter} were recorded in the presence of DMPC/DHPC and DMPG/DHPC bicelles (12.5/25 mM, q=0.5), as well as

in the presence of increasing amounts of PI(4,5)P_2 (1 to 10 equivalents). ^{1}H, ^{15}N chemical shift perturbations (CSP) were calculated using the formula:

$$\Delta\delta = \left|\Delta\delta(1H)\right| + 1/10 \left|\Delta\delta(15N)\right|$$

Binding constant (K_d) was estimated from CSPs upon titration with PI(4,5)P_2 using a fast-exchange, single-site binding model (Ziarek et al., 2011).

5.5.11. Antibodies and immunoblotting

Anti-AtTSPO was designed in the host laboratory as described earlier (Guillaumot et al., 2009). The HisProbe-HRP conjugate was purchased from ThermoFisher Scientific. Antibodies against Arabidopsis RbcL and AtPIP2;7 were from Agrisera. Anti-GFP was purchased from Abcam (ab290). Anti-PI(4,5)P_2 was from Enzo Life Sciences (ADI-915-052-020). Anti-FLAG was a generous gift of Dr. Michel Ghislain (UCLouvain, Louvain-la-Neuve, Belgium). Antibodies against plant H+-ATPase were provided by the lab of Dr. Marc Boutry (UCLouvain, Louvain-la-Neuve, Belgium).

For western blotting, anti-AtTSPO, anti-AtPIP2;7, anti-GFP and anti-RbcL antibodies were diluted 1:5,000. HisProbe-HRP was used at 1:1,000 dilution. Anti-PI(4,5)P_2 and anti-FLAG antibodies were diluted 1:2,000. Anti-H+-ATPase antibodies were diluted 1:100,000. Horseradish peroxidase-coupled anti-rabbit and anti-mouse secondary antibodies were from Sigma and were used at 1:10,000.

Extracted proteins were quantified by Bradford method, mixed with 5x Laemmli buffer and incubated 30 minutes at 37°C prior to classical SDS-PAGE and transfer onto PVDF membrane (Immobilon-P, Millipore). Membranes were saturated for 1h at 25°C in blocking buffer (5% non-fat milk in TBS-Tween20, adding 0.5% Tween20 in 1x TBS) and incubated at room temperature for 1h with primary antibodies diluted in the washing buffer (0.5% milk in TBS-Tween20, adding 0.1% Tween20 in 1x TBS). After washing three times in the washing buffer, membranes were incubated with appropriate secondary HRP-conjugated antibodies for 1h at room temperature. After washing three times in the washing buffer,

membranes were incubated 3-5 minutes with ECL (Roche, #11500694001). The emitted light was detected using either a film processor (OPTIMAX X-RAY FILM PROCESSOR; Protec Medical Systems) or digital imaging device (Amersham Imager 600, GE Healthcare Life Sciences).

5.5.12. Overlay and pull-down assays

Protein-lipid overlay assays were conducted either using commercially available PIP Strips (Echelon Biosciences, #P-6001) according to manufacturer's protocols or using membranes prepared in the host laboratory. Briefly, phosphatidic acid (Sigma, #P9511, dissolved in $CHCl_3$), phosphoinositides PI3P, PI4P and PI(4,5)P_2 (Echelon Biosciences, #P-3016, #P-4016 and #P-4516, respectively; all dissolved in 2% DDM) or SDS-solubilized plasma membrane fractions were spotted on a nitrocellulose membrane (Amersham Protran, GE Healthcare, #10600002) and air-dried for 1h. Then, the membranes were saturated in blocking buffer (3% BSA in TBS-Tween20, adding 0.1% Tween20 in TBS). Incubation with proteins in the blocking buffer was performed at room temperature for 3h. Incubation with primary and secondary antibodies and ECL exposure were as described in immunoblotting section.

In lipid-dependent pull-down assay, purified 10His-AtTSPO or 10His-AtTSPO$^{\Delta N}$ were incubated for 3h at room temperature with phosphatidic acid-coupled agarose beads (Echelon Biosciences, #P-B0PA) followed by flow-through collection, 3 washes with incubation buffer (50 mM Tris-HCl pH 8.0, 150 mM NaCl, 10% glycerol, 0.2% DDM, proteases inhibitors) and elution with Laemmli buffer supplemented with 8M urea. Uncoupled agarose beads were used as a negative control.

5.5.13. Microscale thermophoresis ligand binding analysis

Microscale thermophoresis approach was used to detect and measure binding events between purified TSPO and lipid or aquaporin ligands. All experiments were run on Monolith NT115 instrument (Nanotemper Technologies, Germany) equipped in red and green filters. Standard-threated capillaries were chosen. Both proteins and lipids were stored in the same buffer composed of 50 mM Tris-HCl pH 8.0, 200 mM NaCl, 10%

glycerol, 2% DDM, proteases inhibitors (Sigma). Tested proteins were titrated against a gradient of lipids concentrations and in the AtPIP2;7 aquaporin-AtTSPO interaction assay, the aquaporin was titrated against AtTSPO concentrations. In the phosphatidic acid binding experiment, AtTSPO full length and isolated N-terminus were labeled through lysine residues by the red fluorescent dye NT-647-NHS and in the PI(4,5)P_2 binding assay proteins were labeled through their polyhistidine tags by the RED-tris-NTA dye (Nanotemper). The YFP-AtPIP2;7 aquaporin (mVenus variant) input was a DDM-solubilized microsomal fraction of transgenic *A. thaliana* seedlings (Hachez et al., 2014) and was traced by the YFP fluorescence using the green filter. To generate thermophoresis, the MST laser power was set up for 10%, 20% or 40% and the LED power was maintained at 100%.

5.5.14. Statistical analysis of the data

Number of replicates and statistical method applied for each experiment is stated within appropriate figure legend or in methods section.

GraphPad Prism version 5.03 for Windows (GraphPad Software; San Diego, California, USA; www.graphpad.com) was used to analyze statistical significance of data. For immunoblotting signal quantification we used ImageJ version 1.51j8 (NIH, USA; www.imagej.nih.gov/ij/). For quantification purposes, we ensure that the exposure conditions provided by the digital imager were below the saturation threshold.

For the microscale thermophoresis data analysis, we used the NT Analysis 1.5.37 software (Nanotemper). A non-linear regression model was employed (Graphpad Prism) to fit the normalized fluorescence data and to obtain binding constants.

5.6. Acknowledgements

We thank M. Boutry (LIBST, UCLouvain, Belgium) for sharing purified TEV enzyme and anti-PMA antibodies and M. Ghislain (LIBST, UCLouvain, Belgium) for anti-FLAG antibodies. We also thank K. Moonens (VIB, Center for Structural Biology, VUB, Belgium) for his assistance in thermophoresis experiments, D. Masquelier for preparation of the genetic construct AtTSPO^{Nter}-mTSPO, J. Nader, M.C. Eloy and A. Jurkiewicz

for technical assistance. We acknowledge Y. Jaillais (Laboratoire Reproduction et Développement des Plantes, ENS Lyon, France), T. Munnik (Swammerdam Institute for Life Sciences, University of Amsterdam, The Netherlands), S. Assmann (Department of Biology, Pennsylvania State University, USA) and I. Heilmann (Institute for Biochemistry and Biotechnology, Martin-Luther-University Halle-Wittenberg) for providing reagents and genetic materials. Transgenic Arabidopsis plants expressing mVenus-AtTSPO$^{\Delta N}$ were generated by S. Guillon (UCLouvain). This work was partly funded by the Wallonia-Brussels Federation Joint Research Action (ARC grant #11/16-036 to H.B.), and the Belgian Funds for Scientific Research (FNRS) (CR grant #19516174 and PDR grant # 6794930 and T.0050.18 to H.B.). H.B. is a Senior Research Associate of the FRS-FNRS.

5.7. Author contributions

OL, J-JL and HB conceived and designed the experiments, PJ, LS, OL, J-JL, and HB performed the experiments, analyzed the data. J-JL and HB supervised the research, PJ, J-JL and HB wrote the manuscript.

5.8. Supplemental figures

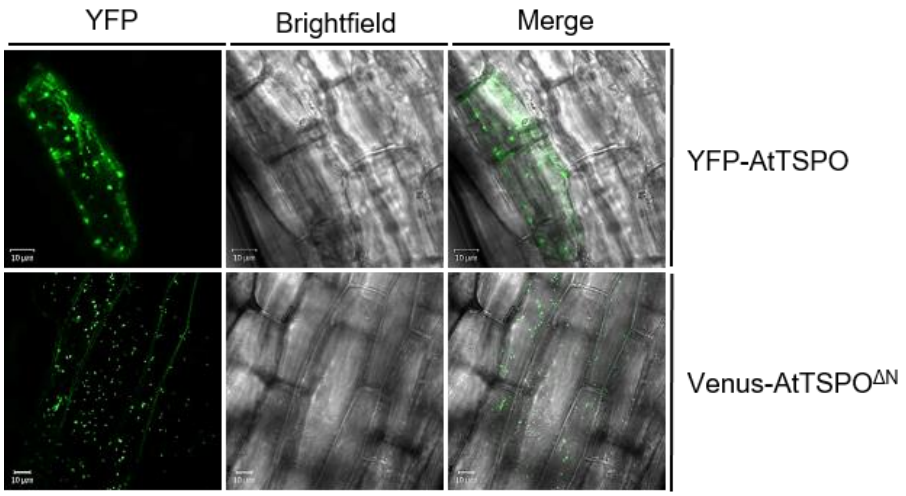

Figure 5.S1. Subcellular localization of AtTSPO and AtTSPO$^{\Delta N}$ expressed in *Arabidopsis thaliana*. Representative confocal images of hypocotyls of transgenic Arabidopsis seedlings overexpressing YFP-AtTSPO or Venus-AtTSPO$^{\Delta N}$. Full-length AtTSPO is detected in the Golgi membranes and in the ER (Guillaumot et al., 2009) and

the N-terminus truncated AtTSPO localizes essentially to the Golgi (Guillon, Batoko et al., unpublished data). Bars = 10 µm.

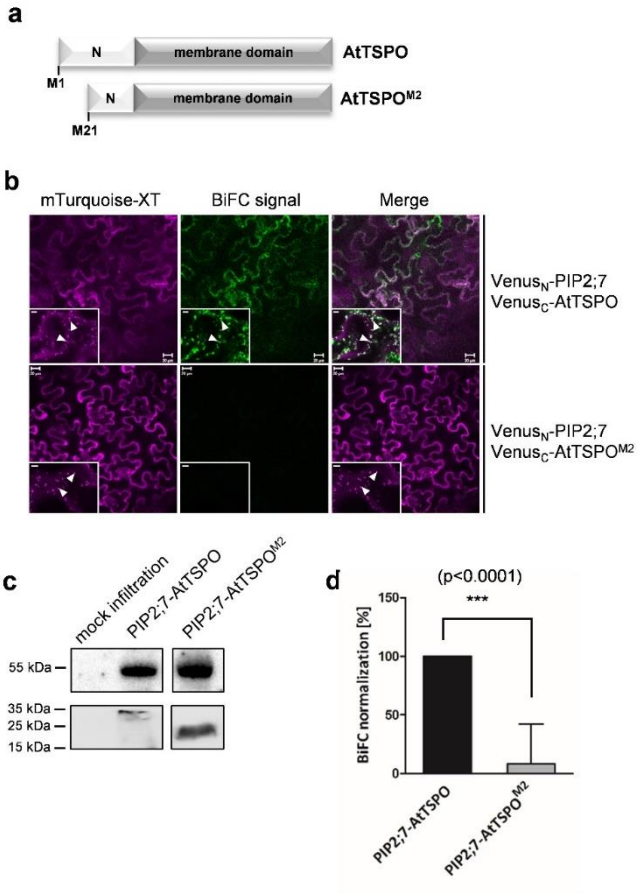

Figure 5.S2. The first 20 amino acids of AtTSPO are required for AtTSPO interaction *in vivo* with PIP2;7. (a) Schematic representation of AtTSPO genetic constructs used in BiFC approach. As a positive control in this assay we used both full-length PIP2;7 and AtTSPO. N-terminus truncated variant (M2) starts with the methionine at the position 21. **(b)** BiFC assay on *Agrobacterium*-infiltrated *Nicotiana benthamiana* leaves. Xylosyltransferase-mTurquoise fluorescent chimera was imaged as cell transfection control (in magenta). Low magnification images qualitatively demonstrate occurrence or lack of BiFC (in green) and the insets with high magnification images show Golgi stacks (arrowheads). Bars = 20 µm and 5 µm for low and high magnification, respectively. Experiment was repeated at least twice. **(c)** Western blot of infiltrated leaves areas used for BiFC microscopy analysis. PIP2;7 expression was detected by anti-GFP. AtTSPO full-length and truncated form were detected by anti-FLAG (the tag was originally cloned in between $Venus_C$ and cloning site for AtTSPO). Non-infiltrated leaf area was used as a negative control. **(d)** Quantitative data of the signal show a drastic reduction of BIFC between PIP2;7 and truncated AtTSPO mutant as compared to full-length AtTSPO. For statistical significance evaluation an independent samples t-test was performed using Graphpad Prism 5 (San Diego, USA). See supplemental data for quantification procedure.

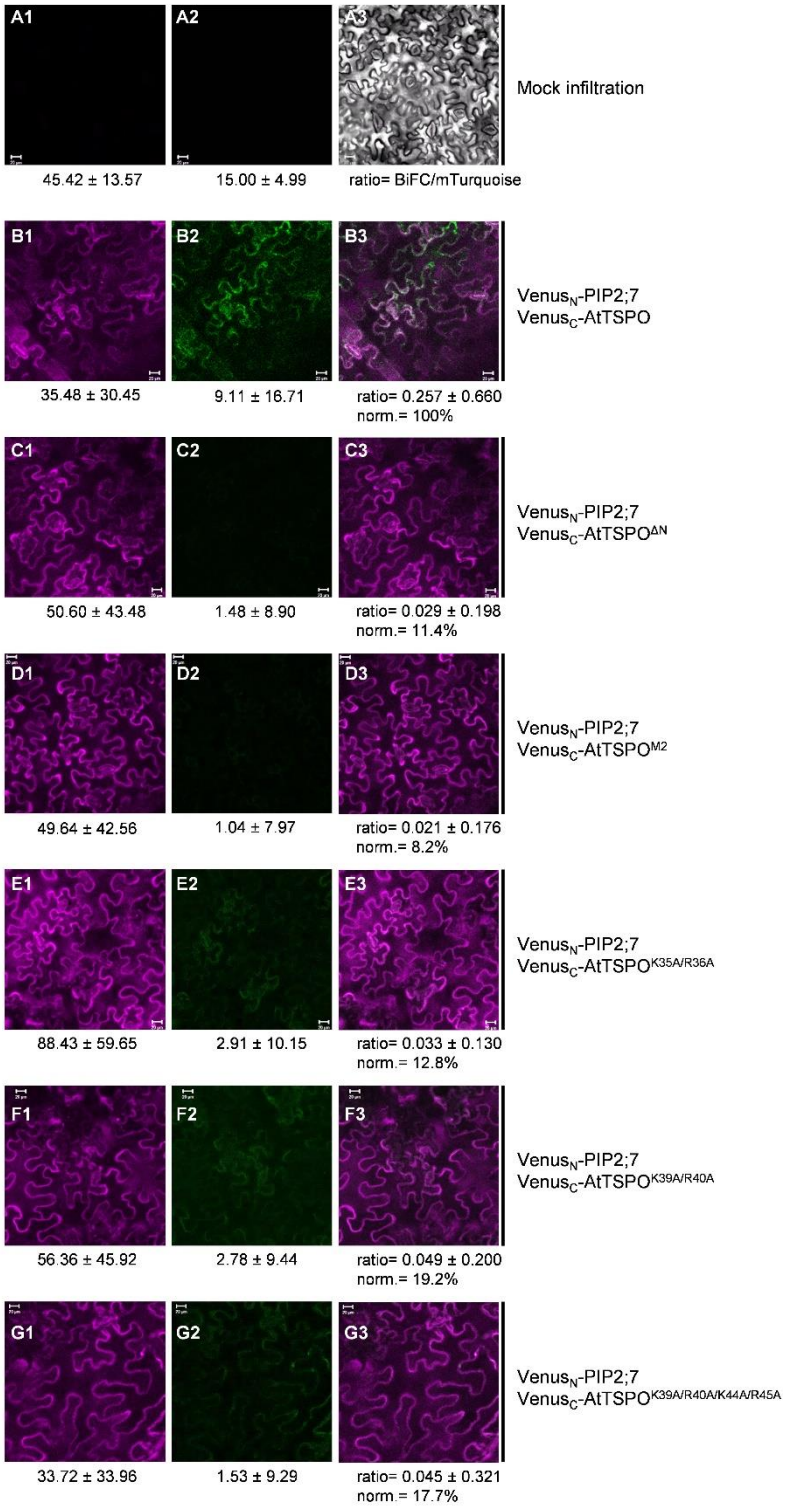
A1
A2
A3
Mock infiltration
45.42 ± 13.57
15.00 ± 4.99
ratio= BiFC/mTurquoise
B1
B2
B3
Venus$_N$-PIP2;7
Venus$_C$-AtTSPO
35.48 ± 30.45
9.11 ± 16.71
ratio= 0.257 ± 0.660
norm.= 100%
C1
C2
C3
Venus$_N$-PIP2;7
Venus$_C$-AtTSPO$^{\Delta N}$
50.60 ± 43.48
1.48 ± 8.90
ratio= 0.029 ± 0.198
norm.= 11.4%
D1
D2
D3
Venus$_N$-PIP2;7
Venus$_C$-AtTSPO^{M2}
49.64 ± 42.56
1.04 ± 7.97
ratio= 0.021 ± 0.176
norm.= 8.2%
E1
E2
E3
Venus$_N$-PIP2;7
Venus$_C$-AtTSPO$^{K35A/R36A}$
88.43 ± 59.65
2.91 ± 10.15
ratio= 0.033 ± 0.130
norm.= 12.8%
F1
F2
F3
Venus$_N$-PIP2;7
Venus$_C$-AtTSPO$^{K39A/R40A}$
56.36 ± 45.92
2.78 ± 9.44
ratio= 0.049 ± 0.200
norm.= 19.2%
G1
G2
G3
Venus$_N$-PIP2;7
Venus$_C$-AtTSPO$^{K39A/R40A/K44A/R45A}$
33.72 ± 33.96
1.53 ± 9.29
ratio= 0.045 ± 0.321
norm.= 17.7%

← **Figure 5.S3. Methodology of BiFC signal quantification.** Five independent randomly chosen (but not overlapping) areas of the infiltrated or non-infiltrated leaf were imaged. Pixel intensities from mTurquoise (magenta) and mVenus (green) channels were acquired along two diagonals of each image (around 700 intensity measurements per one diagonal) using ZEN2012 software (Zeiss). An average signal intensity was calculated from 10 diagonals (around 7000 intensities measurements). An average signal intensity from non-infiltrated leaves was subtracted. Ratio between an average BiFC/mTurquoise signal intensity was calculated and normalized against the control (combination PIP2;7-AtTSPO full-length).

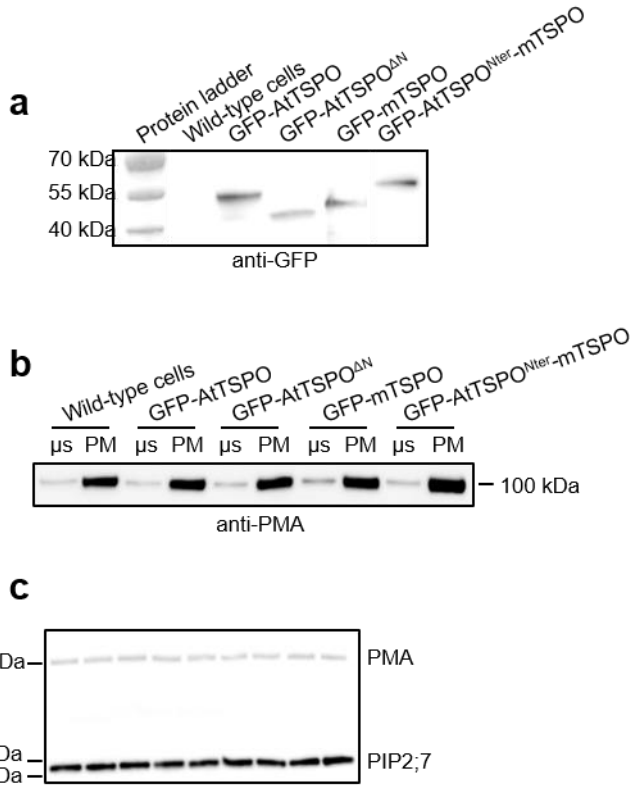

Figure 5.S4. Representative western blots for PIP2;7 aquaporin signal quantification in the plasma membrane-enriched fractions. (a) Expression of GFP-TSPO fusions in Arabidopsis PSB-D suspension cells. Each signal was exposed separately followed by superimposition on the protein ladder. **(b)** Preparation of plasma membrane-enriched fractions (PM) from Arabidopsis suspension cells. The plant plasma membrane H^+-ATPase (PMA) was probed to check for relative enrichment (5 µg protein in each well); µs, microsomal fraction. **(c)** Relative amount of PIP2;7 aquaporin was checked by western blotting. PMA was used as reference protein for the signal quantification. Shown is a representative membrane exposition. Both PMA and PIP2;7 were detected by specific antibodies.

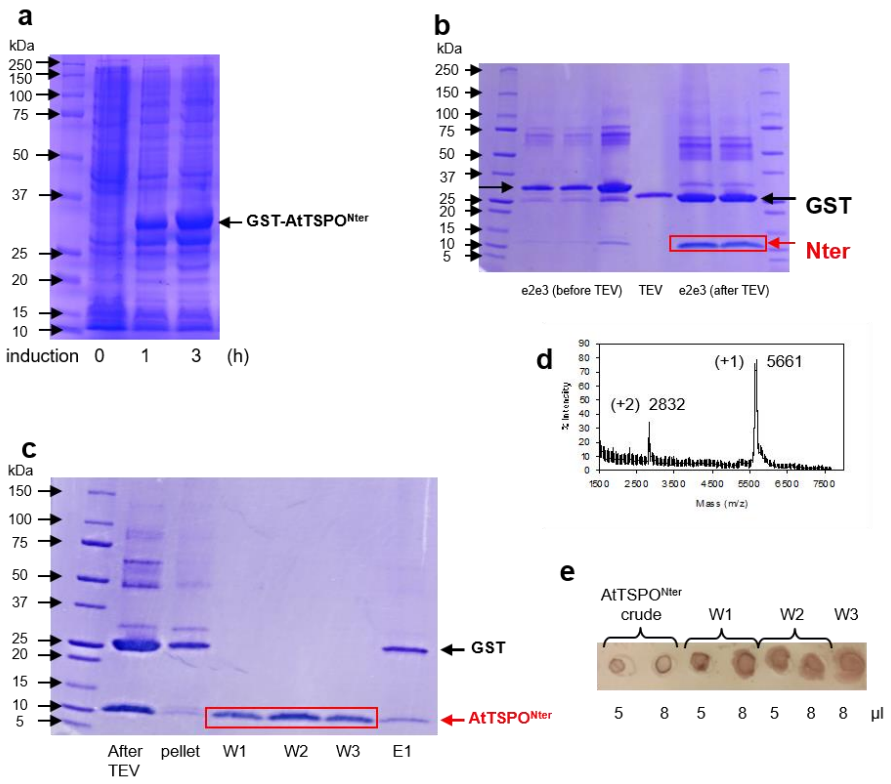

Figure 5.S5. Expression, purification and characterization of the recombinant AtTSPO N-terminal peptide. **(a)** SDS-PAGE of bacterial culture samples taken along the expression time. **(b)** SDS-PAGE of elution fraction (e2 and e3) from the first step of bacterial cytosol purification containing fused protein GST-AtTSPO^{Nter} on Ni-NTA affinity column followed by dialysis to remove imidazole and further proteolytic digestion (TEV) to remove fusion protein (GST). **(c)** SDS-PAGE of the second step of purification on Ni-NTA column to remove His-tagged GST and His-tagged TEV proteins. Digested sample was centrifuged to remove GST precipitated as observed in the pellet. AtTSPO^{Nter} peptide was not retained on the column and collected by washing (W1-W3). GST was removed from the column by imidazole elution **(d)** MALDI-TOF mass spectrum of purified AtTSPO Nter showing the expected molecular weight for [^{15}N] labelled peptide. (**e**) Dot blot of "crude AtTSPO^{Nter}" after proteolytic digestion, before final purification, and samples collected (W1-W3) after Ni-NTA purifcation.

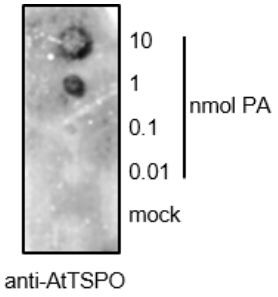

Figure 5.S6. Purified AtTSPO N-terminal peptide binds phosphatidic acid (PA) *in vitro*. Bacterially expressed and purified N-terminal peptide of AtTSPO was incubated with a spotted gradient of PA concentrations and detected with anti-AtTSPO antibodies. Experiment was repeated at least twice.

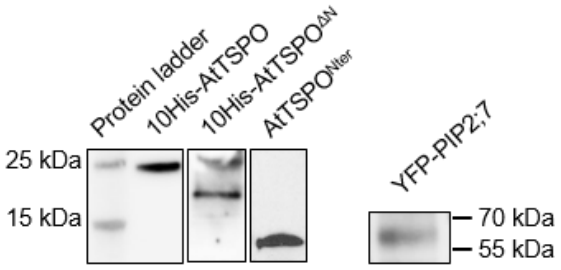

Figure 5.S7. Representative western blot of protein samples used in thermophoresis experiments. AtTSPO and the truncated mutant were detected by HisProbe (Thermo Fisher Scientific) while the purified AtTSPO N-terminus peptide was detected using anti-AtTSPO antibodies. YFP-PIP2;7 fusion was detected using anti-GFP antibodies.

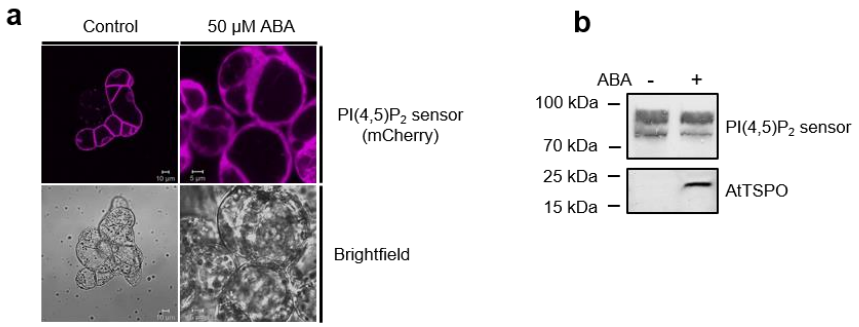

Figure 5.S8. The PI(4,5)P_2 biosensor was depleted from the plasma membrane upon ABA treatment. (a) Arabidopsis PSB-D suspension cells stably expressing the mCherry-tagged PI(4,5)P_2 sensor (double pleckstrin homology domain from phospholipase C) were treated with 50 µM ABA for 24h for endogenous AtTSPO induction. Control cells showed mCherry fluorescence mainly outlining the cell, most likely in the plasma membrane, and some intracellular signals in punctate structures around the nucleus. After ABA treatment, the mCherry fluorescence was essentially detected in the cytosol. Bars = 10 µm and 5 µm for control and treated cells, respectively. **(b)** Western blotting of ABA-dependent AtTSPO induction in cells imaged in **a**. The lipid sensor was detected using anti-mCherry (Abcam ab167453) and served as a loading control. AtTSPO was detected using anti-AtTSPO antibodies.

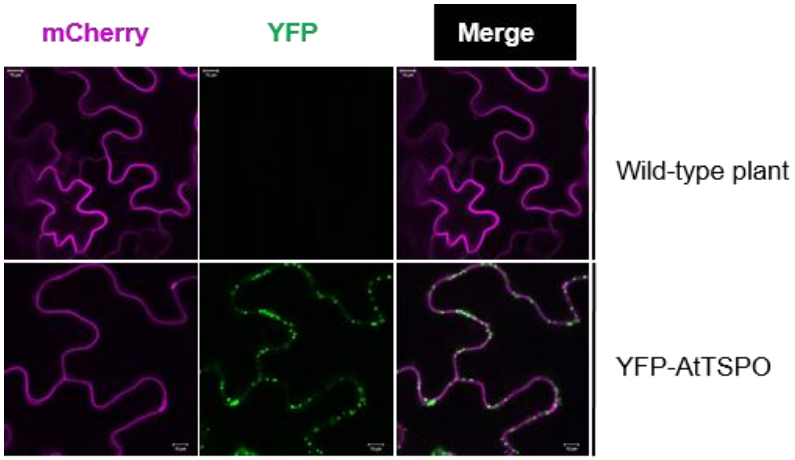

Figure 5.S9. Expression of AtTSPO does not affect the targeting of PI4P 5-kinase to the plasma membrane. The human phosphatidylinositol 4-phosphate 5-kinase type-1 alpha fused to mcherry (mCherry-HsPIPK1α; in magenta) shown to be active in the plant cell was transiently expressed in tobacco wild type or a transgenic line stably expressing YFP-AtTSPO (in green). Bars = 10 µm.

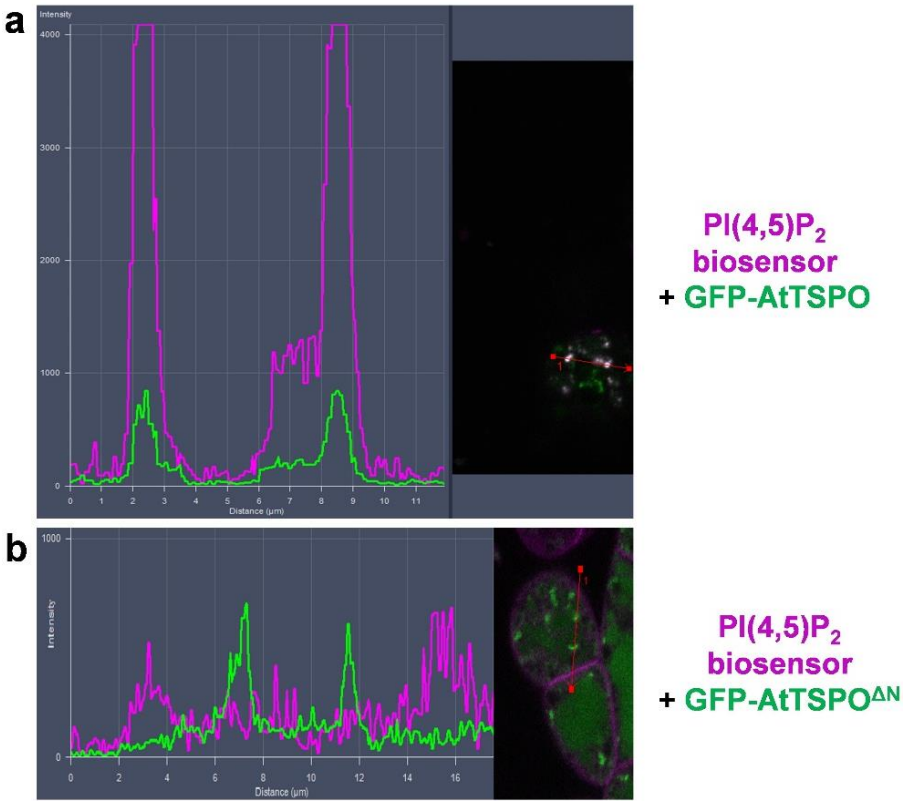

Figure 5.S10. Comparison of colocalization profiles for PI(4,5)P_2 biosensor coexpressed with full-length AtTSPO or with AtTSPO$^{\Delta N}$. (a) Colocalization profile for the lipid biosensor (mCherry-tagged, in magenta) stably expressed with full-length AtTSPO (GFP-tagged, in green). The profile was recorded along the red straight line illustrated on the right-hand side of the figure. A clear presence of both fluorescent signals in punctate structures (most-likely Golgi) could be detected. **(b)** Colocalization profile for the lipid biosensor (mCherry-tagged, in magenta) stably expressed with the N-terminus truncated AtTSPO (GFP-tagged, in green). The profile was recorded along the red straight line illustrated on the right-hand side of the figure. No simultaneous presence of both fluorescent signals could be detected suggesting no colocalization event. Intensities are given in arbitrary units.

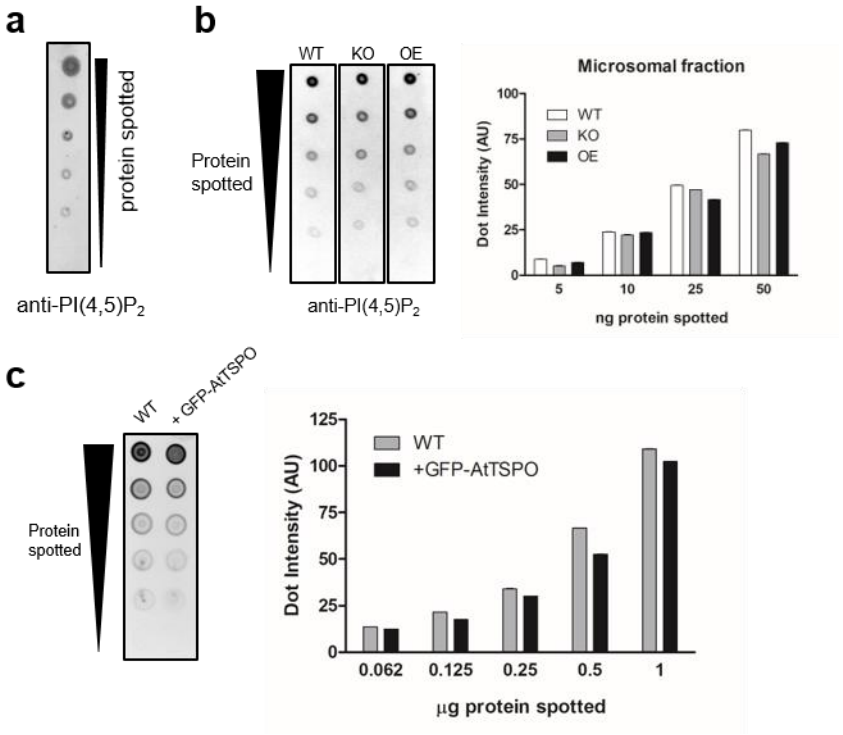

Figure 5.S11. Overexpression of AtTSPO does not impact the overall content of PI(4,5)P_2 lipid in microsomal fraction. (a) SDS-solubilized total extract of Arabidopsis plants was probed for PI(4,5)P_2 to validate the assay and antibodies. **(b)** SDS-solubilized microsomal fractions from the Arabidopsis wild-type (WT), knock-out for AtTSPO (KO) or AtTSPO overexpressing (OE) plant were spotted on the nitrocellulose membrane and probed for PI(4,5)P_2. **(c)** SDS-solubilized microsomal fractions from the Arabidopsis wild-type (WT) and GFP-AtTSPO overexpressing suspension cell lines were spotted on the nitrocellulose membrane and probed for PI(4,5)P_2. Average dot intensities were quantified using the ImageJ software and the plots represent a mean of three technical measurement repetitions.

Table 5.S1. Primers used in this study.

Primers for BiFC

Primer name	Sequence
SpeI-PIP2;7 Fw	5-AAAAAAAACTAGTATGTCGAAAGAAGTGAGCGAAGAAG-3
PIP2;7-XbaI Rv	5-AAAAAAATCTAGATTAATTGGTTGCGTTGCTTCGGAAC-3
AatII-AtTSPO Fw	5-AAAAAGACGTCCATGGATTCTCAGGACATCAG-3
AatII-AtTSPO^{M2} Fw	5-AAAAAGACGTCCATGGCCGAGACAGAGAGGAAAAG-3
AatII-AtTSPO$^{\Delta N}$ Fw	5-AAAAAGACGTCCATGGCGAAACGTGGTCTCAAG-3
AtTSPO-AsiSI Rv	5-AAAAAGCGATCGCTCACGCGACTGCAAGCTTTAC-3
AtTSPO^{K35AR36A} Int Fw	5-GACGACAACAAAGGAGCTGCTGATCAAAAGAGGGCGATG-3
AtTSPO^{K35AR36A} Int Rv	5-CATCGCCCTCTTTTGATCAGCAGCTCCTTTGTTGTCGTC-3
AtTSPO^{K39AR40A} Int Fw	5-GGAAAACGCGATCAAGCTGCTGCGATGGCGAAACGTG-3
AtTSPO^{K39AR40A} Int Rv	5-CACGTTTCGCCATCGCAGCAGCTTGATCGCGTTTTCC-3
AtTSPO$^{K39A/R40A/K44A/R45A}$ Int Fw	5-GAAAACGCGATCAAGCTGCTGCGATGGCGGCTGCTGGTCTCAAGTCTCTG-3
AtTSPO$^{K39A/R40A/K44A/R45A}$ Int Rv	5-CAGAGACTTGAGACCAGCAGCCGCCATCGCAGCAGCTTGATCGCGTTTTC-3

Primers for Arabidopsis transgenic suspension cells

Primer name	Sequence
USER-kozak-GFP Fw	5-GGCTTAAUCCACCATGAGTAAAGGAGAAGAAC-3
GFP-AtTSPO Int Rv	5-CTGATGTCCTGAGAATCCATTTTGTATAGTTCATCCATG-3
GFP-AtTSPO Int Fw	5-CATGGATGAACTATACAAAATGGATTCTCAGGACATCAG-3
USER-AtTSPO Rv	5-GGTTTAAUTCACGCGACTGCAAGCTTTAC-3
L-GFP Rv	5- ACCAGCTCCAGCACCAGCTCCTTTGTATAGTTCATCCATG-3
L-AtTSPO$^{\Delta N}$ Fw	5-GGAGCTGGTGCTGGAGCTGGTCTGACGGTAGCGGTTGCG-3
GFP-mTSPO Int Rv	5-CACCCAGGATTCAGGCATTTTGTATAGTTCATCCATG-3
GFP-mTSPO Int Fw	5-CATGGATGAACTATACAAAATGCCTGAATCCTGGGTG-3
USER-mTSPO Rv	5-GGTTTAAUTCACTCTGGGAGCCGGGAG-3
USER-kozak-AtTSPO Fw	5-GGCTTAAUCCACCATGGATTCTCAGGACATC -3
AtTSPO^{Nter}-GFP Int Rv	5- GTTCTTCTCCTTTACTCATAGACTTGAGACCACGTTTC -3
AtTSPO^{Nter}-GFP Int Fw	5-GAAACGTGGTCTCAAGTCTATGAGTAAAGGAGAAGAAC-3

Primers for TSPOs purification

Primer name	Sequence
XbaI-10His Fw	5-GGGGTCTAGAATGCATCACCATCACCATCACCATCACCATCAC-3
10His^{C}-AtTSPO Fw	5-CATCACCATCACCATCACATGGATTCTCAGGACATCAG-3
AtTSPO-XhoI Rv	5-AAAACTCGAGTCACGCGACTGCAAGC-3
XbaI-10His^{N} Fw	5-GGGGTCTAGAATGCATCACCATCACCATC-3
10His-TEV^{N} Fw	5-CATCACCATCACCATCACCATCACCATCACGGTGAAAATTTATAC-3
TEV-AtTSPO$^{\Delta N}$ Fw	5-GGTGAAAATTTATACTTCCAAGGTATGGCGAAACGTGGTCTC-3
AtTSPO$^{\Delta N}$-XhoI Rv	5-GGGGCTCGAGTCACGCGACTGCAAGC-3
BamHI-10His-TEV^{N} Fw	5-GGGGGGATCCCATCACCATCACCATCACCATCACCATCACGAAAATTTATAC-3
TEV-AtTSPO^{Nter} Fw	5-GAAAATTTATACTTCCAAGGTATGGATTCTCAGGACATCAGATAC-3
AtTSPO^{Nter}-XhoI Rv	5-GGGGCTCGAGTCAAGACTTGAGACCACGTTTC-3
NdeI-mTSPO Fw	5-AAAAACATATGCCTGAATCCTGGGTG-3
mTSPO-BamHI Rv	5-AAAAGGATCCTCACTCTGGGAGCCG-3
AtTSPO^{Nter}-mTSPO Int Fw	5-GAAACGTGGTCTCAAGTCTATGCCTGAATCCTGGGTG-3
AtTSPO^{Nter}-mTSPO Int Rv	5-CACCCAGGATTCAGGCATAGACTTGAGACCACGTTTC-3

PART IV: CONCLUSIONS AND PERSPECTIVES

Chapter 6: Towards a clearer picture of AtTSPO function

The biological role of TSPO protein in animal cells is currently under high debate. Recent findings (Morohaku et al., 2014; Sileikyte et al., 2014; Stocco, 2014; Selvaraj et al., 2016) clearly showed that the absence of TSPO has no effect on cell or whole animal viability and does not affect steroidogenesis, contradicting the almost 40 year-lasting consensus in the field. Nevertheless, high expression of TSPO has been consistently found in steroid-producing cells and recent studies suggested the involvement of TSPO in lipids metabolism in animal cells (Thompson et al., 2013; Taylor et al., 2014; Fan et al., 2015; Tu et al., 2016). Unpublished data from the comparative lipids profiling in Arabidopsis generated in a collaborative research involving the host laboratory uncovered an intriguing observation. Overexpression of AtTSPO significantly reduced the level of sterol esters in seedlings as compared to wild type seedlings attributing a putative function of the Arabidopsis TSPO homolog (AtTSPO) in plant lipids metabolism.

6.1. A role for AtTSPO in lipids metabolism: another mean for the evolutionarily conserved modulation of redox homeostasis?

Multiple environmental stresses affect TSPO expression levels across different organisms. However, oxidative stress appears to be the common stress affecting TSPO expression irrespective of the cell type (Li et al., 2016). So far in the field, the major focus on the regulation of cellular redox status was put on porphyrins. Porphyrins are the best characterized ligands of TSPO from all species characterized to date (Verma et al., 1987; Wendler et al., 2003; Rampon et al., 2009; Vanhee et al., 2011; Li et al., 2013; Gatliff et al., 2014; Marginedas-Freixa et al., 2016) and porphyrin binding seems to control numerous processes that involve TSPO. For instance, TSPO from *R. sphaeroides* was thought to promote the export of porphyrins from the cell to regulate the expression of photosynthetic gene (Yeliseev and Kaplan, 1999). In animals, TSPO

functions possibly in a similar way by regulating the accumulation of porphyrins, although recent studies on mice knocked-out for *TSPO* could not corroborate this data (Zhao et al., 2016). In addition, TSPO regulates the levels of mitochondria-derived ROS, and together with VDAC1 (Voltage-Dependent Anion Channel 1) it establishes a molecular platform for the tuning of mitophagy, a selective autophagic degradation of mitochondria (Gatliff et al., 2014). Characterized plant TSPO are involved, probably indirectly, in redox homeostasis by modulating tetrapyrrole metabolism. TSPO from Arabidopsis acts as a porphyrin scavenger through the autophagy pathway (Vanhee et al., 2011). Likewise, a TSPO homolog in the moss *Physcomitrella patens* controls protoporphyrin IX (PPIX) levels (Frank et al., 2007).

TSPO may also modulate oxidative stress through a direct breakdown of porphyrins. The role for TSPO in catalytic porphyrin degradation was first proposed in *Chlorobium tepidum*, an anaerobic green sulfur bacteria (Ginter et al., 2013). The same conclusion was further made for TSPO purified from a Gram-positive bacterium, *Bacillus cereus* (Guo et al., 2015). Intriguingly, as suggested by crystal structures of TSPO from *Rhodobacter* (Li et al., 2015) and reported in some heme oxygenases (Takayama et al., 2011; Unno et al., 2013), binding of porphyrin to TSPO provokes distortion of the porphyrin ring leading to oxidation even in the absence of light.

Lipid droplets (LD) are no more considered only as a storage form of neutral lipids that are catabolized when energy or fatty acids are required in the cell (Hashemi and Goodman, 2015). Recent evidence suggests that TAG (triacylglycerol), a major component of cytosolic LD are also involved in stress responses, at least in animal cells. Interestingly, LD can act as antioxidant organelles (Bailey et al., 2015), and other studies suggest that oxidative stress boosts the biosynthesis of LD (Liu et al., 2015). During hypoxia-triggered production of ROS in *Drosophila* neuroglia, LD could keep polyunsaturated fatty acids away from the plasma membrane, shielding these lipids from harmful peroxidation (Bailey et al., 2015).

The level of AtTSPO is tightly regulated in the plant cell through the autophagic degradation (Guillaumot et al., 2009; Vanhee et al., 2011;

Hachez et al., 2014). Unexpectedly, we found that overexpression of AtTSPO resulted in an increase of fatty acids levels in seeds. We also showed evidence that constitutive expression of AtTSPO reduced lipids reserves in germinating seeds or seedlings. Inactivation of AtTSPO, in contrast, enhanced lipid droplets (LD) levels in the same tissues. We reported similar observations in yeast cells.

The effect of AtTSPO in seedlings is somewhat similar to the situation described in animal cells. There, TSPO was downregulated in adipose tissues of mouse obesity models as compared to control animals (Thompson et al., 2013). In addition, TSPO absence in steroidogenic cells resulted in the accumulation of LD (Fan et al., 2015). The molecular mechanism of LD anabolism/catabolism regulation by TSPO is not yet clear. We reasoned that in the plant cell LD levels may be strictly correlated to the degradation of detrimental AtTSPO (model presented in Chapter 4.10). Indeed, a stabilized mutant form of AtTSPO harboring the point substitution H91A had a hampered impact on LD content of the cell.

6.2. AtTSPO: a selective autophagy receptor?

Apart from the involvement of AtTSPO in porphyrin scavenging and modulation of lipid homeostasis, the host laboratory revealed an intriguing connection between AtTSPO and aquaporin PIP2;7. These two proteins are targeted to different subcellular compartments but physically interact at membranes of ER and Golgi. The consequence of the interaction is the targeting of the proteins complex to autophagosome and their degradation in the vacuole. However, the underlying molecular mechanism of this interaction was unknown. Plant TSPO differ structurally from their animal and bacterial counterparts. Although plant TSPO also share the relatively conserved membrane domain made of five α-helices, the presence of a N-terminus extension that faces the cytosol appears as an intriguing feature. This extension of about 45 amino acids contains a relatively high number of charged residues. However, the dominance of basic residues over the acidic ones results in an overall positive charge of this peptide. We demonstrated that truncating this plant specific N-terminus in AtTSPO resulted in a mutant incapable of binding PIP2;7 *in vivo* suggesting an evolutionary structure-function

relationship of plant TSPO. Interestingly, this same N-terminal segment, alone or coupled to a TSPO membrane domain, was shown to interact with anionic lipids and in particular with $PI(4,5)P_2$. $PI(4,5)P_2$ is a signaling phosphoinositide involved in response to osmotic stress in plants albeit by an unknown molecular mechanism (Zonia and Munnik, 2004). It seems established in animal cells that $PI(4,5)P_2$ also plays a role in regulation of plasma membrane transporters including channels. Circumstantial evidence suggest a concomitant relationship between the abundance of both aquaporins and $PI(4,5)P_2$ at the plasma membrane of the plant cell (Ma et al., 2014). We reasoned that AtTSPO could regulate the water channel PIP2;7 through $PI(4,5)P_2$ signaling. NMR studies of the purified AtTSPO N-terminus uncovered putative residues involved in $PI(4,5)P_2$ binding. These couples of basic amino acids were mutated and functional analyses of the resultant mutant showed a drastic reduction of their capacity to interact with PIP2;7 *in vivo*. We believe that plant TSPO throughout their evolution have acquired a specific N-terminal domain acting as a $PI(4,5)P_2$ effector domain regulating osmotic stress response of the plant cell through the modulation of water channel levels at the plasma membrane. This plant-evolved function of TSPO argues for a cell-type specific function through the evolution of these enigmatic membrane proteins. These findings have enhanced our fine understanding of the biological role of TSPO and their peculiarities.

Selective autophagy has been characterized both in animal and yeast cells, but only recently similar observations were made in plants. It is suggested that the growing number of target proteins for selective autophagy is accompanied by structurally diverse cognate receptor/adaptor proteins recognizing and recruiting the cargo into the autophagosomes (Veljanovski and Batoko, 2014). Cargo recognition requires a ligand or a structural feature on the target. It was demonstrated before that AtTSPO binds heme *in vivo* and the protein-ligand complex is recruited to the autophagosome through an AIM (Atg8-interacting motif) present in AtTSPO (Vanhee et al., 2011). The tendency of AtTSPO to oligomerize (unpublished data) and the presence of an AIM-like motif (consensus W/YxxL/V/I) favors AtTSPO as a *bona fide* selective autophagy cargo receptor. Heme and PIP2;7 are possible cargo of AtTSPO

as a selective autophagy receptor. It is however speculative if free toxic heme is a simple cargo to be removed or whether it may serve as a ligand activating AtTSPO to recruit PIP2;7 into the nascent autophagosome. It is also tempting to speculate about a potential link between heme binding, lipids binding by AtTSPO, and PIP2;7 downregulation. We demonstrated that the point mutant variant of AtTSPO, H91A, with a reduced ability for heme binding, protected more efficiently plant cells from water loss than the wild-type protein. $AtTSPO^{H91A}$, unable to undergo autophagy is more abundant in the cell as compared to the wild-type protein, thus it could trap more PIP2;7 molecules on their road to the plasma membrane. A missing puzzle in favoring one option or another is whether PIP2;7 could be retained more efficiently in the ER/Golgi membranes in plants overexpressing $AtTSPO^{H91A}$. If so, we would favor heme as a ligand activating AtTSPO to act as PIP2;7 autophagy receptor.

On the other hand, the ligand role could be fulfilled by $PI(4,5)P_2$ (Figure 6.1). Binding of $PI(4,5)P_2$ to AtTSPO could induce structural changes required for the recognition of PIP2;7 molecules and their targeting to the autophagic pathway. It may be that AtTSPO does not directly extract $PI(4,5)P_2$ from the PM but could be a component of a protein complex involved in the recruitment of PI4P 5-kinase to the autophagosome initiation site. AtTSPO-mediated enrichment of the ER and Golgi membranes with $PI(4,5)P_2$ may also help to initiate autophagy. As we now know from animal cells, autophagosome membranes are known to contain PIP5K that generates $PI(4,5)P_2$ and the autophagy regulator Atg14 interacts with both the enzyme and its product. $PI(4,5)P_2$ binding to Atg14 regulates its interaction with the Vps34 complex catalyzing the production of PI3P at the autophagosome initiation site. Generation of $PI(4,5)P_2$ signaling on the autophagosome membrane could facilitate the targeting of AtTSPO-containing complex to this site.

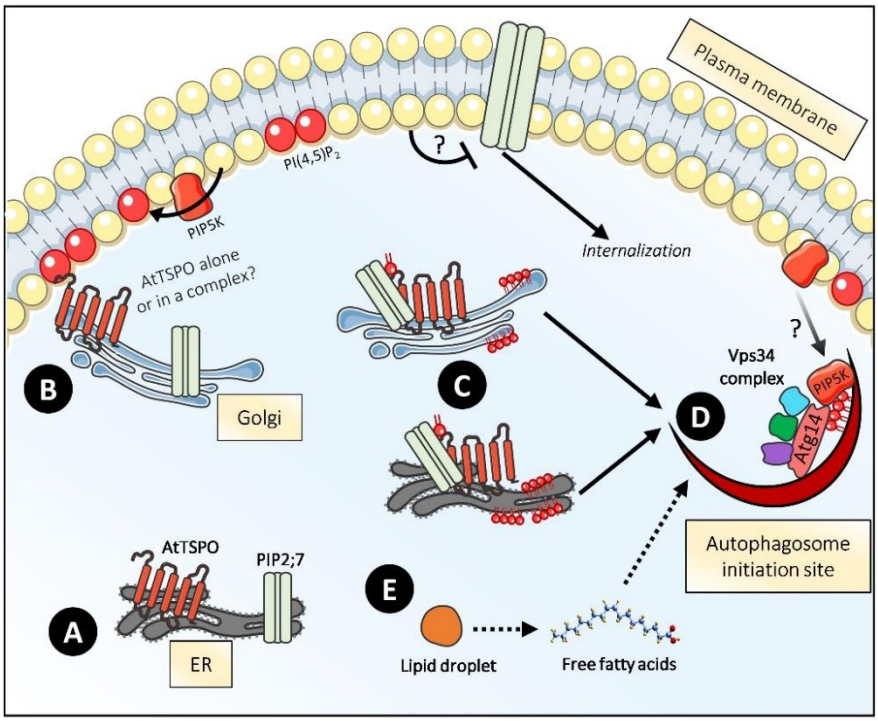

Figure 6.1. A hypothetical model of PI(4,5)P_2-dependent PIP2;7 downregulation by AtTSPO during stress. Under abiotic stress conditions, transiently biosynthesized AtTSPO is targeted to the Golgi via ER (A). Local PI(4,5)P_2 levels at the plasma membrane (PM) increase by the activity of PI4P 5-kinase (PIP5K). How the N-terminus of AtTSPO binds and depletes PI(4,5)P_2 from the PM (B) remains speculative. It likely takes place at the potential contact sites between ER/Golgi and PM. It may be that AtTSPO does not directly extract PI(4,5)P_2 from the PM but could be a part of a protein complex involved in this process or a complex involved in the recruitment of PIP5K to the autophagosome initiation site (question mark). Binding of PI(4,5)P_2 to AtTSPO could induce structural changes and the new conformation could then recognize PIP2;7 molecules *en route* to the PM (C) and incorporate them into nascent autophagosome (D). In parallel, depletion of PI(4,5)P_2 from the PM may reduce the activity of water channels (question mark) and trigger their internalization. Alternatively, enrichment of the ER and/or Golgi membranes with PI(4,5)P_2 may also help to initiate autophagy. Autophagosome has the kinase that generates PI(4,5)P_2 and the autophagy regulator ATG14 (animal nomenclature, a plant counterpart is not yet identified) interacts with both the enzyme and its product during autophagosome initiation. PI(4,5)P_2 binding to ATG14 regulates its interaction with VPS34-Beclin 1/ATG6 complex catalysing the production of PI3P at the autophagosome initiation site. The presence of AtTSPO-PI(4,5)P_2-PIP2;7 complex in the ER/Golgi membrane together with PI(4,5)P_2 and Atg8 in the phagophore inner membrane favors the autophagosome initiation site to be in a close vicinity of the TSPO complex. Also, since PIP5K is a component of phagophore formation, production of PI(4,5)P_2 could be a signal recognized by AtTSPO. (E) Lipid droplets comprise a huge pool of lipids which upon lipophagy and subsequent lipolysis in the vacuole come back as free fatty acids that contribute to the autophagosome formation. Presence of AtTSPO at elevated levels is detrimental to the cell. This triggers increased autophagic degradation of AtTSPO and required enhanced breakdown of lipid droplets. Dotted arrows indicate multi-step processes.

In addition, a mechanism of lipid extraction from the plasma membrane by AtTSPO is not clear. It is known that lipids constantly move across the membrane in lateral way and also by the so-called "flip-flop" transverse, the latter maintaining membrane asymmetry which is critical for membrane functions. Uncatalysed movement of phospholipids between membrane bilayers is possible albeit slow. Instead, phospholipid movement between bilayers is catalyzed by lipid translocator proteins (Contreras et al., 2010). Movement of phospholipids from the outer- to the inner membrane leaflet is catalyzed by flippases and floppases transfer phospholipids in the opposite direction. It is tempting to speculate if AtTSPO could function as lipid translocator protein but in this case AtTSPO would move $PI(4,5)P_2$ from the plasma membrane into the membranes of ER/Golgi. However, these catalyzed movements are typically dependent on ATP hydrolysis (Contreras et al., 2010), reaction not yet reported for AtTSPO.

The question whether PIP2;7 interacts with $PI(4,5)P_2$ remains to be addressed. If so, the PIP2;7-AtTSPO interaction would not only depend on the conformational change of AtTSPO but also on binding of both partners to a common ligand. Despite several experimental trials, we were not able to demonstrate $PI(4,5)P_2$ binding to PIP2;7 (data not shown). Also, a closely related isoform PIP2;5 was shown not to bind $PI(4,5)P_2$ *in vitro* (oral communication, Dr. Ana Romina Fox), although the binding to phosphatidic acid was observed. Interestingly, the sequence analysis of Arabidopsis PIP2;7 does not reveal any positively charged stretch of amino acids facing the cytosol for putative binding of anionic lipids.

The membrane origin for a rapid autophagosome formation in the cell is not yet clear. Studies in yeast and mammalian cells point to the ER as a compartment initiating autophagosomes, and others suggest that several cellular compartments including the Golgi contribute to the phagophore initiation and expansion (Lamb et al., 2013; Puri et al., 2013). It is worth asking why AtTSPO could mislocalize the $PI(4,5)P_2$ sensor to the Golgi but we could not observe sensor fluorescence at the membranes of the ER. It is likely that the local concentration of the free membrane-embedded lipid at the ER was below the detection threshold or all the

available lipid molecules were already bound by AtTSPO. Another intriguing observation is that AtTSPO, when overexpressed in plant cells, was able to colocalize with the PI(4,5)P_2 biosensor at the Golgi membranes but the same sensor remained cytosolic when wild type cells were treated with the plant stress hormone ABA. It is possible that we could not observe the sensor localizing at the Golgi in addition to cytoplasm, because of lack of a Golgi marker.

We found that PI(4,5)P_2 binding is not essential to the autophagy-dependent degradation of AtTSPO since the N-terminus truncated form of the protein could still be translocated to the vacuole. However, binding of PI(4,5)P_2 is necessary for AtTSPO to interact with the aquaporin PIP2;7. This could happen as the autophagosome is initiated at the vicinity of AtTSPO-containing organelles, the cytosolic N-terminus of AtTSPO may come into close contact with the autophagosome initiation membrane enriched in PI(4,5)P_2 and PI3P. The question of how the AtTSPO-containing complex is extracted and translocated to the autophagosomal membrane remains open.

PART V: REFERENCES

Agorio, A., Giraudat, J., Bianchi, M.W., et al. (2017) Phosphatidylinositol 3-phosphate–binding protein AtPH1 controls the localization of the metal transporter NRAMP1 in Arabidopsis. *Proc. Natl. Acad. Sci. U. S. A.*, **114**, E3354–E3363.

Anderson, R.A., Boronenkov, I. V., Doughman, S.D., Kunz, J. and Loijens, J.C. (1999) Phosphatidylinositol phosphate kinases, a multifaceted family of signaling enzymes. *J. Biol. Chem.*, **274**, 9907–9910.

Anholt, R., Pedersen, P.L., Souza, E.B. De and Snyder, S.H. (1986) The peripheral-type benzodiazepine receptor. Localization to the mitochondrial outer membrane. *J. Biol. Chem.*, **261**, 576–583.

Anholt, R.R., Murphy, K.M., Mack, G.E. and Snyder, S.H. (1984) Peripheral-type benzodiazepine receptors in the central nervous system: localization to olfactory nerves. *J. Neurosci.*, **4**, 593–603.

Antoni, R., Gonzalez-Guzman, M., Rodriguez, L., Rodrigues, A., Pizzio, G.A. and Rodriguez, P.L. (2011) Selective inhibition of clade A phosphatases type 2C by PYR/PYL/RCAR abscisic acid receptors. *Plant Physiol.*, **158**, 970–980.

Aroca, R., Amodeo, G., Fernandez-Illescas, S., Herman, E.M., Chaumont, F. and Chrispeels, M.J. (2005) The Role of Aquaporins and Membrane Damage in Chilling and Hydrogen Peroxide Induced Changes in the Hydraulic Conductance of Maize Roots. *Plant Physiol.*, **137**, 341–353.

Audran, C., Borel, C., Frey, A., Sotta, B., Meyer, C., Simonneau, T. and Marion-Poll, A. (1998) Expression Studies of the Zeaxanthin Epoxidase Gene in Nicotiana plumbaginifolia. *Plant Physiol.*, **118**, 1021–1028.

Bae, K.R., Shim, H.J., Balu, D., Kim, S.R. and Yu, S.W. (2014) Translocator protein 18 kDa negatively regulates inflammation in microglia. *J. Neuroimmune Pharmacol.*, **9**, 424–437.

Bailey, A.P., Koster, G., Guillermier, C., Hirst, E.M.A., MacRae, J.I., Lechene, C.P., Postle, A.D. and Gould, A.P. (2015) Antioxidant Role for Lipid Droplets in a Stem Cell Niche of Drosophila. *Cell*, **163**, 340–353.

Bak, G., Lee, E.-J., Lee, Y., Kato, M., Segami, S., Sze, H., Maeshima, M., Hwang, J.-U. and Lee, Y. (2013) Rapid Structural Changes and Acidification of Guard Cell Vacuoles during Stomatal Closure Require Phosphatidylinositol 3,5-Bisphosphate. *Plant Cell*, **25**, 2202–2216.

Balla, T. (2013) Phosphoinositides: Tiny Lipids With Giant Impact on Cell Regulation. *Physiol. Rev.*, **93**, 1019–1137.

Banati, R.B., Middleton, R.J., Chan, R., et al. (2014) Positron emission tomography and functional characterization of a complete PBR/TSPO knockout. *Nat. Commun.*, **5**, 5452.

Bargmann, B., Laxalt, A., ter Riet, B., Testerink, C., et al. (2009) Reassessing the role of phospholipase D in the Arabidopsis wounding response. Plant Cell Environ., **32**, 837-850

Batoko, H., Dagdas, Y., Baluska, F. and Sirko, A. (2017) Understanding and exploiting autophagy signaling in plants. *Essays Biochem.*, **61**, 675–685.

Batoko, H., Veljanovski, V. and Jurkiewicz, P. (2015) Enigmatic Translocator protein (TSPO) and cellular stress regulation. *Trends Biochem. Sci.*, **40**, 497–503.

Batoko, H., Zheng, H.Q., Hawes, C. and Moore, I. (2000) A Rab1 GTPase is required for transport between the endoplasmic reticulum and Golgi apparatus and for normal Golgi movement in plants. *Plant Cell*, **12**, 2201–2217.

Bellati, J., Alleva, K., Soto, G., Vitali, V., Jozefkowicz, C. and Amodeo, G. (2010) Intracellular pH sensing is altered by plasma membrane PIP aquaporin co-expression. *Plant Mol. Biol.*, **74**, 105–118.

Berny, M.C., Gilis, D., Rooman, M. and Chaumont, F. (2016) Single Mutations in the Transmembrane Domains of Maize Plasma Membrane Aquaporins Affect the Activity of Monomers within a Heterotetramer. *Mol. Plant*, **9**, 986–1003.

Berridge, M. (1993) Inositol trisphosphate and calcium signaling. *Nature*, **361**, 315–325.

Bhangoo, A., Anhalt, H., Ten, S. and King, S. (2006) Phenotypic variations in lipoid congenital adrenal hyperplasia. *Pediatr. Endocrinol. Rev.*, **3**, 258–271.

Bhattacharyya, S., Yu, H., Mim, C. and Matouschek, A. (2014) Regulated protein turnover: snapshots of the proteasome in action. *Nat. Rev. Mol. Cell Biol.*, **15**, 122–133.

Bienert, G.P., Cavez, D., Besserer, A., Berny, M.C., Gilis, D., Rooman, M. and Chaumont, F. (2012) A conserved cysteine residue is involved in disulfide bond formation between plant plasma membrane aquaporin monomers. *Biochem. J.*, **445**, 101–111.

Boudsocq, M., Droillard, M.J., Barbier-Brygoo, H. and Laurière, C. (2007) Different phosphorylation mechanisms are involved in the activation of sucrose non-fermenting 1 related protein kinases 2 by osmotic stresses and abscisic acid. *Plant Mol. Biol.*, **63**, 491–503.

Boursiac, Y., Léran, S., Corratgé-Faillie, C., Gojon, A., Krouk, G. and Lacombe, B. (2013) ABA transport and transporters. *Trends Plant Sci.*, **18**, 325–333.

Braestrup, C., Albrechtsen, R. and Squires, R.F. (1977) High densities of benzodiazepine receptors in human cortical areas. *Nature*, **269**, 702–704.

Braestrup, C. and Squires, R.F. (1977) Specific benzodiazepine receptors in rat brain characterized by high affinity [3H] diazepam binding. *Proc. Natl. Acad. Sci. U. S. A.*, **74**, 3805–3809.

Browse, J., McCourt, P.J. and Somerville, C.R. (1986) Fatty acid composition of leaf lipids determined after combined digestion and fatty acid methyl ester formation from fresh tissue. *Anal. Biochem.*, **152**, 141–145.

Browse, J., Warwick, N., Somerville, C.R. and Slack, C.R. (1986) Fluxes through the prokaryotic and eukaryotic pathways of lipid synthesis in the '16:3' plant Arabidopsis thaliana. *Biochem. J.*, **235**, 25–31.

Bueso, E., Rodriguez, L., Lorenzo-Orts, L., Gonzalez-Guzman, M., Sayas, E., Muñoz-Bertomeu, J., Ibañez, C., Serrano, R. and Rodriguez, P.L. (2014) The single-subunit RING-type E3 ubiquitin ligase RSL1 targets PYL4 and PYR1 ABA receptors in plasma membrane to modulate abscisic acid signaling. *Plant J.*, **80**, 1057–1071.

Burbidge, A., Grieve, T.M., Jackson, A., Thompson, A., McCarty, D.R. and Taylor, I.B. (1999) Characterization of the ABA-deficient tomato mutant notabilis and its relationship with maize Vp14. *Plant J.*, **17**, 427–431.

Cai, Y., Goodman, J.M., Pyc, M., Mullen, R.T., Dyer, J.M. and Chapman, K.D. (2015) Arabidopsis SEIPIN Proteins Modulate Triacylglycerol Accumulation and Influence Lipid Droplet Proliferation. *Plant Cell*, **27**, 2616–2636.

Caillon, L., Lequin, O. and Khemtémourian, L. (2013) Evaluation of membrane models and their composition for islet amyloid polypeptide-membrane aggregation. *Biochim. Biophys. Acta - Biomembr.*, **1828**, 2091–2098.

Carayon, P., Portier, M., Dussossoy, D., Bord, A., Petitprêtre, G., Canat, X., Fur, G. Le and Casellas, P. (1996) Involvement of peripheral benzodiazepine receptors in the protection of hematopoietic cells against oxygen radical damage. *Blood J.*, **87**, 3170–3178.

Caron, K.M., Soo, S.C., Wetsel, W.C., Stocco, D.M., Clark, B.J. and Parker, K.L. (1997) Targeted disruption of the mouse gene encoding steroidogenic acute regulatory protein provides insights into congenital lipoid adrenal hyperplasia. *Proc. Natl. Acad. Sci. U. S. A.*, **94**, 11540–11545.

Chapman, K.D. and Ohlrogge, J.B. (2012) Compartmentation of triacylglycerol accumulation in plants. *J. Biol. Chem.*, **287**, 2288–2294.

Chaumont, F., Barrieu, F., Wojcik, E., Chrispeels, M.J. and Jung, R. (2001) Aquaporins Constitute a Large and Highly Divergent Protein Family in Maize. *Plant Physiol.*, **125**, 1206–1215.

Chaumont, F., Moshelion, M. and Daniels, M.J. (2005) Regulation of plant aquaporin activity. *Biol. cell*, **97**, 749–764.

Chaumont, F. and Tyerman, S.D. (2014) Aquaporins: Highly Regulated Channels Controlling Plant Water Relations. *Plant Physiol.*, **164**, 1600–1618.

Chernys, J.T. and Zeevaart, J.A.D. (2000) Characterization of the 9-Cis-Epoxycarotenoid Dioxygenase Gene Family and the Regulation of Abscisic Acid Biosynthesis in Avocado. *Plant Physiol.*, **124**, 343–354.

Chevalier, A.S., Bienert, G.P. and Chaumont, F. (2014) A New LxxxA Motif in the Transmembrane Helix3 of Maize Aquaporins Belonging to the Plasma Membrane Intrinsic Protein PIP2 Group Is Required for Their Trafficking to the Plasma Membrane. *Plant Physiol.*, **166**, 125–138.

Chiabrando, D., Marro, S., Mercurio, S., et al. (2012) The mitochondrial heme exporter FLVCR1b mediates erythroid differentiation. *J. Clin. Invest.*, **122**, 4569–4579.

Cho, H., Kim, Y. a and Ho, W.-K. (2006) Phosphate number and acyl chain length determine the subcellular location and lateral mobility of phosphoinositides. *Mol. Cells*, **22**, 97–103.

Christmann, A., Weiler, E.W., Steudle, E. and Grill, E. (2007) A hydraulic signal in root-to-shoot signaling of water shortage. *Plant J.*, **52**, 167–174.

Chuang, H., Prescott, E., Kong, H. and Shields, S. (2001) Bradykinin and nerve growth factor release the capsaicin receptor from PtdIns(4,5)P_2-mediated inhibition. *Nature*, **411**, 957–962.

Cochard, H., Venisse, J.-S., Barigah, T.S., Brunel, N., Herbette, S., Guilliot, A., Tyree, M.T. and Sakr, S. (2006) Putative Role of Aquaporins in Variable Hydraulic Conductance of Leaves in Response to Light. *Plant Physiol.*, **143**, 122–133.

Contreras, F.X., Sánchez-Magraner, L., Alonso, A. and Gonic, F.M. (2010) Transbilayer (flip-flop) lipid motion and lipid scrambling in membranes. FEBS Lett., **584**, 1779-1786.

Cornforth, J.W., Milborrow, B. V., Ryback, G. and Wareing, P.F. (1965) Chemistry and Physiology of 'Dormins' In Sycamore: Identity of Sycamore 'Dormin' with Abscisin II. *Nature*, **205**, 1269–1270.

Corsi, L., Avallone, R., Geminiani, E., Cosenza, F., Venturini, I. and Baraldi, M. (2004) Peripheral benzodiazepine receptors in potatoes (Solanum tuberosum). *Biochem. Biophys. Res. Commun.*, **313**, 62–66.

Costa, B., Pini, S., Gabelloni, P., et al. (2009) The spontaneous Ala147Thr amino acid substitution within the translocator protein influences pregnenolone production in lymphomonocytes of healthy individuals. *Endocrinology*, **150**, 5438–5445.

Craene, J.O. De, Bertazzi, D.L., Bär, S. and Friant, S. (2017) Phosphoinositides, major actors in membrane trafficking and lipid signaling pathways. *Int. J. Mol. Sci.*, **18**, 634.

Cutler, S.R., Rodriguez, P.L., Finkelstein, R.R. and Abrams, S.R. (2010) Abscisic acid: emergence of a core signaling network. *Annu. Rev. Plant Biol.*, **61**, 651–679.

Danielson, J. and Johanson, U. (2008) Unexpected complexity of the Aquaporin gene family in the moss Physcomitrella patens. *BMC Plant Biol.*, **8**, 45.

Davey, M.E. and Bruijn, F.J. De (2000) A homologue of the tryptophan-rich sensory protein TspO and FixL regulate a novel nutrient deprivation-induced Sinorhizobium meliloti locus. *Appl. Environ. Microbiol.*, **66**, 5353–5359.

Delaglio, F., Grzesiek, S., Vuister, G., Zhu, G., Pfeifer, J. and Bax, A. (1995) NMRPipe: a multidimensional spectral processing system based on UNIX pipes. *J. Biomol. NMR*, **6**, 277–293.

Ding, Y., Lapko, H., Ndamukong, I., et al. (2009) TheArabidopsis Chromatin Modifier ATX1, the Myotubularin-like AtMTM, and the response to Drought; a view from the other end of the pathway. *Plant Signal. Behav.*, **4**, 1049–1058.

Doi, A., Fujimoto, A., Sato, S., et al. (2015) Chemical genomics approach to identify genes associated with sensitivity to rapamycin in the fission yeast Schizosaccharomyces pombe. *Genes to Cells*, **20**, 292–309.

Egan, D.F., Chun, M.G.H., Vamos, M., et al. (2015) Small Molecule Inhibition of the Autophagy Kinase ULK1 and Identification of ULK1 Substrates. *Mol. Cell*, **59**, 285–297.

Eggena, P. (1983) Activation energy for water transport in toad bladder. *Am. J. Physiol.*, **244**, C44-49.

Fahy, E., Cotter, D., Sud, M. and Subramaniam, S. (2011) Lipid classification, structures and tools. *Biochim. Biophys. Acta - Mol. Cell Biol. Lipids*, **1811**, 637–647.

Fahy, E., Subramaniam, S., Brown, H.A., et al. (2005) A comprehensive classification system for lipids. *J. Lipid Res.*, **46**, 839–862.

Fahy, E., Subramaniam, S., Murphy, R.C., et al. (2009) Update of the LIPID MAPS comprehensive classification system for lipids. *J. Lipid Res.*, **50**, S9–S14.

Fan, J., Campioli, E., Midzak, A., Culty, M. and Papadopoulos, V. (2015) Conditional steroidogenic cell-targeted deletion of TSPO unveils a crucial role in viability and hormone-dependent steroid formation. *Proc. Natl. Acad. Sci. U. S. A.*, **112**, 7261–7266.

Fan, J., Lindemann, P., Feuilloley, M.G.J. and Papadopoulos, V. (2012) Structural and Functional Evolution of the Translocator Protein (18 kDa). *Curr. Mol. Med.*, **12**, 369–386.

Fan, J., Rone, M.B. and Papadopoulos, V. (2009) Translocator protein 2 is involved in cholesterol redistribution during erythropoiesis. *J. Biol. Chem.*, **284**, 30484–30497.

Fan, J., Yan, C. and Xu, C. (2013) Phospholipid:diacylglycerol acyltransferase-mediated triacylglycerol biosynthesis is crucial for protection against fatty acid-induced cell death in growing tissues of Arabidopsis. *Plant J.*, **76**, 930–942.

Fan, T. (1996) Metabolite profiling by one- and two-dimensional NMR analysis of complex mixtures. *Prog. Nucl. Magn. Reson. Spectrosc.*, **28**, 161–219.

Ferry-Dumazet, H., Gil, L., Deborde, C., Moing, A., Bernillon, S., Rolin, D., Nikolski, M., Daruvar, A. de and Jacob, D. (2011) MeRy-B: A web knowledgebase for the storage, visualization, analysis and annotation of plant NMR metabolomic profiles. *BMC Plant Biol.*, **11**, 104.

Fetter, K., van Wilder, V., Moshelion, M. and Chaumont, F. (2004) Interactions between Plasma Membrane Aquaporins Modulate Their Water Channel Activity. *Plant Cell*, **16**, 215–228.

Finkelstein, R. (2013) Abscisic Acid synthesis and response. *Arab. B.*, **11**, e0166.

Finley, D. (2009) Recognition and Processing of Ubiquitin-Protein Conjugates by the Proteasome. *Annu. Rev. Biochem.*, **78**, 477–513.

Food and Agriculture Organization of the United Nations. (2009) High level expert forum-How to feed the world 2050, October 12-13, Rome, Italy.

Forcat, S., Bennett, M.H., Mansfield, J.W. and Grant, M.R. (2008) A rapid and robust method for simultaneously measuring changes in the phytohormones ABA, JA and SA in plants following biotic and abiotic stress. *Plant Methods*, **4**, 16.

Fotiadis, D., Jenö, P., Mini, T., Wirtz, S., Müller, S.A., Fraysse, L., Kjellbom, P. and Engel, A. (2001) Structural characterization of two aquaporins isolated from native spinach leaf plasma membranes. *J. Biol. Chem.*, **276**, 1707–1714.

Frank, W., Baar, K.M., Qudeimat, E., Woriedh, M., Alawady, A., Ratnadewi, D., Gremillon, L., Grimm, B. and Reski, R. (2007) A mitochondrial protein homologous to the mammalian peripheral-type benzodiazepine receptor is essential for stress adaptation in plants. *Plant J.*, **51**, 1004–1018.

Frick, A., Järvå, M. and Törnroth-Horsefield, S. (2013) Structural basis for pH gating of plant aquaporins. *FEBS Lett.*, **587**, 989–993.

Fujita, M., Fujita, Y., Noutoshi, Y., Takahashi, F., Narusaka, Y., Yamaguchi-Shinozaki, K. and Shinozaki, K. (2006) Crosstalk between abiotic and biotic stress responses: a current view from the points of convergence in the stress signaling networks. *Curr. Opin. Plant Biol.*, **9**, 436–442.

Funderburk, S.F., Wang, Q.J. and Yue, Z. (2010) The Beclin 1-VPS34 complex - at the crossroads of autophagy and beyond. *Trends Cell Biol.*, **20**, 355–362.

Galvão, R.M., Kota, U., Soderblom, E.J., Goshe, M.B. and Boss, W.F. (2008) Characterization of a new family of protein kinases from Arabidopsis containing phosphoinositide 3/4-kinase and ubiquitin-like domains. *Biochem. J.*, **409**, 117–127.

Gao, C., Zhuang, X., Cui, Y., et al. (2015) Dual roles of an Arabidopsis ESCRT component FREE1 in regulating vacuolar protein transport and autophagic degradation. *Proc. Natl. Acad. Sci. U. S. A.*, **112**, 1886–1891.

Gao, H., Brandizzi, F., Benning, C. and Larkin, R.M. (2008) A membrane-tethered transcription factor defines a branch of the heat stress response in Arabidopsis thaliana. *Proc. Natl. Acad. Sci. U. S. A.*, **105**, 16398–16403.

Gatliff, J., East, D., Crosby, J., Abeti, R., Harvey, R., Craigen, W., Parker, P. and Campanella, M. (2014) TSPO interacts with VDAC1 and triggers a ROS-mediated inhibition of mitochondrial quality control. *Autophagy*, **10**, 2279–2296.

Gatliff, J., East, D.A., Singh, A., et al. (2017) A role for TSPO in mitochondrial Ca2+homeostasis and redox stress signaling. *Cell Death Dis.*, **8**, e2896.

Gavish, M., Bachman, I., Shoukrun, R., Katz, Y., Veenman, L., Weisinger, G. and Weizman, A. (1999) Enigma of the peripheral benzodiazepine receptor. *Pharmacol. Rev.*, **51**, 629–650.

Geng, Y., Wu, R., Wee, C.W., Xie, F., Wei, X., Chan, P.M.Y., Tham, C., Duan, L. and Dinneny, J.R. (2013) A Spatio-Temporal Understanding of Growth Regulation during the Salt Stress Response in Arabidopsis. *Plant Cell*, **25**, 2132–2154.

Gietz, R.D. and Schiest, R.H. (2007) Yeast transformation by the LiAc/SS carrier DNA/PEG method. *Nat. Protoc.*, **2**, 31–34.

Ginter, C., Kiburu, I. and Boudker, O. (2013) Chemical Catalysis by the Translocator Protein (18 kDa). *Biochemistry*, **52**, 3609–3611.

Girard, C., Liu, S., Adams, D., et al. (2012) Axonal regeneration and neuroinflammation: Roles for the translocator protein 18kDa. *J. Neuroendocrinol.*, **24**, 71–81.

Gomez, R.E., Joubès, J., Valentin, N., Batoko, H., Satiat-Jeunemaître, B. and Bernard, A. (2017) Lipids in membrane dynamics during autophagy in plants. *J. Exp. Bot.*, **69**, 1287–1299.

Gonzalez-Guzman, M., Pizzio, G.A., Antoni, R., et al. (2012) Arabidopsis PYR/PYL/RCAR Receptors Play a Major Role in Quantitative Regulation of Stomatal Aperture and Transcriptional Response to Abscisic Acid. *Plant Cell*, **24**, 2483–2496.

Gonzalez-Polo, R.A., Carvalho, G., Braun, T., et al. (2005) PK11195 potently sensitizes to apoptosis induction independently from the peripheral benzodiazepin receptor. *Oncogene*, **24**, 7503–7513.

Gookin, T.E. and Assmann, S.M. (2014) Significant reduction of BiFC non-specific assembly facilitates in planta assessment of heterotrimeric G-protein interactors. *Plant J.*, **80**, 553–567.

Guilarte, T.R., Loth, M.K. and Guariglia, S.R. (2016) TSPO Finds NOX2 in Microglia for Redox Homeostasis. *Trends Pharmacol. Sci.*, **37**, 334–343.

Guillaumot, D., Guillon, S., Planque, T. De, Vanhee, C., Gumy, C., Masquelier, D., Morsomme, P. and Batoko, H. (2009) The Arabidopsis TSPO-related protein is a stress and abscisic acid regulated, endoplasmic reticulum-Golgi-localized membrane protein. *Plant J.*, **60**, 242–256.

Guo, Y., Kalathur, R.C., Liu, Q., Kloss, B., Bruni, R., Ginter, C., Kloppmann, E., Rost, B. and Hendrickson, W.A. (2015) Structure and activity of tryptophan-rich TSPO proteins. *Science*, **347**, 551–555.

Gupta, R. (2002) A Tumor Suppressor Homolog, AtPTEN1, Is Essential for Pollen Development in Arabidopsis. *Plant Cell*, **14**, 2495–2507.

Gut, P., Baeza-Raja, B., Andersson, O., et al. (2013) Whole-organism screening for gluconeogenesis identifies activators of fasting metabolism. *Nat. Chem. Biol.*, **9**, 97–104.

Hachez, C., Heinen, R.B., Draye, X. and Chaumont, F. (2008) The expression pattern of plasma membrane aquaporins in maize leaf highlights their role in hydraulic regulation. *Plant Mol. Biol.*, **68**, 337–353.

Hachez, C., Laloux, T., Reinhardt, H., et al. (2014) Arabidopsis SNAREs SYP61 and SYP121 Coordinate the Trafficking of Plasma Membrane Aquaporin PIP2;7 to Modulate the Cell Membrane Water Permeability. *Plant Cell*, **26**, 3132–3147.

Hachez, C., Moshelion, M., Zelazny, E., Cavez, D. and Chaumont, F. (2006) Localization and quantification of plasma membrane aquaporin expression in maize primary root: A clue to understanding their role as cellular plumbers. *Plant Mol. Biol.*, **62**, 305–323.

Hachez, C., Veljanovski, V., Reinhardt, H., Guillaumot, D., Vanhee, C., Chaumont, F. and Batoko, H. (2014) The Arabidopsis abiotic stress-induced TSPO-related protein reduces cell-surface expression of the aquaporin PIP2;7 through protein-protein interactions and autophagic degradation. *Plant Cell*, **26**, 4974–4990.

Hachez, C., Veselov, D., Ye, Q., Reinhardt, H., Knipfer, T., Fricke, W. and Chaumont, F. (2012) Short-term control of maize cell and root water permeability through plasma membrane aquaporin isoforms. *Plant, Cell Environ.*, **35**, 185–198.

Hachez, C., Zelazny, E. and Chaumont, F. (2006) Modulating the expression of aquaporin genes in planta: A key to understand their physiological functions? *Biochim. Biophys. Acta*, **1758**, 1142–1156.

Hamasaki, M., Furuta, N., Matsuda, A., et al. (2013) Autophagosomes form at ER-mitochondria contact sites. *Nature*, **495**, 389–393.

Hammond, G.R. V, Fischer, M.J., Anderson, K.E., Holdich, J., Koteci, A., Balla, T. and Irvine, R.F. (2012) PI4P and PI(4,5)P_2 are essential but independent lipid determinants of membrane identity. *Science*, **337**, 727–730.

Harris, M.J. and Outlaw, W.H. (1991) Rapid adjustment of guard-cell abscisic acid levels to current leaf-water status. *Plant Physiol.*, **95**, 171–173.

Harris, M.J., Outlaw, W.H., Mertens, R. and Weiler, E.W. (1988) Water-stress-induced changes in the abscisic acid content of guard cells and other cells of Vicia faba L. leaves as determined by enzyme-amplified immunoassay. *Proc. Natl. Acad. Sci. U. S. A.*, **85**, 2584–2588.

Hashemi, H.F. and Goodman, J.M. (2015) The life cycle of lipid droplets. *Curr. Opin. Cell Biol.*, **33**, 119–124.

Heape, A.M., Juguelin, H., Boiron, F. and Cassagne, C. (1985) Improved one-dimensional thin-layer chromatographic technique for polar lipids. *J. Chromatogr. A*, **322**, 391–395.

Hedfalk, K., Törnroth-Horsefield, S., Nyblom, M., Johanson, U., Kjellbom, P. and Neutze, R. (2006) Aquaporin gating. *Curr. Opin. Struct. Biol.*, **16**, 447–456.

Heilmann, I. (2016a) Phosphoinositide signaling in plant development. *Development*, **143**, 2044–2055.

Heilmann, I. (2016b) Plant phosphoinositide signaling - dynamics on demand. *Biochim. Biophys. Acta - Mol. Cell Biol. Lipids*, **1861**, 1345–1351. **Heilmann, M. and Heilmann, I.** (2013) Arranged marriage in lipid signaling? The limited choices of PtdIns(4,5)P_2 in finding the right partner. *Plant Biol.*, **15**, 789–797.

Heilmann, M. and Heilmann, I. (2015) Plant phosphoinositides - complex networks controlling growth and adaptation. *Biochim. Biophys. Acta - Mol. Cell Biol. Lipids*, **1851**, 759–769.

Hermans, C., Vuylsteke, M., Coppens, F., Craciun, A., Inzé, D. and Verbruggen, N. (2010) Early transcriptomic changes induced by magnesium deficiency in Arabidopsis thaliana reveal the alteration of circadian clock gene expression in roots and the triggering of abscisic acid-responsive genes. *New Phytol.*, **187**, 119–131.

Hilgemann, D.W., Feng, S. and Nasuhoglu, C. (2001) The complex and intriguing lives of PIP2 with ion channels and transporters. *Sci. STKE*, **2001**, re19.

Hirano, T., Munnik, T. and Sato, M.H. (2015) Phosphatidylinositol 3-phosphate 5-kinase, FAB1/PIKfyve mediates endosome maturation to establish endosome-cortical microtubule interaction in Arabidopsis. *Plant Physiol.*, **169**, 1961–1974.

Hirayama, T. and Shinozaki, K. (2007) Perception and transduction of abscisic acid signals: keys to the function of the versatile plant hormone ABA. *Trends Plant Sci.*, **12**, 343–351.

Hofmann, N.R. (2011) *How a Transient Response Becomes Transient: Autophagy Cleans up after Abscisic Acid*,

Holthuis, J.C.M. and Menon, A.K. (2014) Lipid landscapes and pipelines in membrane homeostasis. *Nature*, **510**, 48–57.

Horie, T., Karahara, I. and Katsuhara, M. (2012) Salinity tolerance mechanisms in glycophytes: An overview with the central focus on rice plants. *Rice*, **5**, 11.

Horn, P.J., James, C.N., Gidda, S.K., Kilaru, A., Dyer, J.M., Mullen, R.T., Ohlrogge, J.B. and Chapman, K.D. (2013) Identification of a New Class of Lipid Droplet-Associated Proteins in Plants. *Plant Physiol.*, **162**, 1926–1936.

Hua, Z. and Vierstra, R.D. (2011) The Cullin-RING Ubiquitin-Protein Ligases. *Annu. Rev. Plant Biol.*, **62**, 299–334.

Ikegami, K., Okamoto, M., Seo, M. and Koshiba, T. (2009) Activation of abscisic acid biosynthesis in the leaves of Arabidopsis thaliana in response to water deficit. *J. Plant Res.*, **122**, 235–243.

Ischebeck, T., Seiler, S. and Heilmann, I. (2010) At the poles across kingdoms: Phosphoinositides and polar tip growth. *Protoplasma*, **240**, 13–31.

Ischebeck, T., Stenzel, I. and Heilmann, I. (2008) Type B Phosphatidylinositol-4-Phosphate 5-Kinases Mediate Arabidopsis and Nicotiana tabacum Pollen Tube Growth by Regulating Apical Pectin Secretion. *Plant Cell*, **20**, 3312–3330.

Ischebeck, T., Stenzel, I., Hempel, F., Jin, X., Mosblech, A. and Heilmann, I. (2011) Phosphatidylinositol-4,5-bisphosphate influences Nt-Rac5-mediated cell expansion in pollen tubes of Nicotiana tabacum. *Plant J.*, **65**, 453–468.

Iuchi, S., Kobayashi, M., Taji, T., et al. (2001) Regulation of drought tolerance by gene manipulation of 9-cis- epoxycarotenoid dioxygenase, a key enzyme in abscisic acid biosynthesis in Arabidopsis. *Plant J.*, **27**, 325–333.

James, C.N., Horn, P.J., Case, C.R., Gidda, S.K., Zhang, D., Mullen, R.T., Dyer, J.M., Anderson, R.G.W. and Chapman, K.D. (2010) Disruption of the Arabidopsis CGI-58 homologue produces Chanarin–Dorfman-like lipid droplet accumulation in plants. *Proc. Natl. Acad. Sci. U. S. A.*, **107**, 17833–17838.

Jamin, N., Neumann, J.-M., Ostuni, M. a, et al. (2005) Characterization of the cholesterol recognition amino acid consensus sequence of the peripheral-type benzodiazepine receptor. *Mol. Endocrinol.*, **19**, 588–594.

Jao, C.C., Ragusa, M.J., Stanley, R.E. and Hurley, J.H. (2013) A HORMA domain in Atg13 mediates PI 3-kinase recruitment in autophagy. *Proc. Natl. Acad. Sci. U. S. A.*, **110**, 5486–5491.

Jaremko, L., Jaremko, M., Giller, K., Becker, S. and Zweckstetter, M. (2014) Structure of the Mitochondrial Translocator Protein in Complex with a Diagnostic Ligand. *Science*, **343**, 1363–1366.

Jensen, R.B., Cour, T. La, Albrethsen, J., Nielsen, M. and Skriver, K. (2001) FYVE zinc-finger proteins in the plant model Arabidopsis thaliana: identification of PtdIns3P-binding residues by comparison of classic and variant FYVE domains. *Biochem. J.*, **359**, 165–173.

Ji, H., Peng, Y., Meckes, N., Allen, S., Stewart, C.N. and Traw, M.B. (2014) ATP-Dependent Binding Cassette Transporter G Family Member 16 Increases Plant Tolerance to Abscisic Acid and Assists in Basal Resistance against Pseudomonas syringae DC3000. *Plant Physiol.*, **166**, 879–888.

Johanson, U., Karlsson, M., Johansson, I., Gustavsson, S., Sjovall, S., Fraysse, L., Weig, A.R. and Kjellbom, P. (2001) The Complete Set of Genes Encoding Major Intrinsic Proteins in Arabidopsis Provides a Framework for a New Nomenclature for Major Intrinsic Proteins in Plants. *Plant Physiol.*, **126**, 1358–1369.

Jurkiewicz, P. and Batoko, H. (2018) Protein degradation mechanisms modulate abscisic acid signaling and responses during abiotic stress. *Plant Sci.*, **267**, 48–54.

Kang, B.H., Nielsen, E., Preuss, M.L., Mastronarde, D. and Staehelin, L.A. (2011) Electron Tomography of RabA4b- and PI-4Kb1-Labeled Trans Golgi Network Compartments in Arabidopsis. *Traffic*, **12**, 313–329.

Kang, J., Hwang, J.-U., Lee, M., Kim, Y.-Y., Assmann, S.M., Martinoia, E. and Lee, Y. (2010) PDR-type ABC transporter mediates cellular uptake of the phytohormone abscisic acid. *Proc. Natl. Acad. Sci. U. S. A.*, **107**, 2355–2360.

Kang, J., Yim, S., Choi, H., Kim, A., Lee, K.P., Lopez-Molina, L., Martinoia, E. and Lee, Y. (2015) Abscisic acid transporters cooperate to control seed germination. *Nat. Commun.*, **6**, 8113.

Kanno, Y., Hanada, A., Chiba, Y., Ichikawa, T., Nakazawa, M., Matsui, M., Koshiba, T., Kamiya, Y. and Seo, M. (2012) Identification of an abscisic acid transporter by functional screening using the receptor complex as a sensor. *Proc. Natl. Acad. Sci. U. S. A.*, **109**, 9653–9658.

Kapilan, R., Vaziri, M. and Zwiazek, J.J. (2018) Regulation of aquaporins in plants under stress. *Biol. Res.*, **51**, 4.

Kihara, A., Noda, T., Ishihara, N. and Ohsumi, Y. (2001) Two distinct Vps34 phosphatidylinositol 3-kinase complexes function in autophagy and carboxypeptidase Y sorting in Saccharomyces cerevisiae. *J. Cell Biol.*, **153**, 519–530.

Koga, H., Kaushik, S. and Cuervo, A.M. (2010) Altered lipid content inhibits autophagic vesicular fusion. *FASEB J.*, **24**, 3052–3065.

Kong, L., Cheng, J., Zhu, Y., et al. (2015) Degradation of the ABA co-receptor ABI1 by PUB12/13 U-box E3 ligases. *Nat. Commun.*, **6**, 8630.

König, S., Mosblech, A. and Heilmann, I. (2007) Stress-inducible and constitutive phosphoinositide pools have distinctive fatty acid patterns in Arabidopsis thaliana. *FASEB J.*, **21**, 1958–1967.

Kooijman, E.E., Tieleman, D.P., Testerink, C., Munnik, T., Rijkers, D.T.S., Burger, K.N.J. and Kruijff, B. De (2007) An electrostatic/hydrogen bond switch as the basis for the specific interaction of phosphatidic acid with proteins. *J. Biol. Chem.*, **282**, 11356–11364.

Korkhov, V.M., Sachse, C., Short, J.M. and Tate, C.G. (2010) Three-Dimensional Structure of TspO by Electron Cryomicroscopy of Helical Crystals. *Structure*, **18**, 677–687.

Korolnek, T. and Hamza, I. (2014) Like iron in the blood of the people: The requirement for heme trafficking in iron metabolism. *Front. Pharmacol.*, **5**, 126.

Kreps, J. a, Wu, Y., Chang, H.-S., Zhu, T., Wang, X. and Harper, J.F. (2002) Transcriptome changes for Arabidopsis in response to salt, osmotic, and cold stress. *Plant Physiol.*, **130**, 2129–2141.

Krinke, O., Novotná, Z., Valentová, O. and Martinec, J. (2007) Inositol trisphosphate receptor in higher plants: Is it real? *J. Exp. Bot.*, **58**, 361–376.

Krueger, K.E. and Papadopoulos, V. (1992) Mitochondrial Benzodiazepine Receptors and the Regulation of Steroid Biosynthesis. *Annu. Rev. Pharmacol. Toxicol.*, **32**, 211–237.

Krueger, K.E. and Papadopoulos, V. (1990) Peripheral-type benzodiazepine receptors mediate translocation of cholesterol from outer to inner mitochondrial membranes in adrenocortical cells. *J. Biol. Chem.*, **265**, 15015–15022.

KUNTAM, S., PUSKÁS, L.G. AND AYAYDIN, F. (2015) CHARACTERIZATION OF A NEW CLASS OF BLUE-FLUORESCENT LIPID DROPLET MARKERS FOR LIVE-CELL IMAGING IN PLANTS. *PLANT CELL REP.*, **34**, 655–665.

KUROMORI, T., MIYAJI, T., YABUUCHI, H., SHIMIZU, H., SUGIMOTO, E., KAMIYA, A., MORIYAMA, Y. AND SHINOZAKI, K. (2010) ABC TRANSPORTER ATABCG25 IS INVOLVED IN ABSCISIC ACID TRANSPORT AND RESPONSES. *PROC. NATL. ACAD. SCI. U. S. A.*, **107**, 2361–2366.

KUROMORI, T., SUGIMOTO, E. AND SHINOZAKI, K. (2011) ARABIDOPSIS MUTANTS OF ATABCG22, AN ABC TRANSPORTER GENE, INCREASE WATER TRANSPIRATION AND DROUGHT SUSCEPTIBILITY. *PLANT J.*, **67**, 885–894.

KUSANO, H., TESTERINK, C., VERMEER, J.E.M., TSUGE, T., SHIMADA, H., OKA, A., MUNNIK, T. AND AOYAMA, T. (2008) THE ARABIDOPSIS PHOSPHATIDYLINOSITOL PHOSPHATE 5-KINASE PIP5K3 IS A KEY REGULATOR OF ROOT HAIR TIP GROWTH. *PLANT CELL*, **20**, 367–380.

KUSHIRO, T., OKAMOTO, M., NAKABAYASHI, K., ET AL. (2004) THE ARABIDOPSIS CYTOCHROME P450 CYP707A ENCODES ABA 8-HYDROXYLASES: KEY ENZYMES IN ABA CATABOLISM. *EMBO J.*, **23**, 1647–1656.

LACAPERE, J.-J. AND PAPADOPOULOS, V. (2003) PERIPHERAL-TYPE BENZODIAZEPINE RECEPTOR: STRUCTURE AND FUNCTION OF A CHOLESTEROL-BINDING PROTEIN IN STEROID AND BILE ACID BIOSYNTHESIS. *STEROIDS*, **68**, 569–585.

LALOI, M., PERRET, A.-M., CHATRE, L., ET AL. (2007) INSIGHTS INTO THE ROLE OF SPECIFIC LIPIDS IN THE FORMATION AND DELIVERY OF LIPID MICRODOMAINS TO THE PLASMA MEMBRANE OF PLANT CELLS. *PLANT PHYSIOL.*, **143**, 461–472.

LAMB, C.A., YOSHIMORI, T. AND TOOZE, S.A. (2013) THE AUTOPHAGOSOME: ORIGINS UNKNOWN, BIOGENESIS COMPLEX. *NAT. REV. MOL. CELL BIOL.*, **14**, 759–774.

LAPIERRE, L.R., GELINO, S., MELÉNDEZ, A. AND HANSEN, M. (2011) AUTOPHAGY AND LIPID METABOLISM COORDINATELY MODULATE LIFE SPAN IN GERMLINE-LESS C. ELEGANS. *CURR. BIOL.*, **21**, 1507–1514.

LEE, C.B., KIM, S. AND MCCLURE, B. (2008) A POLLEN PROTEIN, NAPCCP, THAT BINDS PISTIL ARABINOGALACTAN PROTEINS ALSO BINDS PHOSPHATIDYLINOSITOL 3-PHOSPHATE AND ASSOCIATES WITH THE POLLEN TUBE ENDOMEMBRANE SYSTEM. *PLANT PHYSIOL.*, **149**, 791–802.

LEE, G.-J., KIM, H., KANG, H., JANG, M., LEE, D.W., LEE, S. AND HWANG, I. (2007) EPSINR2 INTERACTS WITH CLATHRIN, ADAPTOR PROTEIN-3, ATVTI12, AND PHOSPHATIDYLINOSITOL-3-PHOSPHATE. IMPLICATIONS FOR EPSINR2 FUNCTION IN PROTEIN TRAFFICKING IN PLANT CELLS. *PLANT PHYSIOL.*, **143**, 1561–1575.

LEE, K.H., PIAO, H.L., KIM, H.Y., ET AL. (2006) ACTIVATION OF GLUCOSIDASE VIA STRESS-INDUCED POLYMERIZATION RAPIDLY INCREASES ACTIVE POOLS OF ABSCISIC ACID. *CELL*, **126**, 1109–1120.

LEE, S.H., JIN, J.B., SONG, J., MIN, M.K., PARK, D.S., KIM, Y.W. AND HWANG, I. (2002) THE INTERMOLECULAR INTERACTION BETWEEN THE PH DOMAIN AND THE C-TERMINAL DOMAIN OF ARABIDOPSIS DYNAMIN-LIKE 6 DETERMINES LIPID BINDING SPECIFICITY. *J. BIOL. CHEM.*, **277**, 31842–31849.

LEE, W., TONELLI, M. AND MARKLEY, J.L. (2015) NMRFAM-SPARKY: ENHANCED SOFTWARE FOR BIOMOLECULAR NMR SPECTROSCOPY. *BIOINFORMATICS*, **31**, 1325–1327.

LEE, Y., KIM, E.-S., CHOI, Y., HWANG, I., STAIGER, C.J., CHUNG, Y.-Y. AND LEE, Y. (2008) THE ARABIDOPSIS PHOSPHATIDYLINOSITOL 3-KINASE IS IMPORTANT FOR POLLEN DEVELOPMENT. *PLANT PHYSIOL.*, **147**, 1886–1897.

LEE, Y., KIM, Y.W., JEON, B.W., ET AL. (2007) PHOSPHATIDYLINOSITOL 4,5-BISPHOSPHATE IS IMPORTANT FOR STOMATAL OPENING. *PLANT J.*, **52**, 803–816.

LI-BEISSON, Y., SHORROSH, B., BEISSON, F., ET AL. (2013) ACYL-LIPID METABOLISM. *ARAB. B.*, **11**, E0161.

LI, D., SONG, J.Z., LI, H., SHAN, M.H., LIANG, Y., ZHU, J. AND XIE, Z. (2015) STORAGE LIPID SYNTHESIS IS NECESSARY FOR AUTOPHAGY INDUCED BY NITROGEN STARVATION. *FEBS LETT.*, **589**, 269–276.

Li, F., Liu, J., Liu, N., Kuhn, L.A., Garavito, R.M. and Ferguson-Miller, S. (2016) Translocator Protein 18 kDa (TSPO): An Old Protein with New Functions? *Biochemistry*, **55**, 2821–2831.

Li, F., Liu, J., Zheng, Y., Garavito, R.M. and Ferguson-Miller, S. (2015) Crystal structures of translocator protein (TSPO) and mutant mimic of a human polymorphism. *Science*, **347**, 555–558.

Li, F., Xia, Y., Meiler, J. and Ferguson-Miller, S. (2013) Characterization and modeling of the oligomeric state and ligand binding behavior of purified Translocator Protein 18 kDa from Rhodobacter sphaeroides. *Biochemistry*, **52**, 5884–5899.

Li, H. and Papadopoulos, V. (1998) Peripheral-type benzodiazepine receptor function in cholesterol transport. Identification of a putative cholesterol recognition/interaction amino acid sequence and consensus pattern. *Endocrinology*, **139**, 4991–4997.

Li, N., Gügel, I.L., Giavalisco, P., Zeisler, V., Schreiber, L., Soll, J. and Philippar, K. (2015) FAX1, a Novel Membrane Protein Mediating Plastid Fatty Acid Export. *PLoS Biol.*, **13**, e1002053.

Li, N., Xu, C., Li-Beisson, Y. and Philippar, K. (2016) Fatty Acid and Lipid Transport in Plant Cells. *Trends Plant Sci.*, **21**, 145–158.

Lim, P.O. and Nam, H.G. (2005) The Molecular and Genetic Control of Leaf Senescence and Longevity in Arabidopsis. *Curr. Top. Dev. Biol.*, **67**, 49–83.

Lin, D., Sugawara, T., 3rd, J.S., Clark, B., Stocco, D., Saenger, P., Rogol, A. and Miller, W. (1995) Role of steroidogenic acute regulatory protein in adrenal and gonadal steroidogenesis. *Science*, **267**, 1828–1831.

Lin, R., Angelin, A., Settimo, F. Da, Martini, C., Taliani, S., Zhu, S. and Wallace, D.C. (2014) Genetic analysis of dTSPO, an outer mitochondrial membrane protein, reveals its functions in apoptosis, longevity, and Aβ42-induced neurodegeneration. *Aging Cell*, **13**, 507–518.

Lindemann, P., Koch, A., Degenhardt, B., Hause, G., Grimm, B. and Papadopoulos, V. (2004) A novel Arabidopsis thaliana protein is a functional peripheral-type benzodiazepine receptor. *Plant Cell Physiol.*, **45**, 723–733.

Liu, J.-X. and Howell, S. (2016) Managing the protein folding demands in the endoplasmic reticulum of plants. *New Phytol.*, **211**, 418–428.

Liu, J.-X., Srivastava, R., Che, P. and Howell, S.H. (2007) Salt stress responses in Arabidopsis utilize a signal transduction pathway related to endoplasmic reticulum stress signaling. *Plant J.*, **51**, 897–909.

Liu, K., Li, L. and Luan, S. (2005) An essential function of phosphatidylinositol phosphates in activation of plant shaker-type K+channels. *Plant J.*, **42**, 433–443.

Liu, L., Zhang, K., Sandoval, H., et al. (2015) Glial lipid droplets and ROS induced by mitochondrial defects promote neurodegeneration. *Cell*, **160**, 177–190.

Liu, Y. and Bassham, D.C. (2012) Autophagy: pathways for self-eating in plant cells. *Annu. Rev. Plant Biol.*, **63**, 215–237.

Liu, Y., Burgos, J.S., Deng, Y., Srivastava, R., Howell, S.H. and Bassham, D.C. (2012) Degradation of the Endoplasmic Reticulum by Autophagy during Endoplasmic Reticulum Stress in Arabidopsis. *Plant Cell*, **24**, 4635–4651.

Lopez, F., Bousser, A., Sissoëff, I., Gaspar, M., Lachaise, B., Hoarau, J. and Mahé, A. (2003) Diurnal Regulation of Water Transport and Aquaporin Gene Expression in Maize Roots: Contribution of PIP2 Proteins. *Plant Cell Physiol.*, **44**, 1384–1395.

Luu, D.T. and Maurel, C. (2005) Aquaporins in a challenging environment: Molecular gears for adjusting plant water status. *Plant, Cell Environ.*, **28**, 85–96.

Lyzenga, W.J. and Stone, S.L. (2012) Abiotic stress tolerance mediated by protein ubiquitination. *J. Exp. Bot.*, **63**, 599–616.

Ma, X., Shatil-Cohen, A., Ben-Dor, S., et al. (2014) Do phosphoinositides regulate membrane water permeability of tobacco protoplasts by enhancing the aquaporin pathway? *Planta*, **241**, 741–755.

Ma, Y., Szostkiewicz, I., Korte, A., Moes, D., Yang, Y., Christmann, A. and Grill, E. (2009) Regulators of PP2C Phosphatase Activity Function as Abscisic Acid Sensors. *Science*, **324**, 1064–1069.

Macala, L.J., Yu, R.K. and Ando, S. (1983) Analysis of brain lipids by high performance thin-layer chromatography and densitometry. *J. Lipid Res.*, **24**, 1243–1250.

Malara, A., Fresia, C., Buduo, C.A. Di, Soprano, P.M., Moccia, F., Balduini, C., Zocchi, E., Flora, A. De and Balduini, A. (2017) The plant hormone abscisic acid is a prosurvival factor in human and murine megakaryocytes. *J. Biol. Chem.*, **292**, 3239–3251.

Marginedas-Freixa, I., Hattab, C., Bouyer, G., et al. (2016) TSPO ligands stimulate ZnPPIX transport and ROS accumulation leading to the inhibition of P. falciparum growth in human blood. *Sci. Rep.*, **6**, 33516.

Marsh, J.A., Singh, V.K., Jia, Z. and Forman-Kay, J.D. (2006) Sensitivity of secondary structure propensities to sequence differences between α- and γ-synuclein: Implications for fibrillation. *Protein Sci.*, **15**, 2795–2804.

Marshall, R.S., Li, F., Gemperline, D.C., Book, A.J. and Vierstra, R.D. (2015) Autophagic Degradation of the 26S Proteasome Is Mediated by the Dual ATG8/Ubiquitin Receptor RPN10 in Arabidopsis. *Mol. Cell*, **58**, 1053–1066.

Maurel, C., Boursiac, Y., Luu, D.-T., Santoni, V., Shahzad, Z. and Verdoucq, L. (2015) Aquaporins in Plants. *Physiol. Rev.*, **95**, 1321–1358.

Maurel, C., Reizer, J., Schroeder, J.I. and Chrispeels, M.J. (1993) The vacuolar membrane protein gamma-TIP creates water specific channels in Xenopus oocytes. *EMBO J.*, **12**, 2241–2247.

May, M.J. and Leaver, C.J. (1993) Oxidative Stimulation of Glutathione Synthesis in Arabidopsis thaliana suspension cultures. *Plant Physiol.*, **103**, 621–627.

McCourt, P. and Creelman, R. (2008) The ABA receptors - we report you decide. *Curr. Opin. Plant Biol.*, **11**, 474–478.

McLachlan, D.H., Lan, J., Geilfus, C.M., et al. (2016) The Breakdown of Stored Triacylglycerols is Required during Light-Induced Stomatal Opening. *Curr. Biol.*, **26**, 707–712.

McLaughlin, S. and Murray, D. (2005) Plasma membrane phosphoinositide organization by protein electrostatics. *Nature*, **438**, 605–611.

Mehrotra, R., Bhalothia, P., Bansal, P., Basantani, M.K., Bharti, V. and Mehrotra, S. (2014) Abscisic acid and abiotic stress tolerance - Different tiers of regulation. *J. Plant Physiol.*, **171**, 486–496.

Meijer, H.J., Berrie, C.P., Iurisci, C., Divecha, N., Musgrave, A. and Munnik, T. (2001) Identification of a new polyphosphoinositide in plants, phosphatidylinositol 5-monophosphate (PtdIns5P), and its accumulation upon osmotic stress. *Biochem. J.*, **360**, 491–8.

Merilo, E., Jalakas, P., Kollist, H. and Brosch, M. (2015) The Role of ABA recycling and transporter proteins in rapid stomatal responses to reduced air humidity, elevated CO2, and exogenous ABA. *Mol. Plant*, **8**, 657–659.

Merlot, S., Gosti, F., Guerrier, D., Vavasseur, A. and Giraudat, J. (2001) The ABI1 and ABI2 protein phosphatases 2C act in a negative feedback regulatory loop of the abscisic acid signaling pathway. *Plant J.*, **25**, 295–303.

Michaeli, S., Galili, G., Genschik, P., Fernie, A.R. and Avin-Wittenberg, T. (2016) Autophagy in Plants - What's New on the Menu? *Trends Plant Sci.*, **21**, 134–144.

Millar, A.A., Smith, M.A. and Kunst, L. (2000) All fatty acids are not equal: Discrimination in plant membrane lipids. *Trends Plant Sci.*, **5**, 95–101.

Miller, W.L. (2013) Steroid hormone synthesis in mitochondria. *Mol. Cell. Endocrinol.*, **379**, 62–73.

Miyazono, K., Miyakawa, T., Sawano, Y., et al. (2009) Structural basis of abscisic acid signaling. *Nature*, **462**, 609–614.

Mohler, H. and Okada, T. (1977) Benzodiazepine receptor: demonstration in the central nervous system. *Science*, **198**, 849–851.

Moing, A., Maucourt, M., Renaud, C., et al. (2004) Quantitative metabolic profiling by 1-dimensional 1H-NMR analyses: Application to plant genetics and functional genomics. *Funct. Plant Biol.*, **31**, 889–902.

Moldavski, O., Amen, T., Levin-Zaidman, S., Eisenstein, M., Rogachev, I., Brandis, A., Kaganovich, D. and Schuldiner, M. (2015) Lipid Droplets Are Essential for Efficient Clearance of Cytosolic Inclusion Bodies. *Dev. Cell*, **33**, 603–610.

Moore, D.T., Berger, B.W. and DeGrado, W.F. (2008) Protein-Protein Interactions in the Membrane: Sequence, Structural, and Biological Motifs. *Structure*, **16**, 991–1001.

Morin, D., Musman, J., Pons, S., Berdeaux, A. and Ghaleb, B. (2016) Mitochondrial translocator protein (TSPO): From physiology to cardioprotection. *Biochem. Pharmacol.*, **105**, 1–13.

Morohaku, K., Pelton, S.H., Daugherty, D.J., Butler, W.R., Deng, W. and Vimal, S. (2014) Translocator Protein/Peripheral Benzodiazepine Receptor Is Not Required for Steroid Hormone Biosynthesis. *Endocrinology*, **155**, 89–97.

Moshelion, M., Becker, D., Biela, A., Uehlein, N., Hedrich, R., Otto, B., Levi, H., Moran, N. and Kaldenhoff, R. (2002) Plasma membrane aquaporins in the motor cells of Samanea saman: diurnal and circadian regulation. *Plant Cell*, **14**, 727–739.

Mueller-Roeber, B. and Pical, C. (2002) Inositol Phospholipid Metabolism in Arabidopsis. Characterized and Putative Isoforms of Inositol Phospholipid Kinase and Phosphoinositide-Specific Phospholipase C. *Plant Physiol.*, **130**, 22–46.

Mukherjee, S., Soe, T.T. and Maxfield, F.R. (1999) Endocytic sorting of lipid analogues differing solely in the chemistry of their hydrophobic tails. *J. Cell Biol.*, **144**, 1271–1284.

Mukhin, A., Papadopoulos, V., Costa, E. and Krueger, K.E. (1989) Mitochondrial benzodiazepine receptors regulate steroid biosynthesis. *Proc. Natl. Acad. Sci. U. S. A.*, **86**, 9813–9816.

Munnik, T. and Nielsen, E. (2011) Green light for polyphosphoinositide signals in plants. *Curr. Opin. Plant Biol.*, **14**, 489–497.

Munnik, T. and Testerink, C. (2009) Plant phospholipid signaling: "in a nutshell." *J. Lipid Res.*, **50**, S260–S265.

Munnik, T. and Vermeer, J.E.M. (2010) Osmotic stress-induced phosphoinositide and inositol phosphate signaling in plants. *Plant, Cell Environ.*, **33**, 655–669.

Murashige, T. and Skoog, F. (1962) A revised medium for rapid growth and bio-assays with tobacco tissue cultures. *Physiol. Plant.*, **15**, 473–497.

Murata, K., Mitsuoka, K., Hiral, T., Walz, T., Agre, P., Heymann, J.B., Engel, A. and Fujiyoshi, Y. (2000) Structural determinants of water permeation through aquaporin-1. *Nature*, **407**, 599–605.

Nakamura, Y. (2017) Plant Phospholipid Diversity: Emerging Functions in Metabolism and Protein–Lipid Interactions. *Trends Plant Sci.*, **22**, 1027–1040.

Nakazawa, F., Alev, C., Shin, M., Nakaya, Y., Jakt, L.M. and Sheng, G. (2009) PBRL, a putative peripheral benzodiazepine receptor, in primitive erythropoiesis. *Gene Expr. Patterns*, **9**, 114–121.

Nambara, E. and Marion-Poll, A. (2005) Abscisic Acid Biosynthesis and Catabolism. *Annu. Rev. Plant Biol.*, **56**, 165–185.

Nazio, F., Strappazzon, F., Antonioli, M., et al. (2013) mTOR inhibits autophagy by controlling ULK1 ubiquitylation, self-association and function through AMBRA1 and TRAF6. *Nat. Cell Biol.*, **15**, 406–416.

Ng, L.M., Melcher, K., Teh, B.T. and Xu, H.E. (2014) Abscisic acid perception and signaling: structural mechanisms and applications. *Acta Pharmacol. Sin.*, **35**, 567–584.

Nishimura, N., Hitomi, K., Arvai, A.S., Rambo, R.P., Hitomi, C., Cutler, S.R., Schroeder, J.I. and Getzoff, E.D. (2009) Structural Mechanism of Abscisic Acid Binding and Signaling by Dimeric PYR1. *Science*, **326**, 1373–1380.

Nishimura, N., Sarkeshik, A., Nito, K., et al. (2010) PYR/PYL/RCAR family members are major in-vivo ABI1 protein phosphatase 2C-interacting proteins in Arabidopsis. *Plant J.*, **61**, 290–299.

Nour-Eldin, H.H., Hansen, B.G., Nørholm, M.H.H., Jensen, J.K. and Halkier, B.A. (2006) Advancing uracil-excision based cloning towards an ideal technique for cloning PCR fragments. *Nucleic Acids Res.*, **34**, e122.

Nyblom, M., Frick, A., Wang, Y., Ekvall, M., Hallgren, K., Hedfalk, K., Neutze, R., Tajkhorshid, E. and Törnroth-Horsefield, S. (2009) Structural and Functional Analysis of SoPIP2;1 Mutants Adds Insight into Plant Aquaporin Gating. *J. Mol. Biol.*, **387**, 653–668.

Ohtsuka, H., Ogawa, S., Kawamura, H., Sakai, E., Ichinose, K., Murakami, H. and Aiba, H. (2013) Screening for long-lived genes identifies Oga1, a guanine-quadruplex associated protein that affects the chronological lifespan of the fission yeast Schizosaccharomyces pombe. *Mol. Genet. Genomics*, **288**, 285–295.

Ozaki, H., Zoghbi, S.S., Hong, J., Verma, A., Pike, V.W., Innis, R.B. and Fujita, M. (2010) In vivo binding of protoporphyrin IX to rat Translocator protein imaged with positron emission tomography. *Synapse*, **64**, 649–653.

Papadopoulos, V., Amri, H., Boujrad, N., et al. (1997) Peripheral benzodiazepine receptor in cholesterol transport and steroidogenesis. *Steroids*, **62**, 21–28.

Papadopoulos, V., Amri, H., Li, H., Boujrad, N., Vidic, B. and Garnier, M. (1997) Targeted Disruption of the Peripheral-type Benzodiazepine Receptor Gene Inhibits Steroidogenesis in the R2C Leydig Tumor Cell Line. *J. Biol. Chem.*, **272**, 32129–32135.

Papadopoulos, V., Baraldi, M., Guilarte, T.R., et al. (2006) Translocator protein (18 kDa): new nomenclature for the peripheral-type benzodiazepine receptor based on its structure and molecular function. *Trends Pharmacol. Sci.*, **27**, 402–409.

Park, J.M., Jung, C.H., Seo, M., et al. (2016) The ULK1 complex mediates MTORC1 signaling to the autophagy initiation machinery via binding and phosphorylating ATG14. *Autophagy*, **12**, 547–564.

Park, S., Fung, P., Nishimura, N., et al. (2009) Abscisic acid inhibits type 2C protein phosphatases via the PYR/PYL family of START proteins. *Science*, **324**, 1068–1069.

Patel, J. and Marangos, P. (1982) Differential effects of GABA on peripheral and central type benzodiazepine binding sites in brain. *Neurosci. Lett.*, **30**, 157–160.

Payrastre, B., Missy, K., Giuriato, S., Bodin, S., Plantavid, M. and Gratacap, M.P. (2001) Phosphoinositides: key players in cell signaling, in time and space. *Cell. Signal.*, **13**, 377–387.

Phan, N.Q., Kim, S.J. and Bassham, D.C. (2008) Overexpression of arabidopsis sorting nexin AtSNX2b inhibits endocytic trafficking to the vacuole. *Mol. Plant*, **1**, 961–976.

Prado, K., Boursiac, Y., Tournaire-Roux, C., et al. (2013) Regulation of Arabidopsis Leaf Hydraulics Involves Light-Dependent Phosphorylation of Aquaporins in Veins. *Plant Cell*, **25**, 1029–1039.

Prado, K. and Maurel, C. (2013) Regulation of leaf hydraulics: from molecular to whole plant levels. *Front. Plant Sci.*, **4**, 255.

Prasad, M., Kaur, J., Pawlak, K.J., Bose, M., Whittal, R.M. and Bose, H.S. (2015) Mitochondria-associated endoplasmic reticulum membrane (MAM) regulates steroidogenic activity via steroidogenic acute regulatory protein (StAR)-voltage-dependent anion channel 2 (VDAC2) interaction. *J. Biol. Chem.*, **290**, 2604–2616.

Preston, G.M., Carroll, T.P., Guggino, W.B. and Agre, P. (1992) Appearance of Water Channels in Xenopus Oocytes Expressing Red Cell CHIP28 Protein. *Science*, **256**, 385–387.

Preuss, M.L., Schmitz, A.J., Thole, J.M., Bonner, H.K.S., Otegui, M.S. and Nielsen, E. (2006) A role for the RabA4b effector protein PI-4Kb1 in polarized expansion of root hair cells in Arabidopsis thaliana. *J. Cell Biol.*, **172**, 991–998.

Puri, C., Renna, M., Bento, C.F., Moreau, K. and Rubinsztein, D.C. (2013) Diverse autophagosome membrane sources coalesce in recycling endosomes. *Cell*, **154**, 1285–1299.

Qin, X. and Zeevaart, J.A.D. (1999) The 9-cis-epoxycarotenoid cleavage reaction is the key regulatory step of abscisic acid biosynthesis in water-stressed bean. *Proc. Natl. Acad. Sci. U. S. A.*, **96**, 15354–15361.

Raghavendra, A.S., Gonugunta, V.K., Christmann, A. and Grill, E. (2010) ABA perception and signaling. *Trends Plant Sci.*, **15**, 395–401.

Rampon, C., Bouzaffour, M., Ostuni, M.A., Dufourcq, P., Girard, C., Freyssinet, J.M., Lacapere, J.-J., Schweizer-Groyer, G. and Vriz, S. (2009) Translocator protein (18 kDa) is involved in primitive erythropoiesis in zebrafish. *FASEB J.*, **23**, 4181–4192.

Rupprecht, R., Papadopoulos, V., Rammes, G., Baghai, T.C., Fan, J., Akula, N., Groyer, G., Adams, D. and Schumacher, M. (2010) Translocator protein (18 kDa) (TSPO) as a therapeutic target for neurological and psychiatric disorders. *Nat. Rev. Drug Discov.*, **9**, 971–988.

Russell, R.C., Tian, Y., Yuan, H., et al. (2013) ULK1 induces autophagy by phosphorylating Beclin-1 and activating VPS34 lipid kinase. *Nat. Cell Biol.*, **15**, 741–750.

Sadanandom, A., Bailey, M., Ewan, R., Lee, J. and Nelis, S. (2012) The ubiquitin-proteasome system: Central modifier of plant signaling. *New Phytol.*, **196**, 13–28.

Sah, S.K., Reddy, K.R. and Li, J. (2016) Abscisic Acid and Abiotic Stress Tolerance in Crop Plants. *Front. Plant Sci.*, **7**, 571.

Saito, S., Hirai, N., Matsumoto, C., Ohigashi, H. and Ohta, D. (2004) Arabidopsis CYP707As encode (+)-abscisic acid 8-hydroxylase, a key enzyme in the oxidative catabolism of abscisic acid. *Plant Physiol.*, **134**, 1439–1449.

Sakurai, J., Ishikawa, F., Yamaguchi, T., Uemura, M. and Maeshima, M. (2005) Identification of 33 rice aquaporin genes and analysis of their expression and function. *Plant Cell Physiol.*, **46**, 1568–1577.

Santelia, D., Trost, P. and Sparla, F. (2015) New insights into redox control of starch degradation. *Curr. Opin. Plant Biol.*, **25**, 1–9.

Santiago, J., Rodrigues, A., Saez, A., et al. (2009) Modulation of drought resistance by the abscisic acid receptor PYL5 through inhibition of clade A PP2Cs. *Plant J.*, **60**, 575–588.

Santoni, V. (2007) *Plant plasma membrane protein extraction and solubilization for proteomic analysis*,

Seki, M., Narusaka, M., Ishida, J., et al. (2002) Monitoring the expression profiles of 7000 Arabidopsis genes under drought, cold and high-salinity stresses using a full-length cDNA microarray. *Plant J.*, **31**, 279–292.

Selvaraj, V. and Stocco, D.M. (2015) The changing landscape in translocator protein (TSPO) function. *Trends Endocrinol. Metab.*, **26**, 341–348.

Selvaraj, V., Tu, L. and Stocco, D. (2016) Crucial Role Reported for TSPO in Viability and Steroidogenesis is a Misconception. *Front. Endocrinol.*, **7**, 91.

Seo, M., Peeters, A.J.M., Koiwai, H., Oritani, T., Marion-Poll, A., Zeevaart, J.A.D., Koornneef, M., Kamiya, Y. and Koshiba, T. (2000) The Arabidopsis aldehyde oxidase 3 (AAO3) gene product catalyzes the final step in abscisic acid biosynthesis in leaves. *Proc. Natl. Acad. Sci. U. S. A.*, **97**, 12908–12913.

Shpilka, T., Welter, E., Borovsky, N., Amar, N., Mari, M., Reggiori, F. and Elazar, Z. (2015) Lipid droplets and their component triglycerides and steryl esters regulate autophagosome biogenesis. *EMBO J.*, **34**, 2117–2131.

Sileikyte, J., Blachly-Dyson, E., Sewell, R., Carpi, A., Menabo, R., Lisa, F. Di, Ricchelli, F., Bernardi, P. and Forte, M. (2014) Regulation of the Mitochondrial Permeability Transition Pore by the Outer Membrane does not Involve the Peripheral Benzodiazepine Receptor (TSPO). *J. Biol. Chem.*, **289**, 13769–13781.

Simon, M.L.A., Platre, M.P., Assil, S., Wijk, R. van, Chen, W.Y., Chory, J., Dreux, M., Munnik, T. and Jaillais, Y. (2014) A multi-colour/multi-affinity marker set to visualize phosphoinositide dynamics in Arabidopsis. *Plant J.*, **77**, 322–337.

Smalle, J. and Vierstra, R.D. (2004) the Ubiquitin 26S Proteasome Proteolytic Pathway. *Annu. Rev. Plant Biol.*, **55**, 555–590.

Sohn, M., Korzeniowski, M., Zewe, J.P., et al. (2018) PI(4,5)P_2 controls plasma membrane PI4P and PS levels via ORP5/8 recruitment to ER-PM contact sites. *J. Cell Biol.*, **217**, 1797–1813.

Spandl, J., White, D.J., Peychl, J. and Thiele, C. (2009) Live cell multicolor imaging of lipid droplets with a new dye, LD540. *Traffic*, **10**, 1579–1584.

Squires, R.F. and Braestrup, C. (1977) Benzodiazepine receptors in rat brain. *Nature*, **266**, 732–734.

Stein, W.D. and Danielli, J.F. (1956) Structure and function in red cell permeability. *Discuss. Faraday Soc.*, **21**, 238–251.

Stenzel, I., Ischebeck, T., Konig, S., Holubowska, A., Sporysz, M., Hause, B. and Heilmann, I. (2008) The Type B Phosphatidylinositol-4-Phosphate 5-Kinase 3 Is Essential for Root Hair Formation in Arabidopsis thaliana. *Plant Cell*, **20**, 124–141.

Stocco, D.M. (2014) The role of PBR/TSPO in steroid biosynthesis challenged. *Endocrinology*, **155**, 6–9.

Stoebner, P.E., Carayon, P., Casellas, P., Portier, M., Lavabre-Bertrand, T., Cuq, P., Cano, J.P., Meynadier, J. and Meunier, L. (2001) Transient protection by peripheral benzodiazepine receptors during the early events of ultraviolet light-induced apoptosis. *Cell Death Differ.*, **8**, 747–753.

Stone, S.L. (2014) The role of ubiquitin and the 26S proteasome in plant abiotic stress signaling. *Front. Plant Sci.*, **5**, 135.

Suh, B.-C., Inoue, T., Meyer, T. and Hille, B. (2006) Rapid Chemically Induced Changes of PtdIns(4,5)P_2 Gate KCNQ Ion Channels. *Science*, **314**, 1454–1457.

Suh, B.C. and Hille, B. (2005) Regulation of ion channels by phosphatidylinositol 4,5-bisphosphate. *Curr. Opin. Neurobiol.*, **15**, 370–378.

Sui, H., Han, B.G., Lee, J.K., Walian, P. and Jap, B.K. (2001) Structural basis of water-specific transport through the AQP1 water channel. *Nature*, **414**, 872–878.

Suttangkakul, A., Li, F., Chung, T. and Vierstra, R.D. (2011) The ATG1/ATG13 Protein Kinase Complex Is Both a Regulator and a Target of Autophagic Recycling in Arabidopsis. *Plant Cell*, **23**, 3761–3779.

Suzuki, K., Akioka, M., Kondo-Kakuta, C., Yamamoto, H. and Ohsumi, Y. (2013) Fine mapping of autophagy-related proteins during autophagosome formation in Saccharomyces cerevisiae. *J. Cell Sci.*, **126**, 2534–2544.

Tajima, H., Iwata, Y., Iwano, M., Takayama, S. and Koizumi, N. (2008) Identification of an Arabidopsis transmembrane bZIP transcription factor involved in the endoplasmic reticulum stress response. *Biochem. Biophys. Res. Commun.*, **374**, 242–247.

Takayama, S. -i. J., Ukpabi, G., Murphy, M.E.P. and Mauk, A.G. (2011) Electronic properties of the highly ruffled heme bound to the heme degrading enzyme IsdI. *Proc. Natl. Acad. Sci. U. S. A.*, **108**, 13071–13076.

Tan, B.C., Schwartz, S.H., Zeevaart, J. a and McCarty, D.R. (1997) Genetic control of abscisic acid biosynthesis in maize. *Proc. Natl. Acad. Sci. U. S. A.*, **94**, 12235–12240.

Tan, X., Thapa, N., Choi, S. and Anderson, R.A. (2015) Emerging roles of PtdIns(4,5)P_2 - beyond the plasma membrane. *J. Cell Sci.*, **128**, 4047–4056.

Tan, X., Thapa, N., Liao, Y., Choi, S. and Anderson, R.A. (2016) PtdIns(4,5)P_2 signaling regulates ATG14 and autophagy. *Proc. Natl. Acad. Sci. U. S. A.*, **113**, 10896–10901.

Taylor, I.B., Burbidge, A. and Thompson, A.J. (2000) Control of abscisic acid synthesis. *J. Exp. Bot.*, **51**, 1563–1574.

Taylor, J.M.W., Allen, A.-M. and Graham, A. (2014) Targeting mitochondrial 18 kDa translocator protein (TSPO) regulates macrophage cholesterol efflux and lipid phenotype. *Clin. Sci.*, **127**, 603–613.

Teboul, D., Beaufils, S., Taveau, J.C., Iatmanen-Harbi, S., Renault, A., Venien-Bryan, C., Vie, V. and Lacapere, J.J. (2012) Mouse TSPO in a lipid environment interacting with a functionalized monolayer. *Biochim. Biophys. Acta - Biomembr.*, **1818**, 2791–2800.

Temmei, Y., Uchida, S., Hoshino, D., Kanzawa, N., Kuwahara, M., Sasaki, S. and Tsuchiya, T. (2005) Water channel activities of Mimosa pudica plasma membrane intrinsic proteins are regulated by direct interaction and phosphorylation. *FEBS Lett.*, **579**, 4417–4422.

Testerink, C. and Munnik, T. (2005) Phosphatidic acid: A multifunctional stress signaling lipid in plants. *Trends Plant Sci.*, **10**, 368–375.

Thole, J.M., Vermeer, J.E.M., Zhang, Y., Gadella, T.W.J. and Nielsen, E. (2008) ROOT HAIR DEFECTIVE4 Encodes a Phosphatidylinositol-4-Phosphate Phosphatase Required for Proper Root Hair Development in Arabidopsis thaliana. *Plant Cell*, **20**, 381–395.

Thompson, A.J., Jackson, A.C., Parker, R.A., Morpeth, D.R., Burbidge, A. and Taylor, I.B. (2000) Abscisic acid biosynthesis in tomato: Regulation of zeaxanthin epoxidase and 9-cis-epoxycarotenoid dioxygenase mRNAs by light/dark cycles, water stress and abscisic acid. *Plant Mol. Biol.*, **42**, 833–845.

Thompson, M.M., Manning, H.C. and Ellacott, K.L.J. (2013) Translocator protein 18 kDa (TSPO) is regulated in white and brown adipose tissue by obesity. *PLoS One*, **8**, e79980.

Tilman, D., Balzer, C., Hill, J. and Befort, B.L. (2011) Global food demand and the sustainable intensification of agriculture. *Proc. Natl. Acad. Sci. U. S. A.*, **108**, 20260–20264.

Törnroth-Horsefield, S., Wang, Y., Hedfalk, K., Johanson, U., Karlsson, M., Tajkhorshid, E., Neutze, R. and Kjellbom, P. (2006) Structural mechanism of plant aquaporin gating. *Nature*, **439**, 688–694.

Troncoso-Ponce, M.A., Nikovics, K., Marchive, C., Lepiniec, L. and Baud, S. (2016) New insights on the organization and regulation of the fatty acid biosynthetic network in the model higher plant Arabidopsis thaliana. *Biochimie*, **120**, 3–8.

Tu, L.N., Morohaku, K., Manna, P.R., Pelton, S.H., Butler, W.R., Stocco, D.M. and Selvaraj, V. (2014) Peripheral Benzodiazepine Receptor/Translocator Protein Global Knockout Mice are Viable with no Effects on Steroid Hormone Biosynthesis. *J. Biol. Chem.*, **289**, 27444–27454.

Tu, L.N., Zhao, A.H., Hussein, M., Stocco, D.M. and Selvaraj, V. (2016) Translocator protein (TSPO) affects mitochondrial fatty acid oxidation in steroidogenic cells. *Endocrinology*, **157**, 1110–1121.

Tuteja, N. (2007) Abscisic acid and abiotic stress signaling. *Plant Signal. Behav.*, **2**, 135–138.

Ulrich, E.L., Akutsu, H., Doreleijers, J.F., et al. (2008) BioMagResBank. *Nucleic Acids Res.*, **36**, 402–408.

United Nations, Department of Economic and Social Affairs, Population Division. (2015) World Population Prospects: The 2015 Revision, Key Findings and Advance Tables. Working Paper No. ESA/P/WP.241.

Unno, M., Ardevol, A., Rovira, C. and Ikeda-Saito, M. (2013) Structures of the substrate-free and product-bound forms of HmuO, a heme oxygenase from corynebacterium diphtheriae: X-ray crystallography and molecular dynamics investigation. *J. Biol. Chem.*, **288**, 34443–34458.

VAN ECHTEN-DECKERT, G. (2000) SPHINGOLIPID EXTRACTION AND ANALYSIS BY THIN-LAYER CHROMATOGRAPHY. *METHODS ENZYMOL.*, **312**, 64–79.

VAN LEENE, J., STALS, H., EECKHOUT, D., ET AL. (2007) A TANDEM AFFINITY PURIFICATION-BASED TECHNOLOGY PLATFORM TO STUDY THE CELL CYCLE INTERACTOME IN ARABIDOPSIS THALIANA. *MOL. CELL. PROTEOMICS*, **6**, 1226–1238.

VAN LEEUWEN, W., ÖKRÉSZ, L., BÖGRE, L. AND MUNNIK, T. (2004) LEARNING THE LIPID LANGUAGE OF PLANT SIGNALING. *TRENDS PLANT SCI.*, **9**, 378–384.

VAN LEEUWEN, W., VERMEER, J.E.M., GADELLA, T.W.J. AND MUNNIK, T. (2007) VISUALIZATION OF PHOSPHATIDYLINOSITOL 4,5-BISPHOSPHATE IN THE PLASMA MEMBRANE OF SUSPENSION-CULTURED TOBACCO BY-2 CELLS AND WHOLE ARABIDOPSIS SEEDLINGS. *PLANT J.*, **52**, 1014–1026.

VAN MEER, G., VOELKER, D.R. AND FEIGENSON, G.W. (2008) MEMBRANE LIPIDS: WHERE THEY ARE AND HOW THEY BEHAVE. *NAT. REV. MOL. CELL BIOL.*, **9**, 112–124.

VAN ROSSUM, D.B., PATTERSON, R.L., SHARMA, S., BARROW, R.K., KORNBERG, M., GILL, D.L. AND SNYDER, S.H. (2005) PHOSPHOLIPASE CΓ1 CONTROLS SURFACE EXPRESSION OF TRPC3 THROUGH AN INTERMOLECULAR PH DOMAIN. *NATURE*, **434**, 99–104.

VANDELEUR, R.K., MAYO, G., SHELDEN, M.C., GILLIHAM, M., KAISER, B.N. AND TYERMAN, S.D. (2009) THE ROLE OF PLASMA MEMBRANE INTRINSIC PROTEIN AQUAPORINS IN WATER TRANSPORT THROUGH ROOTS: DIURNAL AND DROUGHT STRESS RESPONSES REVEAL DIFFERENT STRATEGIES BETWEEN ISOHYDRIC AND ANISOHYDRIC CULTIVARS OF GRAPEVINE. *PLANT PHYSIOL.*, **149**, 445–460.

VANDELEUR, R.K., SULLIVAN, W., ATHMAN, A., JORDANS, C., GILLIHAM, M., KAISER, B.N. AND TYERMAN, S.D. (2014) RAPID SHOOT-TO-ROOT SIGNALING REGULATES ROOT HYDRAULIC CONDUCTANCE VIA AQUAPORINS. *PLANT, CELL ENVIRON.*, **37**, 520–538.

VANHEE, C. AND BATOKO, H. (2011) AUTOPHAGY INVOLVEMENT IN RESPONSES TO ABSCISIC ACID BY PLANT CELLS. *AUTOPHAGY*, **7**, 655–656.

VANHEE, C., GUILLON, S., MASQUELIER, D., DEGAND, H., DELEU, M., MORSOMME, P. AND BATOKO, H. (2010) A TSPO-RELATED PROTEIN LOCALIZES TO THE EARLY SECRETORY PATHWAY IN ARABIDOPSIS, BUT IS TARGETED TO MITOCHONDRIA WHEN EXPRESSED IN YEAST. *J. EXP. BOT.*, **62**, 497–508.

VANHEE, C., ZAPOTOCZNY, G., MASQUELIER, D., GHISLAIN, M. AND BATOKO, H. (2011) THE ARABIDOPSIS MULTISTRESS REGULATOR TSPO IS A HEME BINDING MEMBRANE PROTEIN AND A POTENTIAL SCAVENGER OF PORPHYRINS VIA AN AUTOPHAGY-DEPENDENT DEGRADATION MECHANISM. *PLANT CELL*, **23**, 785–805.

VELJANOVSKI, V. AND BATOKO, H. (2014) SELECTIVE AUTOPHAGY OF NON-UBIQUITYLATED TARGETS IN PLANTS: LOOKING FOR COGNATE RECEPTOR/ADAPTOR PROTEINS. *FRONT. PLANT SCI.*, **5**, 308.

VERDOUCQ, L., GRONDIN, A. AND MAUREL, C. (2008) STRUCTURE–FUNCTION ANALYSIS OF PLANT AQUAPORIN ATPIP2;1 GATING BY DIVALENT CATIONS AND PROTONS. *BIOCHEM. J.*, **415**, 409–416.

VERMA, A., NYE, J.S. AND SNYDER, S.H. (1987) PORPHYRINS ARE ENDOGENOUS LIGANDS FOR THE MITOCHONDRIAL (PERIPHERAL-TYPE) BENZODIAZEPINE RECEPTOR. *PROC. NATL. ACAD. SCI. U. S. A.*, **84**, 2256–2260.

VERMEER, J.E.M., VAN LEEUWEN, W., TOBEÑA-SANTAMARIA, R., LAXALT, A.M., JONES, D.R., DIVECHA, N., GADELLA, T.W.J. AND MUNNIK, T. (2006) VISUALIZATION OF PTDINS3P DYNAMICS IN LIVING PLANT CELLS. *PLANT J.*, **47**, 687–700.

VERMEER, J.E.M., THOLE, J.M., GOEDHART, J., NIELSEN, E., MUNNIK, T. AND GADELLA, T.W.J. (2009) IMAGING PHOSPHATIDYLINOSITOL 4-PHOSPHATE DYNAMICS IN LIVING PLANT CELLS. *PLANT J.*, **57**, 356–372.

VIERSTRA, R.D. (2009) THE UBIQUITIN–26S PROTEASOME SYSTEM AT THE NEXUS OF PLANT BIOLOGY. *NAT. REV. MOL. CELL BIOL.*, **10**, 385–397.

VIERSTRA, R.D. (2003) THE UBIQUITIN/26S PROTEASOME PATHWAY, THE COMPLEX LAST CHAPTER IN THE LIFE OF MANY PLANT PROTEINS. *TRENDS PLANT SCI.*, **8**, 135–142.

VON BERLEPSCH, S., KUNZ, H.-H., BRODESSER, S., FINK, P., MARIN, K., FLUGGE, U.-I. AND GIERTH, M. (2012) THE ACYL-ACYL CARRIER PROTEIN SYNTHETASE FROM SYNECHOCYSTIS SP. PCC 6803 MEDIATES FATTY ACID IMPORT. *PLANT PHYSIOL.*, **159**, 606–617.

WAADT, R., HITOMI, K., NISHIMURA, N., HITOMI, C., ADAMS, S.R., GETZOFF, E.D. AND SCHROEDER, J.I. (2014) FRET-BASED REPORTERS FOR THE DIRECT VISUALIZATION OF ABSCISIC ACID CONCENTRATION CHANGES AND DISTRIBUTION IN ARABIDOPSIS. *ELIFE*, **3**, E01739.

WANG, C., ZIEN, C., AFITLHILE, M., WELTI, R., HILDEBRAND, D., AND WANG X. (2000) INVOLVEMENT OF PHOSPHOLIPASE D IN WOUND-INDUCED ACCUMULATION OF JASMONIC ACID IN ARABIDOPSIS. *PLANT CELL*, **12**, 2237-2246.

WANG, M., WANG, X., ZHAO, L., MA, W., RODRIGUEZ, I.R., FARISS, R.N. AND WONG, W.T. (2014) MACROGLIA-MICROGLIA INTERACTIONS VIA TSPO SIGNALING REGULATES MICROGLIAL ACTIVATION IN THE MOUSE RETINA. *J. NEUROSCI.*, **34**, 3793–3806.

WASILEWSKA, A., VLAD, F., SIRICHANDRA, C., REDKO, Y., JAMMES, F., VALON, C., FREI DIT FREY, N. AND LEUNG, J. (2008) AN UPDATE ON ABSCISIC ACID SIGNALING IN PLANTS AND MORE. *MOL. PLANT*, **1**, 198–217.

WELTERS, P., TAKEGAWA, K., EMR, S.D. AND CHRISPEELS, M.J. (1994) ATVPS34, A PHOSPHATIDYLINOSITOL 3-KINASE OF ARABIDOPSIS THALIANA, IS AN ESSENTIAL PROTEIN WITH HOMOLOGY TO A CALCIUM-DEPENDENT LIPID BINDING DOMAIN. *PROC. NATL. ACAD. SCI. U. S. A.*, **91**, 11398–11402.

WENDLER, G., LINDEMANN, P., LACAPÈRE, J.-J. AND PAPADOPOULOS, V. (2003) PROTOPORPHYRIN IX BINDING AND TRANSPORT BY RECOMBINANT MOUSE PBR. *BIOCHEM. BIOPHYS. RES. COMMUN.*, **311**, 847–852.

WHITLEY, P., REAVES, B.J., HASHIMOTO, M., RILEY, A.M., POTTER, B.V.L. AND HOLMAN, G.D. (2003) IDENTIFICATION OF MAMMALIAN VPS24P AS AN EFFECTOR OF PHOSPHATIDYLINOSITOL 3,5-BISPHOSPHATE-DEPENDENT ENDOSOME COMPARTMENTALIZATION. *J. BIOL. CHEM.*, **278**, 38786–38795.

WILKINSON, S. AND DAVIES, W.J. (2010) DROUGHT, OZONE, ABA AND ETHYLENE: NEW INSIGHTS FROM CELL TO PLANT TO COMMUNITY. *PLANT, CELL ENVIRON.*, **33**, 510–525.

WINTER, D., VINEGAR, B., NAHAL, H., AMMAR, R., WILSON, G. V AND PROVART, N.J. (2007) AN "ELECTRONIC FLUORESCENT PICTOGRAPH" BROWSER FOR EXPLORING AND ANALYZING LARGE-SCALE BIOLOGICAL DATA SETS. *PLOS ONE*, **2**, E718.

WISHART, D.S., JEWISON, T., GUO, A.C., ET AL. (2013) HMDB 3.0-THE HUMAN METABOLOME DATABASE IN 2013. *NUCLEIC ACIDS RES.*, **41**, 801–807.

WU, Q., ZHANG, X., PEIRATS-LLOBET, M., BELDA-PALAZON, B., WANG, X., CUI, S., YU, X., RODRIGUEZ, P.L. AND AN, C. (2016) UBIQUITIN LIGASES RGLG1 AND RGLG5 REGULATE ABSCISIC ACID SIGNALING BY CONTROLLING THE TURNOVER OF PHOSPHATASE PP2CA. *PLANT CELL*, **28**, 2178–2196.

WYWIAL, E. AND SINGH, S.M. (2010) IDENTIFICATION AND STRUCTURAL CHARACTERIZATION OF FYVE DOMAIN-CONTAINING PROTEINS OF ARABIDOPSIS THALIANA. *BMC PLANT BIOL.*, **10**, 157.

XIONG, L., ISHITANI, M., LEE, H. AND ZHU, J.-K. (2001) THE ARABIDOPSIS LOS5/ABA3 LOCUS ENCODES A MOLYBDENUM COFACTOR SULFURASE AND MODULATES COLD STRESS- AND OSMOTIC STRESS-RESPONSIVE GENE EXPRESSION. *PLANT CELL*, **13**, 2063–2083.

XIONG, L., LEE, H., ISHITANI, M. AND ZHU, J.K. (2002) REGULATION OF OSMOTIC STRESS-RESPONSIVE GENE EXPRESSION BY THE LOS6/ABA1 LOCUS IN ARABIDOPSIS. *J. BIOL. CHEM.*, **277**, 8588–8596.

XIONG, L. AND ZHU, J. (2003) REGULATION OF ABSCISIC ACID BIOSYNTHESIS. *PLANT PHYSIOL.*, **133**, 29–36.

XU, C. AND SHANKLIN J. (2016) TRIACYLGLYCEROL METABOLISM, FUNCTION, AND ACCUMULATION IN PLANT VEGETATIVE TISSUES. *ANNU. REV. PLANT BIOL*, **67,** 179–206.

XU, Z.-Y., LEE, K.H., DONG, T., ET AL. (2012) A VACUOLAR B-GLUCOSIDASE HOMOLOG THAT POSSESSES GLUCOSE-CONJUGATED ABSCISIC ACID HYDROLYZING ACTIVITY PLAYS AN IMPORTANT ROLE IN OSMOTIC STRESS RESPONSES IN ARABIDOPSIS. *PLANT CELL*, **24**, 2184–2199.

Yakir-Tamang, L. and Gerst, J.E. (2009) A Phosphatidylinositol-Transfer Protein and Phosphatidylinositol-4-phosphate 5-Kinase Control Cdc42 to Regulate the Actin Cytoskeleton and Secretory Pathway in Yeast. *Mol. Biol. Cell*, **20**, 3583–3597.

Yamaguchi-Shinozaki, K. and Shinozaki, K. (2006) Transcriptional regulatory networks in cellular responses and tolerance to dehydration and cold stresses. *Annu. Rev. Plant Biol.*, **57**, 781–803.

Yamamoto, M., Arimura, H., Fukushige, T., et al. (2014) Abcb10 Role in Heme Biosynthesis In Vivo: Abcb10 Knockout in Mice Causes Anemia with Protoporphyrin IX and Iron Accumulation. *Mol. Cell. Biol.*, **34**, 1077–1084.

Yaneff, A., Vitali, V. and Amodeo, G. (2015) PIP1 aquaporins: Intrinsic water channels or PIP2 aquaporin modulators? *FEBS Lett.*, **589**, 3508–3515.

Yang, D., Song, D., Kind, T., Ma, Y., Hoefkens, J. and Fiehn, O. (2015) Lipidomic analysis of chlamydomonas reinhardtii under nitrogen and sulfur deprivation. *PLoS One*, **10**, e0137948.

Yang, W., Zhang, W. and Wang, X. (2017) Post-translational control of ABA signaling: the roles of protein phosphorylation and ubiquitination. *Plant Biotechnol. J.*, **15**, 4–14.

Yang, Y. and Benning, C. (2018) Functions of triacylglycerols during plant development and stress. *Curr. Opin. Biotechnol.*, **49**, 191–198.

Yang, Y.G., Lv, W.T., Li, M.J., Wang, B., Sun, D.M. and Deng, X. (2013) Maize membrane-bound transcription factor zmbzip17 is a key regulator in the cross-talk of er quality control and aba signaling. *Plant Cell Physiol.*, **54**, 2020–2033.

Yeliseev, A.A. and Kaplan, S. (1999) A novel mechanism for the regulation of photosynthesis gene expression by the TspO outer membrane protein of Rhodobacter sphaeroides 2.4.1. *J. Biol. Chem.*, **274**, 21234–21243.

Yin, P., Fan, H., Hao, Q., et al. (2009) Structural insights into the mechanism of abscisic acid signaling by PYL proteins. *Nat. Struct. Mol. Biol.*, **16**, 1230–1236.

Yoshida, T., Fujita, Y., Sayama, H., Kidokoro, S., Maruyama, K., Mizoi, J., Shinozaki, K. and Yamaguchi-Shinozaki, K. (2010) AREB1, AREB2, and ABF3 are master transcription factors that cooperatively regulate ABRE-dependent ABA signaling involved in drought stress tolerance and require ABA for full activation. *Plant J.*, **61**, 672–685.

Yu, F., Wu, Y. and Xie, Q. (2016) Ubiquitin-Proteasome System in ABA Signaling: From Perception to Action. *Mol. Plant*, **9**, 21–33.

Zelazny, E., Borst, J.W., Muylaert, M., Batoko, H., Hemminga, M.A. and Chaumont, F. (2007) FRET imaging in living maize cells reveals that plasma membrane aquaporins interact to regulate their subcellular localization. *Proc. Natl. Acad. Sci. U. S. A.*, **104**, 12359–12364.

Zelicourt, A. de, Colcombet, J. and Hirt, H. (2016) The Role of MAPK Modules and ABA during Abiotic Stress Signaling. *Trends Plant Sci.*, **21**, 677–685.

Zeng, X. and Kaplan, S. (2001) TspO as a modulator of the repressor/antirepressor (PpsR/AppA) regulatory system in Rhodobacter spaeroides 2.4.1. *J. Bacteriol.*, **183**, 6355–6364.

Zeno, S., Veenman, L., Katz, Y., Bode, J., Gavish, M. and Zaaroor, M. (2012) The 18 kDa mitochondrial translocator protein (TSPO) prevents accumulation of protoporphyrin IX. Involvement of reactive oxygen species (ROS). *Curr. Mol. Med.*, **12**, 494–501.

Zhang, H., Zhu, H., Pan, Y., Yu, Y., Luan, S. and Li, L. (2014) A DTX/MATE-type transporter facilitates abscisic acid efflux and modulates ABA sensitivity and drought tolerance in Arabidopsis. *Mol. Plant*, **7**, 1522–1532.

Zhao, A.H., Tu, L.N., Mukai, C., Sirivelu, M.P., Pillai, V. V., Morohaku, K., Cohen, R. and Selvaraj, V. (2016) Mitochondrial translocator protein (TSPO) function is not essential for heme biosynthesis. *J. Biol. Chem.*, **291**, 1591–1603.

Zhao, H. and Lappalainen, P. (2012) A simple guide to biochemical approaches for analyzing protein-lipid interactions. *Mol. Biol. Cell*, **23**, 2823–2830.

Zhao, L., Katavic, V., Li, F., Haughn, G.W. and Kunst, L. (2010) Insertional mutant analysis reveals that long-chain acyl-CoA synthetase 1 (LACS1), but not LACS8, functionally overlaps with LACS9 in Arabidopsis seed oil biosynthesis. *Plant J.*, **64**, 1048–1058.

Zheng, L., Shan, J., Krishnamoorthi, R. and Wang, X. (2002) Activation of plant phospholipase Db by phosphatidylinositol 4,5-bisphosphate: characterization of binding site and mode of action. *Biochemistry*, **41**, 4546–4553.

Zhou, S.F., Sun, L., Valdés, A.E., Engström, P., Song, Z.T., Lu, S.J. and Liu, J.X. (2015) Membrane-associated transcription factor peptidase, site-2 protease, antagonizes ABA signaling in Arabidopsis. *New Phytol.*, **208**, 188–197.

Zhu, J.-K. (2016) Abiotic Stress Signaling and Responses in Plants. *Cell*, **167**, 313–324.

Zhu, J.-K. (2002) Salt and drought stress signal transduction in plants. *Annu. Rev. Plant Biol.*, **53**, 247–273.

Ziarek, J., Peterson, F., Lytle, B. and Volkman, B. (2011) Binding site identification and structure determination of protein-ligand complexes by NMR a semiautomated approach. *Methods Enzymol.*, **493**, 241–275.

Zimmermann, P., Hirsch-Hoffmann, M., Hennig, L. and Gruissem, W. (2004) GENEVESTIGATOR. Arabidopsis microarray database and analysis toolbox. *Plant Physiol.*, **136**, 2621–2632.

Zoncu, R., Perera, R.M., Sebastian, R., Nakatsu, F., Chen, H., Balla, T., Ayala, G., Toomre, D. and Camilli, P. V. De (2007) Loss of endocytic clathrin-coated pits upon acute depletion of phosphatidylinositol 4,5-bisphosphate. *Proc. Natl. Acad. Sci. U. S. A.*, **104**, 3793–3798.

Zonia, L. and Munnik, T. (2004) Osmotically induced cell swelling versus cell shrinking elicits specific changes in phospholipid signals in tobacco pollen tubes. *Plant Physiol.*, **134**, 813–823.